5-2020

Strategic Infrastructure Planning for Autonomous Vehicles

Zhaocai Liu
Utah State University

STRATEGIC INFRASTRUCTURE PLANNING FOR AUTONOMOUS VEHICLES

by

Zhaocai Liu

A dissertation submitted in partial fulfillment
of the requirements for the degree

of

DOCTOR OF PHILOSOPHY

in

Civil and Environmental Engineering

Approved:

_____	_____
Ziqi Song Major Professor	Patrick Singleton Committee Member
_____	_____
Michelle Mekker Committee Member	Haitao Wang Committee Member
_____	_____
Marvin W. Halling Committee Member	Richard Inouye, Ph.D. Vice Provost of Graduate Studies

UTAH STATE UNIVERSITY
Logan, Utah

2020

ABSTRACT

Strategic Infrastructure Planning for Autonomous Vehicles

by

Zhaocai Liu

Utah State University, 2020

Major Professor: Dr. Ziqi Song
Department: Civil and Environmental Engineering

Emerging autonomous vehicle (AV) technology is expected to bring dramatic societal, environmental, and economic benefits. To promote the realization of the potential benefits of AV technology, this dissertation aims at investigating the modeling and optimization of network infrastructure modification and enhancement planning for autonomous vehicles. This dissertation first examines the traffic assignment and congestion pricing problems in a network with mixed AVs and human-driven vehicles (HVs). The impact of AVs on road capacity and drivers' value of travel time is explicitly considered. Numerical results reveal a paradoxical phenomenon that the adoption of AVs may increase network congestion under certain situations. The effectiveness of congestion pricing is also demonstrated with numerical studies.

This dissertation then studies the optimization problem for dedicating lanes for priority or exclusive use by AVs. Deploying dedicated lanes for autonomous vehicles is foreseen as an effective way to amplify the road-capacity-improvement benefit from autonomous vehicles and boost the market penetration of autonomous vehicles. However, dedicated autonomous vehicle lanes may be underutilized when autonomous vehicle

flows are relatively low. This dissertation introduces a new form of managed lanes for autonomous vehicles, designated as autonomous-vehicle/toll lanes, which are freely accessible to autonomous vehicles while allowing human-driven vehicles to utilize the lanes by paying a toll. Numerical results demonstrate that the joint use of dedicated autonomous vehicle lanes and autonomous-vehicle/toll lanes can better improve the system efficiency of transportation networks with mixed human-driven vehicles and autonomous vehicles.

This dissertation further explores an infrastructure-enabled autonomous driving system. The system combines vehicles and infrastructure in the realization of autonomous driving. Equipped with roadside sensor and control systems, a regular road can be upgraded into an automated road providing autonomous driving service to vehicles. Vehicles only need to carry minimum required on-board devices to enable their autonomous driving on an automated road. The costs of vehicles can thus be significantly reduced. Moreover, the liability associated with autonomous driving can now be shared by vehicle makers, infrastructure providers, and/or some third-party players. A network modeling framework is proposed for the evaluation and planning of the infrastructure-enabled autonomous driving system. Numerical studies demonstrate that the infrastructure-enabled autonomous driving system is of great potential in promoting the adoption of autonomous driving technology.

(202 pages)

PUBLIC ABSTRACT

Strategic Infrastructure Planning for Autonomous Vehicles

Zhaocai Liu

Compared with conventional human-driven vehicles (HVs), AVs have various potential benefits, such as increasing road capacity and lowering vehicular fuel consumption and emissions. Road infrastructure management, adaptation, and upgrade plays a key role in promoting the adoption and benefit realization of AVs. This dissertation investigated several strategic infrastructure planning problems for AVs. First, it studied the potential impact of AVs on the congestion patterns of transportation networks. Second, it investigated the strategic planning problem for a new form of managed lanes for autonomous vehicles, designated as autonomous-vehicle/toll lanes, which are freely accessible to autonomous vehicles while allowing human-driven vehicles to utilize the lanes by paying a toll. This new type of managed lanes has the potential of increasing traffic capacity and fully utilizing the traffic capacity by selling redundant road capacity to HVs. Last, this dissertation studied the strategic infrastructure planning problem for an infrastructure-enabled autonomous driving system. The system combines vehicles and infrastructure in the realization of autonomous driving. Equipped with roadside sensor and control systems, a regular road can be upgraded into an automated road providing autonomous driving service to vehicles. Vehicles only need to carry minimum required on-board devices to enable their autonomous driving on an automated road. The costs of vehicles can thus be significantly reduced.

To my parents,

who gave me a love of life

To my wife Yi He,

who gave me a life of love

ACKNOWLEDGMENTS

I would like to express my deepest gratitude and appreciation to my advisor Dr. Ziqi Song for his guidance and support during my studies. It is a great honor for me to be his first Ph.D. student. He is a patient teacher, a supportive friend, and a talented and passionate researcher. He introduced me to this amazing venue of transportation research as my career, guided me through the academic jungle, and sharped my views towards transportation systems.

I would also like to thank Dr. Patrick Singleton, Dr. Michelle Mekker, Dr. Haitao Wang, and Dr. Marvin W. Halling, for serving on my dissertation committee and giving me valuable comments and suggestions on my dissertation research.

I would like to acknowledge U.S. Department of Energy, Utah Department of Transportation, Mountain-Plains Consortium, and Transportation Research Center for Livable Communities for providing financial support.

Zhaocai Liu

CONTENTS

Page

LIST OF TABLES

Table Page

Table Page

LIST OF FIGURES

Figure Page

CHAPTER 1

INTRODUCTION

1.1 Background

Compared with conventional human-driven vehicles (HVs), autonomous vehicles (AVs) have various potential benefits, such as reducing deadly crashes, increasing road capacity, lowering vehicular fuel consumption and emissions, and providing critical mobility to the elderly and disabled (Fagnant and Kockelman, 2015; Chen et al., 2016; Levin and Boyles, 2016a,b; Bagloee et al., 2016; Meyer et al., 2017; Pan et al., 2019). Although commercial AVs have not been offered in the market, recent progress suggests they are on the horizon. In partnership with Lyft, nuTonomy, a software company, has launched the nation's first self-driving ridesharing service in Boston in December 2017 (nuTonomy, 2018). At the end of 2018, Waymo, formerly the Google self-driving car project, launched its first commercial self-driving service in the Metro Phoenix area, Arizona (Waymo, 2018a). Moreover, Waymo plans to add up to 20,000 I-PACE vehicles to its fleet in the next few years (Waymo, 2019). Many automakers such as Nissan (Nissan, 2017), Honda (Honda, 2019), and Toyota (TOYOTA, 2019) have announced their intentions to provide commercially-viable autonomous-driving capabilities by 2020 in some of their vehicle models. Many researchers (e.g., Litman, 2017; Bansal and Kockelman, 2017; Talebian and Mishra, 2018) have predicted that AVs will constitute a significant or even dominant portion of the vehicle market in the next few decades. Therefore, it is imperative to modify existing travel demand and network flow models to capture the characteristics of AVs.

Employing vehicle communication and automated control technologies, AVs can

have smaller time headways than HVs and thus may increase road capacity. This benefit of AVs has been demonstrated by both simulation (e.g., Shladover et al., 2012; Ntousakis et al., 2015) and analytical modeling analyses (e.g., Levin and Boyles, 2015; van den Berg and Verhoef, 2016). The impact of AVs on traffic capacity will inevitably influence the traffic flow distributions and congestion patterns of networks with AVs. Moreover, by allowing drivers to conduct other activities, AVs may also reduce the value of travel time (VOT) of drivers (Le Vine et al., 2015; van den Berg and Verhoef, 2016; Noruzoliaee et al., 2018). The VOT change of drivers will influence their reactions to congestion pricing.

Deploying dedicated lanes for AVs is foreseen as an effective way to amplify the capacity-improvement benefit from AVs and boost the market penetration of AVs (Chen et al., 2016; Chen et al., 2019; Ghiasi et al., 2017; Lamotte et al., 2017; Lu et al., 2019). However, dedicated AV lanes may be underutilized when AV flows are relatively low (Chen et al., 2016). We thus consider a new form of managed lanes for AVs, designated as autonomous-vehicle/toll (AVT) lanes, which are freely accessible to AVs while allowing HVs to utilize the lanes by paying a toll. The idea of AVT lanes is derived from high-occupancy vehicle (HOV) lanes and high-occupancy/toll (HOT) lanes (Fielding and Klein, 1993; Dahlgren, 2002). The joint use of dedicated AV lanes and AVT lanes can better improve the system efficiency of transportation networks with mixed AV and HV traffic.

Currently the development of autonomous driving is focusing on autonomous vehicle (AV) technology and mainly led by the private sector, which includes technology

companies such as Google and Baidu, automakers such as Audi, Toyota, Ford, and Volvo, and transportation network companies such as Uber, Lyft, and DiDi. As of July 2018, Google's AV fleet has self-driven over eight million miles on public roads (Waymo, 2018b), and numerous manufacturers, including BMW, Nissan, Ford, General Motors, Tesla, Mercedes-Benz, and Bosch, have begun testing their prototype AVs (Wang, 2018).

However, focusing on AV technology alone may potentially slow the penetration of AVs and consequently slowing the realization of societal benefits of AVs. In order to safely drive itself in various road environment, an AV needs to be equipped with expensive sensor systems and additional hardware and software. The high cost of AVs can be a significant barrier to their broad adoption (Fagnant and Kockelman, 2015; Jun and Markel, 2017). Moreover, if autonomous driving only relies on AVs, the AV makers will be saddled with both the responsibility and liabilities associated with the traditional capabilities of the vehicle, but also those associated with functions that human beings routinely perform (Gopalswamy and Rathinam, 2018). The liability threats associated with AVs will be an important and potentially limiting consideration for AV makers, and have the potential to present a significant deterrent to the development of AVs (Marchant and Lindor, 2012). Integrating transportation infrastructure enhancement into the realization of autonomous driving can potentially promote the development and adoption of AVs (Rebsamen et al., 2012; Horst et al., 2016; Jun and Markel, 2017; Ran et al., 2019a,b; Sanchez et al., 2016). With the development of vehicle to vehicle and vehicle to infrastructure technologies, researchers have suggested that an infrastructure-enabled or

infrastructure-based autonomous driving system provides a promising alternative to the development of autonomous driving (Gopalswamy and Rathinam, 2018; Ran et al., 2019a,b).

1.2 Research objectives

The main objective of this dissertation is to investigate the modeling and optimization of network infrastructure modification and enhancement planning for AVs. More specifically, this dissertation will make the following contributions.

First, this dissertation investigates traffic assignment and congestion pricing problems in a network with mixed AVs and HVs. It is assumed that both HVs and AVs will selfishly choose their routes to minimize their individual travel costs, i.e., they follow the user equilibrium routing principle. Considering headway realizations in different AV technology scenarios, this dissertation analyzes the impact of AVs on road traffic capacity and provides an analytical capacity model for road segments with mixed HV and AV flows. This dissertation formulates a user equilibrium traffic assignment model, proves the solution existence of the user equilibrium, and establishes the uniqueness conditions for the solutions of link travel time and system delay. This dissertation then investigates the system optimal, the first-best and second-best congestion pricing problems in networks with mixed HV and AV flows.

Second, this dissertation proposes the concept of autonomous vehicle/toll (AVT) lanes, which is a promising alternative to dedicated AV lanes when AV flows are relatively low. A network modeling framework is then proposed to determine the optimal deployment of dedicated AV lanes and AVT lanes in a transportation network with

mixed HV and AV flows. Considering the user equilibrium problem with mixed HVs and AVs may have non-unique flow distribution and system delay, this dissertation proposed a robust optimal deployment model to deploy dedicated AV lanes and AVT lanes in a manner that minimizes the social cost under the worst-case flow distribution. The robust optimal deployment model is formulated as a generalized semi-infinite min-max program and is solved using a genetic-algorithm-based approach.

Last, this dissertation explores the potential of an infrastructure-enabled autonomous driving system and develop a modeling framework for the planning and evaluation of such a system. It is envisioned that there will three major types of vehicles in the market: conventional human-driven vehicles (HVs), infrastructure-independent autonomous vehicles (IIAVs), and infrastructure-enabled autonomous vehicles (IEAVs). This dissertation will develop a new network equilibrium model to describe road users' vehicle type and route choice behaviors in a transportation network with automated roads. The model will consider two special characteristics of IEAVs: (1) IEAVs are driven by human drivers on regular roads and will be driven autonomously on automated roads; (2) IEAV users will experience different value of travel time on regular and automated roads. Based on the proposed network equilibrium model, this dissertation will further investigate the strategic planning of automated roads in a general transportation network. To the best of our knowledge, this study will be the first in the literature that develops a modeling framework for the planning and evaluation of the infrastructure-enabled autonomous driving system in a general transportation network.

1.3 Dissertation organization

The remainder of this dissertation is organized as follows. Chapter 2 reviews related work and highlights how this dissertation can contribute to the existing literature. Chapter 3 first investigates the network equilibrium problem in networks with mixed HVs and AVs. The system optimal, first-best and second-best pricing problems are then studied. Chapter 4 formulates the robust optimization model for the deployment of dedicated AV lanes and AVT lanes and proposes a genetic-algorithm-based algorithm to solve it. Numerical studies are provided to demonstrate the model and the solution algorithm. Chapter 5 develops a network modeling framework for the planning and evaluation of the infrastructure-based autonomous driving system. Chapter 6 concludes the dissertation and discuss future research directions.

CHAPTER 2

LITERATURE REVIEW

2.1 Review of network equilibrium and congestion pricing studies

Several studies have investigated the network equilibrium problem involving AVs. Chen et al. (2016) proposed a multi-class network equilibrium model for a transportation network with dedicated AV lanes and mixed AV and HV flows. The model assumes that AVs will significantly improve road capacity on dedicated AV lanes, whereas they will have no influence on the traffic capacity of roads with mixed flows. Chen et al. (2017b) further developed a network equilibrium model for a transportation network with dedicated AV zones and mixed AV and HV flows. In the model, travelers are assumed to minimize their perceived travel times when they make route choices. Perceived travel times are actual trip times for HV users, while for AV users they represent the actual travel times spent outside of the dedicated AV zones plus perceived marginal travel times within the dedicated AV zones (i.e., AVs are controlled by a central manager and follow a system-optimum (SO) routing principle within the dedicated AV zones). The model also assumes that AVs will improve road capacity within the dedicated AV zones while having no influence on road capacity outside the dedicated AV zones. Considering mixed AV and HV travel demands, Jiang (2017) proposed a combined mode split and traffic assignment model. The model assumes that AVs and HVs travel on separate lanes throughout the network and respectively follow the Cournot-Nash (CN) principle (i.e., AVs try to minimize their total travel cost through cooperation) and the user equilibrium (UE) principle when choosing routes. Based on the

assumption that a central agent can fully control a fraction of the AV fleet in a network, Zhang and Nie (2018) proposed a mixed network equilibrium model with multi-class users. The model assumes that users who are not controlled by the central agent will try to minimize their own travel time through selfishly choosing their routes (i.e., following the UE routing principle), whereas users who are controlled by the central agent will try to minimize total system travel time through cooperative routing behavior (i.e., following the SO routing principle). The above studies either do not consider the case with mixed AV and HV flows (i.e., Jiang, 2017) or neglect the potential impact of AVs on the capacity of roads with mixed flows (i.e., Chen et al., 2016, 2017b; Zhang and Nie, 2018). However, because it will be many years before AVs are widely adopted and it may be impractical to completely separate AV and HV flows throughout a transportation network, a heterogeneous traffic flow consisting of both AVs and HVs will inevitably exist for a long time. In addition, as reported by many studies (e.g., Ghiasi et al., 2017; Bierstedt et al., 2014; Shladover, 2012), the potential impact of AVs on the capacity of roads with mixed AV and HV flows can be significant. Therefore, it is of great theoretical and practical importance to study the network equilibrium problem with mixed AV and HV flows and to specifically consider the impact of AVs on road capacity with mixed traffic.

Levin and Boyles (2015) proposed a multiclass user equilibrium model for traffic assignment in a network with mixed HVs and AVs. They adopted the well-known Bureau of Public Roads (BPR) travel time function in their model. They considered that AVs will have smaller headways than HVs and the traffic capacity of a road is a function of the

proportion of AVs on the road. Mehr and Horowitz (2019) developed a user equilibrium model for a network with mixed autonomy. They also adopted the BPR travel time function and considered that the traffic capacity of a road is a function of the proportion of AVs on the road. However, the road capacity function adopted in both Levin and Boyles (2015) and Mehr and Horowitz (2019) only considered two types of deterministic time headways and neglected the stochasticity of mixed traffic (Ghiasi et al., 2017).

Only a limited number of studies have investigated the congestion pricing problems in networks with mixed traffic of both HVs and AVs. Ye and Wang (2018) proposed a bi-level network design model compromising dedicated AV links and congestion pricing to reduce traffic congestion. They assume that congestion pricing is only implemented for HVs. They also assume that dedicated AV links can only be accessed by AVs and will have significantly increased capacity, whereas regular links will have unchanged capacity although they will be used by mixed HVs and AVs. As discussed above, the impact of AVs on the capacity of roads with mixed traffic may be significant and thus should not be neglected. Tscharaktschiew and Evangelinos (2019) studied the interactions between the transition in automated driving capabilities on road congestion pricing. They considered the interdependencies between traffic flow, the choice level of autonomous driving, effective road capacity, and marginal travel cost. To make the analysis simple and clear, they adopted the classical continuous static model of traffic congestion pricing. They considered a single origin-destination pair connected by a single road in their numerical study. Their study focuses on the economic analysis of congestion pricing rather than network-level congestion pricing design. Recently,

considering different potential future scenarios with different market penetration of AVs and shared AVs, Simoni et al. (2019) developed multiple congestion pricing and tolling strategies and investigated their effects on the Austin, Texas network conditions and traveler welfare, using the agent-based simulation model MATsim (www.matsim.org). An agent-based model allows a higher level of realism compared to conventional static traffic assignment model because it is possible to explicitly model several factors concerning transportation demand and traffic. However, it requires demanding computational effort.

Also worth noting here are a few recent studies that propose new and futuristic tolling schemes in a connected and automated vehicles environment. Basar and Cetin (2017) proposed a novel tolling system based on descending price auction. They conducted an online survey to assess the public acceptance of the auction-based tolling systems over current dynamic and fixed tolling methodologies on highways. Based on the analysis of the survey data and, the authors found that, among those who are familiar with the current tolling methods, there is no outright rejection of the new tolling method. In addition, they found that, compared to fixed tolling, the new tolling method generates more revenue and improves the capacity utilization of the toll road. Sharon et al. (2017) presented a mechanism for setting dynamic and adaptive tolls denoted Delta-toll for connected and automated vehicles. The Delta-toll is a model-free adaptive tolling scheme which only requires travel time observations on links. They showed the effectiveness of Delta-tolling using traffic simulators. They also proved that the Delta-tolling will yield

system optimal flow for the special case of the static network equilibrium model with BPR-style delay functions.

2.2 Review of lane management studies

Traffic capacity analysis for a road with mixed AVs and HVs have been conducted in many studies (e.g., Shladover et al., 2012; Ntousakis et al., 2015; Levin and Boyles, 2015; van den Berg and Verhoef, 2016). Based on the anticipation that AVs will have reduced time headways when following other vehicles, majority of these studies concluded that traffic capacity would increase substantially with the increase of the AV flow proportion. A number of studies (e.g., Chen et al., 2016; Ghiasi et al., 2017; Talebpour et al., 2017; Ye and Yamamoto, 2018) have indicated that reserving dedicated lanes for AVs can possibly further amplify their benefits in improving traffic capacity. Tientrakool et al. (2011) showed that, due to the benefits of reduced inter-vehicle safe distance, the capacity of lanes used by pure AV flows will approximately become tripled compared to the capacity in the case of pure HV flows. Using microscopic simulation, Talebpour et al. (2017) investigated the impacts of reserved lanes for AVs on congestion and travel time reliability. They found that reserving a lane for autonomous vehicles is beneficial only when the market penetration rates of AVs is above 50% for the tested two-lane highway and 30% for the tested four-lane highway. Ye and Yamamoto (2018) introduced a fundamental diagram approach to reveal the pros and cons of setting dedicated lanes for connected AVs under various connected AV penetration rates and demand levels. They found that setting dedicated AV lanes will deteriorate the performance of the overall traffic throughput at a low AV penetration rate. Ghiasi et al.

(2017) proposed an analytical stochastic capacity model for highways with mixed HV and AV flows. They considered the stochasticity and heterogeneity of headways in mixed traffic and different future realizations of AV technology scenarios. Based on the capacity model, the authors further built a lane management model to optimize the number of dedicated AV lanes on a multi-lane highway segment. They found that, if future AV technology is conservative (i.e., AVs have larger headways than HVs), setting dedicated AV lanes is not beneficial. They also found that setting dedicated AV lanes is not beneficial when AV penetration rate is low even when future AV technology is aggressive (i.e., AVs have much smaller headways than HVs). In the recently published National Cooperative Highway Research Program (NCHRP) research report 891 (NASEM, 2018), researchers have developed specific guidance for agencies on operational characteristic and impacts of dedicating lanes to priority (i.e., only AVs and high occupancy vehicles (HOVs) can use dedicated lanes) or exclusive use by AVs. The report also pointed out that, at low market penetration of AVs, dedicated AV lanes will be underutilized and will even compromise the overall network performance.

To the best of our knowledge, only two studies in the literature has investigated the deployment problem of managed lanes for AVs at the network level (i.e., Chen et al., 2016; Chen et al., 2019). Chen et al. (2016) developed a time-dependent network design model to determine when, where and how many AV lanes should be deployed in a general network. The model assumes that AVs and HVs follow the UE principle in choosing their routes and that AVs will significantly improve road capacity on AV lanes while having no impact on the traffic capacity of roads with mixed flows. However, as

discussed above, the impacts of AVs on the traffic capacity of roads with mixed flows can be significant and thus should not be neglected. Chen et al. (2019) proposed an AV incentive program design problem, in which both dedicated AV lanes and AV purchase subsidies are implemented to promote the adoption of AVs. They formulated the AV incentive program design problem as a two-stage stochastic programming model with equilibrium constraints and developed a solution method based on linear approximation and duality to solve the model. They also assumed that AVs will significantly improve road capacity on AV lanes while having no impact on the traffic capacity of roads with mixed flows.

2.3 Review of infrastructure-enabled autonomous driving studies

As discussed in the Chapter one, researchers have pointed out the potential of integrating transportation infrastructure enhancement into the realization of autonomous driving (Rebsamen et al., 2012; Horst et al., 2016; Jun and Markel, 2017; Sanchez et al., 2016; Ran et al., 2019a,b). Sanchez et al. (2016) indicate that cooperative technologies, which enable cooperation between vehicles, vulnerable road users, and infrastructure, will be vital to the development of highly autonomous vehicles operating in complex urban environments. Based on simulation and field experiment results, Rebsamen et al. (2012) argued that utilizing infrastructure sensors can improve the operation safety and reduce the on-board sensor cost of AVs. Jun and Markel (2017) proposed a data sharing strategy in which the expensive AV component, the light detection and ranging (LIDAR) sensors, are moved from vehicles to the infrastructure to be used as shared sensors by all vehicles within the vicinity. They argued that the infrastructure-based strategy will reduce

the cost of automobiles and can accelerate the introduction of AVs.

More recently, Gopalswamy and Rathinam (2018) introduce a concept of infrastructure enabled autonomy (IEA), in which autonomous driving is enabled only on certain corridors equipped with necessary sensing, computing and communicating devices, while outside these corridors vehicles will be driven by human drivers. Under the IEA concept, the autonomous driving can be treated as a service jointly provided by automakers, infrastructure players and third-party players, consequently the responsibility and liability associated with autonomous driving can be shared by these players rather than undertaken primarily by automakers. The authors believe that the re-distribution of the responsibility and liability associated with autonomous driving will incentivize the eco-system of businesses to accelerate the deployment of AVs.

Ran et al. (2019a) and Ran et al. (2019b) defined a connected automated vehicle highway (CAVH) system, in which connected and automated vehicle (CAV) technology and automated highway system (AHS) (Congress, 1994) are integrated to dramatically promote the development and adoption of AVs. Ran et al. (2019a) pointed out that the majority of the sensor functions can be achieved using sensor systems on highway infrastructure, and that the majority of the vehicle operation and control functions can be achieved via the cooperation of control systems on highway infrastructure and vehicle. Based on implementation cost analysis in different metropolitan areas, Ran et al. (2019a) reported that, the total societal investment of the CAVH approach for autonomous driving will be 1/2000 to 1/100 that of vehicle-only approach.

In summary, the infrastructure-enabled autonomous driving system or the CAVH

system has the following main advantages: (1) It can promote the adoption of AVs by reducing vehicle cost; (2) It can promote the development of AVs by alleviating the liability threats facing AV makers; (3) It is a cost effective way for the society to implement autonomous driving; (4) It endows transportation agencies a more active role in the realization of autonomous driving.

To the best of our knowledge, no study exists in the literature that provides a modeling framework for the planning and evaluation of the infrastructure-enabled autonomous driving system in a general transportation network.

CHAPTER 3

USER EQUILIBRIUM AND CONGESTION PRICING PROBLEMS FOR THE MIXED AUTONOMOUS VEHICLES AND HUMAN-DRIVEN VEHICLES

This chapter examines the user equilibrium and congestion pricing problems in a network with mixed autonomous vehicles and human-driven vehicles. Autonomous vehicles can maintain shorter headways than human-driven vehicles, thereby possibly increasing road capacity and change the current traffic congestion patterns. Autonomous vehicles may also reduce drivers' value of travel time by allowing them to perform other activities and thus may affect the effectiveness of congestion pricing. We first investigate the impact of autonomous vehicles on the capacity of a road with mixed autonomous vehicles and human-driven vehicles. Using the well-known Bureau of Public Roads (BPR) travel time models, we then show that the user equilibrium problem for a network with mixed autonomy can have unique or non-unique flow patterns depending on the capacity model of mixed traffic. We then further investigate the system optimum and the first-best pricing problems for a network with mixed autonomy. Last, we study the second-best pricing problem for a network with mixed autonomy. Considering the that the user equilibrium problem may have non-unique flow patterns and system delays, we proposed a robust congestion pricing model to determine a robust optimal toll scheme that can optimize the system performance under the worst-case flow pattern. The model is solved using a genetic-algorithm-based approach. Numerical examples are presented to illustrate key concepts and to demonstrate the proposed models.

3.1 User equilibrium problem in networks with mixed HVs and AVs

3.1.1 Basic considerations and notations

In this study, we consider transportation networks with both HVs and AVs. All HVs and AVs in the network are passenger cars. AVs in the network are homogenous in terms of driving speed and time headway settings. Assume that HVs and AVs will have identical average driving speed in mixed traffic. This assumption is reasonable because AVs may be set to always match the speed of surrounding vehicles (Levin and Boyles, 2016b). Further assume that when travelling between origins and destinations, both HV and AV users will selfishly choose their routes to minimize their individual travel costs.

Let graph $G(N, L)$ denote a transportation network, where N is the set of nodes and L is the set of directed links. Links in the road network are designated by $l \in L$ or represented as node pairs $(i, j) \in L$, where $i, j \in N$. The set of origin-destination (O-D) pairs are denoted by W. For each O-D pair $w \in W$, let $\mathrm{O}(w)$ and $\mathrm{D}(w)$ denote the origin and the destination nodes, respectively. Let $M = \{h, a\}$ denote the set of vehicle classes, where class h refers to HVs and class a refers to AVs. Let $q^{w,h}$ and $q^{w,a}$ be the travel demands of HVs and AVs between O-D pair $w \in W$, respectively. Let $x_l^{w,h}$ and $x_l^{w,a}$ be the traffic flow of HVs and AVs on link $l \in L$ between O-D pair $w \in W$, respectively. Let x_l^h and x_l^a denote the aggregate traffic flows of HVs and AVs on link $l \in L$, respectively. Let t_l denote the travel time on link $l \in L$.

Assume that the link travel times are specified by the well-known Bureau of Public Roads (BPR) travel time function with capacity as a function of the proportion of AVs on the road:

$$t_l\left(x_l^h, x_l^a\right) = \hat{t}_l\left[1 + \alpha_l\left(\frac{x_l^h + x_l^a}{c_l\left(x_l^h, x_l^a\right)}\right)^{\beta_l}\right] \qquad \forall l \in L \qquad (3\text{-}1)$$

where $\hat{t}_l$ is the free flow travel time; $c_l\left(x_l^h, x_l^a\right)$ is the link capacity which is a function of $\left(x_l^h, x_l^a\right)$; and α_l and β_l are positive calibration constants for link $l \in L$. This link travel time function for mixed traffic of HVs and AVs was first proposed by Levin and Boyles (2015) and has also been adopted by Noruzoliaee et al. (2018) and Mehr and Horowitz (2019).

3.1.2 Traffic capacity for links with mixed flows of HVs and AVs

In Levin and Boyles (2015), Noruzoliaee et al. (2018) and Mehr and Horowitz (2019) the capacity function $c_l\left(x_l^h, x_l^a\right)$ was derived based on the assumption that the headway between two vehicles only depends on the type of the following vehicle. However, this assumption may not be valid because an HV or AV may choose different trailing distances when it follows different types of vehicles (Chen et al., 2017a; Ghiasi et al., 2017). As shown in Figure 3-1, there are four different types of headways: (1) η^{ha} for an AV following an HV, (2) η^{hh} for an HV following another HV, (3) η^{ah} for an HV following an AV, and (4) η^{aa} for an AV following an AV. In the literature, different studies have assumed quite different values for the above four different types of headways. As summarized by Ghiasi et al. (2017), the values of η^{ha} range from 0.6 to 2.6 seconds, the values of η^{hh} range from 0.7 to 2.4 seconds, the values of η^{ah} range from 0.5 to 2.6 seconds, and the values of η^{aa} range from 0.3 to 2 seconds. Since we are trying

to derive the traffic capacity function, each headway mentioned above refers to the minimum headway between the corresponding vehicles.

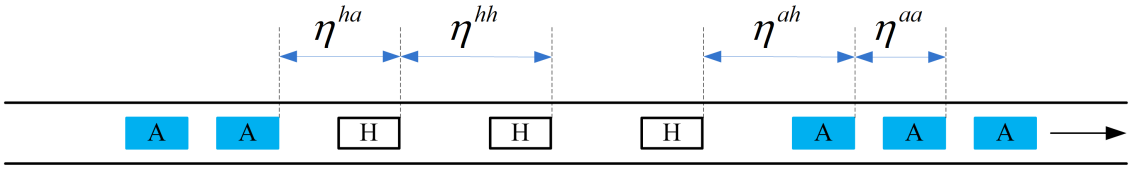

Figure 3-1. Illustration of inter-vehicle headways.

Let $\bar{\eta}_l^{ha}$, $\bar{\eta}_l^{hh}$, $\bar{\eta}_l^{ah}$, and $\bar{\eta}_l^{aa}$ denote the mean values of η^{ha}, η^{hh}, η^{ah}, and η^{aa} on link $l \in L$, respectively. Let p_l^a and p_l^h denote the proportion of AV flow and HV flow in the total link flow.p_l^a and p_l^h are given by

$$p_l^m = \frac{x_l^m}{\sum_{m' \in M} x_l^{m'}} \qquad \forall l \in L, m \in M \tag{3-2}$$

It is easy to see that $p_l^h + p_l^a = 1$. Further assume that both HVs and AVs are randomly distributed in a mixed traffic. Vehicle type can then be modeled as a Bernoulli process (Lazar et al., 2017), i.e., each vehicle is an HV with probability p_l^h and an AV with probability p_l^a independently. For a pair of vehicles, they are an AV following an HV with probability $p_l^a p_l^h$, an HV following an HV with probability $p_l^h p_l^h$, an HV following an AV with probability $p_l^h p_l^a$, and an AV following an AV with probability $p_l^a p_l^a$. The average headway in mixed flow on link $l \in L$, denoted by $\bar{\eta}_l$, is then calculated as follows:

$$\bar{\eta}_l = \bar{\eta}_l^{ha} p_l^h p_l^a + \bar{\eta}_l^{hh} p_l^h p_l^h + \bar{\eta}_l^{ah} p_l^a p_l^h + \bar{\eta}_l^{aa} p_l^a p_l^a \qquad \forall l \in L \tag{3-3}$$

According to traffic flow theory (see e.g., Hoogendoorn, 2010; van Wee et al., 2013;), the per-lane capacity (in veh/h) of a link equals the reciprocal of the mean minimum headway (in h). The traffic capacity of link $l \in L$ can thus be given by

$$c_l = \frac{\iota_l}{\bar{\eta}_l} \qquad \forall l \in L \qquad (3\text{-}4)$$

where ι_l denote the number of lanes on link $l \in L$.

Combining equations (3-3) and (3-4) and considering $p_l^a + p_l^h = 1$, we further have the following function that relates the traffic capacity of a link to the proportion of AV flow on the link:

$$c_l = \frac{\iota_l}{\left(\bar{\eta}_l^{ha} + \bar{\eta}_l^{ah}\right)(1-p_l^a)p_l^a + \bar{\eta}_l^{hh}(1-p_l^a)^2 + \bar{\eta}_l^{aa}(p_l^a)^2} \qquad \forall l \in L \qquad (3\text{-}5)$$

Proposition 3-1. Link capacity function c_{ij} is an increasing function of $p_l^a \in [0,1]$ if and only if $\bar{\eta}_l^{aa} \le \frac{\left(\bar{\eta}_l^{ha}+\bar{\eta}_l^{ah}\right)}{2} \le \bar{\eta}_l^{hh}$.

Proof. We derive $\frac{dc_l}{dp_l^a}$ as follows

$$\frac{dc_l}{dp_l^a} = \frac{\iota_l\left(\left(2\bar{\eta}_l^{hh} - \bar{\eta}_l^{ha} - \bar{\eta}_l^{ah}\right)(1-p_l^a) + \left(\bar{\eta}_l^{ha} + \bar{\eta}_l^{ah} - 2\bar{\eta}_l^{aa}\right)p_l^a\right)}{\left(\left(\bar{\eta}_l^{ha} + \bar{\eta}_l^{ah}\right)(1-p_l^a)p_l^a + \bar{\eta}_l^{hh}(1-p_l^a)^2 + \bar{\eta}_l^{aa}(p_l^a)^2\right)^2}$$

c_l is an increasing function of p_l^a if and only if $\frac{dc_l}{dp_l^a} \ge 0$. In the above, the denominator is always positive. Therefore, $\frac{dc_l}{dp_l^a} \ge 0$ is equivalent to $\left(2\bar{\eta}_l^{hh} - \bar{\eta}_l^{ha} - \bar{\eta}_l^{ah}\right)(1-p_l^a) + \left(\bar{\eta}_l^{ha} + \bar{\eta}_l^{ah} - 2\bar{\eta}_l^{aa}\right)p_l^a \ge 0$. For $p_l^a \in [0,1]$, the two extreme values of $\left(2\bar{\eta}_l^{hh} - \bar{\eta}_l^{ha} -\right.$

$\bar{\eta}_l^{ah}\big)(1-p_l^a)+\big(\bar{\eta}_l^{ha}+\bar{\eta}_l^{ah}-2\bar{\eta}_l^{aa}\big)p_l^a$ are $\big(2\bar{\eta}_l^{hh}-\bar{\eta}_l^{ha}-\bar{\eta}_l^{ah}\big)$ and $\big(\bar{\eta}_l^{ha}+\bar{\eta}_l^{ah}-2\bar{\eta}_l^{aa}\big)$. $\big(2\bar{\eta}_l^{hh}-\bar{\eta}_l^{ha}-\bar{\eta}_l^{ah}\big)(1-p_l^a)+\big(\bar{\eta}_l^{ha}+\bar{\eta}_l^{ah}-2\bar{\eta}_l^{aa}\big)p_l^a \geq 0, \forall p_l^a \in [0,1]$ is equivalent to $\big(2\bar{\eta}_l^{hh}-\bar{\eta}_l^{ha}-\bar{\eta}_l^{ah}\big) \geq 0$ and $\big(\bar{\eta}_l^{ha}+\bar{\eta}_l^{ah}-2\bar{\eta}_l^{aa}\big) \geq 0$, or $\bar{\eta}_l^{aa} \leq \frac{\left(\bar{\eta}_l^{ha}+\bar{\eta}_l^{ah}\right)}{2} \leq \bar{\eta}_l^{hh}$. Therefore, Link capacity function c_{ij} is an increasing function of $p_l^a \in [0,1]$ if and only if $\bar{\eta}_l^{aa} \leq \frac{\left(\bar{\eta}_l^{ha}+\bar{\eta}_l^{ah}\right)}{2} \leq \bar{\eta}_l^{hh}$ □

Proposition 3-2. Link capacity function c_l is an decreasing function of $p_l^a \in [0,1]$ if and only if $\bar{\eta}_l^{aa} \geq \frac{\left(\bar{\eta}_l^{ha}+\bar{\eta}_l^{ah}\right)}{2} \geq \bar{\eta}_l^{hh}$.

The proof process of proposition 3-2 is similar to that of proposition 3-1. Propositions 3-1 and 3-2 are consistent with the corollaries 5 and 6 in Ghiasi et al. (2017). Proposition 3-2 indicates that under conservative AV technologies with headways satisfying $\bar{\eta}_l^{aa} \geq \frac{\left(\bar{\eta}_l^{ha}+\bar{\eta}_l^{ah}\right)}{2} \geq \bar{\eta}_l^{hh}$, a higher proportion of AV flow will reduce rather than increase traffic capacity.

Let $\hat{c}_l^h$ denote the traffic capacity of link $l \in L$ when it is used by pure HVs. According to equation (3-5), $\hat{c}_l^h = \frac{\iota_l}{\bar{\eta}_l^{hh}}$. Substituting $\hat{c}_l^h = \frac{\iota_l}{\bar{\eta}_l^{hh}}$ into equation (3-5) gives

$$c_l = \frac{\hat{c}_l^h}{\left(\frac{\bar{\eta}_l^{ha}}{\bar{\eta}_l^{hh}}+\frac{\bar{\eta}_l^{ah}}{\bar{\eta}_l^{hh}}\right)(1-p_l^a)p_l^a+(1-p_l^a)^2+\frac{\bar{\eta}_l^{aa}}{\bar{\eta}_l^{hh}}(p_l^a)^2} \qquad \forall l \in L \qquad (3\text{-}6)$$

3.1.3 HV equivalents for AVs

Substituting equations (3-2) and (3-6) into equation (3-1) and performing some algebra* yield the following travel time function

$$t_l\left(x_l^h, x_l^a\right) = \hat{t}_l \left[1 + \alpha_l \left(\frac{x_l^h + \left(\frac{\bar{\eta}_l^{hh} + \bar{\eta}_l^{aa} - \bar{\eta}_l^{ha} - \bar{\eta}_l^{ah}}{\bar{\eta}_l^{hh}} p_l^a + \frac{\bar{\eta}_l^{ha} + \bar{\eta}_l^{ah} - \bar{\eta}_l^{hh}}{\bar{\eta}_l^{hh}} \right) x_l^a}{\hat{c}_l^h} \right)^{\beta_l} \right] \quad \forall l \in L \qquad (3\text{-}7)$$

One can observe from the above equation that, the travel time of link $l \in L$ with mixed traffic of x_l^h HV flow and x_l^a AV flow can be calculated as the travel time on the link with $x_l^h + \left(\frac{\bar{\eta}_l^{hh} + \bar{\eta}_l^{aa} - \bar{\eta}_l^{ha} - \bar{\eta}_l^{ah}}{\bar{\eta}_l^{hh}} p_l^a + \frac{\bar{\eta}_l^{ha} + \bar{\eta}_l^{ah} - \bar{\eta}_l^{hh}}{\bar{\eta}_l^{hh}} \right) x_l^a$ pure HV flow. In conventional multiclass user equilibrium with multiple types of vehicles (e.g., trucks and cars), different types of vehicle flows are usually converted into equivalent passenger car equivalent (de Andrade et al., 2017). Inspired by the concept of passenger car equivalent,

---

* $\frac{x_l^h + x_l^a}{c_l(x_l^h, x_l^a)} = \frac{x_l^h + x_l^a}{\frac{\hat{c}_l^h}{\left(\frac{\bar{\eta}_l^{ha}}{\bar{\eta}_l^{hh}} + \frac{\bar{\eta}_l^{ah}}{\bar{\eta}_l^{hh}} \right)\left(1 - p_l^a\right)p_l^a + \left(1 - p_l^a\right)^2 + \frac{\bar{\eta}_l^{aa}}{\bar{\eta}_l^{hh}}\left(p_l^a\right)^2}} = \frac{\left(x_l^h + x_l^a\right)\left(\left(\frac{\bar{\eta}_l^{ha}}{\bar{\eta}_l^{hh}} + \frac{\bar{\eta}_l^{ah}}{\bar{\eta}_l^{hh}} \right)\left(1 - p_l^a\right)p_l^a + \left(1 - p_l^a\right)^2 + \frac{\bar{\eta}_l^{aa}}{\bar{\eta}_l^{hh}}\left(p_l^a\right)^2 \right)}{\hat{c}_l^h} =$

$\frac{\left(\frac{\bar{\eta}_l^{ha}}{\bar{\eta}_l^{hh}} + \frac{\bar{\eta}_l^{ah}}{\bar{\eta}_l^{hh}} \right)\left(1 - p_l^a\right)x_l^a + \left(1 - p_l^a\right)x_l^h + \frac{\bar{\eta}_l^{aa}}{\bar{\eta}_l^{hh}}\left(p_l^a\right)x_l^a}{\hat{c}_l^h} = \frac{\left(\frac{\bar{\eta}_l^{ha}}{\bar{\eta}_l^{hh}} + \frac{\bar{\eta}_l^{ah}}{\bar{\eta}_l^{hh}} \right)\left(1 - p_l^a\right)x_l^a + x_l^h - p_l^a x_l^h + \frac{\bar{\eta}_l^{aa}}{\bar{\eta}_l^{hh}}\left(p_l^a\right)x_l^a}{\hat{c}_l^h} =$

$\frac{\left(\frac{\bar{\eta}_l^{ha}}{\bar{\eta}_l^{hh}} + \frac{\bar{\eta}_l^{ah}}{\bar{\eta}_l^{hh}} \right)\left(1 - p_l^a\right)x_l^a + x_l^h - \frac{\bar{\eta}_l^{hh}}{\bar{\eta}_l^{hh}}\left(x_l^a - p_l^a x_l^a\right) + \frac{\bar{\eta}_l^{aa}}{\bar{\eta}_l^{hh}}\left(p_l^a\right)x_l^a}{\hat{c}_l^h} = \frac{x_l^h + \left(\frac{\bar{\eta}_l^{hh} + \bar{\eta}_l^{aa} - \bar{\eta}_l^{ha} - \bar{\eta}_l^{ah}}{\bar{\eta}_l^{hh}} p_l^a + \frac{\bar{\eta}_l^{ha} + \bar{\eta}_l^{ah} - \bar{\eta}_l^{hh}}{\bar{\eta}_l^{hh}} \right)x_l^a}{\hat{c}_l^h}$

we propose a new concept named human-driven vehicle equivalent (HVE) to denote the term $\left(\frac{\bar{\eta}_l^{hh}+\bar{\eta}_l^{aa}-\bar{\eta}_l^{ha}-\bar{\eta}_l^{ah}}{\bar{\eta}_l^{hh}} p_l^a + \frac{\bar{\eta}_l^{ha}+\bar{\eta}_l^{ah}-\bar{\eta}_l^{hh}}{\bar{\eta}_l^{hh}}\right)$. For each link $l \in L$, HVE_l is defined as

$$HVE_l = \frac{\bar{\eta}_l^{hh} + \bar{\eta}_l^{aa} - \bar{\eta}_l^{ha} - \bar{\eta}_l^{ah}}{\bar{\eta}_l^{hh}} p_l^a + \frac{\bar{\eta}_l^{ha} + \bar{\eta}_l^{ah} - \bar{\eta}_l^{hh}}{\bar{\eta}_l^{hh}} \qquad \forall l \in L \qquad (3\text{-}8)$$

Since $p_l^a \in [0, 1]$, the two extreme values of HVE_l is $\frac{\bar{\eta}_l^{ha}+\bar{\eta}_l^{ah}-\bar{\eta}_l^{hh}}{\bar{\eta}_l^{hh}}$ and $\frac{\bar{\eta}_l^{aa}}{\bar{\eta}_l^{hh}}$, respectively. It is reasonable to assume that $\bar{\eta}_l^{ah} \geq \bar{\eta}_l^{hh}$ since a HV following an AV is likely to at least maintain the same headway as when it follows a HV (Chen et al., 2017a). Therefore $\frac{\bar{\eta}_l^{ha}+\bar{\eta}_l^{ah}-\bar{\eta}_l^{hh}}{\bar{\eta}_l^{hh}} \geq 0$ and $HVE_l \geq 0$. Note that the concept of HVE was first introduced in another study of the authors (Liu and Song, 2019). The definition given in Equation (3-8) further generalizes the definition in Liu and Song (2019).

We further define a new concept named aggregate link flow in HVE, denoted as v_l. For each link $l \in L$, v_l is defined as

$$v_l = x_l^h + HVE_l x_l^a \qquad \forall l \in L \qquad (3\text{-}9)$$

Substituting equations (3-8) and (3-9) into equation (3-7) gives

$$t_l(v_l) = \hat{t}_l \left[1 + \alpha_l \left(\frac{v_l}{\hat{c}_l^h}\right)^{\beta_l}\right] \qquad \forall l \in L \qquad (3\text{-}10)$$

With a slight abuse of notation, we still use $t_l(v_l)$ to represent the functional relationship between link travel time and the aggregate link flow in HVE.

Based on the above derivations of link capacity and travel time functions, we can then formulate and analyze the user equilibrium problem in networks with mixed flows of HVs and AVs.

3.1.4 User equilibrium model

The flow distributions of both HVs and AVs can be described by the following multiclass user equilibrium model:

Equations (3-8)-(3-10)

$$\boldsymbol{\Delta x}^{w,m} = \boldsymbol{E}^{w} q^{w,m} \qquad \forall w \in W, m \in M \qquad (3\text{-}11)$$

$$x_l^m = \sum_{w \in W} x_l^{w,m} \qquad \forall l \in L \qquad (3\text{-}12)$$

$$x_l^{w,m} \geq 0 \qquad \forall w \in W, m \in M, (i,j) = \ l \in L \qquad (3\text{-}13)$$

$$\left(t_l(v_l) + \rho_i^{w,m} - \rho_j^{w,m}\right) x_l^{w,m} = 0 \qquad \forall w \in W, m \in M, (i,j) = \ l \in L \qquad (3\text{-}14)$$

$$t_l(v_l) + \rho_i^{w,m} - \rho_j^{w,m} \geq 0 \qquad \forall w \in W, m \in M, (i,j) = l \in L \qquad (3\text{-}15)$$

where $\boldsymbol{\Delta}$ is the node-link incidence matrix associated with the network;$\boldsymbol{x}^{w,m}$ is the vector of $\{\cdots, x_l^{w,m}, \cdots\}$; and $\boldsymbol{E}^{w}$ represents an "input-output" vector, which has exactly two non-zero components: one has the value 1 corresponding to the origin node $\mathrm{O}(w)$ and the other has the value -1 corresponding to the destination node $\mathrm{D}(w)$; $\rho_i^{w,m}$ is an auxiliary variable representing the node potentials.

In the above, equations (3-8)-(3-10) are definitional constraints; constraint (3-11) ensures flow balance between each O-D pair; constraint (3-12) aggregates link flows across all O-D pairs; constraint (3-13) makes sure the non-negativity of link flows; constraints (3-13)-(3-15) ensure that, for each O-D pair, the travel costs on all utilized

paths are the same and equal to $\rho_{D(w)}^{w,m} - \rho_{O(w)}^{w,m}$, and are less than or equal to those on unutilized paths.

3.1.5 Solution existence and uniqueness for the user equilibrium model

The following proposition establishes the solution existence of the user equilibrium model.

Proposition 3-3. The user equilibrium defined by equations (3-8)-(3-15) has at least one solution.

Proof. Let set $\Phi = \{(\boldsymbol{x}, \boldsymbol{v}) | \ \boldsymbol{x} \text{ and } \boldsymbol{v} \text{ satisfies constraints } (3-8)-(3-13)\}$ denote the feasible domain of $(\boldsymbol{x}, \boldsymbol{v})$. The user equilibrium conditions (3-8)-(3-15) are equivalent to finding $(\boldsymbol{x}^*, \boldsymbol{v}^*) \in \Phi$ that solves the following variational inequality (VI):

$$\sum_{m \in M} \sum_{l \in L} t_l(v_l^*)(x_l^m - x_l^{m*}) \geq 0, \forall (\boldsymbol{x}, \boldsymbol{v}) \in \Phi \tag{3-16}$$

The equivalence can be established by deriving the Karush-Kuhn-Tucker (KKT) conditions of the above VI and comparing them with the user equilibrium conditions. Since the demands of HVs and AVs are fixed and finite, all link flows must be bounded from above. Therefore, set Φ is compact and convex. Given that all the functions are continuous, the vatiational inequality problem (3-16) has at least one solution as per Theorem 3.1 of Harker and Pang (1990). □

The following proposition gives the sufficient conditions for the solution uniqueness of the aggregate link flow in HVE for the user equilibrium problem.

Proposition 3-4. If $\bar{\eta}_l^{hh} + \bar{\eta}_l^{aa} - \bar{\eta}_l^{ha} - \bar{\eta}_l^{ah} = 0, \forall l \in L$ and

$\exists\ a$ constant λ such that $\frac{\bar{\eta}_l^{aa}}{\bar{\eta}_l^{hh}} = \lambda, \forall l \in L$, then:

(a) The aggregate link flow in HVE, $\boldsymbol{v}$, for the user equilibrium problem defined by equations (3-8)-(3-15) is unique.

(b) For two travel demand vectors $(\overline{\boldsymbol{q}}^h, \overline{\boldsymbol{q}}^a)$ and $(\widetilde{\boldsymbol{q}}^h, \widetilde{\boldsymbol{q}}^a)$, if $\overline{\boldsymbol{q}}^h + \lambda\overline{\boldsymbol{q}}^a = \widetilde{\boldsymbol{q}}^h + \lambda\widetilde{\boldsymbol{q}}^a$, then the user equilibrium problems defined by equations (3-8)-(3-15) with these two demand vectors have identical solutions for the aggregate link flow in HVE.

Proof. If $\bar{\eta}_l^{hh} + \bar{\eta}_l^{aa} - \bar{\eta}_l^{ha} - \bar{\eta}_l^{ah} = 0, \forall l \in L$ and $\exists\ a$ constant λ such that $\frac{\bar{\eta}_l^{aa}}{\bar{\eta}_l^{hh}} = \lambda, \forall l \in L$, HVE_l defined in equations (3-8) is an identical constant for all links, i.e., $HVE_l = \frac{\bar{\eta}_l^{aa}}{\bar{\eta}_l^{hh}} = \lambda, \forall l \in L$. The user equilibrium conditions (3-8)-(3-15) are equivalent to finding $(\boldsymbol{x}^*, \boldsymbol{v}^*) \in \Phi$ that solves the following VI:

$$\sum_{w \in W} \sum_{l \in L} t_l(v_l^*)\left(x_l^{w,h} - x_l^{w,h*} + \lambda x_l^{w,a} - \lambda x_l^{w,a*}\right) \geq 0, \forall \boldsymbol{x} \in X \tag{3-17}$$

The equivalence can be established by deriving the Karush-Kuhn-Tucker (KKT) conditions of the above VI and comparing them with the user equilibrium conditions. Let set $V = \{\boldsymbol{v} |\ \boldsymbol{v}$ satisfies constraints $(3-8)-(3-13)\}$ denote the feasible domain of $\boldsymbol{v}$. By performing simple algebra, variational inequality (3-17) can be rewritten as

$$\sum_{l \in L} t_l(v_l^*)(v_l - v_l^*) \geq 0, \forall \boldsymbol{v} \in V \tag{3-18}$$

Because t_{ij} is continuous and strictly monotone with respect to v_l, $\boldsymbol{t}(\boldsymbol{v})$ is continuous and strictly monotone with respect to $\boldsymbol{v}$. In addition, V is compact and convex. Therefore, there exists a unique solution to the VI problem (3-18) as per Theorem 3.1 and Proposition 3.2 of Harker and Pang (1990). This completes the proof of the first part.

Constraint (3-11) can be specified for the two vehicle classes as follows:

$$\boldsymbol{\Delta x}^{w,h} = \boldsymbol{E}^w q^{w,h} \qquad \forall w \in W \qquad (3\text{-}19)$$

$$\boldsymbol{\Delta x}^{w,a} = \boldsymbol{E}^w q^{w,a} \qquad \forall w \in W \qquad (3\text{-}20)$$

By performing simple algebra, constraints (3-19) and (3-20) can deduce the following equation:

$$\boldsymbol{\Delta}(\boldsymbol{x}^{w,h} + \lambda \boldsymbol{x}^{w,a}) = \boldsymbol{E}^w (q^{w,h} + \lambda q^{w,a}) \qquad \forall w \in W \qquad (3\text{-}21)$$

Define an auxiliary variable v_{ij}^{rs} as follows:

$$v_l^w = x_l^{w,h} + \lambda x_l^{w,a} \qquad \forall w \in W, l \in L \qquad (3\text{-}22)$$

By definition, $\lambda > 0$. Equation (3-22) and constraint (3-13) then lead to the following non-negativity constraint for v_l^w:

$$v_l^w \geq 0 \qquad \forall w \in W, l \in L \qquad (3\text{-}23)$$

Substituting equation (3-22) into equation (3-21) gives

$$\boldsymbol{\Delta v}^w = \boldsymbol{E}^w (q^{w,h} + \lambda q^{w,a}) \qquad \forall w \in W \qquad (3\text{-}24)$$

Substituting equations (3-12) and (3-22) into equation (3-9) gives

$$v_l = \sum_{w \in W} v_l^w \qquad \forall l \in L \qquad (3\text{-}25)$$

Set $V = \{\boldsymbol{v}|\ \boldsymbol{v}$ satisfies constraints $(3-8)-(3-13)\}$ can then be reduced to $V = \{\boldsymbol{v}|\ \boldsymbol{v}$ satisfies constraints $(3-23)-(3-25)\}$. For two travel demand vectors $(\bar{\boldsymbol{q}}^h, \bar{\boldsymbol{q}}^a)$ and $(\tilde{\boldsymbol{q}}^h, \tilde{\boldsymbol{q}}^a)$, if $\bar{\boldsymbol{q}}^h + \lambda\bar{\boldsymbol{q}}^a = \tilde{\boldsymbol{q}}^h + \lambda\tilde{\boldsymbol{q}}^a$, the corresponding sets V and VI problems defined in (3-18) are identical, thus leading to identical solutions for the aggregate link flow in HVE. This finishes the proof of the second part. □

Remark 3-1. The uniqueness of $\boldsymbol{v}$ can further guarantee the uniqueness of travel time on each link and the equilibrium total travel time between each O-D pair. However, the link flow by class may not be unique even when the aggregate link flow in HVE is unique. A possible scenario for $\bar{\eta}_l^{hh} + \bar{\eta}_l^{aa} - \bar{\eta}_l^{ha} - \bar{\eta}_l^{ah} = 0, \forall l \in L$ is that $\bar{\eta}_l^{hh} = \bar{\eta}_l^{ah}$ and $\bar{\eta}_l^{aa} = \bar{\eta}_l^{ha}, \forall l \in L$, i.e., an HV follows the preceding vehicle (whether it is an HV or an AV) with identical time headway and an AV follows the preceding vehicle (whether it is an AV or an HV) with identical time headway. This scenario is adopted in both Levin and Boyles (2015) and Noruzoliaee et al. (2018). Moreover, the above two studies also assumed that $\bar{\eta}_l^{aa}$ and $\bar{\eta}_l^{hh}$ are link-independent constants. Under this assumption, $\frac{\bar{\eta}_l^{aa}}{\bar{\eta}_l^{hh}}$ is a link-independent constant, i.e., $\exists\ a$ constant λ such that $\frac{\bar{\eta}_l^{aa}}{\bar{\eta}_l^{hh}} = \lambda, \forall l \in L$.

Remark 3-2. Based on the second part of Proposition 3-4, we can always convert a travel demand vector $(\bar{\boldsymbol{q}}^h, \bar{\boldsymbol{q}}^a)$ into $(\tilde{\boldsymbol{q}}^h, \tilde{\boldsymbol{q}}^a)$, which satisfies $\tilde{\boldsymbol{q}}^h = \bar{\boldsymbol{q}}^h + \lambda\bar{\boldsymbol{q}}^a$ and $\tilde{\boldsymbol{q}}^a = 0$, without changing the solution of the aggregate link flow in HVE (consequently, the solution of link travel time and equilibrium O-D travel time also remain unchanged).

With $\tilde{\boldsymbol{q}}^a = 0$, the user equilibrium actually reduces to the conventional user equilibrium with only HV users. Note that this property has also been proved by Mehr and Horowitz (2019) in a different manner.

In more general scenarios, however, the user equilibrium problem may admit multiple solutions for the aggregate link flow in HVE, link travel time, and equilibrium O-D travel time. To see this non-uniqueness property, consider the network in Figure 3-2 with three links and one O-D pair (1, 3). The travel demands and the link parameters are given as follows:

(1) Travel demands: $q^{13,a} = 16000$ veh/h, $q^{13,h} = 4000$ veh/h.

(2) Free flow travel times: $\hat{t}_{12} = 5$ min, $\hat{t}_{23} = 5$ min, $\hat{t}_{13} = 10$ min.

(3) Number of lanes: $\iota_{12} = \iota_{23} = \iota_{13} = 2$.

(4) Calibration constants: $\alpha_l = 0.15, \beta_l = 4, \forall l \in \{(1,2),(2,3),(1,3)\}$.

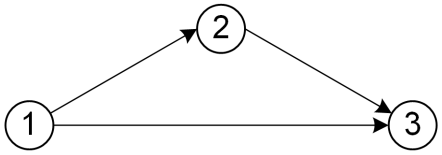

Figure 3-2. A toy network with one O-D pair and three links.

Scenario 1. First consider the scenario that an HV always follows the preceding vehicle (whether it is an HV or AV) with identical time headway of 1.8 seconds, an AV follows an HV with a time headway of 0.9 seconds, and an AV follows an AV with a time headway of 0.45 seconds, i.e., $\bar{\eta}_l^{hh} = \bar{\eta}_l^{ah} = 1.8$ seconds, $\bar{\eta}_l^{ha} = 0.9$ seconds and $\bar{\eta}_l^{aa} = 0.45$ seconds, $\forall l \in \{(1,2),(2,3),(1,3)\}$. The link capacities with pure HVs are $\hat{c}_l^h =$

$\frac{\iota_l}{\bar{\eta}_l^{hh}} = 4000$ veh/h, $\forall l \in \{(1,2),(2,3),(1,3)\}$ and the HVE_l defined in equation (3-8) becomes $HVE_l = -\frac{1}{4}p_l^a + \frac{1}{2}$. In this scenario, $\frac{\bar{\eta}_l^{aa}}{\bar{\eta}_l^{hh}} = \frac{1}{4}$ is a link-independent constant but $\bar{\eta}_l^{hh} + \bar{\eta}_l^{aa} - \bar{\eta}_l^{ha} - \bar{\eta}_l^{ah} \neq 0$. This scenario is possible because: (1) when following AVs, human drivers may keep identical safe distance as when they follow HVs, (2) with automated control, AVs may have reduced following distance than HVs when they follow HVs, (3) with vehicle communication and automated control, AVs can further reduce their following distance when they follow AVs, and (4) the three links may be homogeneous and both HVs and AVs adopt consistent time headways on them. Note that the link capacity is consistent with the base-condition value for a multilane highway segment with a 50-mi/h free flow speed in highway capacity manual (TRB, 2016).

As indicated in Table 3-1, two different sets of aggregate link flows in HVE both satisfy the user equilibrium conditions. The O-D equilibrium travel times associated with the two solutions are 11.50 and 12.20, respectively. The total system travel time of the solution 2 is 6.1% higher than that of the solution 1.

Table 3-1: Flow distributions and link travel times for the toy network in the first scenario

Link	AV flow (x_l^a)	HV flow (x_l^h)	Proportion of AV flow (p_l^a)	HV equivalent (HVE_l)	Aggregate flow in HVE (v_l)	Travel time (t_l)
Solution 1						
(1, 2)	16000	0	1/1	1/4	4000	5.75
(2, 3)	16000	0	1/1	1/4	4000	5.75
(1, 3)	0	4000	0/1	1/2	4000	11.50
Solution 2						
(1, 2)	8000	2000	4/5	3/10	4400	6.10
(2, 3)	8000	2000	4/5	3/10	4400	6.10
(1, 3)	8000	2000	4/5	3/10	4400	12.20

Scenario 2. Consider another scenario when $\bar{\eta}_l^{ha} = \bar{\eta}_l^{aa} = 0.45$ seconds, $\forall l \in \{(1,2),(2,3),(1,3)\}$, $\bar{\eta}_l^{hh} = \bar{\eta}_l^{ah} = 1.8$ seconds, $\forall l \in \{(1,2),(2,3)\}$, and $\bar{\eta}_{13}^{hh} = \bar{\eta}_{13}^{ah} = 1.5$ seconds. The link capacities with pure HVs are $\hat{c}_{12}^h = \hat{c}_{23}^h = 4000$ veh/h, $\hat{c}_{13}^h = 4800$ veh/h and the HVE_l values defined in equation (3-8) are $\text{HVE}_{12} = \text{HVE}_{23} = 1/4, \text{HVE}_{13} = 3/10$. In this scenario, $\bar{\eta}_l^{hh} + \bar{\eta}_l^{aa} - \bar{\eta}_l^{ha} - \bar{\eta}_l^{ah} = 0, \forall l \in L$ but $\frac{\bar{\eta}_l^{aa}}{\bar{\eta}_l^{hh}}$ is not a link-independent constant. This scenario is also possible because: (1) controlled by computers, AVs may adopt consistent time headways on different types of links; (2) the three links are not homogeneous and HVs may adopt different time headways on them. The link capacities of links (1, 2) and (2, 3) are consistent with the base-condition value for a multilane highway segment with a 50-mi/h free flow speed in the highway capacity manual (TRB, 2016). The link capacity of link (1, 3) is consistent with the base-condition value for a freeway segment with a 75-mi/h free flow speed in the highway capacity manual (TRB, 2016)

As shown in Table 3-2, two different sets of aggregate link flows in HVE both satisfy the user equilibrium conditions. The O-D equilibrium travel times associated with the two solutions are 11.06 and 11.50, respectively. The total system travel time of the solution 2 is 4.0% higher than that of the solution 1.

Table 3-2: Flow distributions and link travel times for the toy network in the second scenario

Link	AV flow (x_l^a)	HV flow (x_l^h)	HV equivalent (HVE_l)	Aggregate flow in HVE (v_l)	Travel time (t_l)
Solution 1					
(1, 2)	14666.67	0	1/4	3666.67	5.53

(2, 3)	14666.67	0	1/4	3666.67	5.53
(1, 3)	1333.33	4000	3/10	4400	11.06
Solution 2					
(1, 2)	0	4000	1/4	4000	5.75
(2, 3)	0	4000	1/4	4000	5.75
(1, 3)	16000	0	3/10	4800	11.50

The above two scenarios demonstrate that the uniqueness of aggregate link flow in HVE for the user equilibrium problem cannot be guaranteed if either of the two conditions in Proposition 3-4 (i.e., $\bar{\eta}_l^{hh} + \bar{\eta}_l^{aa} - \bar{\eta}_l^{ha} - \bar{\eta}_l^{ah} = 0, \forall l \in L$ and $\exists\ a$ constant λ such that $\frac{\bar{\eta}_l^{aa}}{\bar{\eta}_l^{hh}} = \lambda, \forall l \in L$) is not satisfied.

3.1.6 Solution algorithm

Based on the travel time function defined by equations (3-7) and (3-10), we derive partial derivatives $\frac{\partial t_l\left(x_l^h, x_l^a\right)}{\partial x_l^h}$ and $\frac{\partial t_l\left(x_l^h, x_l^a\right)}{\partial x_l^a}$ as follows:

$$\frac{\partial t_l\left(x_l^h, x_l^a\right)}{\partial x_l^h} = \frac{\hat{t}_l \alpha_l \beta_l}{\left(\hat{c}_l^h\right)^{\beta_l}} (v_l)^{\beta_l - 1} \frac{\bar{\eta}_l^{hh}\left(\left(x_l^h\right)^2 + 2x_l^h x_l^a\right) + \left(\bar{\eta}_l^{ha} + \bar{\eta}_l^{ah} - \bar{\eta}_l^{aa}\right)(x_l^a)^2}{\bar{\eta}_l^{hh}\left(x_l^h + x_l^a\right)^2}$$

$$\frac{\partial t_l\left(x_l^h, x_l^a\right)}{\partial x_l^a} = \frac{\hat{t}_l \alpha_l \beta_l}{\left(\hat{c}_l^h\right)^{\beta_l}} (v_l)^{\beta_l - 1} \frac{\bar{\eta}_l^{aa}\left((x_l^a)^2 + 2x_l^h x_l^a\right) + \left(\bar{\eta}_l^{ha} + \bar{\eta}_l^{ah} - \bar{\eta}_l^{hh}\right)\left(x_l^h\right)^2}{\bar{\eta}_l^{hh}\left(x_l^h + x_l^a\right)^2}$$

3.1.6.1 Diagonalization algorithm

Chen et al. (2017a) believe it is reasonable to assume that $\bar{\eta}_l^{ha} \geq \bar{\eta}_l^{aa}$ since an AV following an HV is likely to at least maintain the same headway as when it follows an HV, and that $\bar{\eta}_l^{ah} \geq \bar{\eta}_l^{hh}$ since a HV following an AV is likely to at least maintain the same headway as when it follows a HV. Under this assumption, we have $\left(\bar{\eta}_l^{ha} + \bar{\eta}_l^{ah} -\right.$

$\bar{\eta}_l^{aa}\big) \geq 0$ and $\big(\bar{\eta}_l^{ha} + \bar{\eta}_l^{ah} - \bar{\eta}_l^{hh}\big) \geq 0$. It is then straightforward to verify that $\frac{\partial t_l\left(x_l^h, x_l^a\right)}{\partial x_l^h} > 0$ and $\frac{\partial t_l\left(x_l^h, x_l^a\right)}{\partial x_l^a} > 0$. Note that $\frac{\partial t_l\left(x_l^h, x_l^a\right)}{\partial x_l^h} \neq \frac{\partial t_l\left(x_l^h, x_l^a\right)}{\partial x_l^a}$ in general.

Due to the asymmetric impact on link travel time between HVs and AVs, the multi-class user equilibrium problem cannot be readily formulated as a convex optimization problem. The diagonalization algorithm can be used to solve the multi-class user equilibrium problem. Note that the derived results in the above that $\frac{\partial t_l\left(x_l^h, x_l^a\right)}{\partial x_l^h} > 0$ and $\frac{\partial t_l\left(x_l^h, x_l^a\right)}{\partial x_l^a} > 0$ ensure that the diagonalized subproblems are convex. In addition, the streamlined version of the diagonalization algorithm suggested by Sheffi (1985), in which diagonalized subproblems are solved by using only one iteration of the convex combinations algorithm, can be adopted to improve the efficiency. Following the presentation in Sheffi (1985), the algorithm is given as follows:

Step 0: *Initialization.* Set $k = 0$. Find a feasible flow pattern vector $\boldsymbol{x^k}$.

Step 1: *Travel-time update.* Set $t_l^k = t_l\left(x_l^{h,k}, x_l^{a,k}\right), \forall l \in L$.

Step 2: *Direction finding.* Assign the O-D demands, $\{q^{w,m}\}$, to the network using the all-or-nothing approach based on $\left\{t_l^k\right\}$. This yields a flow pattern $\left\{y_l^{m,k}\right\}$.

Step 3: *Move-size determination.* Find a scalar, θ^k, which solves the following program:

$$\min_{\theta} \sum_{l \in L} \left(\int_0^{x_l^{h,k} + \theta\left(y_l^{h,k} - x_l^{h,k}\right)} t_l\left(\omega, x_l^{a,k}\right) d\omega + \int_0^{x_l^{a,k} + \theta\left(y_l^{a,k} - x_l^{a,k}\right)} t_l\left(x_l^{h,k}, \omega\right) d\omega \right)$$

s.t.

$$0 \le \theta \le 1$$

Step 4: *Updating.* Set $x_l^{m,k+1} = x_l^{m,k} + \theta^k\left(y_l^{m,k} - x_l^{m,k}\right), \forall m \in M, l \in L.$

Step 5: *Convergence test.* If $x_l^{m,k+1} \cong x_l^{m,k}, \forall m \in M, l \in L$, stop and the solution is $\boldsymbol{x^{k+1}}$. Otherwise, set $k = k + 1$ and go to step 1.

At Step 3, the objective function of the minimization program is convex because $\frac{\partial t_l\left(x_l^h, x_l^a\right)}{\partial x_l^h} > 0$ and $\frac{\partial t_l\left(x_l^h, x_l^a\right)}{\partial x_l^a} > 0$.

3.1.6.2 A gap function approach

Different from Chen et al. (2017a), Ghiasi et al. (2017) didn't assume $\bar{\eta}_l^{ha} \ge \bar{\eta}_l^{aa}$ or $\bar{\eta}_l^{ah} \ge \bar{\eta}_l^{hh}$. They thought AV technologies are yet to be fully developed and thus may have quite some uncertainties. Ghiasi et al. (2017) pointed out that, if future AV technologies are conservative, headways between vehicles will increase rather than decrease.

In general cases, if $\bar{\eta}_l^{ha} \ge \bar{\eta}_l^{aa}$ and $\bar{\eta}_l^{ah} \ge \bar{\eta}_l^{hh}$ don't hold simultaneously, the above diagonalization algorithm is no longer usable because the subproblem at Step 3 may not be convex. We thus adopt a more general algorithm to solve the multi-class user equilibrium problem. According to the proof process of Proposition 3-3, the user equilibrium conditions (3-8)-(3-15) are equivalent to finding $(\boldsymbol{x}^*, \boldsymbol{v}^*) \in \Phi$ that solves the following variational inequality (VI):

UE-VI:

$$\sum_{m\in M}\sum_{l\in L} t_l(v_l^*)(x_l^m - x_l^{m*}) \geq 0, \forall(\boldsymbol{x},\boldsymbol{v}) \in \Phi$$

To solve the UE-VI, we apply the technique developed by Aghassi et al. (2006) using duality to reformulate the UE-VI as the following nonlinear optimization problem:

UE-NLP:

$$\min_{(\boldsymbol{v},\boldsymbol{x},\boldsymbol{\rho})} \sum_{m\in M}\sum_{l\in L} t_l(v_l)x_l^m - \sum_{m\in M}\sum_{w\in W} q^{w,m}\left(\rho_{D(w)}^{w,m} - \rho_{O(w)}^{w,m}\right)$$

s.t.

$$-\rho_i^{w,m} + \rho_j^{w,m} \leq t_l(v_l) \qquad \forall(i,j) = l \in L, w \in W, m \in M$$
$$(\boldsymbol{v},\boldsymbol{x}) \in \Phi$$

In solving the above optimization problem, if the optimal value of the objective function is zero, then one part of the optimal solution, $(\boldsymbol{v},\boldsymbol{x})$, would be the solution to the UE-VI problem. Because the UE-NLP model is a regular nonlinear program, it can be solved using commercial nonlinear solvers such as CONOPT (Drud, 1994). This gap function approach has been widely adopted in the literature in solving VI formulations of UE problems (see, e.g., Chen et al., 2017b; Liu and Song, 2018a; Liu and Song, 2018b).

3.1.7 Quantifying network delay under best and worst cases

As discussed in Section 3.1.5, the user equilibrium with mixed autonomy may have non-unique flow patterns and network delays. This non-uniqueness property makes it difficult to predict congestion pattern in a network with mixed autonomy. In practice, to evaluate the performance of a network, decision makers may want to know the network

delay under best and worst cases. The following two models are proposed to find the best- and worst-case flow patterns for a network with mixed autonomy.

BC/WC-UE

$$\min/\max_{\boldsymbol{x},\boldsymbol{v},\boldsymbol{\rho}} \sum_{m\in M}\sum_{l\in L} t_l(v_l)x_l^m$$

s.t. (3-8)-(3-15)

In the above, constraints (3-8)-(3-15) are the user equilibrium conditions. The objective function of BC-UE is to minimize the total network delay while the objective function of WC-UE is to maximize the total network delay. The models BC/WC-UE belong to mathematical program with complementarity constraints (MPCC), which is difficult to solve. In this paper, we adopt the algorithm proposed by Lawphongpanich and Yin (2010) using manifold suboptimization to solve them. The algorithm guarantees convergence to a strongly stationary solution within a finite number of iterations.

3.1.8 Numerical studies

In this section, numerical studies are conducted to show the potential impact of AVs on the congestion patterns of a network with mixed autonomy.

Numerical studies in this section are based on a toy network, as shown in Figure 3-3, with four nodes, five links, and one O-D pair. The free flow travel time on each link is given by: $\hat{t}_{12} = 5$ min, $\hat{t}_{13} = 20$ min, $\hat{t}_{23} = 5$ min, $\hat{t}_{24} = 20$ min, $\hat{t}_{34} = 5$ min. The number of lanes on each link is set to $\iota_l = 2, \forall l \in \{(1,2),(1,3),(2,3),(2,4),(3,4)\}$. The calibration constants are given by $\alpha_l = 0.15, \beta_l = 4, \forall l \in \{(1,2),(1,3),(2,3),(2,4),(3,4)\}$. Note that the parameter values are for illustration

purposes only. In the following, three different scenarios are considered. The first two scenarios assume homogeneous links. The third scenario considers heterogeneity among links. Other link characteristics are specified independently for each of the following scenarios.

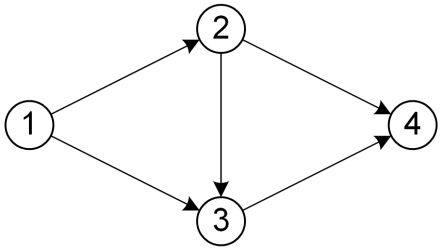

Figure 3-3. A toy network with one O-D pair and five links.

Scenario 1. The total travel demand of HVs and AVs is set to 8000 veh/h, i.e., $q^{14,a} + q^{14,h} = 8000$ veh/h. Set headway $\bar{\eta}_l^{hh} = \bar{\eta}_l^{ah} = 1.8\ s, \forall l \in \{(1,2),(1,3),(2,3),(2,4),(3,4)\}$, consequently link capacities with pure HVs are $\hat{c}_l^h = \frac{\iota_l}{\bar{\eta}_l^{hh}} = 4000\ veh/h, \forall l \in \{(1,2),(1,3),(2,3),(2,4),(3,4)\}$. Suppose $\bar{\eta}_l^{ha} = \bar{\eta}_l^{aa} = \bar{\eta}^{aa}, \forall l \in \{(1,2),(1,3),(2,3),(2,4),(3,4)\}$, where $\bar{\eta}^{aa}$ is a link-independent constant. The HVE defined in Equation (3-8) is then given by $HVE_l = \frac{\bar{\eta}^{aa}}{1.8\ s}$, which is a link-independent constant. As discussed in Remark 1, the user equilibrium problem will have unique solution for total system travel time. To investigate the impact of the headway setting of AVs on system travel time, seven groups of the headway $\bar{\eta}^{aa}$ are considered, with $\bar{\eta}^{aa}$ ranging from 1.8 s to 0.6 s with a step size of $-0.2\ s$. To investigate the impact of AV penetration rate (denoted by PR) on total system delay, 11 groups of AV penetration rate PR are considered with PR ranging from 0.0 to 1.0 with a step size of 0.1.

Figure 3-4 shows the total equilibrium system travel time with different combinations of $\bar{\eta}^{aa}$ and PR. Several observations can be made from Figure 3-4. First, when $\bar{\eta}^{aa} = 1.8\ s$, the total system travel time remain unchanged when the AV penetration rate increase from 0.0 to 1.0. This result is expected because when $\bar{\eta}^{aa} = 1.8\ s$, there is no behavioral difference between AVs and HVs in mixed traffic. Second, when AV penetration rate $\text{PR} = 0.0$, the total system travel time remain unchanged when $\bar{\eta}^{aa}$ decreases from 1.8 s to 0.6 s. This result is self-explanatory. Third, for a given headway value less than 1.8 s, the total system travel time decreases with the increase of AV penetration rate. Last, for a given positive AV penetrative rate, the total system travel time decreases with the decrease of AV headway value $\bar{\eta}^{aa}$. With these two observations, one straightforward question is whether the increase of AV penetration rate and the decrease of AV headway value $\bar{\eta}^{aa}$ can increase the total system travel time. For this scenario, the answer is no. As discussed in Remark 2, we can convert the mixed travel demand with $q^{14,a} = 8000 \times \text{PR}\ (\text{veh/h})$ and $q^{14,h} = 8000 \times (1 - \text{PR})\ (\text{veh/h})$ into a pure HV demand of $8000 \times \text{PR} \times \frac{\bar{\eta}^{aa}}{1.8\ s} + 8000 \times (1 - \text{PR})\ (\text{veh/h})$, without charging the solution of the equilibrium O-D travel time. When $\text{PR} > 0$ and $\frac{\bar{\eta}^{aa}}{1.8\ s} < 1$, the converted HV demand $8000 \times \text{PR} \times \frac{\bar{\eta}^{aa}}{1.8\ s} + 8000 \times (1 - \text{PR}) = 8000 \times \left(1 + \text{PR} \times \left(\frac{\bar{\eta}^{aa}}{1.8\ s} - 1\right)\right)\ (\text{veh/h})$ decreases with the increase of PR (given other parameters fixed), and decreases with the decrease of $\bar{\eta}^{aa}$ (given other parameters fixed). According to the Theorem 3 in Hall (1978), the equilibrium travel time of an O-D pair is a non-decreasing function of the travel demand of the O-D pair, when the travel demands of all

other O-D pairs are held constant. For the current scenario with only one O-D pair, the O-D equilibrium travel time must be non-increasing with the decrease of the converted HV demand. Therefore, given fixed total travel demand for the one O-D pair, the total system travel time must be non-increasing with the increase of AV penetration rate and the decrease of AV headway value $\bar{\eta}^{aa}$. This conclusion can be extended to an arbitrary network with a single O-D pair and with the solution uniqueness conditions given in Proposition 3-4 holding. Note that one part of the conclusion has also been discovered and proved by Mehr and Horowitz (2019).

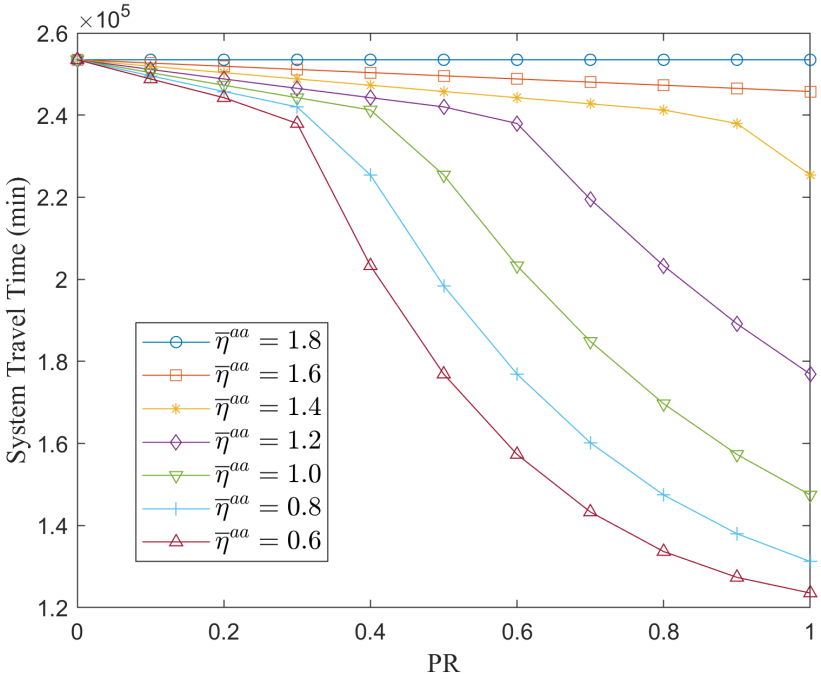

Figure 3-4. System travel times for Scenario 1.

Scenario 2. The total travel demand of HVs and AVs is set to 8000 veh/h, i.e., $q^{14,a} + q^{14,h} = 8000$ veh/h. Set headway $\bar{\eta}_l^{ha} = \bar{\eta}_l^{aa} = 1.5\ s, \forall l \in \{(1,2),(1,3),(2,3),(2,4),(3,4)\}$; $\bar{\eta}_l^{hh} = \bar{\eta}_l^{ah} = 1.5\ s, \forall l \in \{(1,2),(1,3),(2,4),(3,4)\}$; $\bar{\eta}_{23}^{hh} = \bar{\eta}_{23}^{ah} = 1.8$ s. The link capacities with pure HVs are

$\hat{c}_l^h = \frac{\iota_l}{\bar{\eta}_l^{hh}} = 4800\ veh/h, \forall l \in \{(1,2),(1,3),(2,4),(3,4)\}$ and $\hat{c}_{23}^h = 4000$ veh/h. The HVE_l values defined in equation (3-8) are $HVE_l = 1, \forall l \in \{(1,2),(1,3),(2,4),(3,4)\}$ and $\text{HVE}_{23} = 5/6$. To investigate the impact of AV penetration rate (denoted by PR) on total system delay, 11 groups of AV penetration rate PR are considered with PR ranging from 0.0 to 1.0 with a step size of 0.1.

Figure 3-5 displays the total system travel times of best- and worst-case UE (denoted as BC-UE and WC-UE, respectively) flow distributions with AV penetration rate PR varying from 0 to 1.0. One can observe that when $\text{PR} = 0$ or $\text{PR} = 1$, there is no difference between the best- and worst-case total system travel time. This result is expected because the UE link flow solution is unique when traffic flows in the network are pure HVs (when $\text{PR} = 0$) or pure AVs (when $\text{PR} = 1$). For $0 < \text{PR} < 1$, the best-case UE always has smaller total system travel time than the worst-case UE. Moreover, the system travel times of both best- and worst-case UE flow distributions increase with the increase of the AV penetration rate PR. This result might be counter intuitive as people expect that the adoption of AVs will reduce the system delay. However, the results of this scenario show that the market penetration increase of AVs might actually increase the system delay. To investigate the reason for this counter-intuitive result, we further compare the UE solutions between the case with $\text{PR} = 0$ and the case with $\text{PR} = 1$ in Table 3-3. Note that the link capacity in the fourth column is calculated based on Equation (3-5). Several observations can be made from Table 3-3. First, compared with the case with $\text{PR} = 0$, the case with $\text{PR} = 1$ has increased link capacity on link (2, 3) (i.e., from 4000 veh/h to 4800 veh/h). Second, the link capacities for all other links, i.e.,

links (1, 2), (1, 3), (2, 4), and (3, 4), do not change when PR is changed from 0 to 1. These two observations remind us that the tested scenario is actually a special instance of the classical Braess' Paradox (Braess et al., 2005), where an extension of the road network may lead to increased travel times in unfavorable situations. Therefore, although the adoption of AVs increases the capacity of link (2, 3), this capacity increase leads to increased system travel time due to the presence of Braess' Paradox. We note that the above paradoxical fact has also been discussed in Mehr and Horowitz (2019).

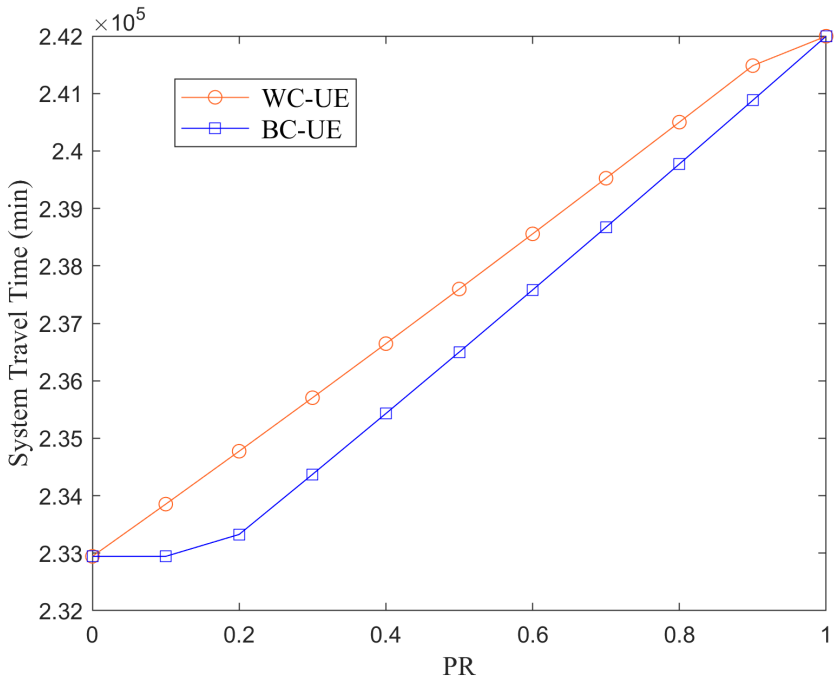

Figure 3-5. System travel times for Scenario 2.

Table 3-3: UE solutions for Scenario 2 with PR = 0 and PR = 1

Link	AV flow x_l^a (veh/h)	HV flow x_l^h (veh/h)	Link Capacity c_l (veh/h)	Travel time t_l (min)
PR=0				
(1, 2)	0	7347.2	4800	9.117
(1, 3)	0	652.8	4800	20.001
(2, 3)	0	6694.4	**4000**	10.884
(2, 4)	0	652.8	4800	20.001
(3, 4)	0	7347.2	4800	9.117

PR=1				
(1, 2)	7807.4	0	4800	10.250
(2, 3)	192.6	0	4800	20.000
(2, 3)	7614.8	0	**4800**	9.750
(2, 4)	192.6	0	4800	20.000
(3, 4)	7807.4	0	4800	10.250

Scenario 3. The total travel demand of HVs and AVs is set to 24000 veh/h, i.e., $q^{14,a} + q^{14,h} = 24000$ veh/h. Set headway $\bar{\eta}_l^{hh} = \bar{\eta}_l^{ah} = \bar{\eta}_l^{ha} = 1.8\ s,\ \bar{\eta}_l^{aa} = 0.6\ s, \forall l \in \{(1,2),(1,3),(2,3),(2,4),(3,4)\}$, consequently link capacity $\hat{c}_l^h = \frac{\iota_l}{\bar{\eta}_l^{hh}} = 4000\ veh/h, \forall l \in \{(1,2),(1,3),(2,3),(2,4),(3,4)\}$. The HVE defined in Equation (3-8) is then given by $HVE_l = -\frac{2}{3}p_l^a + 1$, which is a function of the proportion of AV flow on a link. To investigate the impact of AV penetration rate (denoted by PR) on total system delay, 11 groups of AV penetration rate PR are considered with PR ranging from 0.0 to 1.0 with a step size of 0.1.

Table 3-4 compares the system optimal (SO), best- and worst-case UE flow distributions with AV penetration rate PR $= 0.7$. Note that the flows shown in the table are aggregate link flows in HVE. Figure 3-6 displays the total system travel times of SO, best- and worst-case UE (denoted as BC-UE and WC-UE, respectively) flow distributions, as well as the relative system travel time difference between best- and worst-case UE flow distributions with AV penetration rate PR varying from 0 to 1.0. The relative difference is calculated by dividing the system travel time difference between best- and worst-case UE flow distributions by the best-case system travel time. One can observe that the system travel times of SO, best- and worst-case UE flow distributions all decrease with the increase of the AV penetration rate PR. When $PR = 0$ or $PR = 1$, the

UE flow distribution in HVE is unique and there is no difference between the best- and worst-case performances. This result is expected because traffic flows in the network are pure HVs when $PR = 0$ and pure AVs when $PR = 1$. Note that the total system travel time of SO is less than that of best- and worst-case UE when $PR = 0$, although the marginal difference is almost invisible in Figure 3-6. When $PR = 0$, the total system travel time of SO is 3,211,474 min and the total system travel times of best- and worst-case UE are both 3,219,585 min. For PR between 0 and 1, the absolute and relative difference between the best- and worst-case performances increases initially as PR increase from 0 to 0.6, and then decreases as PR increases from 0.6 to 1. The maximum relative difference is 37.5% and is reached when $PR = 0.6$. The system travel time associated with the SO flow distribution is always the minimum and it provides a valid lower bound for the best-case UE performance.

This numerical example reveals the difficulty of designing and evaluating improving strategies to highway networks with mixed HV and AV flows as the resulting performances are likely to be uncertain.

Table 3-4: Flow distributions for Scenario 3 with PR = 0.7

Link	WC-UE	BC-UE	SO
(1, 2)	9673.9	9518.2	8397.3
(1, 3)	4775.3	4646.5	7316.6
(2, 3)	3726.5	4338.5	2283.4
(2, 4)	5946.7	4703.7	4800.0
(3, 4)	10395.9	9545.2	9600.0

3.2 System optimum and first-best pricing

The system optimal flow distribution will minimize the total system travel disutility, which can be measured in terms of either time or monetary units (Yang and

Huang, 2004). It is well known that the marginal-cost link toll evaluated at the system optimum link flow can support a system optimum (SO) as a user equilibrium (UE) flow pattern (Yang and Huang, 2004; Yang and Huang, 2005). In this section, we first provide tolled user equilibrium conditions, we then investigate the system optimum and first-best pricing problems for networks with mixed flows of HVs and AVs.

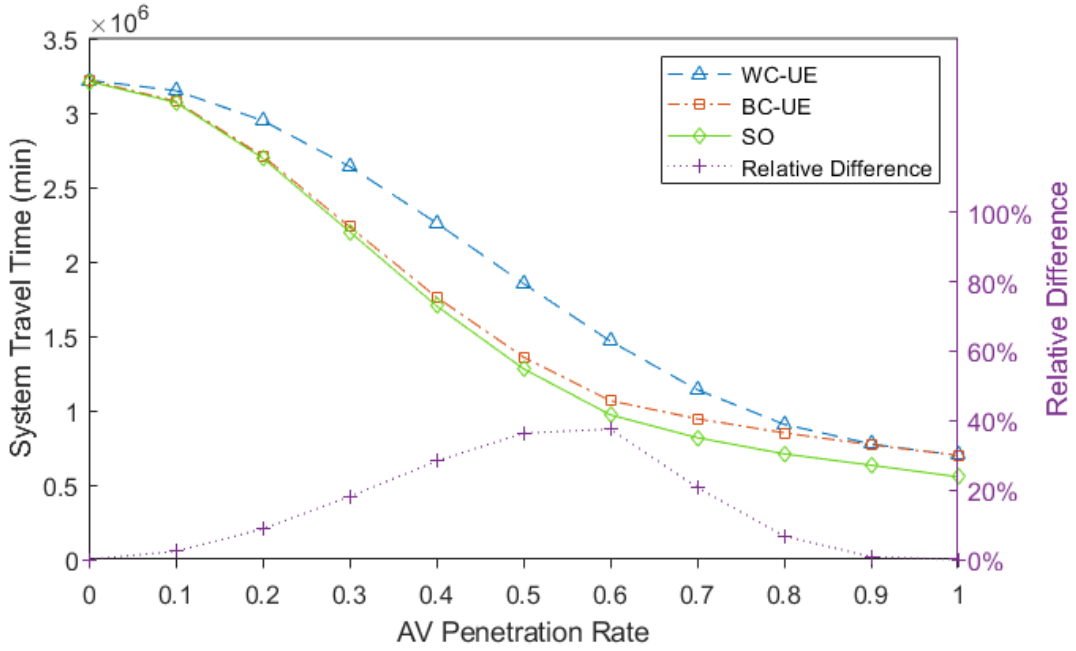

Figure 3-6. Comparison of system performances for Scenario 3.

3.2.1 Tolled user equilibrium flow distribution

Let τ_l^m denote the toll on link $l \in L$ for class $m \in M$ vehicles. Let VOT^m represent the value of time (VOT) of for users of class $m \in M$ vehicles. When tolls are present, the user equilibrium flow distributions of both HVs and AVs can be described by the following conditions:

Equations (3-8)-(3-13)

$$\left(t_l(v_l) + \frac{\tau_l^m}{VOT^m} + \rho_i^{w,m} - \rho_j^{w,m}\right) x_l^{w,m} = 0 \quad \forall w \in W, m \in M, (i,j) = l \in L \quad (3\text{-}26)$$

$$t_l(v_l) + \frac{\tau_l^m}{VOT^m} + \rho_i^{w,m} - \rho_j^{w,m} \geq 0 \quad \forall w \in W, m \in M, (i,j) = l \in L \quad (3\text{-}27)$$

where. $t_l(v_l) + \frac{\tau_l^m}{VOT^m}$ is the generalized travel cost (in time unit) on link $l \in L$ for users of class $m \in M$ vehicles. The above time-based user equilibrium conditions can be equivalently formulated as user equilibrium conditions on the basis of generalized travel cost in monetary units as per Theorem 2.3 of Yang and Huang (2005). Specifically, multiplying both sides of the equilibrium conditions (3-26) and (3-27) by VOT^m and letting $\hat{\rho}_i^{w,m} = \text{VOT}^m \rho_i^{w,m}, \forall w \in W, m \in M, i \in N$, we have

$$\left(VOT^m t_l(v_l) + \tau_l^m + \hat{\rho}_i^{w,m} - \hat{\rho}_j^{w,m}\right) x_l^{w,m} = 0 \quad \forall w \in W, m \in M, (i,j) = l \in L \quad (3\text{-}28)$$

$$VOT^m t_l(v_l) + \tau_l^m + \hat{\rho}_i^{w,m} - \hat{\rho}_j^{w,m} \geq 0 \quad \forall w \in W, m \in M, (i,j) = l \in L \quad (3\text{-}29)$$

where $VOT^m t_l(v_l) + \tau_l^m$ is the generalized travel cost (in monetary unit) on link $l \in L$ for users of class $m \in M$ vehicles. Clearly, equations (3-8)-(3-13), (3-28) and (3-29) are the tolled user equilibrium conditions on the basis of generalized travel cost in monetary units.

When $\tau_l^m = 0, \forall m \in M, l \in L$, the tolled user equilibrium conditions reduce to the user equilibrium conditions (3-8)-(3-15), which involves no tolls. The following proposition extends Proposition 3-4 and gives the sufficient conditions for the solution uniqueness of the aggregate link flow in HVE for the tolled user equilibrium problem.

Proposition 3-5. If $\bar{\eta}_l^{hh} + \bar{\eta}_l^{aa} - \bar{\eta}_l^{ha} - \bar{\eta}_l^{ah} = 0, \forall l \in L$ and $\exists\ a$ constant λ such that $\frac{\bar{\eta}_l^{aa}}{\bar{\eta}_l^{hh}} = \lambda, \forall l \in L$, then the aggregate link flow in HVE, $\boldsymbol{v}$, for the tolled user equilibrium problem defined by equations (3-8)-(3-13), (3-26) and (3-27) is unique.

Proof. If $\bar{\eta}_l^{hh} + \bar{\eta}_l^{aa} - \bar{\eta}_l^{ha} - \bar{\eta}_l^{ah} = 0, \forall l \in L$ and $\exists\ a$ constant λ such that $\frac{\bar{\eta}_l^{aa}}{\bar{\eta}_l^{hh}} = \lambda, \forall l \in L$, HVE_l defined in equations (3-8) is an identical constant for all links, i.e., $HVE_l = \frac{\bar{\eta}_l^{aa}}{\bar{\eta}_l^{hh}} = \lambda, \forall l \in L$. The tolled user equilibrium conditions (3-8)-(3-13)), (3-26) and (3-27) are equivalent to finding $(\boldsymbol{x}^*, \boldsymbol{v}^*) \in \Phi$ that solves the following VI:

$$\sum_{w \in W} \sum_{l \in L} \left\{ \left(t_l(v_l^*) + \frac{\tau_l^h}{VOT^h} \right) \left(x_l^{w,h} - x_l^{w,h*} \right) + \left(t_l(v_l^*) + \frac{\tau_l^a}{VOT^a} \right) \left(\lambda x_l^{w,a} - \lambda x_l^{w,a*} \right) \right\} \geq 0, \forall \boldsymbol{x} \in X$$

The equivalence can be established by deriving the Karush-Kuhn-Tucker (KKT) conditions of the above VI and comparing them with the user equilibrium conditions.

Suppose that $(\boldsymbol{v}^*, \boldsymbol{x}^*)$ and $(\boldsymbol{v}^\dagger, \boldsymbol{x}^\dagger)$ are two solutions of the above VI, then

$$\sum_{w \in W} \sum_{l \in L} \left\{ \left(t_l(v_l^*) + \frac{\tau_l^h}{VOT^h} \right) \left(x_l^{w,h\dagger} - x_l^{w,h*} \right) + \left(t_l(v_l^*) + \frac{\tau_l^a}{VOT^a} \right) \left(\lambda x_l^{w,a\dagger} - \lambda x_l^{w,a*} \right) \right\} \geq 0$$

$$\sum_{w \in W} \sum_{l \in L} \left\{ \left(t_l(v_l^\dagger) + \frac{\tau_l^h}{VOT^h} \right) \left(x_l^{w,h*} - x_l^{w,h\dagger} \right) + \left(t_l(v_l^\dagger) + \frac{\tau_l^a}{VOT^a} \right) \left(\lambda x_l^{w,a*} - \lambda x_l^{w,a\dagger} \right) \right\} \geq 0$$

Summing up both sides of the above two inequalities and performing simple algebra gives

$$\sum_{w\in W}\sum_{l\in L}\left(t_l\left(v_l^{\dagger}\right)-t_l\left(v_l^{*}\right)\right)\left(x_l^{w,h\dagger}+\lambda x_l^{w,a\dagger}-x_l^{w,h*}-\lambda x_l^{w,a*}\right)\le 0$$

With $v_l = x_l^h + HVE_l x_l^a$, $\forall l \in L$, the above inequality can be rewritten as

$$\sum_{w\in W}\sum_{l\in L}\left(t_l\left(v_l^{\dagger}\right)-t_l\left(v_l^{*}\right)\right)\left(v_l^{\dagger}-v_l^{*}\right)\le 0$$

Because $t_l(v_l)$ is a strictly increasing function of v_l, the above inequality implies that $v_l^{\dagger} = v_l^{*}$, or v_l^{*} is unique. □

Again, the uniqueness of $\boldsymbol{v}$ can further guarantee the uniqueness of travel time on each link and the equilibrium total travel time between each O-D pair. However, the link flow by class may not be unique even when the aggregate link flow in HVE is unique. In more general scenarios, however, the tolled user equilibrium problem may admit multiple solutions for the aggregate link flow in HVE, link travel time, and equilibrium O-D travel time.

3.2.2 System optimum in time units and pricing for user equilibrium

The system optimum in time units can be formulated as the following minimization program:

SO-Time:

$$\min_{\boldsymbol{x},\boldsymbol{v}} \sum_{m\in M}\sum_{l\in L} t_l(v_l)x_l^m$$

s.t. (3-8)-(3-13)

In the above, the objective is to minimize the total system travel time. Constraints (3-8)-(3-13) are flow conservation constraints ensuring that all O-D travel demands are assigned to the network.

The following proposition establishes the sufficient conditions for the solution uniqueness of the aggregate link flow in HVE for the SO-Time problem.

Proposition 3-6. If $\bar{\eta}_l^{hh} + \bar{\eta}_l^{aa} - \bar{\eta}_l^{ha} - \bar{\eta}_l^{ah} = 0, \forall l \in L$ and $\frac{\bar{\eta}_l^{aa}}{\bar{\eta}_l^{hh}} = 1, \forall l \in L$, then the solution of the aggregate link flow in HVE, $\boldsymbol{v}$, for the SO-Time problem is unique.

Proof. If $\bar{\eta}_l^{hh} + \bar{\eta}_l^{aa} - \bar{\eta}_l^{ha} - \bar{\eta}_l^{ah} = 0, \forall l \in L$ and $\frac{\bar{\eta}_l^{aa}}{\bar{\eta}_l^{hh}} = 1, \forall l \in L$, HVE_l defined in equations (3-8) is constant 1 for all links, i.e., $HVE_l = 1, \forall l \in L$. With $v_l = x_l^h + HVE_l x_l^a = x_l^h + x_l^a, \forall l \in L$, the objective function of SO-Time can then be rewritten as $\sum_{l\in L} t_l(v_l)v_l$, which is convex in v_l. Therefore, the solution of the aggregate link flow in HVE, $\boldsymbol{v}$, for the SO-Time problem is unique. □

Note that the uniqueness of $\boldsymbol{v}$ can further guarantee the uniqueness of travel time on each link and the total system travel time (i.e., the objective function value of SO-Time). However, the link flow by class may not be unique even when the aggregate link flow in HVE is unique. A possible scenario for $\bar{\eta}_l^{hh} + \bar{\eta}_l^{aa} - \bar{\eta}_l^{ha} - \bar{\eta}_l^{ah} = 0, \forall l \in L$ and

$\frac{\bar{\eta}_l^{aa}}{\bar{\eta}_l^{hh}} = 1, \forall l \in L$ is that $\bar{\eta}_l^{hh} = \bar{\eta}_l^{ah} = \bar{\eta}_l^{aa} = \bar{\eta}_l^{ha}, \forall l \in L$, i.e., HVs and AVs have identical mean time headways when following other vehicles (whether they are HVs or AVs). In more general scenarios, however, the SO-Time problem may have multiple local minima because its objective function is not necessarily convex in x_{ij}^m. It is thus important to identify the global minimum targeted for meaningful pricing.

For SO-Time, its first-order optimality conditions at an optimum $(\bar{\boldsymbol{x}}, \bar{\boldsymbol{v}})$ are Constraints (3-8)-(3-13) and

$$\bar{x}_l^m \left(t_l(\bar{v}_l) + \left(\bar{x}_l^h + \bar{x}_l^a\right) \frac{\partial t_l(\bar{v}_l)}{\partial x_l^m} + \rho_i^{w,m} - \rho_j^{w,m} \right) = 0 \qquad \forall w \in W, m \in M, (i,j) = l \in L \tag{3-30}$$

$$t_l(\bar{v}_l) + \left(\bar{x}_l^h + \bar{x}_l^a\right) \frac{\partial t_l(\bar{v}_l)}{\partial x_l^m} + \rho_i^{w,m} - \rho_j^{w,m} \geq 0 \qquad \forall w \in W, m \in M, (i,j) = l \in L \tag{3-31}$$

Clearly, the optimality conditions (3-30) and (3-31) for the SO-Time can be regarded as the time-based user equilibrium conditions. The requirement for such an equilibrium is that each user should face a marginal social travel time consisting of an experienced travel time and a class-specific travel time externality when using each link in the network.

If $\bar{\eta}_l^{hh} + \bar{\eta}_l^{aa} - \bar{\eta}_l^{ha} - \bar{\eta}_l^{ah} = 0, \forall l \in L$ and $\frac{\bar{\eta}_l^{aa}}{\bar{\eta}_l^{hh}} = 1, \forall l \in L$, we have $v_l = x_l^h + HVE_l x_l^a = x_l^h + x_l^a$, and consequently $\left(x_l^h + x_l^a\right) \frac{\partial t_l(v_l)}{\partial x_l^a} = \left(x_l^h + x_l^a\right) \frac{\partial t_l(v_l)}{\partial x_l^h} = v_l \frac{\partial t_l(v_l)}{\partial v_l}$, i.e., the link travel time externality is identical for AVs and HVs. However, the anonymous link travel time externality can be internalized only when the toll charge for each link is differentiated according to each user's VOT:

$$\tau_l^m = VOT^m v_l \frac{\partial t_l(\bar{v}_l)}{\partial v_l} \qquad \forall m \in M, l \in L \qquad (3\text{-}32)$$

This class-specific toll is difficult to implement in practice because we may not be able to easily distinguish between AVs and HVs. Yang and Huang (2004) proved that a uniform link toll pattern across user classes can be obtained by solving the following linear program:

$$\max_{\boldsymbol{\tau},\boldsymbol{\mu}} \sum_{w \in W} \sum_{m \in M} q^{w,m} \mu^{w,m} - \sum_{l \in L} \bar{v}_l \tau_l$$

s.t.

$$\mu^{w,m} \leq \sum_{l \in L} (VOT^m t_l(\bar{v}_l) + \tau_l) \delta_l^r \qquad \forall r \in R^w, w \in W, m \in M$$

where the optimal solution of τ_l is the uniform link toll; the optimal solution of $\mu^{w,m}$ represents the travel cost of class $m \in M$ between O-D pair $w \in W$ under the induced tolled user equilibrium; R^w is set of routes connecting O-D pair $w \in W$; δ_l^r is link route indicator, $\delta_l^r = 1$ if link $l \in L$ is a part of route $r \in R^w$, and $\delta_l^r = 0$ otherwise. Detailed derivation and proof can be found in Yang and Huang (2004) and Theorem 6.2 of Yang and Huang (2005). Note that the toll given by the above linear program can be positive (charge) or negative (subsidy) to link users. Yang and Huang (2004) further showed that nonnegative tolls can be obtained by solving the above linear program with additional constraints $\tau_l \geq 0, \forall l \in L$.

In general scenarios when conditions $\bar{\eta}_l^{hh} + \bar{\eta}_l^{aa} - \bar{\eta}_l^{ha} - \bar{\eta}_l^{ah} = 0, \forall l \in L$ and $\frac{\bar{\eta}_l^{aa}}{\bar{\eta}_l^{hh}} = 1, \forall l \in L$ do not hold simultaneously, we may not be able to identify an anonymous toll to decentralize the time-based system optimal as a tolled user equilibrium. The link travel time congestion externality $\left(\bar{x}_l^h + \bar{x}_l^a\right)\frac{\partial t_l(\bar{v}_l)}{\partial x_l^m}$ can always be internalized by the following class-specific link tolls:

$$\tau_l^m = VOT^m\left(\bar{x}_l^h + \bar{x}_l^a\right)\frac{\partial t_l(\bar{v}_l)}{\partial x_l^m} \qquad \forall m \in M, l \in L \qquad (3\text{-}33)$$

From Proposition 3-5 we know that if $\bar{\eta}_l^{hh} + \bar{\eta}_l^{aa} - \bar{\eta}_l^{ha} - \bar{\eta}_l^{ah} = 0, \forall l \in L$ and $\exists\ a \text{ constant } \lambda \text{ such that} \frac{\bar{\eta}_l^{aa}}{\bar{\eta}_l^{hh}} = \lambda, \forall l \in L$, the tolled user equilibrium will have unique solution for the aggregate link flow in HVE. If we can identify the global minimum solution for SO-Time and set link tolls according to equation (3-33), we can achieve system optimal flow distribution. However, if conditions $\bar{\eta}_l^{hh} + \bar{\eta}_l^{aa} - \bar{\eta}_l^{ha} - \bar{\eta}_l^{ah} = 0, \forall l \in L$ and $\exists\ a \text{ constant } \lambda \text{ such that} \frac{\bar{\eta}_l^{aa}}{\bar{\eta}_l^{hh}} = \lambda, \forall l \in L$ do not hold simultaneously, we may not be able to successfully realize a target system optimal flow distribution with link tolls because the tolled user equilibrium may have non-unique solutions for the aggregate link flow in HVE.

3.2.3 System optimum in monetary units and pricing for user equilibrium

The system optimum in monetary units can be formulated as the following minimization program:

SO-Money:

$$\min_{\boldsymbol{x},\boldsymbol{v}} \sum_{m\in M}\sum_{l\in L} t_l(v_l)x_l^m VOT^m$$

s.t. (3-8)-(3-13)

In the above, the objective is to minimize the total system travel cost in monetary units. Constraints (3-8)-(3-13) are flow conservation constraints ensuring that all O-D travel demands are assigned to the network.

The following proposition establishes the sufficient conditions for the solution uniqueness of the aggregate link flow in HVE for the SO-Money problem.

Proposition 3-7. If $\bar{\eta}_l^{hh} + \bar{\eta}_l^{aa} - \bar{\eta}_l^{ha} - \bar{\eta}_l^{ah} = 0, \forall l \in L$ and $\frac{\bar{\eta}_l^{aa}}{\bar{\eta}_l^{hh}} = \frac{VOT^a}{VOT^h}, \forall l \in L$, then the solution of the aggregate link flow in HVE, $\boldsymbol{v}$, for the SO-Money problem is unique.

Proof. If $\bar{\eta}_l^{hh} + \bar{\eta}_l^{aa} - \bar{\eta}_l^{ha} - \bar{\eta}_l^{ah} = 0, \forall l \in L$ and $\frac{\bar{\eta}_l^{aa}}{\bar{\eta}_l^{hh}} = \frac{VOT^a}{VOT^h}, \forall l \in L$, HVE_l defined in equations (3-8) is constant $\frac{\mathrm{VOT}^a}{\mathrm{VOT}^h}$ for all links, i.e., $HVE_l = \frac{VOT^a}{VOT^h}, \forall l \in L$. With $v_l = x_l^h + HVE_l x_l^a = \frac{1}{VOT^h}\left(VOT^h x_l^h + VOT^a x_l^a\right), \forall l \in L$, the objective function of SO-Time can then be rewritten as $\sum_{l\in L} VOT^h t_l(v_l)v_l$, which is convex in v_l. Therefore, the solution of the aggregate link flow in HVE, $\boldsymbol{v}$, for the SO-Money problem is unique. □

Note that the uniqueness of $\boldsymbol{v}$ can further guarantee the uniqueness of travel time on each link and the total system travel cost (i.e., the objective function value of SO-Money). However, the link flow by class may not be unique even when the aggregate link flow in HVE is unique. In general scenarios, the SO-Money problem may have multiple

local minima because its objective function is not necessarily convex in x_l^m. It is thus important to identify the global minimum targeted for meaningful pricing.

For SO-Money, its first-order optimality conditions at an optimum $(\bar{\boldsymbol{x}}, \bar{\boldsymbol{v}})$ are Constraints (3-8)-(3-13) and

$$x_l^m \left(VOT^m t_l(\bar{v}_l) + \left(VOT^h \bar{x}_l^h + VOT^a \bar{x}_l^a \right) \frac{\partial t_l(\bar{v}_l)}{\partial x_l^m} + \hat{\rho}_i^{w,m} - \hat{\rho}_j^{w,m} \right) = 0 \quad \forall w \in W, m \in M, (i,j) = l \in L \tag{3-34}$$

$$VOT^m t_l(\bar{v}_l) + \left(VOT^h \bar{x}_l^h + VOT^a \bar{x}_l^a \right) \frac{\partial t_l(\bar{v}_l)}{\partial x_l^m} + \hat{\rho}_i^{w,m} - \hat{\rho}_j^{w,m} \geq 0 \quad \forall w \in W, m \in M, (i,j) = l \in L \tag{3-35}$$

Clearly, the optimality conditions (3-34) and (3-35) for the SO-Money can be regarded as the cost-based user equilibrium conditions. The requirement for such an equilibrium is that each user should be charged a toll given by the following equation:

$$\tau_l^m = \left(VOT^h \bar{x}_l^h + VOT^a \bar{x}_l^a \right) \frac{\partial t_l(\bar{v}_l)}{\partial x_l^m} \quad \forall m \in M, l \in L \tag{3-36}$$

If $\bar{\eta}_l^{hh} + \bar{\eta}_l^{aa} - \bar{\eta}_l^{ha} - \bar{\eta}_l^{ah} = 0, \forall l \in L$ and $\frac{\bar{\eta}_l^{aa}}{\bar{\eta}_l^{hh}} = 1, \forall l \in L$, we have $v_l = x_l^h + HVE_l x_l^a = x_l^h + x_l^a$, and consequently $\left(VOT^h \bar{x}_l^h + VOT^a \bar{x}_l^a \right) \frac{\partial t_l(\bar{v}_l)}{\partial x_l^a} = \left(VOT^h \bar{x}_l^h + VOT^a \bar{x}_l^a \right) \frac{\partial t_l(\bar{v}_l)}{\partial x_l^h} = \left(VOT^h \bar{x}_l^h + VOT^a \bar{x}_l^a \right) \frac{\partial t_l(v_l)}{\partial v_l}$ or $\tau_l^a = \tau_l^h$, i.e., the link tolls given by equations (3-36) are anonymous to AVs and HVs. In general scenarios when conditions $\bar{\eta}_l^{hh} + \bar{\eta}_l^{aa} - \bar{\eta}_l^{ha} - \bar{\eta}_l^{ah} = 0, \forall l \in L$ and $\frac{\bar{\eta}_l^{aa}}{\bar{\eta}_l^{hh}} = 1, \forall l \in L$ do not hold simultaneously, we

may not be able to identify an anonymous toll to decentralize the cost-based system optimal as a tolled user equilibrium.

Like discussion in previous Section 3.2.2, if $\bar{\eta}_l^{hh} + \bar{\eta}_l^{aa} - \bar{\eta}_l^{ha} - \bar{\eta}_l^{ah} = 0, \forall l \in L$ and $\exists\ a$ constant λ such that $\frac{\bar{\eta}_l^{aa}}{\bar{\eta}_l^{hh}} = \lambda, \forall l \in L$, and if we can identify the global minimum solution for SO-Money and set link tolls according to equation (3-36), we can realize the targeted system optimal flow distribution. However, if conditions $\bar{\eta}_l^{hh} + \bar{\eta}_l^{aa} - \bar{\eta}_l^{ha} - \bar{\eta}_l^{ah} = 0, \forall l \in L$ and $\exists\ a$ constant λ such that $\frac{\bar{\eta}_l^{aa}}{\bar{\eta}_l^{hh}} = \lambda, \forall l \in L$ do not hold simultaneously, we may not be able to successfully realize a target system optimal flow distribution with link tolls.

3.3 Robust congestion pricing

The first-best or marginal-cost pricing scheme, although with perfect theoretical basis, is of little practical interest due to the fact that it is impractical to charge users on each network link in view of the operating cost and public acceptance (Yang and Huang, 2005). In this section, we further investigated the second-best (link-based) toll pricing problems for networks with mixed flows of HVs and AVs, in which toll levels are determined for a subset of selected links. As discussed in Section 3.1.5 and Section 3.2.1, the system performance for a network with mixed HV and AV flows may be nonunique in general scenarios. This non-uniqueness property makes it difficult to design and evaluate a congestion pricing strategy. In real-world applications, decision makers and planners tend to be risk averse and may prefer a plan or design that can optimize the worst-case performance (Lou et al., 2010). Therefore, we formulate the second-best pricing problem

as a robust min-max optimization problem, inspired by the pioneering works of Lou et al., 2010, Di et al., 2016 who investigated second-best toll pricing within the framework of bounded rationality.

3.3.1 Model formulation

The robust congestion pricing problem (RCPP) can be formulated as the following min-max program:

RCPP:

$$\min_{\boldsymbol{\tau}} \max_{\boldsymbol{x},\boldsymbol{v},\boldsymbol{\rho}} \sum_{m\in M}\sum_{l\in L} t_l(v_l)x_l^m$$

s.t. (3-8)-(3-13), (3-26), (3-27)

$$\tau_l^m \geq 0 \qquad \forall m \in M, l \in L \qquad (3\text{-}37)$$

$$\tau_l^m \leq \tau_{max} \qquad \forall m \in M, l \in L \qquad (3\text{-}38)$$

where parameter τ_{max} is a predetermined upper bound of link tolls.

Note that, the system travel cost in the objective function of RCPP can be in time or monetary units depending on the real concern of the system manager or toll designer (Yin and Yang, 2004; Yang and Huang, 2005). It is straightforward to convert the proposed time-based formulation in RCPP into a monetary-based formulation. Moreover, if class-specific toll is difficult to implement in practice, anonymous toll can be ensured by simply replace each class-specific toll variable τ_l^m with a new anonymous toll variable τ_l.

For convenience, let $\Psi(\boldsymbol{\tau})$ denote the feasible region of the inner problem, or the maximization part of RCPP, $\boldsymbol{\psi}$ represent the decision variable vector $(\boldsymbol{x}, \boldsymbol{v}, \boldsymbol{\rho})$, and $\phi(\boldsymbol{\psi})$ denote the objective function. Then the inner problem can be written as:

RCPP-IN:

$$\lambda(\boldsymbol{\tau}) = \max_{\boldsymbol{\psi}}\{\phi(\boldsymbol{\psi}): \boldsymbol{\psi} \in \Psi(\boldsymbol{\tau})\}$$

Consequently, the RCPP can be written as:

$$\min_{\boldsymbol{\tau}} \lambda(\boldsymbol{\tau})$$

s.t. (3-37)-(3-38) and

$$\lambda(\boldsymbol{\tau}) = \max_{\boldsymbol{\psi}}\{\phi(\boldsymbol{\psi}): \boldsymbol{\psi} \in \Psi(\boldsymbol{\tau})\}$$

One can observe that the feasible region of the inner problem depends on the decision variables of the outer problem. Therefore, RCPP is essentially a generalized semi-infinite min-max problem (see, e.g., Polak and Royset, 2005), which is difficult to solve. Moreover, the MPCC property of the inner problem further increases the difficulty of solving RCPP. Lou et al. (2010) proposed a heuristic algorithm based on penalization and a cutting-plane scheme to solve their robust congestion pricing models, which have similar structure with RCPP and are also generalized semi-infinite min-max problems. In their robust congestion pricing models, the decision variable of the outer problem, i.e., the link toll, appears in one set of equality constraints in the inner problem. Lou et al. (2010) formulated a penalized inner problem in which the set of equality constraints involving the toll variables are removed and a penalty term is added in the objective function. By doing so, the original generalized semi-infinite min-max problem is converted into an ordinary semi-infinite min-max problem. They then further reformulate the problem as an equivalent ordinary semi-infinite optimization problem and solve it using a cutting-plane scheme. However, as mentioned by Lou et al. (2010), their algorithm does not guarantee convergence. Moreover, it is difficult to determine the value of the penalty parameter in the penalized inner problem. Therefore, we solve our RCPP

using a genetic-algorithm-based approach, which may be less efficient but easier to implement.

3.3.2 Solution algorithm

This paper proposes a genetic-algorithm-based approach shown in Figure 3-7 to solve the RCPP. The solution procedure mainly includes two modules, i.e., inner problem solution module and genetic algorithm module. The inner problem is a MPCC, which is difficult to solve. An iterative solution procedure is designed to solve it based on the algorithm proposed by Lawphongpanich and Yin (2010) using manifold suboptimization. The algorithm enables convergence to a strongly stationary solution with a finite number of iterations. Genetic algorithm module (including the reproduction, crossover and mutation operations) is adopted to determine the link tolls.

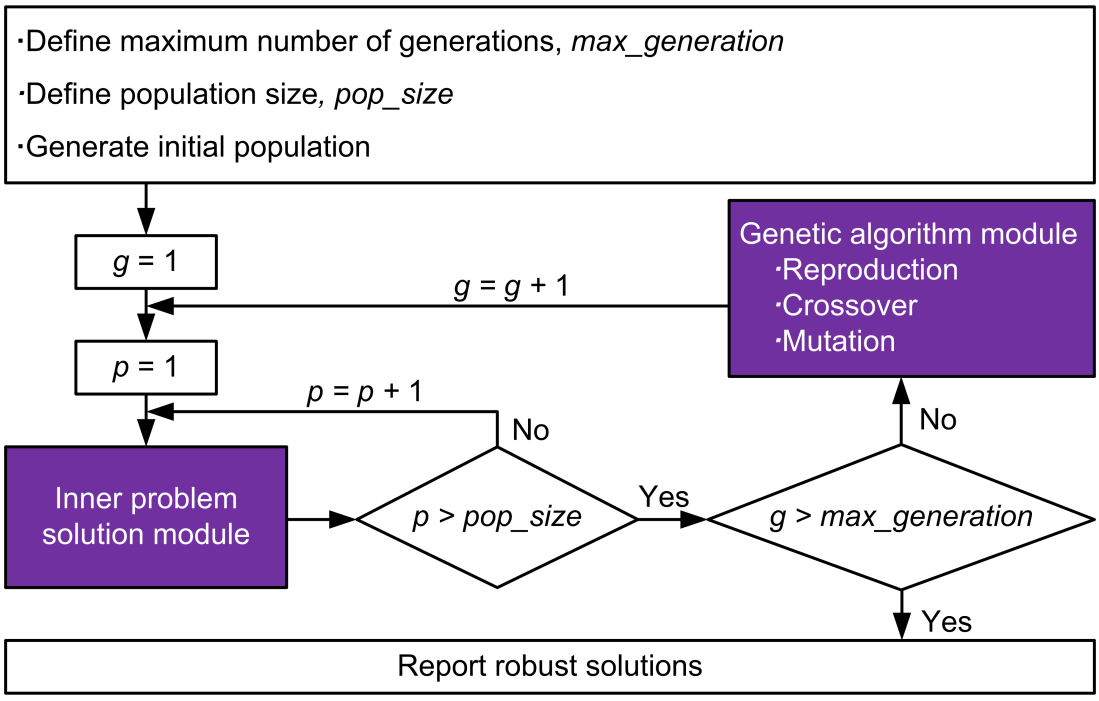

Figure 3-7. Flowchart of the genetic-algorithm-based approach.

3.3.2.1 Inner problem solution module

In the inner problem RCPP-IN, constraints (3-13), (3-26), and (3-27) form a set of complementarity constraints, which can be given as the following compact form:

$$0 \le \left(t_l(v_l) + \frac{\tau_l^m}{VOT^m} + \rho_i^{w,m} - \rho_j^{w,m} \right) \perp x_l^{w,m} \ge 0, \quad \forall w \in W, m \in M, (i,j) = l \in L$$

where $\perp$ is the orthogonal sign representing that the inner product of two vectors is zero. To track whether $\left(t_l(v_l) + \frac{\tau_l^m}{VOT^m} + \rho_i^{w,m} - \rho_j^{w,m} \right)$ or $x_l^{w,m}$ is zero, two index sets are defined as follows:

$$\Omega^k = \{(l,w,m): x_l^{w,m} = 0, w \in W, m \in M, l \in L\}$$
$$\bar{\Omega}^k = \left\{ (l,w,m): t_l(v_l) + \frac{\tau_l^m}{VOT^m} + \rho_i^{w,m} - \rho_j^{w,m} = 0, w \in W, m \in M, (i,j) = l \in L \right\}$$

where superscript k indicates the current iteration of the solution procedure. With the above index sets, a restricted version of RCPP-IN, denoted as R-RCPP-IN can be formulated as the following nonlinear program:

R-RCPP-IN:

$$\max_{\boldsymbol{x},\boldsymbol{v},\boldsymbol{\rho}} \sum_{m \in M} \sum_{l \in L} t_l(v_l) x_l^m$$

s.t. (3-8)-(3-12)

$$x_l^{w,m} = 0 \qquad \forall (l,w,m) \in \Omega^k \qquad (3\text{-}39)$$

$$t_l(v_l) + \frac{\tau_l^m}{VOT^m} + \rho_i^{w,m} - \rho_j^{w,m} = 0 \qquad \forall \big((i,j) = l, w, m\big) \in \bar{\Omega}^k \qquad (3\text{-}40)$$

$$x_l^{w,m} \geq 0 \qquad \forall (l,w,m) \notin \Omega^k \qquad (3\text{-}41)$$

$$t_l(v_l) + \frac{\tau_l^m}{VOT^m} + \rho_i^{w,m} - \rho_j^{w,m} \geq 0 \qquad \forall \big((i,j) = l,w,m\big) \notin \bar{\Omega}^k \qquad (3\text{-}42)$$

Given a toll design $\boldsymbol{\tau}$, the solution procedure of RCPP-IN is outlined below.

Step 0: Solve the tolled user equilibrium problem and obtain the solution of vectors $\boldsymbol{x}$, $\boldsymbol{v}$ and $\boldsymbol{\rho}$. Set $k = 1$ and initialize index sets Ω^1 and $\bar{\Omega}^1$.

Step 1: Let $(\boldsymbol{x}^k, \boldsymbol{v}^k, \boldsymbol{\rho}^k)$ solve the R-RCPP-IN and obtain the multipliers associated with constraints $x_l^{w,m} = 0$, denoted as $\xi_l^{w,m}$.

Step 2: Update a new index set defined as follows:

$$\Gamma^k = \{(l,w,m) \in \Omega^k \cap \bar{\Omega}^k : \xi_l^{w,m} < 0\}$$

If $\Gamma^k = \emptyset$, stop and $(\boldsymbol{x}^k, \boldsymbol{v}^k, \boldsymbol{\rho}^k)$ is strongly stationary. Otherwise, do the following and go to Step 1: (1) set $\Omega^{k+1} = \Omega^k - \Gamma^k$, (2) set $\bar{\Omega}^{k+1} = \left\{\big((i,j) = l,w,m\big) : t_l^k\big(v_l^k\big) + \frac{\tau_l^m}{VOT^m} + \rho_i^{w,m,k} - \rho_j^{w,m,k} = 0, w \in W, m \in M, (i,j) = l \in L\right\}$, and (3) set $k = k + 1$.

3.3.2.2 Genetic algorithm module

Genetic algorithms are search and optimization procedures motivated by natural principles and selection (Goldberg, 1989). Due to its extensive generality, global perspective, strong robustness and implicit parallelism, genetic algorithm has been applied to a wide variety of problems in transportation engineering, including road

network design problem (Xiong and Schneider, 1992; Drezner and Salhi, 2002; Chen et al., 2010), transit network design problem (Fan and Machemehl, 2006; Arbex and da Cunha, 2015), traffic signal timing (Park et al., 1999; Ceylan and Bell, 2004) and road pricing (Yin, 2000; Shepherd and Sumalee, 2004; Zhang and Yang, 2004).

The basic idea of the genetic-algorithm-based approach is to code the decision variables of the outer problem to a number of chromosomes (i.e., strings) and calculate the fitness of each chromosome by solving the inner problem. By iteratively conducting reproduction, crossover and mutation operations of genetic algorithms, the optimal string may be obtained.

The toll variable $\boldsymbol{\tau} = \{\tau_l^m | \, m \in M, l \in L\}$ is coded as a chromosome $\boldsymbol{p} = \{p_n | n = 1, 2, \ldots, |M| \times |L|\}$ (see Figure 3-8). Initially, a group of chromosomes is generated randomly. The fitness of each chromosome is evaluated by solving the inner problem. By iteratively conducting reproduction, crossover and mutation operations of genetic algorithms, the optimal chromosome may be obtained. The process is outlined below.

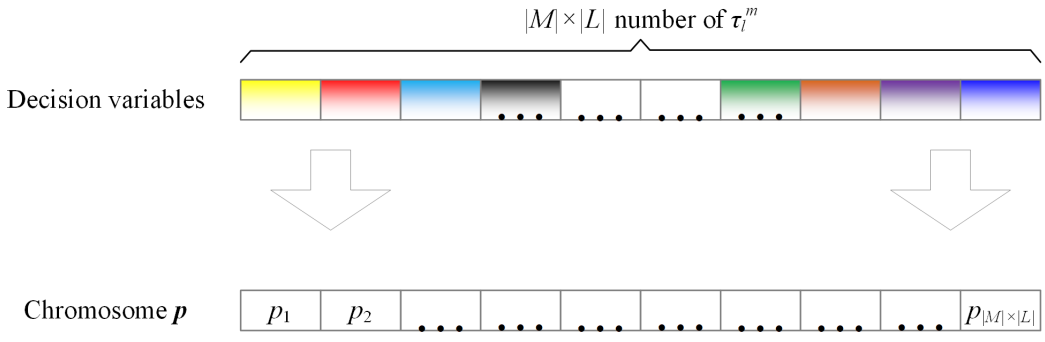

Figure 3-8. Structure of a chromosome (Figure adapted from Yang et al., 2016).

Step 0: Define genetic algorithm parameters: mutation probability (P_{mt}), crossover probability (P_{co}), population size (pop_size), and maximal number of generations ($max\_generation$). Randomly generate a set of initial toll solutions of size pop_size and set generation index $g = 1$.

Step 1: Solve the inner problem RCPP-IN for each toll solution. Collect distribution of the objective function values.

Step 2: Improve all toll solutions via genetic algorithm operators: reproduction, crossover, and mutation.

Step 3: If $g = max\_generation$, the solution with the best performance is adopted as the optimal solution of the problem. Else, set $g = g + 1$, and go to Step 1.

3.3.3 Numerical studies

The following set of tests are conducted on the Nguyen-Dupuis network (Nguyen and Dupuis, 1984). As shown in Figure 3-9, the network consists of 13 nodes, 19 regular links, 7 candidate toll links, and four O-D pairs. In the travel time function, $\alpha_l = 0.15$ and $\beta_l = 4$. Table 3-5 lists the link input parameters, including link free flow travel time, and number of lanes on each link. Set headway $\bar{\eta}_l^{hh} = \bar{\eta}_l^{ah} = \bar{\eta}_l^{ha} = 1.8$ seconds and $\bar{\eta}_l^{aa} = 0.6$ seconds, $\forall l \in L$. The per-lane capacity for each link with pure HVs is $\hat{c}_l^h = \frac{1}{\bar{\eta}_l^{hh}} = 2000$ veh/h, $\forall l \in L$ and the HVE_l defined in equation (3-8) becomes $HVE_l = -\frac{2}{3}p_l^a + 1$. The total travel demand between each O-D pair is set to $q^{1\text{-}2} = 9600\ veh/h$, $q^{1\text{-}3} = 19200\ veh/h$, $q^{4\text{-}2} = 14400\ veh/h$, $q^{4\text{-}3} = 4800\ veh/h$. The AV penetration rates for all O-D pairs are set to 50%. The upper bound of toll rate τ_{max} is set to \$10. The

value of time of drivers using HVs is assumed to be $VOT^h = \$7.5/h$.† For drivers using AVs, the value of time is assumed to be half of VOT^h, i.e., $VOT^a = 0.5VOT^h = \$3.75/h$.

The genetic-algorithm-based solution procedure was implemented using MATLAB R2018b interfaced with GAMs (Rosenthal, 2012) on a 3.40 GHz Dell Computer with 16 GB of RAM. CONOPT (Drud, 1994) was used to solve the UE-NLP and R-RCPP-IN problems. The genetic-algorithm-based procedure was performed with $pop\_size = 30$, $P_{co} = 0.6$, $P_{mt} = 0.15$ and $max\_generation = 120$. Because the inner problem is a MPCC, using multiple initial solutions to solve it can yield better local optimal solutions. Three different initial solutions were used in solving each inner problem. The computation time thus increased significantly. It took about two hours to solve the model.

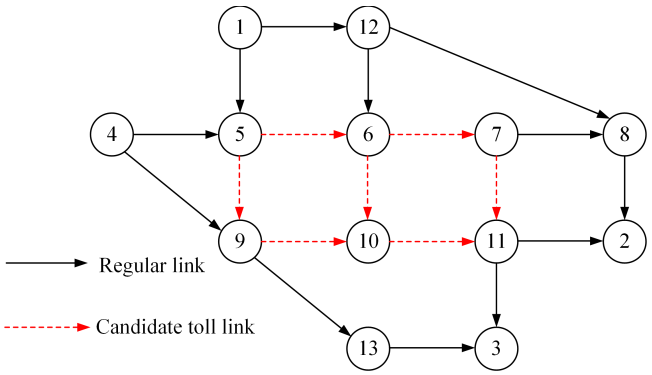

Figure 3-9. Nguyen-Dupuis network with candidate toll links.

Table 3-5: Link characteristics of the Nguyen-Dupuis network

Link	Free-flow travel time $\hat{t}_l$ (min)	Number of lanes ι_l	Link	Free-flow travel time $\hat{t}_l$ (min)	Number of lanes ι_l
1-5	7	3	8-2	9	4

† The value of time is assumed to be 50% of the hourly wage rate of road users (Concas and Kolpakov, 2009; Zhang et al., 2004). The hourly wage rate is set to be \$15/h, which is computed based on the annual average income of \$31,128 (Department of Numbers, 2018) and the working time of 52 weeks with 40 hours per week.

1-12	9	4	9-10	10	4
4-5	9	3	9-13	9	2
4-9	12	2	10-11	6	4
5-6	3	3	11-2	7	3
5-9	9	3	11-3	8	4
6-7	5	3	12-6	7	4
6-10	13	4	12-8	14	2
7-8	5	2	13-3	11	2
7-11	9	3			

The toll rates are reported in Table 3-6. Table 3-7 compares the system performance of the Nguyen-Dupuis network in the status quo condition (i.e., no toll) and in the robust toll design. It can be observed that the robust toll design reduces the worst-case total system travel time from 3,284,549.6 min to 2,587,730.4 min, a reduction of 21.2 percent. We further note that, in the status quo condition, the relative difference between the worst- and best-case total system travel time is 17.2%, while under the robust toll design, the relative difference becomes 0.0%. With the designed link tolls, the system performance of the network becomes more stable. The worst-case equilibrium AV flow ratios on each link are compared in Figure 3-10. It can be observed that, with the robust link tolls, all AVs between O-D pair (4,3) are forced to use route 4-5-6-7-11-3, all AVs between O-D pair (4,2) are forced to use route 4-5-6-7-8-2, all AVs between O-D pair (1,3) are forced to use route 1-5-6-7-11-3, and majority of AVs between O-D pair (1,2) are forced to use route 1-5-6-7-8-2. Compared to the status quo condition, the robust toll design better clusters AV flows together (on those blue links as shown in Figure 3-10(b)) so that they have better chances to form platoons, utilize less road capacity, and reduce congestion. We note that the robust links tolls even make the traffic flows on links (5,6), (6,7), (7,8), (7,11) pure AV flows.

Table 3-6: Robust toll design in the Nguyen-Dupuis network

Candidate toll links	Tolls for HVs ($)	Tolls for AVs ($)
5-6	9.69	0.16
5-9	1.57	9.14
6-7	9.48	0.09
6-10	0.83	6.19
7-11	6.91	0.97
9-10	0.74	0.17
10-11	0.13	6.17

Table 3-7: System performances in status quo condition and robust toll design

	Total system travel time (min)		Relative difference
	Worst-case	Best-case	
The status quo	3,284,549.6	2,802,075.4	17.2%
Robust toll design	2,587,730.4	2,587,730.4	0.0%

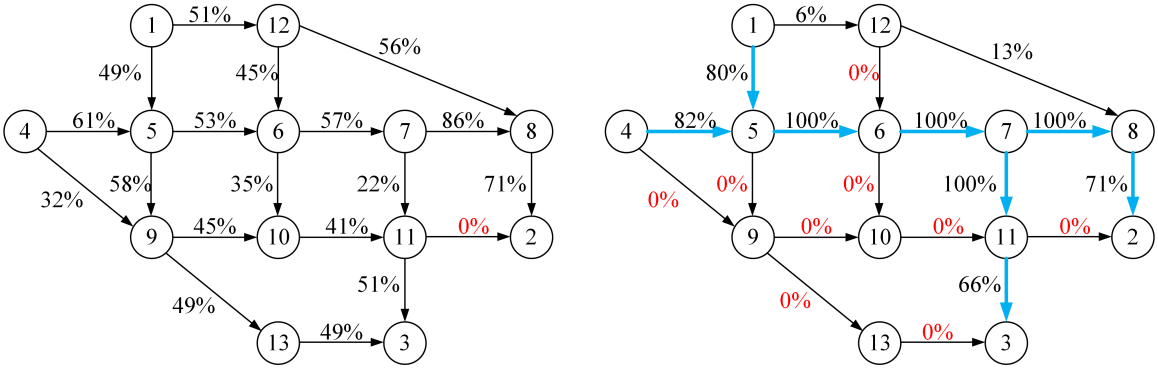

(a) The status quo **(b) Robust toll design**

Figure 3-10. AV flow ratios in status quo condition and robust toll design.

3.4 Summary

In this chapter, we investigated the UE and congestion pricing problems in transportation networks with mixed AV and HV flows. UE models were formulated to describe the flow distributions of AVs and HVs. It was found that with different time headway patterns in mixed AV and HV flows, the UE problems might have unique or non-unique flow patterns. Numerical examples based on a toy network were provided to

show the potential impact of AVs on the congestion patterns of a network with mixed autonomy. The first-best pricing problem was then studied. The uniqueness of the system optimum problems (in monetary or time units) and the corresponding pricing for UE were explicitly discussed. It was found that, under general scenarios, it may be difficult to identify and realize system optimal flow distributions with the marginal-cost pricing scheme. At last, the second-best (link-based) toll pricing problems for networks with mixed flows of HVs and AVs were investigated. Because the UE problems may have non-unique flow distributions, a robust optimal pricing model was proposed to design link tolls so that the system performance under the worst-case flow distributions is optimized. The robust model is a generalized semi-infinite min-max problem, which is not easy to solve. A genetic-algorithm-based approach was proposed for its solution in the present study. The Nguyen-Dupuis network was used for the numerical demonstration of the proposed robust congestion pricing model. The results demonstrate that properly designed tolls can significantly improve the system performance.

CHAPTER 4

STRATEGIC PLANNING OF DEDICATED AUTONOMOUS VEHICLE LANES AND AUTONOMOUS VEHICLE/TOLL LANES IN TRANSPORTATION NETWORKS

Employing vehicle communication and automated control technologies, autonomous vehicles (AVs) can safely drive closer together than human-driven vehicles (HVs), thereby potentially improving traffic efficiency. Separation between AV and HV traffic through the deployment of dedicated AV lanes is foreseen as an effective method of amplifying the benefits of AVs and promoting their adoption. However, it is important to consider mixed AV and HV traffic in a transportation network. On the one hand, it may be impractical to deploy dedicated AV lanes throughout the network, while on the other hand, dedicated AV lanes may even reduce the total traffic efficiency of a road segment when the AV flow rate is low. In this chapter, we considered a new form of managed lanes for AVs, designated as autonomous vehicle/toll (AVT) lanes, which grant free access to AVs while allowing HVs to access the lanes by paying a toll. We investigated the optimal deployment of dedicated AV lanes and AVT lanes in transportation networks with mixed AV and HV flows. The user equilibrium (UE) problem in a transportation network with mixed flows of AVs and HVs is first explored. We formulated the UE problem as a link-based variational inequality (VI) and identified that, with different impacts of AVs on road capacity, the UE problem can have unique or non-unique flow patterns. Considering that the UE problem may have non-unique flow distributions, we proposed a robust optimal deployment model, which is a generalized

semi-infinite min-max program, to deploy the dedicated AV lanes and AVT lanes so that the system performance under the worst-case flow distributions is optimized. We proposed effective solution algorithms to solve these models and presented numerical studies to demonstrate the models and the solution algorithms. The results show that the system performance can be significantly improved through the deployment of AV and AVT lanes.

4.1. Potential benefits of AV lanes and AVT lanes

As discussed in Chapter 3, road capacity increases with the increase of AV flow proportion. If used by pure AV flows, dedicated AV lanes have maximized traffic capacity. However, dedicated AV lanes may be underutilized when AV flow rate is low. AVT lanes are a promising substitution and complementarity to dedicated AV lanes. On the one hand, by charging HVs tolls, AVT lanes will have increased AV flow proportion and thus have improved traffic capacity. On the other hand, when AV flow rate is low, the capacity of an AVT lane can be more effectively used.

Dedicated AV lanes and AVT lanes may benefit a transportation network with mixed AVs and HVs in two aspects: First, they may amplify the benefits of AVs and improve the traffic capacity of individual roads. Second, they may be able to improve the system-wide flow distribution in the network.

To show the first benefit, consider a single O-D pair (1, 2) connected by one road segment with two lanes, as shown in Figure 4-1. Lane 1 and lane 2 can be represented as link 1 and link 2, respectively. Assume that $\bar{\eta}^{hh} = \bar{\eta}^{ah} = \bar{\eta}^{ha} = 1.8$ s and $\bar{\eta}^{aa} = 0.9$ s, then the HVE_l is given by $HVE_l = 1 - \frac{p_l}{2}$. The per-lane capacity is 2000 veh/h for pure

HV flows, i.e., $\hat{c}_1^h = \hat{c}_2^h = 2000$ veh/h. The free flow travel time is 10 min. The parameters α_l and β_l in the travel time function are both equal to 1. The toll on an AVT lane is equivalent to $\frac{5}{3}$ min. Table 4-1 presents the efficiency of road segment (1, 2) under different scenarios.

Based upon the data in Table 4-1, we make several observations. Under scenario 1, converting lane 1 into an AV lane can reduce the total system travel time from 75000 min to 70000 min. Under scenario 2, converting lane 1 into an AV lane will increase the total travel time from 51250 min to 52500 min, while converting lane 1 into an AVT lane can reduce the total travel time to 50000 min. The results of scenario 1 demonstrate that converting existing lanes into dedicated AV lanes may improve the efficiency of a road segment with a high proportion of AV flows. The results of scenario 2 suggest that AVT lanes may exhibit better performance than AV lanes when AV flow rate is low.

If $\bar{\eta}^{hh} + \bar{\eta}^{aa} - \bar{\eta}^{ah} - \bar{\eta}^{ha} = 0$, then $HVE_l = \frac{\bar{\eta}^{aa}}{\bar{\eta}^{hh}}$ is a constant and converting lane 1 or lane 2 into AV or AVT lanes will not improve efficiency under any demand scenarios. This result can be extended to a general road segment with an arbitrary number of lanes (intuitively, a unit of AV flow will always be transformed to $\frac{\bar{\eta}^{aa}}{\bar{\eta}^{hh}}$ HV flow regardless of the distribution of mixed traffic among the lanes of a road segment). That being said, for general transportation networks, AV/AVT lanes may still be able to improve system-wide flow distribution when HVE_l is constant.

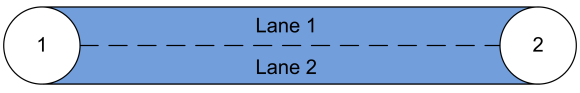

Figure 4-1. A road segment with two lanes.

Table 4-1: Efficiency of road segment (1, 2) under different scenarios

Scenario 1: Demand between (1, 2) is $q^{1\text{-}2,h} = 2000$ veh/h and $q^{1\text{-}2,a} = 2000$ veh/h				
Lane setting	Flow distribution $(x_1^h, x_1^a, x_2^h, x_2^a)$	HVE (HVE_1, HVE_2)	Aggregate flow in HVE (v_1, v_2)	Total travel time (min)
Both lanes 1 and 2 are regular	(1000, 1000, 1000, 1000)	(3/4, 3/4)	(1750, 1750)	75000
Lane 1 is AV lane, lane 2 is regular	(0, 2000, 2000, 0)	(1/2, 1)	(1000, 2000)	70000
Scenario 2: Demand between (1, 2) is $q^{1\text{-}2,h} = 2000$ vehh and $q^{1\text{-}2,a} = 1000$ veh/h				
Lane setting	Flow distribution $(x_1^h, x_1^a, x_2^h, x_2^a)$	HVE (HVE_1, HVE_2)	Aggregate flow in HVE (v_1, v_2)	Total travel time (min)
Both lanes 1 and 2 are regular	(1000, 500, 1000, 500)	(5/6, 5/6)	$(1417, 1417)$	51250
Lane 1 is AV lane, lane 2 is regular	(0, 1000, 2000, 0)	(0.5, 1)	(500, 2000)	52500
Lane 1 is AVT lane, Lane 2 is regular	(500, 1000, 1500, 0)	(2/3, 1)	(1167,1500)	50000

4.2 UE model with AV/AVT lanes

Let $\hat{L}$ represent the set of AV/AVT candidate links in the network. Note that if a directed road segment has some lanes that are designated as AV/AVT lanes, this road segment can be represented as a pair of parallel links, i.e., one AV/AVT link and one regular link. Further, let H denote the set of these link pairs. Each link pair is designated by $h \in H$ or represented as $[l, \hat{l}]$, where $l \in L \backslash \hat{L}$ is a regular link, $\hat{l} \in \hat{L}$ is a candidate AV/AVT link, and l and $\hat{l}$ belong to the same directed road segment.

For example, Figure 4-2 (a) shows a small traffic network with three directed road segments. If road segment 1 is considered a candidate road to deploy AV/AVT lanes, then the network topology of the traffic network is given by Figure 4-2 (b), and we have $L = \{1, 2, 3, 4\}$, $\hat{L} = \{4\}$, and $H = \{[1, 4]\}$, where $h = [1, 4] \in H$ denote a link pair of regular link 1 and AV/AVT candidate link 4. This link pair representation is inspired by Chen et al. (2016).

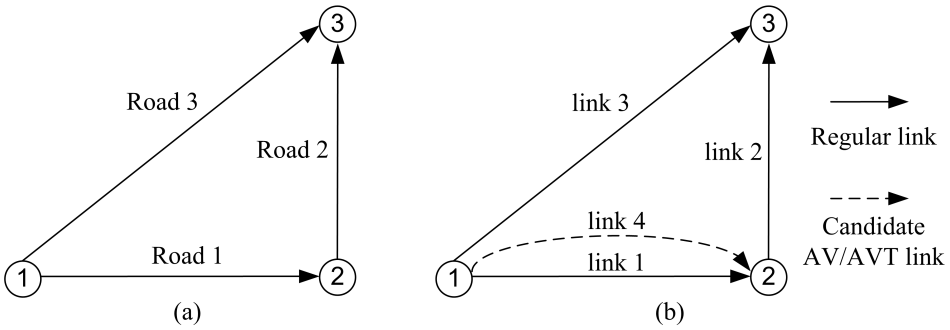

Figure 4-2. A small illustrative network.

An integer variable y_l is introduced for each candidate AV/AVT link $l \in \hat{L}$ to represent the number of lanes that are converted to AV/AVT lanes. Note that link $l \in \hat{L}$ is a real link that can be utilized only when $y_l > 0$; otherwise the link is only a virtual link that cannot be utilized. A binary variable z_l is introduced to differentiate dedicated AV lanes and AVT lanes. It is stipulated that $z_l = 1$ if link $l \in \hat{L}$ is converted into an AVT link and $z_l = 0$ if link $l \in \hat{L}$ is converted into a dedicated AV link. Let τ_l^h denote tolls that are measured in units of time for HVs to access AVT lanes. Since a toll is only enacted on HVs using AVT lanes, τ_l^h can be simplified as τ_l when there is no confusion.

Given the deployment of AV/AVT lanes and the toll rates on AVT lanes (i.e., given y_l, z_l, and τ_l), the flow distribution of HVs and AVs can be described by the following UE conditions:

$$\boldsymbol{\Delta x}^{w,m} = \boldsymbol{E}^{w} q^{w,m} \qquad \forall w \in W, m \in M \qquad (4\text{-}1)$$

$$x_l^m = \sum_{w \in W} x_l^{w,m} \qquad \forall l \in L, m \in M \qquad (4\text{-}2)$$

$$\sum_{w \in W} x_l^{w,h} \le G z_l \qquad \forall l \in \hat{L} \qquad (4\text{-}3)$$

$$\sum_{m \in M} \sum_{w \in W} x_l^{w,m} \le G y_l \qquad \forall l \in \hat{L} \qquad (4\text{-}4)$$

$$x_l^{w,m} \ge 0 \qquad \forall l \in L, w \in W, m \in M \qquad (4\text{-}5)$$

$$\left(t_l(v_l) + \rho_i^{w,m} - \rho_j^{w,m}\right) x_l^{w,m} = 0 \qquad \forall (i,j) = l \in L \backslash \hat{L}, w \in W, m \in M \qquad (4\text{-}6)$$

$$t_l(v_l) + \rho_i^{w,m} - \rho_j^{w,m} \ge 0 \qquad \forall (i,j) = l \in L \backslash \hat{L}, w \in W, m \in M \qquad (4\text{-}7)$$

$$\left(t_l(v_l) + \tau_l + \rho_i^{w,h} - \rho_j^{w,h} + \pi_l + \varpi_l\right) x_l^{w,h} = 0 \qquad \forall (i,j) = l \in \hat{L}, w \in W \qquad (4\text{-}8)$$

$$t_l(v_l) + \tau_l + \rho_i^{w,h} - \rho_j^{w,h} + \pi_l + \varpi_l \ge 0 \qquad \forall (i,j) = l \in \hat{L}, w \in W \qquad (4\text{-}9)$$

$$\left(t_l(v_l) + \rho_i^{w,a} - \rho_j^{w,a} + \varpi_l\right) x_l^{w,a} = 0 \qquad \forall (i,j) = l \in \hat{L}, w \in W \qquad (4\text{-}10)$$

$$t_l(v_l) + \rho_i^{w,a} - \rho_j^{w,a} + \varpi_l \ge 0 \qquad \forall (i,j) = l \in \hat{L}, w \in W \qquad (4\text{-}11)$$

$$\left(\sum_{w \in W} x_l^{w,h} - G z_l\right) \pi_l = 0 \qquad \forall l \in \hat{L}, w \in W \qquad (4\text{-}12)$$

$$\left(\sum_{m \in M} \sum_{w \in W} x_l^{w,m} - G y_l\right) \varpi_l = 0 \qquad \forall l \in \hat{L}, w \in W \qquad (4\text{-}13)$$

$$\pi_l \ge 0 \qquad \forall l \in \hat{L}, w \in W \qquad (4\text{-}14)$$

$$\varpi_l \ge 0 \qquad \forall l \in \hat{L}, w \in W \qquad (4\text{-}15)$$

where G is a sufficiently large positive constant; π_a and ϖ_a are auxiliary variables.

In the above, constraint (4-1) ensures flow balance between each O-D pair; constraint (4-2) aggregates link flows across all O-D pairs; constraint (4-3) prohibits HVs to use AV links; constraint (4-4) makes sure that, a candidate AV/AVT link cannot be

utilized by HVs and AVs if it is only a virtual link, i.e., if $y_l = 0$; constraint (4-5) ensures the non-negativity of link flows; constraints (4-3)-(4-15) make sure that, for each O-D pair, the travel costs on all utilized paths are the same and equal to $\rho_{D(w)}^{w,m} - \rho_{O(w)}^{w,m}$, and less than or equal to those on unutilized paths.

Define a vector $(\boldsymbol{v}, \boldsymbol{x})$, whose feasible region $\bar{\Phi}$ is defined by constraints (4-1)-(4-5). Finding a solution to the system of UE conditions (4-1)-(4-15) is equivalent to solving the following VI:

UE-VI-2:

$$\sum_{w\in W}\sum_{m\in M}\sum_{l\in L\setminus\hat{L}} t_l(v_l^*)\left(x_l^{w,m} - x_l^{w,m*}\right) + \sum_{w\in W}\sum_{l\in\hat{L}}\left[(t_l(v_l^*)+\tau_l)\left(x_l^{w,h} - x_l^{w,h*}\right) + t_l(v_l^*)\left(x_l^{w,a} - x_l^{w,a*}\right)\right] \geq 0, \forall(\boldsymbol{v},\boldsymbol{x}) \in \bar{\Phi}$$

The equivalence can be established by comparing the KKT conditions of the VI with the defined UE conditions (4-1)-(4-15). It can be proved that UE-VI-2 also has unique solution for the aggregate link flow in HVE when the conditions in Proposition 3-4 hold, similar to the situation without AV/AVT lanes.

Again, we solve UE-VI-2 by reformulating it to be the following nonlinear optimization problem via the technique proposed by Aghassi et al. (2006):

UE-NLP-2:

$$\min_{(\boldsymbol{v},\boldsymbol{x},\boldsymbol{\rho},\boldsymbol{\pi},\boldsymbol{\varpi})} \sum_{w\in W}\sum_{m\in M}\sum_{l\in L\setminus\hat{L}} t_l(v_l)x_l^{w,m} + \sum_{w\in W}\sum_{a\in\hat{L}}\left[(t_l(v_l)+\tau_l)x_l^{w,h} + t_l(v_l)x_l^{w,a}\right] - \sum_{w\in W}\sum_{m\in M} q^{w,m}\left(\rho_{D(w)}^{w,m} - \rho_{O(w)}^{w,m}\right) + \sum_{a\in\hat{L}} G z_l \pi_l + \sum_{a\in\hat{L}} G y_l \varpi_l$$

s.t.

$-\rho_i^{w,m} + \rho_j^{w,m} \le t_l(v_l)$ $\forall (i,j) = l \in L \backslash \hat{L}, w \in W, m \in M$

$-\rho_i^{w,h} + \rho_j^{w,h} - \pi_l - \varpi_l \le t_l(v_l) + \tau_l$ $\forall (i,j) = l \in \hat{L}, w \in W$

$-\rho_i^{w,a} + \rho_j^{w,a} - \varpi_l \le t_l(v_l)$ $\forall (i,j) = l \in \hat{L}, w \in W$

$\pi_l \ge 0$ $\forall l \in \hat{L}, w \in W$

$\varpi_l \ge 0$ $\forall l \in \hat{L}, w \in W$

$(\boldsymbol{v}, \boldsymbol{x}) \in \Phi$

The objective function of UE-NLP-2 is to minimize the gap between a primal and duel problem associated with UE-VI-2, and the constraints are those from the primal and duel problems. The optimal solution $(\boldsymbol{v}^*, \boldsymbol{x}^*)$ to UE-NLP-2 solves UE-VI-2 if the gap is zero. UE-NLP-2 can be solved using commercial nonlinear solvers such as CONOPT (Drud, 1994).

4.3 Deployment model

Based on the UE model with AV/AVT lanes, this section investigates the problem of optimally deploying AV/AVT lanes and designing toll rates for AVT lanes. As discussed in Section 3.1.5, when the two conditions in Proposition 3-4 are not satisfied simultaneously, the system performance for a network with mixed HV and AV flows may be non-unique, and consequently, it is difficult to design and evaluate improving strategies for the network. In real-world applications, a plan or design that can optimize the worst-case performance is more robust and preferable for planners, who tend to be risk-averse. Therefore, we propose a robust optimal deployment problem (RODP) of AV/AVT lanes and formulate it as the following min-max program:

RODP:

$$\min_{\boldsymbol{y},\boldsymbol{z},\boldsymbol{\tau}} \max_{\boldsymbol{v},\boldsymbol{x},\boldsymbol{\rho},\boldsymbol{\pi},\boldsymbol{\varpi}} \sum_{l \in L} \sum_{m \in M} t_l(v_l) x_l^m$$

s.t. (4-1)-(4-15)

$$\hat{c}_{\hat{l}}^{h} = \bar{u}_{\hat{l}} + \bar{\sigma}_{\hat{l}} y_{\hat{l}} \qquad \forall \hat{l} \in \hat{L} \qquad (4\text{-}16)$$

$$\hat{c}_{l}^{h} = \bar{u}_{l} - \bar{\sigma}_{l} y_{\hat{l}} \qquad \forall \left[l, \hat{l}\right] \in H \qquad (4\text{-}17)$$

$$\hat{c}_{l}^{h} \geq \bar{\gamma}_{l} \qquad \forall l \in L \qquad (4\text{-}18)$$

$$y_{\hat{l}} \in \{0, 1, \cdots, I_{\hat{l}}\} \qquad \forall \hat{l} \in \hat{L} \qquad (4\text{-}19)$$

$$\tau_{l} \geq 0 \qquad \forall l \in \hat{L} \qquad (4\text{-}20)$$

$$\tau_{l} \leq \tau_{max} \qquad \forall l \in \hat{L} \qquad (4\text{-}21)$$

where $\bar{u}_l$ is the initial capacity of link $l \in L$, $\bar{\sigma}_l$ denotes the per-lane capacity of link $l \in L$, $\bar{\gamma}_l$ is given parameter that represents the minimum capacity required for link $l \in L$, $I_{\hat{l}}$ is a given integer parameter that denotes the maximum number of lanes that can be converted to AV/AVT lanes for candidate link pair $\hat{l} \in \hat{L}$, τ_{max} is the toll rate upper bound. Note that all capacities refer to the traffic capacities when used by pure HV flows, and the per-lane capacities of an AV/AVT link and its paired regular link are thus identical.

In the above, the objective function is to minimize the maximum, or worst-case total system travel time. Constraints (4-1)-(4-15) ensure that the travelers' behavior follows the UE conditions. Constraints (4-16) and (4-17) capture the change of link capacity due to the deployment of AV/AVT lanes for each candidate link $\hat{l} \in \hat{L}$ and its paired regular link $l \in L \backslash \hat{L}$ (here $\left[l, \hat{l}\right] \in H$). Constraint (4-18) ensures that the capacity of a link $l \in L$ is no less than a required minimum capacity. For instance, all of the regular links should have at least one regular lane so that the network is still freely accessible for HV users. Constraint (4-19) specifies that $y_{\hat{l}}$ is an integer variable and no greater than its upper bound $I_{\hat{l}}$. Constraint (4-20) ensures the non-negativity of τ_l. Constraint (4-21) specifies the upper bound of τ_l.

The model RODP can be readily extended to consider the potential construction cost for the deployment of AV and AVT lanes, via adding a term $\varsigma \sum_{l\in\hat{L}} y_l \left((1-z_l)b_l^{AV} + z_l b_l^{AVT}\right)$ to the objective function or adding a budget constraint $\sum_{l\in\hat{L}} y_l \left((1-z_l)b_l^{AV} + z_l b_l^{AVT}\right) \leq B$, where b_l^{AV} represents the cost for converting one regular lane into a dedicated AV lane on link $l \in \hat{L}$, b_l^{AVT} represents the cost for converting one regular lane into an AVT lane on link $l \in \hat{L}$, ς is a conversion factor that converts the total construction cost from a monetary basis to a time basis, and parameter B is the total available budget.

For convenience, let $\Psi(\boldsymbol{y}, \boldsymbol{z}, \boldsymbol{\tau})$ denote the feasible region of the inner problem, or the maximization part of RODP, $\boldsymbol{\psi}$ represent the decision variable vector $(\boldsymbol{v}, \boldsymbol{x}, \boldsymbol{\rho}, \boldsymbol{\pi}, \boldsymbol{\varpi})$, and $\phi(\boldsymbol{\psi})$ denote the objective function. Then the inner problem can be written as:

RODP-IN:

$$\lambda(\boldsymbol{y}, \boldsymbol{z}, \boldsymbol{\tau}) = \max_{\boldsymbol{\psi}} \{\phi(\boldsymbol{\psi}): \boldsymbol{\psi} \in \Psi(\boldsymbol{y}, \boldsymbol{z}, \boldsymbol{\tau})\}$$

Consequently, the RODP can be written as:

$$\min_{\boldsymbol{y},\boldsymbol{z},\boldsymbol{\tau}} \lambda(\boldsymbol{y}, \boldsymbol{z}, \boldsymbol{\tau})$$

s.t. (4-16)-(4-21)

$$\lambda(\boldsymbol{y}, \boldsymbol{z}, \boldsymbol{\tau}) = \max_{\boldsymbol{\psi}} \{\phi(\boldsymbol{\psi}): \boldsymbol{\psi} \in \Psi(\boldsymbol{y}, \boldsymbol{z}, \boldsymbol{\tau})\}$$

RODP is also a generalized semi-infinite min-max problem (see, e.g., Polak and Royset, 2005), which is not easy to solve. We adopt the genetic-algorithm-based approach proposed in Chapter 3 to solve it.

4.4 Solution algorithm

The genetic-algorithm-based approach mainly includes two modules, i.e., inner problem solution module and genetic algorithm module. The inner problem solution module is designed based on the algorithm proposed by Lawphongpanich and Yin (2010) using manifold suboptimization. The algorithm guarantees convergences to a strongly stationary solution in a finite number of iterations. The genetic algorithm module (including the reproduction, crossover and mutation operations) is adopted to determine the deployment of AV/AVT lanes and the toll rate on AVT lanes.

4.4.1 Inner problem solution module

All complementarity constraints in the inner problem RODP-IN, i.e., constraints (4-3)-(4-15), can be represented by the following generalized form:

$$0 \le F_{ind}(\boldsymbol{x_{ind}}) \perp x_{ind} \ge 0$$

where $\perp$ is the orthogonal sign representing the inner product of two vectors is zero, x_{ind} is a variable with index ind and $F_{ind}(\boldsymbol{x_{ind}})$ is a function of vector $\boldsymbol{x_{ind}}$. To illustrate, for constraints $0 \le \left(t_l(v_l) + \rho_i^{w,m} - \rho_j^{w,m}\right) \perp x_l^{w,m} \ge 0, \forall (i,j) = l \in L \backslash \hat{L}, w \in W, m \in M$, $x_{ind} = x_l^{w,m}$, $ind = (l,w,m)$, and $F_{ind}(\boldsymbol{x_{ind}}) = t_l(v_l) + \rho_i^{w,m} - \rho_j^{w,m}$. For each group of complementarity constraints, we define two index sets Λ_x and $\overline{\Lambda}_x$ to respectively track the component of single variable x_{ind} and formula $F_{ind}(\boldsymbol{x_{ind}})$ required to be zero:

$$\Lambda_x^k = \{ind: x_{ind} = 0\}$$
$$\overline{\Lambda}_x^k = \{ind: F_{ind}(\boldsymbol{x_{ind}}) = 0\}$$

Note that, here superscript k indicates the iteration of the solution procedure, which will be introduced below. Based on Λ_x and $\overline{\Lambda}_x$, a restricted version of RODP-IN, denoted as R-RODP-IN, can be formulated as the following nonlinear programs:

R-RODP-IN:

$$\max_{\boldsymbol{v},\boldsymbol{x},\boldsymbol{\rho},\boldsymbol{\pi},\boldsymbol{\varpi}} \sum_{l\in L}\sum_{m\in M} t_l(v_l)x_l^m$$

s.t. (4-1), (4-2) and

$$\begin{aligned} x_{ind} &= 0 && \forall\, ind \in \Lambda_x^k \\ F_{ind}(\boldsymbol{x_{ind}}) &= 0 && \forall\, ind \in \overline{\Lambda}_x^k \\ x_{ind} &\geq 0 && \forall\, ind \notin \Lambda_x^k \\ F_{ind}(\boldsymbol{x_{ind}}) &\geq 0 && \forall\, ind \notin \overline{\Lambda}_x^k \end{aligned}$$

where $\boldsymbol{x_{ind}} = (\boldsymbol{v}, \boldsymbol{x}, \boldsymbol{\rho}, \boldsymbol{\pi}, \boldsymbol{\varpi})$; the right part of $F_{ind}(\boldsymbol{x_{ind}}) \perp x_{ind}$, i.e., x_{ind}, can be π_l, ϖ_l, $x_l^{w,m}$and each of them has a corresponding $F_{ind}(\boldsymbol{x_{ind}})$.

Given a design for $(\boldsymbol{y}, \boldsymbol{z}, \boldsymbol{\tau})$, the iterative procedure of solving RODP-IN is as follows:

Step 0: Solve the problem UE-NLP-2 and obtain the solution of vector $(\boldsymbol{v}, \boldsymbol{x}, \boldsymbol{\rho}, \boldsymbol{\pi}, \boldsymbol{\varpi})$. Based on the solution, set $k = 1$ and initialize all index sets Λ_x^k and $\overline{\Lambda}_x^k$.

Step 1: Let $(\boldsymbol{v}, \boldsymbol{x}, \boldsymbol{\rho}, \boldsymbol{\pi}, \boldsymbol{\varpi})^k$ solve R-RODP-IN, and obtain the multipliers associated with constraints $x_{ind} = 0$, denoted as g_{ind}^x.

Step 2: Update index sets defined as follows:

$$\Gamma^{x,k} = \{ind \in \Lambda_x^k \cap \overline{\Lambda}_x^k : g_{ind}^x > 0\}$$

If all these index sets are empty, stop and $(\boldsymbol{v}, \boldsymbol{x}, \boldsymbol{\rho}, \boldsymbol{\pi}, \boldsymbol{\varpi})^k$ is strongly stationary. Otherwise, do the following and go to Step 1:

(a) Set

$$\Lambda_x^{k+1} = \Lambda_x^k - \Gamma^{x,k}$$

(b) Set

$\overline{\Lambda}_x^{k+1} = \{ind: F_{ind}(\boldsymbol{x_{ind}}) = 0\}$

(c) Set $k = k + 1$

To solve the problem UE-NLP-2 more efficiently, we propose a technique to avoid using the parameter G, i.e., a sufficiently large positive constant, in the solution procedure. The technique is outlined below:

Check the value of y_l and z_l for each link $l \in \hat{L}$ and do the following:

(a) If $y_l = 0$, set $x_l^{w,m} = 0$, $\forall m \in M, w \in W$.

(b) If $y_l > 0$, set $\varpi_l = 0$.

(c) If $z_l = 0$, set $x_l^{w,h} = 0$, $\forall w \in W$..

(d) If $z_l > 0$, set $\pi_l = 0$.

(e) Remove constraints (4-3) and (4-4) that involves *G*.

(f) Remove the term $\sum_{l \in \hat{L}} G z_l \pi_l + \sum_{l \in \hat{L}} G y_l \varpi_l$ in the objective function of UE-NLP-2.

We briefly explain the rationale of the above technique. First, if $y_l = 0$ for a link $l \in \hat{L}$, the constraint (4-4) for this link can be reduced to $\sum_{m \in M} \sum_{w \in W} x_l^{w,m} \leq 0$, which can further be reduced to $x_l^{w,m} = 0$, $\forall m \in M, w \in W$ given $x_l^{w,m} \geq 0$, $\forall l \in \hat{L}, m \in M, w \in W$. If $y_l > 0$ for an $l \in \hat{L}$, we set the multiplier associated with constraint (4-4), i.e., ϖ_l, to be zero and remove constraint (4-4) for this link l. Note that because the total traffic flow on a link is upper bounded by the total travel demand between all O-D pairs,

i.e., $\sum_{m\in M}\sum_{w\in W} x_l^{w,m} \le \sum_{m\in M}\sum_{w\in W} q^{w,m}$, we can always make constraint (4-4) unbinding by choosing a sufficiently large constant G when $y_l > 0$, consequently constraint (4-4) for a link $l \in \hat{L}$ with $y_l > 0$ can be safely removed without affecting the solution of the problem UE-NLP-2. Similarly, if $z_l = 0$ for a link $l \in \hat{L}$, the constraint (4-3) for this link can be reduced to $\sum_{w\in W} x_l^{w,h} \le 0$, which can further be reduced to $x_l^{w,h} = 0, \forall w \in W$ given $x_l^{w,h} \ge 0, \forall l \in \hat{L}, w \in W$. If $z_l > 0$ for an $l \in \hat{L}$, we set the multiplier associated with constraint (4-3), i.e., π_l, to be zero and remove constraint (4-3) for this link l. Again, because the total HV flow on a link is upper bounded by the total HV demand between all O-D pairs, i.e., $\sum_{w\in W} x_l^{w,h} \le \sum_{w\in W} q^{w,h}$, we can always make constraint (4-3) unbinding by choosing a sufficiently large constant G when $z_l > 0$, consequently constraint (4-3) for a link $l \in \hat{L}$ with $z_l > 0$ can be safely removed without affecting the solution of the problem UE-NLP-2. Under the above settings, for any link $l \in \hat{L}$, either $y_l = 0$ or $\varpi_l = 0$ and either $z_l = 0$ or $\pi_l = 0$, consequently the term $\sum_{l\in\hat{L}} G z_l \pi_l + \sum_{l\in\hat{L}} G y_l \varpi_l$ will always be zero.

4.4.2 Genetic algorithm module

The decision variables of the outer problem, i.e., $\boldsymbol{y} = \{y_l | l \in \hat{L}\}$, $\boldsymbol{z} = \{z_l | l \in \hat{L}\}$, and $\boldsymbol{\tau} = \{\tau_l | l \in \hat{L}\}$ is coded as a chromosome $\boldsymbol{p} = \{p_n | n = 1, 2, \dots, 3 \times |\hat{L}|\}$ (see Figure 4-3). A group of chromosomes is first generated randomly. Following the evaluation, selection, crossover, and mutation operations, a new population of chromosomes is generated at each iteration. After a given number of iterations, genetic algorithm will terminate and return the best-found solution. The process is outlined below.

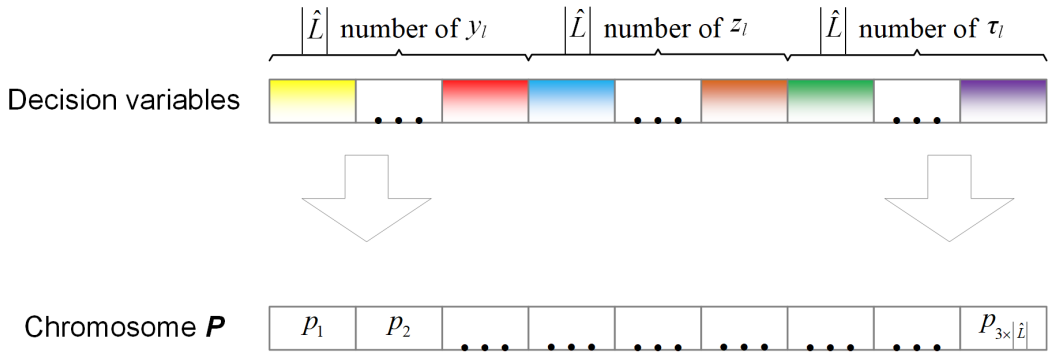

Figure 4-3. Structure of a chromosome (Figure adapted from Yang et al., 2016).

Step 0: Initialize parameters: population size pop_size, crossover probability P_{co}, mutation probability P_{mt}, and maximal number of generations $max\_generation$.

Step 1: Randomly generate pop_size feasible chromosomes as the initial population. Set generation index $g = 1$.

Step 2: Calculate the fitness for all chromosomes by solving the inner problem RODP-IN, and reproduce the population according to the distribution of the fitness values.

Step 3: Carry out the crossover and mutation operations.

Step 4: If $g = max\_generation$, the chromosome with the highest fitness is adopted as the optimal solution of the problem. Else, set $g = g + 1$, and go to Step 2.

4.5 Numerical studies

In this section, two numerical examples are presented to demonstrate the proposed models and algorithms.

4.5.1 The Nguyen-Dupuis network

The following set of tests are conducted on the Nguyen-Dupuis network (Nguyen and Dupuis, 1984). As shown in Figure 4-4, the network consists of 13 nodes, 19 regular links, 19 candidate AV/AVT links, and four O-D pairs. In the travel time function, $\alpha_l = 0.15$ and $\beta_l = 4$. Table 4-2 lists the link input parameters for regular links, including link free flow travel time, initial number of lanes and initial capacity. The per-lane capacity is set to 2000 veh/h, which means $\bar{\eta}_l^{hh} = 1.8$ s, $\forall l \in L$. The minimum capacity for each regular link is set as the per-lane capacity. Table 4-3 shows the link pairs, in which each candidate AV/AVT link is paired with one regular link. A candidate AV/AVT link has the same free flow travel time and per-lane capacity as its paired regular link. The initial capacity and the minimum capacity for each AV/AVT link are set to 0. Note that all the capacities mentioned here refer to the capacities for pure HV flows. The total travel demand between each O-D pair is given by: $q^{1\text{-}2} = 9600\ veh/h$, $q^{1\text{-}3} = 19200\ veh/h$, $q^{4\text{-}2} = 14400\ veh/h$, $q^{4\text{-}3} = 4800\ veh/h$. The AV penetration rates for all O-D pairs are set to 40%. Suppose headway $\bar{\eta}_l^{hh} = \bar{\eta}_l^{ah} = \bar{\eta}_l^{ha} = 1.8$ s, $\bar{\eta}_l^{aa} = \frac{\bar{\eta}_l^{hh}}{2.5} = 0.72$ s, $\forall l \in L$, then HVE_l is given by $HVE_l = 1 - \frac{3}{5} p_l^a, \forall l \in L$. The upper bound of toll rate τ_{max} is set equivalent to 3 minutes.

The genetic-algorithm-based solution procedure was implemented using MATLAB R2018b interfaced with GAMs (Rosenthal, 2012) on a 3.40 GHz Dell Computer with 16 GB of RAM. CONOPT (Drud, 1994) was used to solve the UE-NLP-2 and R-RODP-IN problems. The genetic-algorithm-based procedure was performed with $pop\_size = 30$, $P_{co} = 0.6$, $P_{mt} = 0.15$ and $max\_generation = 120$. Because the inner

problem is a MPCC, using multiple initial solutions to solve it can yield better local optimal solutions. Three different initial solutions were used in solving each inner problem. The computation time thus increased significantly. It took about 2.6 hours to solve the model.

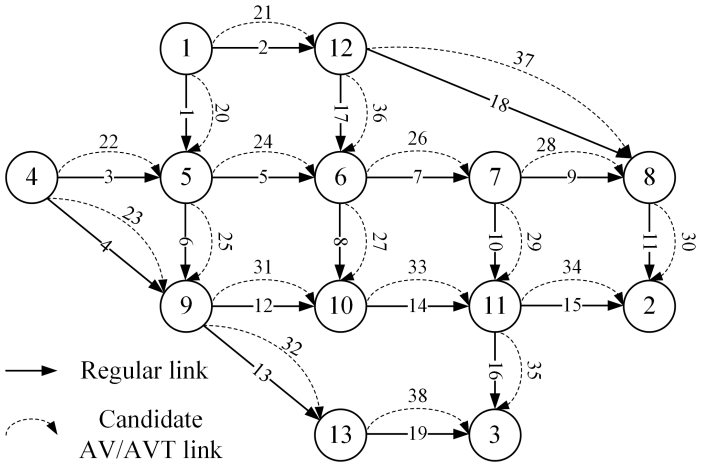

Figure 4-4. Nguyen-Dupuis network with candidate AV/AVT links.

Table 4-2: Link characteristics of the Nguyen-Dupuis network with candidate AV/AVT links

Link	Free-flow travel time $\hat{t}_l$ (min)	Initial number of lanes	Initial capacity $\bar{u}_l$ (veh/h)	Link	Free-flow travel time $\hat{t}_l$ (min)	Initial number of lanes	Initial capacity $\bar{u}_l$ (veh/h)
1-5	7	3	6000	8-2	9	4	8000
1-12	9	4	8000	9-10	10	4	8000
4-5	9	3	6000	9-13	9	2	4000
4-9	12	2	4000	10-11	6	4	8000
5-6	3	3	6000	11-2	7	3	6000
5-9	9	3	6000	11-3	8	4	8000
6-7	5	3	6000	12-6	7	4	8000
6-10	13	4	8000	12-8	14	2	4000
7-8	5	2	4000	13-3	11	2	4000
7-11	9	3	6000				

Table 4-3: Link pairs in the Nguyen-Dupuis network

Pair	Candidate AV/AVT link	Regular link	Pair	Candidate AV/AVT link	Regular link
1	20	1	11	30	11
2	21	2	12	31	12
3	22	3	13	32	13
4	23	4	14	33	14
5	24	5	15	34	15
6	25	6	16	35	16
7	26	7	17	36	17
8	27	8	18	37	18
9	28	9	19	38	19
10	29	10			

The robust deployment plan is shown in Figure 4-5. In total, three dedicated AV links and eight AVT links are deployed. The number of lanes of AV/AVT links, and the toll rates and HV flows (under the worst-case UE) on AVT links are reported in Table 4-4. Toll is only enacted on HVs using AVT lanes and is zero for all other link types. The last column shows the HV flow using AVT links. It can be observed that HVs are willing to pay a toll to access AVT links. Table 4-5 compares the travel times between deployed AVT links and their paired regular links. It can be observed that the travel time difference between an AVT link and its paired regular link is equal to the toll rate on the AVT link. This result verifies that for a HV using a AVT link, the total travel costs (including travel time and toll) on the AVT link and on its paired regular link are identical.

Table 4-4: Robust optimal deployment of AV/AVT lanes in the Nguyen-Dupuis network

Selected candidate links	Optimal deployment type	Number of lanes	HV toll	HV flow
21	AVT	2	2.96	751.9
22	AV	1	-	-
24	AVT	1	2.69	255.4
26	AV	2	-	-
27	AVT	1	0.46	1227.2

29	AVT	2	0.59	593.5
30	AVT	3	2.46	3174.9
31	AVT	2	1.84	2732.5
32	AVT	1	2.91	3061.6
35	AVT	2	2.09	1480.3
36	AV	1	-	-

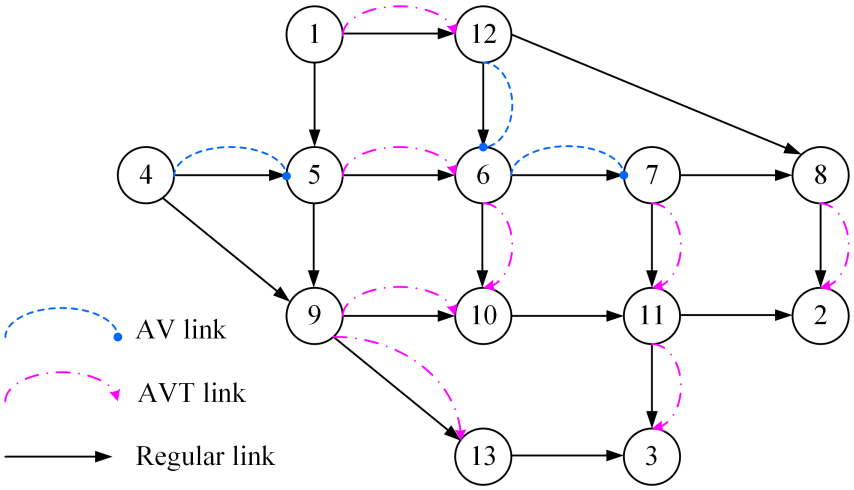

Figure 4-5. Robust optimal deployment of AV/AVT lanes in the Nguyen-Dupuis network.

Table 4-5: Travel time comparison between AVT links and their paired regular links

Pair	AVT link	Regular link	Travel time on AVT link (min)	Travel time on regular link (min)	Travel time difference (min)	Toll on AVT link (min)
2	21	2	14.90	17.86	2.96	2.96
5	24	5	7.10	9.79	2.69	2.69
8	27	8	13.28	13.73	0.46	0.46
10	29	10	11.73	12.32	0.59	0.59
11	30	11	14.30	16.77	2.46	2.46
12	31	12	10.33	12.17	1.84	1.84
13	32	13	16.41	19.33	2.91	2.91
16	35	16	14.45	16.53	2.09	2.09

Table 4-6 compares the system performance of the Nguyen-Dupuis network in the status quo condition (i.e., no AV/AVT links are deployed) and in the robust deployment

plan. It can be observed that the robust deployment plan reduces the worst-case total system travel time from 3,964,807.7 min to 2,956,840.8 min, a reduction of 25.4 percent. We further note that, in the status quo condition, the relative difference between the worst- and best-case total system travel time is 18.31%, while under the robust deployment plan, the relative difference is only 0.02%. With the deployed AV and AVT links, the system performance of the network becomes more stable. The worst-case equilibrium O-D travel costs are compared in Table 4-7. It can be observed that, compared to the status quo condition, the robust deployment plan reduces the worst-case equilibrium O-D travel cost for each O-D pair and for both AVs and HVs. This result implies that it may be possible to realize a Pareto-improving design (Song et al., 2009, 2014; Liu et al., 2009; Guo and Yang, 2010; Lawphongpanich and Yin, 2010) with AV/AVT lanes. Moreover, in the status quo condition, the worst-case equilibrium O-D travel costs for AVs and HVs are identical for each O-D pair, while under the robust deployment plan, the equilibrium O-D travel cost for AVs is less than that for HVs. This result is expected because AVs will always have equal or lower equilibrium travel cost (including travel time and toll) than HVs on deployed AV/AVT links.

We also solved a restricted version of the deployment model, in which only dedicated AV lanes are considered. The deployment plan can only reduce the worst-case system travel time from 3,964,807.7 min to 3,144,559.7 min, a reduction of 20.7 percent. Therefore, compared with the scenario with only dedicated AV lanes, the combination use of AV and AVT lanes brings more reduction to the total system travel time. Note that

the full deployment model will always have equal or better performance than its restricted version as the feasible region of the latter is a subset of the former.

Table 4-6: System performances in status quo condition and robust deployment plan

	Total system travel time (min)		Relative difference
	Worst-case	Best-case	
The status quo	3,964,807.7	3,351,335.0	18.31%
Robust deployment plan	2,956,840.8	2,956,124.5	0.02%

Table 4-7: Comparison of worst-case equilibrium O-D travel costs

O-D	Mode	Travel cost (min)		Travel cost change
		The status quo	Robust deployment plan	
(1, 2)	HV	78.89	61.93	-21.5%
	AV	78.89	56.50	-28.4%
(1, 3)	HV	87.19	67.93	-22.1%
	AV	87.19	62.28	-28.6%
(4, 2)	HV	77.79	60.49	-22.2%
	AV	77.79	55.34	-28.9%
(4, 3)	HV	86.09	66.49	-22.8%
	AV	86.09	61.12	-29.0%

4.5.2 The Sioux Falls network

To further test the proposed model, we solve it for the Sioux Falls network, which consists of 24 nodes, 76 regular links, 20 candidate AV/AVT links as shown in Figure 4-6. In the travel time function, $\alpha_l = 0.15$ and $\beta_l = 4$. Table 4-8 lists the link input parameters for regular links. Again, $\bar{\eta}_l^{hh}$ is assumed to be 1.8 s, which leads to a per-lane capacity of 2000 veh/h when used by pure HVs. The minimum capacity for each regular link is set to the per-lane capacity. The initial capacity and the minimum capacity for each AV/AVT link are set to 0. The total O-D demands for HVs and AVs are listed in Table 4-9. The penetration rate of AVs is assumed to be 40% and identical for all O-D pairs.

Suppose headway $\bar{\eta}_l^{hh} = \bar{\eta}_l^{ah} = \bar{\eta}_l^{ha} = 1.8$ s, $\bar{\eta}_l^{aa} = \frac{\bar{\eta}_l^{hh}}{2.5} = 0.72$ s, $\forall l \in L$, then HVE_l is given by $HVE_l = 1 - \frac{3}{5} p_l^a, \forall l \in L$. The upper bound of toll rate τ_{max} is set is set equivalent to 3 minutes.

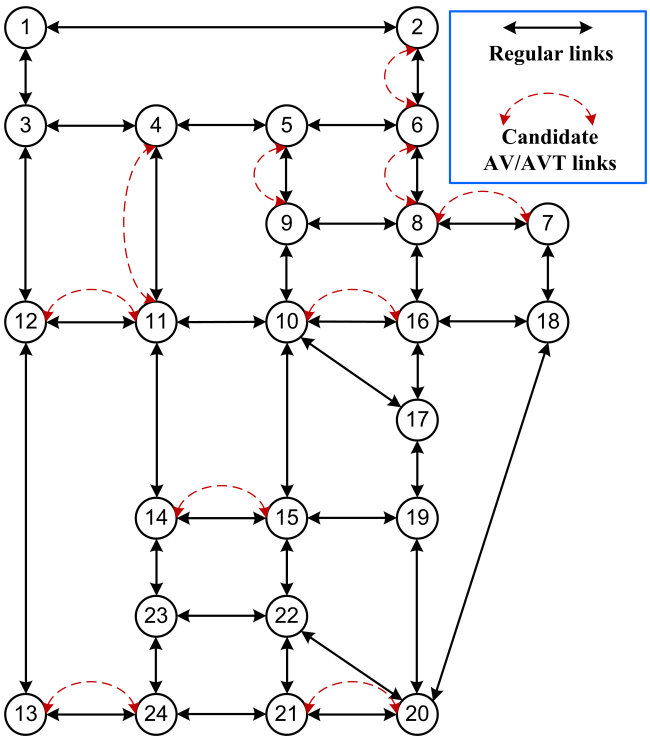

Figure 4-6. Sioux Falls network with candidate AV/AVT links.

Table 4-8: Link characteristics of the Sioux Falls network with candidate AV/AVT links

Link	Free-flow travel time (min)	Initial number of lanes	Initial capacity (veh/h)	Link	Free-flow travel time (min)	Initial number of lanes	Initial capacity (veh/h)
1-2	6	5	10000	13-24	4	3	6000
1-3	4	5	10000	14-11	4	2	4000
2-1	6	5	10000	14-15	3	3	6000
2-6	8	3	6000	14-23	4	2	4000
3-1	4	5	10000	15-10	6	4	8000
3-4	4	4	8000	15-14	3	3	6000

3-12	4	5	10000	15-19	3	4	8000
4-3	4	4	8000	15-22	3	4	8000
4-5	2	4	8000	16-8	5	3	6000
4-11	6	3	6000	16-10	4	3	6000
5-4	2	4	8000	16-17	2	3	6000
5-6	4	2	4000	16-18	3	4	8000
5-9	5	3	6000	17-10	8	2	4000
6-2	8	3	6000	17-16	2	3	6000
6-5	4	2	4000	17-19	2	2	4000
6-8	2	3	6000	18-7	2	5	10000
7-8	3	3	6000	18-16	3	4	8000
7-18	2	5	10000	18-20	14	5	10000
8-6	2	3	6000	19-15	3	4	8000
8-7	3	3	6000	19-17	2	2	4000
8-9	3	2	4000	19-20	4	2	4000
8-16	5	3	6000	20-18	14	5	10000
9-5	5	3	6000	20-19	4	2	4000
9-8	3	2	4000	20-21	6	3	6000
9-10	3	4	8000	20-22	5	3	6000
10-9	3	4	8000	21-20	6	3	6000
10-11	1	3	6000	21-22	2	3	6000
10-15	6	4	8000	21-24	3	2	4000
10-16	4	3	6000	22-15	3	4	8000
10-17	8	2	4000	22-20	5	3	6000
11-4	6	3	6000	22-21	2	3	6000
11-10	1	3	6000	22-23	4	2	4000
11-12	6	3	6000	23-14	4	2	4000
11-14	4	2	4000	23-22	4	2	4000
12-3	4	5	10000	23-24	2	3	6000
12-11	6	3	6000	24-13	4	3	6000
12-13	3	5	10000	24-21	3	2	4000
13-12	3	5	10000	24-23	2	3	6000

Table 4-9: Total O-D demands of AVs and HVs of the Sioux Falls network (veh/h)

O-D	Demand	O-D	Demand	O-D	Demand	O-D	Demand
1-6	5000	6-15	3000	11-1	5000	21-7	1000
1-7	5000	6-21	3000	11-6	3000	21-11	2000
1-11	5000	7-1	5000	11-7	5000	21-15	3000
1-15	5000	7-6	2000	11-21	2000	15-1	5000
1-21	2000	7-11	5000	11-15	3000	15-6	3000
6-1	5000	7-21	4000	21-1	2000	15-7	3000

6-11	3000	7-15	3000	21-6	3000	15-11	3000

The genetic-algorithm-based procedure is performed with $pop\_size = 30$, $P_{co} = 0.6$, $P_{mt} = 0.15$ and $max\_generation = 120$. Three different initial solutions were used in solving each inner problem. It took 70.5 hours to solve the model. Although not particularly efficient, the generic-algorithm-based procedure generated reasonable solutions. The robust deployment plan is listed in Table 4-10. Compared to the status quo condition, the robust deployment plan reduces the worst-case total system travel time from 7,812,395.3 minutes to 6,840,264.9 minutes, a reduction of 12.4 percent.

Table 4-10: Robust deployment of AV/AVT lanes for the Sioux Falls network

Selected candidate links	Optimal deployment type	Number of lanes	HV toll	HV flows
2-6	AVT	1	1.84	579
6-2	AVT	1	2.74	510
4-11	AV	1	-	-
6-8	AVT	1	2.57	98
8-6	AV	1	-	-
7-8	AVT	1	1.65	478
8-7	AVT	2	2.50	2554
10-16	AVT	2	2.24	2819
12-11	AV	1	-	-
15-14	AVT	2	0.20	1427
24-13	AVT	2	2.78	1049
13-24	AV	1	-	-

4.6 Summary

This chapter investigated the strategic development of AV and AVT lanes in transportation networks with mixed AV and HV flows. Different from dedicated AV lanes that can only be used by AVs, AVT lanes allow HVs to use by paying tolls. AVT

lanes provide a promising alternative to dedicated AV lanes when AV flows are low. A UE model was first formulated to describe the flow distributions of AVs and HVs. It was found that with different time headway patterns in mixed AV and HV flows, the UE problem might have unique or non-unique flow patterns. Because the UE problem may have non-unique flow distributions, a robust optimal deployment model is proposed to deploy AV and AVT lanes so that the system performance under the worst-case flow distributions is optimized. The robust model is a generalized semi-infinite min-max problem, which is not easy to solve. A genetic-algorithm-based approach was proposed for its solution in the present study. The Nguyen-Dupuis network and the Sioux Falls network were used for the numerical demonstration of the proposed AV and AVT lane deployment models. The results demonstrate that AV and AVT lanes can significantly improve the system performance.

CHAPTER 5

STRATEGIC PLANNING OF AUTOMATED ROADS FOR INFRASTRUCTURE-ENABLED AUTONOMOUS VEHICLES

Although autonomous vehicle (AV) technology is expected to bring dramatic societal, environmental, and economic benefits, the high cost of AVs and the liability threats facing AV makers may slow the development and adoption of AVs. This chapter explored an infrastructure-enabled autonomous driving system, which is a potential remedy to the cost and liability issues. The system combines vehicles and infrastructure in the realization of autonomous driving. Equipped with roadside sensor and control systems, a regular road can be upgraded into an automated road providing autonomous driving service to vehicles. Vehicles only need to carry minimum required on-board devices to enable their autonomous driving on an automated road. The costs of vehicles can thus be significantly reduced. Moreover, the liability associated with autonomous driving can now be shared by vehicle makers, infrastructure providers, and/or some third-party players. This chapter developed a modeling framework for the evaluation and planning of the infrastructure-enabled autonomous driving system. The authors envision there will be three types of vehicles: human-driven vehicles (HVs) that can only be driven by human drivers, infrastructure-independent autonomous vehicles (IIAVs) that can be driven autonomously on any roads, and infrastructure-enabled autonomous vehicles (IEAVs) that can be driven autonomously on automated roads but must be driven by human drivers on regular roads. A network equilibrium model is first developed to describe both road users' vehicle type choice and route choice behaviors in

a network with automated roads. Based on the established network equilibrium conditions, the optimal deployment problem of automated roads is then formulated as a mathematical program with complementarity constraints (MPCC) and solved by an efficient algorithm. Numerical studies are presented to demonstrate the proposed models. The results show that the infrastructure-enabled autonomous driving system is promising in promoting the adoption and benefit realization of autonomous driving technology. Lastly, several extensions of the proposed models are briefly discussed.

5.1 Network equilibrium model

In this section, a set of UE conditions is first proposed to describe the route choice behaviors of HVs, IEAVs, and IIAVs in a transportation network with automated roads. A multinomial logit model is then adopted to model the vehicle type choice behaviors of road users. Finally, a variational inequality model is developed to simultaneously capture the route choice and vehicle type choice behaviors of road users. For the convenience of readers, frequently used notations are listed below.

Sets	**Description**
N	Set of nodes, indexed by i, j
L	Set of links, indexed by $l = (i, j)$
$\hat{L}$	Set of automated links
W	Set of O-D pairs, indexed by w
M	Set of vehicles classes, indexed by $m = h, a, \tilde{a}$
Parameters	**Description**
q^w	Total travel demand for O-D pair $w \in W$ by all classes
$\hat{t}_l$	Free flow travel time of link $l \in L$
η_{HV}	Average headway of HVs
η_{AV}	Average headway of autonomous driving vehicles
c_l^{HV}	The base capacity of link l when used by pure HVs

θ	The ratio between the average headway of autonomous driving vehicles and the average headway of HVs, $\theta = \frac{\eta_{AV}}{\eta_{HV}}$
γ^{HV}	Value of time of drivers in human-driven mode
γ^{AV}	Value of time of drivers in autonomous driving mode
p^m	Purchasing price of vehicle type m
l^m	Life time of vehicle type m
ϕ	Annual average number of trips made by each driver
ζ_p, ζ_t	Coefficients for vehicle purchase cost and travel cost in utility definition model
ζ_0^m	Vehicle-specific constant in utility definition model
η_l	The cost for converting link l into an automated link
B	Budget
Variables	**Description**
$q^{w,m}$	Travel demand between O-D pair $w \in W$ by class $m \in M$
$x_l^{w,m}$	Traffic flow of class $m \in M$ between O-D pair $w \in W$ on link $l \in L$
x_l^m	Aggregate flow of class $m \in M$ on link $l \in L$
r_l	Percentage of flow of autonomous driving vehicles on link $l \in L$
$c_l(r_l)$	Capacity of link $l \in L$ with r_l percentage of autonomous driving vehicles
t_l	Travel time on link $l \in L$ specified by the link performance function
$\rho_i^{w,m}$	Node potential at node i for class $m \in M$ between O-D pair $w \in W$
$u^{w,m}$	Utility of road users between O-D pair $w \in W$ choosing vehicle type $m \in M$
$\lambda^{w,m}$	The probability of road users between O-D pair w choosing vehicle type m
y_l	A binary variable, representing whether to convert link l into automated link. If yes, $y_l = 1$; otherwise, $y_l = 0$
τ_l	Service charge for IEAV users on link l

5.1.1 UE conditions

In this study, we consider a transportation network with mixed HVs, infrastructure-independent autonomous vehicles (IIAVs), and infrastructure-enabled autonomous vehicles (IEAVs). All vehicles in the network are passenger cars. We envision that a government agency strategically deploys automated roads in a road network. An automated road is equipped with smart roadside devices that have the

functionalities of sensing, communicating, and/or computing and can enable autonomous driving for IEAVs (Gopalswamy and Rathinam, 2018; Nayak et al., 2018). HVs are driven by human drivers on any roads in the network. IIAVs are driven autonomously on any roads in the network. IEAVs are driven by human drivers on regular links and will be driven autonomously on automated links. In a traffic flow, an IEAV in human-driven mode is identical to a HV and an IEAV in autonomous driving mode is identical to an IIAV. When travelling between origins and destinations, all road users will selfishly choose their routes to minimize their individual travel costs.

Let $G(N, L)$ denote a directed road network, where N is the set of nodes and L is the set of directed links. Links in the road network are designated by $l \in L$, or represented as node pairs (i, j), where $i, j \in N$. Let $\hat{L}$ represent the set of automated links in the network. Let W denote the set of origin-destination (O-D) pairs. Let $o(w)$ and $d(w)$ represent the origin node and destination node of O-D pair $w \in W$, respectively. Let $M = \{h, a, \tilde{a}\}$ denote the set of vehicle classes, where class h refers to HV, class a refers to IIAV, and class $\tilde{a}$ refers to IEAV. Let $q^{w,m}$ be the demand between O-D pair $w \in W$ by class $m \in M$, and q^w be the total demand between O-D pair $w \in W$ by all classes. In this study, the total demand q^w for each O-D pair is assumed to be known and fixed. Let $x_l^{w,m}$ denote the traffic flow of class $m \in M$ between O-D pair $w \in W$ on link $l \in L$, x_l^m denote the aggregate flow of class $m \in M$ on link $l \in L$.

Let t_l denote the travel time on link l. Assume t_l is given by the well-known Bureau of Public Roads (BPR) travel time function with capacity being a function of the proportion of self-driving vehicles on link $l \in L$:

$$t_l = \hat{t}_l \left[1 + \alpha_l \left(\frac{x_l^h + x_l^a + x_l^{\tilde{a}}}{c_l(r_l)} \right)^{\beta_l} \right] \tag{5-1}$$

where $\hat{t}_l$ represents the free-flow travel time of link $l \in L$; r_l denotes the percentage of flow of autonomous driving vehicles on link $l \in L$; $c_l(r_l)$ represents the capacity of link $l \in L$; and α_l and β_l are two positive parameters. This assumption is also adopted by Levin and Boyles (2015) and more recently by Noruzoliaee et al. (2018).

Compared to vehicles driven by human drivers, vehicles driven automatically by computers can have smaller vehicle spacing, thus can improve road traffic capacity. Results from both simulation (e.g., Shladover et al., 2012; Ntousakis et al., 2015) and analytical modeling (e.g., Levin and Boyles, 2015; van den Berg and Verhoef, 2016) have shown that, in a mixed traffic with HVs and autonomous driving vehicles, road traffic capacity increases significantly with the increase of the proportion of autonomous driving vehicles on the road. On an automated road, both IIAVs and IEAVs are autonomous driving vehicles. On a regular link, however, only IIAVs are autonomous driving vehicles. The percentage of flow of autonomous driving vehicles is given by

$$r_l = \frac{x_l^a + x_l^{\tilde{a}}}{x_l^h + x_l^a + x_l^{\tilde{a}}} \qquad \forall l \in \hat{L} \tag{5-2}$$

$$r_l = \frac{x_l^a}{x_l^h + x_l^a + x_l^{\tilde{a}}} \qquad \forall l \in L \backslash \hat{L} \tag{5-3}$$

For the road traffic capacity $c_l(r_l)$, this chapter adopted a model proposed by Noruzoliaee et al. (2018), which is based on the Greenshields relationship and the following two assumptions: (1) the average vehicle spacing in mixed flow is a weighted average of vehicle spacing with only autonomous driving vehicles and only HVs,

weighted by the proportions of autonomous driving vehicles and HVs in the total flow (Bose and Ioannou, 2003); (2) autonomous driving vehicles and HVs have identical speeds in mixed traffic. The road capacity with mixed traffic, i.e., $c_l(r_l)$, is given as follows:

$$c_l(r_l) = \frac{\eta_{HV}}{\eta_{HV}(1-r_l) + \eta_{AV} r_l} c_l^{HV} \tag{5-4}$$

where h_{HV} is the average headway of HVs, h_{AV} is the average headway of autonomous driving vehicles, and c_l^{HV} is the base capacity with only HVs. Let $\theta = \frac{\eta_{AV}}{\eta_{HV}}$ denote the ratio between the average headway of autonomous driving vehicles and the average headway of HVs. Substituting $\theta = \frac{\eta_{AV}}{\eta_{HV}}$ in equation (5-4) gives

$$c_l(r_l) = \frac{1}{1 - r_l + \theta r_l} c_l^{HV} \tag{5-5}$$

Substituting equations (5-2), (5-3), and (5-5) in equation (5-1) gives

$$t_l = \hat{t}_l \left[1 + \alpha_l \left(\frac{x_l^h + \theta x_l^a + \theta x_l^{\tilde{a}}}{c_l^{HV}} \right)^{\beta_l} \right] \qquad \forall l \in \hat{L} \tag{5-6}$$

$$t_l = \hat{t}_l \left[1 + \alpha_l \left(\frac{x_l^h + \theta x_l^a + x_l^{\tilde{a}}}{c_l^{HV}} \right)^{\beta_l} \right] \qquad \forall l \in L \backslash \hat{L} \tag{5-7}$$

One can see from equation (5-6) that the performance of an automated link $l \in \hat{L}$ (i.e., the average travel time on the link) with x_l^h human-driven vehicles and $x_l^a + x_l^{\tilde{a}}$ autonomous driving vehicles is equivalent to the performance of the link with $x_l^h + \theta x_l^a + \theta x_l^{\tilde{a}}$ pure HV flow. Similarly, one can see from equation (5-7) that the performance of a regular link $l \in L \backslash \hat{L}$ with $x_l^h + x_l^{\tilde{a}}$ human-driven vehicles and x_l^a autonomous driving vehicles is equivalent to the performance of the link with $x_l^h +$

$\theta x_l^a + x_l^{\tilde{a}}$ pure HV flows. The parameter θ can thus be treated as a parameter that converts autonomous driving vehicles into equivalent human-driven vehicles in a mixed flow.

In a network with automated links, the flow distribution of HVs, IIAVs, and IEAVs can be described by the following UE conditions:

(5-6)-(5-7)

$$\boldsymbol{\Delta x}^{w,m} = \boldsymbol{E}^w q^{w,m} \qquad \forall w \in W, m \in M \qquad (5\text{-}8)$$

$$x_l^m = \sum_{w \in W} x_l^{w,m} \qquad \forall l \in L, m \in M \qquad (5\text{-}9)$$

$$x_l^{w,m} \geq 0 \qquad \forall l \in L, w \in W, m \in M \qquad (5\text{-}10)$$

$$\left(\gamma^{HV} t_l + \rho_i^{w,h} - \rho_j^{w,h}\right) x_l^{w,h} = 0 \qquad \forall (i,j) = l \in L, w \in W \qquad (5\text{-}11)$$

$$\gamma^{HV} t_l + \rho_i^{w,h} - \rho_j^{w,h} \geq 0 \qquad \forall (i,j) = l \in L, w \in W \qquad (5\text{-}12)$$

$$\left(\gamma^{AV} t_l + \rho_i^{w,a} - \rho_j^{w,a}\right) x_l^{w,a} = 0 \qquad \forall (i,j) = l \in L, w \in W \qquad (5\text{-}13)$$

$$\gamma^{AV} t_l + \rho_i^{w,a} - \rho_j^{w,a} \geq 0 \qquad \forall (i,j) = l \in L, w \in W \qquad (5\text{-}14)$$

$$\left(\gamma^{HV} t_l + \rho_i^{w,\tilde{a}} - \rho_j^{w,\tilde{a}}\right) x_l^{w,\tilde{a}} = 0 \qquad \forall (i,j) = l \in L \backslash \hat{L}, w \in W \qquad (5\text{-}15)$$

$$\gamma^{HV} t_l + \rho_i^{w,\tilde{a}} - \rho_j^{w,\tilde{a}} \geq 0 \qquad \forall (i,j) = l \in L \backslash \hat{L}, w \in W \qquad (5\text{-}16)$$

$$\left(\gamma^{AV} t_l + \rho_i^{w,\tilde{a}} - \rho_j^{w,\tilde{a}}\right) x_a^{w,3} = 0 \qquad \forall (i,j) = l \in \hat{L}, w \in W \qquad (5\text{-}17)$$

$$\gamma^{AV} t_l + \rho_i^{w,\tilde{a}} - \rho_j^{w,\tilde{a}} \geq 0 \qquad \forall (i,j) = l \in \hat{L}, w \in W \qquad (5\text{-}18)$$

where $\boldsymbol{\Delta}$ is the node-link incidence matrix associated with the network; $\boldsymbol{x}^{w,m}$ is the vector of $\{\cdots, x_l^{w,m}, \cdots\}$; $\boldsymbol{E}^w$ represents an "input-output" vector, which has exactly two non-zero components: one has the value 1 corresponding to the origin node $o(w)$ and the other has the value -1 corresponding to the destination node $d(w)$; γ^{HV} and γ^{AV} represent the value of time of drivers in human-driven mode and in autonomous driving mode, respectively; $\rho_i^{w,m}$ is an auxiliary variable representing the node potential.

In the above, constraints (5-6)-(5-7) are definitional constraints; constraint (5-8) ensures flow balance between each O-D pair for each class; constraint (5-9) is a

definitional constraint; constraint (5-10) describes the non-negativity of link flows; constraints (5-10)-(5-18) makes sure that, for the same class between each O-D pair, the travel costs on all utilized paths are the same and equal to $\rho_{d(w)}^{w,m} - \rho_{o(w)}^{w,m}$, and less than or equal to those on unutilized paths. Note that the travel costs are all in monetary unit.

5.1.2 Road users' vehicle type choice

Road users' vehicle type choice is modeled using a multinomial logit model. Constraint (5-19) specifies the probability of road users between O-D pair w choosing vehicle type m following the logit function, where $\lambda^{w,m}$ represents the probability of road users between O-D pair w choosing vehicle type m and $u^{w,m}$ denotes the utility of road users between O-D pair w choosing vehicle type m. Note that the scale factor is normalized to 1 in the logit model. The utility $u^{w,m}$ is defined in constraint (5-20), where p^m and l^m are respectively purchasing price and life time of vehicle type m, ϕ is the annual average number of trips made by each driver, $\rho_{d(w)}^{w,m} - \rho_{o(w)}^{w,m}$ is the equilibrium travel cost of road users between O-D pair w choosing vehicle type m, ζ_p and ζ_t are respectively the coefficients for vehicle purchase cost and travel cost, and ζ_0^m is a vehicle-specific constant that encapsulates all "hidden" attributes. Note that $\frac{p^m}{\phi l^m}$ represents vehicle's capital cost per trip, and that we assume the equilibrium travel cost $\rho_{d(w)}^{w,m} - \rho_{o(w)}^{w,m}$ can represent the average travel cost for all the trips made by a road user. In addition, coefficients ζ_p and ζ_t should have a negative sign. Similar utility definition has been adopted by the studies of Nie et al. (2016) and Liu and Wang (2017) to model road users' choice of different type of electric vehicles. Finally, constraint (5-21)

calculates the demand of road users between O-D pair w using vehicle type m, i.e., $q^{w,m}$. We note that users may also consider other vehicle or trip related costs when choosing vehicle types, such as government subsidy, auto insurance and parking cost. For simplicity and to highlight the price and travel cost differences, this study assumes that all other vehicle or trip related costs are identical for the three types of vehicles. The utility model (5-20) can be readily extended to consider government subsidy, auto insurance and parking cost, via adding corresponding terms to the model.

$$\lambda^{w,m} = \frac{\exp(u^{w,m})}{\sum_{m' \in W} \exp\left(u^{w,m'}\right)} \qquad \forall w \in W, m \in M \qquad (5\text{-}19)$$

$$u^{w,m} = \frac{\zeta_p p^m}{\phi l^m} + \zeta_t\left(\rho^{w,m}_{d(w)} - \rho^{w,m}_{o(w)}\right) + \zeta_0^m \qquad \forall w \in W, m \in M \qquad (5\text{-}20)$$

$$q^{w,m} = q^w \lambda^{w,m} \qquad \forall w \in W, m \in M \qquad (5\text{-}21)$$

5.1.3 Variational inequality formulation

The multi-class network equilibrium model, i.e., equations (5-6)-(5-21), can be formulated as a variational inequality. For this purpose, we define a vector $(\boldsymbol{x}, \boldsymbol{q})$, whose feasible region Φ is defined by constraints (5-6)-(5-10) and the following constraint:

$$\sum_{m \in M} q^{w,m} = q^w \qquad \forall w \in W, m \in M \qquad (5\text{-}22)$$

Proposition 5-1. The network equilibrium conditions (5-6)-(5-21) are equivalent to finding the solution to the following variational inequality (VI).

NE-VI:

$$\sum_{w\in W}\sum_{l\in L}\left[\gamma^{HV}t_l^*\left(x_l^{w,h}-x_l^{w,h*}\right)+\gamma^{AV}t_l^*\left(x_l^{w,a}-x_l^{w,a*}\right)\right]+\sum_{w\in W}\sum_{l\in L\setminus\hat{L}}\gamma^{HV}t_l^*\left(x_l^{w,\tilde{a}}-x_l^{w,\tilde{a}*}\right)$$
$$+\sum_{w\in W}\sum_{l\in\hat{L}}\gamma^{AV}t_l^*\left(x_l^{w,\tilde{a}}-x_l^{w,\tilde{a}*}\right)$$
$$-\sum_{w\in W}\sum_{m\in M}\frac{1}{\zeta_t}\left(ln\,q^{w,m*}-\zeta_0^m-\frac{\zeta_p p^m}{\phi l^m}\right)\left(q^{w,m}-q^{w,m*}\right)\geq 0,\forall(\boldsymbol{x},\boldsymbol{q})\in\Phi$$

The equivalence can be established by deriving the Karush-Kuhn-Tucker (KKT) conditions of the above VI and comparing them with the multi-class user equilibrium conditions. See Appendix A for the proof.

Proposition 5-2. There exists a solution to the problem NE-VI.

Proof. Because the total demand of HVs, IIAVs and IEAVs is fixed and finite, all link flows must be bounded from the above. Therefore, Φ is a compact and convex set. In addition, all functions of the VI formulation are continuous. According to the theory of the VI problem (see, e.g., Hartman and Stampacchia, 1966; Harker and Pang, 1990), the VI has at least one solution. □

The proposed network equilibrium model has two special characteristics: First, the travel time function has different structures for regular links and automated links (i.e., the difference of equations (5-6) and (5-7)); Second, the value of time for IEAV users are different on regular links and automated links. These two special characteristics make it non-trivial to discuss the uniqueness of NE-VI. In this paper, we will only briefly discuss the solution uniqueness for link travel time t_a and O-D travel demand by class $q^{w,m}$ under three special cases. We leave the work of further investigating the uniqueness of

NE-VI to our future study. Note that unique solution for link travel time means unique solution for equilibrium O-D travel cost.

Proposition 5-3. The solution of link travel time and O-D travel demand by class to the NE-VI, i.e., t_l^* and $q^{w,m*}$, is unique if one of the follow conditions is satisfied:

(a) All links are regular links, i.e., $\hat{L} = \emptyset$;

(b) All links are automated links, i.e., $\hat{L} = L$;

(c) The ratio between the value of time in autonomous driving mode and the value of time in human-driven mode is equal to the ratio between the average head way of autonomous driving vehicles and the average headway of human-driven vehicles, i.e., $\frac{\gamma^{AV}}{\gamma^{HV}} = \theta$.

Proof. Define a new variable v_l as follows:

$$v_l = x_l^h + \theta x_l^a + \theta x_l^{\tilde{a}} \qquad \forall l \in \hat{L} \qquad (5\text{-}23)$$

$$v_l = x_l^h + \theta x_l^a + x_l^{\tilde{a}} \qquad \forall l \in L \backslash \hat{L} \qquad (5\text{-}24)$$

then the travel time function (6)-(7) can be rewritten as

$$t_l(v_l) = \hat{t}_l \left[1 + \alpha_l \left(\frac{v_l}{c_l^{HV}} \right)^{\beta_l} \right] \qquad \forall l \in L \qquad (5\text{-}25)$$

(a) If $\hat{L} = \emptyset$, we reformulate the NE-VI as the following equivalent VI:

$$\sum_{w \in W} \sum_{l \in L} \left[t_l(v_l^*) \left(x_l^{w,h} - x_l^{w,h*} \right) + t_l(v_l^*) \theta \left(x_l^{w,a} - x_l^{w,a*} \right) + t_l(v_l^*) \left(x_l^{w,\tilde{a}} - x_l^{w,\tilde{a}*} \right) \right]$$
$$- \sum_{w \in W} \sum_{m \in M} \frac{1}{\zeta_t} \left(ln\, q^{w,m*} - \zeta_0^m - \frac{\zeta_p p^m}{\phi l^m} \right) (q^{w,m} - q^{w,m*}) \geq 0, \forall (\boldsymbol{x}, \boldsymbol{q})$$
$$\in \Phi \text{ and } v_l \text{ and } t_l(v_l) \text{ are defined by constraints } (5-23)\text{-}(5-25)$$

The equivalence can be easily proved through comparing their KKT conditions.

Suppose that $(\boldsymbol{v}^*, \boldsymbol{x}^*, \boldsymbol{q}^*)$ and $(\boldsymbol{v}^\dagger, \boldsymbol{x}^\dagger, \boldsymbol{q}^\dagger)$ are two solutions of the above VI, then

$$\sum_{w\in W}\sum_{l\in L}\left[t_l(v_l^*)\left(x_l^{w,h\dagger}-x_l^{w,h*}\right)+t_l(v_l^*)\theta\left(x_l^{w,a\dagger}-x_l^{w,a*}\right)+t_l(v_l^*)\left(x_l^{w,\tilde{a}\dagger}-x_l^{w,\tilde{a}*}\right)\right] - \sum_{w\in W}\sum_{m\in M}\frac{1}{\zeta_t}\left(ln\, q^{w,m*}-\zeta_0^m-\frac{\zeta_p p^m}{\phi l^m}\right)\left(q^{w,m\dagger}-q^{w,m*}\right)\geq 0$$

$$\sum_{w\in W}\sum_{l\in L}\left[t_l\left(v_l^\dagger\right)\left(x_l^{w,h*}-x_l^{w,h\dagger}\right)+t_l\left(v_l^\dagger\right)\theta\left(x_l^{w,a*}-x_l^{w,a\dagger}\right)+t_l\left(v_l^\dagger\right)\left(x_l^{w,\tilde{a}*}-x_l^{w,\tilde{a}\dagger}\right)\right] - \sum_{w\in W}\sum_{m\in M}\frac{1}{\zeta_t}\left(ln\, q^{w,m\dagger}-\zeta_0^m-\frac{\zeta_p p^m}{\phi l^m}\right)\left(q^{w,m*}-q^{w,m\dagger}\right)\geq 0$$

and consequently

$$\sum_{w\in W}\sum_{l\in L}\left(t_l\left(v_l^\dagger\right)-t_l(v_l^*)\right)\left(x_l^{w,h\dagger}+\theta x_l^{w,a\dagger}+x_l^{w,\tilde{a}\dagger}-x_l^{w,h*}-\theta x_l^{w,a*}-x_l^{w,\tilde{a}*}\right) - \sum_{w\in W}\sum_{m\in M}\frac{1}{\zeta_t}\left(ln\, q^{w,m\dagger}-ln\, q^{w,m*}\right)\left(q^{w,m\dagger}-q^{w,m*}\right)\leq 0$$

or

$$\sum_{l\in L}\left(t_l\left(v_l^\dagger\right)-t_l(v_l^*)\right)\left(v_l^\dagger-v_l^*\right)-\sum_{w\in W}\sum_{m\in M}\frac{1}{\zeta_t}\left(ln\, q^{w,m\dagger}-ln\, q^{w,m*}\right)\left(q^{w,m\dagger}-q^{w,m*}\right) \leq 0$$

Because $t_l(v_l)$ is a strictly increasing function of v_l and $\frac{-1}{\zeta_t}\ln q^{w,m}$ is a strictly increasing function of $q^{w,m}$, the above inequality implies that $v_l^\dagger = v_l^*$ and $q^{w,m\dagger} = q^{w,m*}$, or v_l^* and $q^{w,m*}$ are unique. Unique v_l^* further implies t_l^* is unique.

(b) If $\hat{L} = L$, we reformulate the NE-VI as the following equivalent VI:

$$\sum_{w\in W}\sum_{l\in L}\left[t_l(v_l^*)\left(x_l^{w,h}-x_l^{w,h*}\right)+t_l(v_l^*)\theta\left(x_l^{w,a}-x_l^{w,a*}\right)+t_l(v_l^*)\theta\left(x_l^{w,\tilde{a}}-x_l^{w,\tilde{a}*}\right)\right]$$
$$-\sum_{w\in W}\sum_{m\in M}\frac{1}{\zeta_t}\left(\ln q^{w,m*}-\zeta_0^m-\frac{\zeta_p p^m}{\phi l^m}\right)\left(q^{w,m}-q^{w,m*}\right)\geq 0,\forall(\boldsymbol{x},\boldsymbol{q})$$
$$\in \Phi \text{ and } v_l \text{ and } t_l(v_l) \text{ are defined by constraints } (5-23)\text{-}(5-25)$$

The equivalence can be easily proved through comparing their KKT conditions.

Suppose that $(\boldsymbol{v}^*,\boldsymbol{x}^*,\boldsymbol{q}^*)$ and $(\boldsymbol{v}^\dagger,\boldsymbol{x}^\dagger,\boldsymbol{q}^\dagger)$ are two solutions of the above VI, then

$$\sum_{w\in W}\sum_{l\in L}\left[t_l(v_l^*)\left(x_l^{w,h\dagger}-x_l^{w,h*}\right)+t_l(v_l^*)\theta\left(x_l^{w,a\dagger}-x_l^{w,a*}\right)+t_l(v_l^*)\theta\left(x_l^{w,\tilde{a}\dagger}-x_l^{w,\tilde{a}*}\right)\right]$$
$$-\sum_{w\in W}\sum_{m\in M}\frac{1}{\zeta_t}\left(\ln q^{w,m*}-\zeta_0^m-\frac{\zeta_p p^m}{\phi l^m}\right)\left(q^{w,m\dagger}-q^{w,m*}\right)\geq 0$$
$$\sum_{w\in W}\sum_{l\in L}\left[t_l\left(v_l^\dagger\right)\left(x_l^{w,h*}-x_l^{w,h\dagger}\right)+t_l\left(v_l^\dagger\right)\theta\left(x_l^{w,a*}-x_l^{w,a\dagger}\right)+t_l\left(v_l^\dagger\right)\theta\left(x_l^{w,\tilde{a}*}-x_l^{w,\tilde{a}\dagger}\right)\right]$$
$$-\sum_{w\in W}\sum_{m\in M}\frac{1}{\zeta_t}\left(\ln q^{w,m\dagger}-\zeta_0^m-\frac{\zeta_p p^m}{\phi l^m}\right)\left(q^{w,m*}-q^{w,m\dagger}\right)\geq 0$$

and consequently

$$\sum_{w\in W}\sum_{l\in L}\left(t_l\left(v_l^\dagger\right)-t_l(v_l^*)\right)\left(x_l^{w,h\dagger}+\theta x_l^{w,a\dagger}+\theta x_l^{w,\tilde{a}\dagger}-x_l^{w,h*}-\theta x_l^{w,a*}-\theta x_l^{w,\tilde{a}*}\right)$$
$$-\sum_{w\in W}\sum_{m\in M}\frac{1}{\zeta_t}\left(\ln q^{w,m\dagger}-\ln q^{w,m*}\right)\left(q^{w,m\dagger}-q^{w,m*}\right)\leq 0$$

or

$$\sum_{l\in L}\left(t_l\left(v_l^\dagger\right)-t_l(v_l^*)\right)\left(v_l^\dagger-v_l^*\right)-\sum_{w\in W}\sum_{m\in M}\frac{1}{\zeta_t}\left(\ln q^{w,m\dagger}-\ln q^{w,m*}\right)\left(q^{w,m\dagger}-q^{w,m*}\right)$$
$$\leq 0$$

Because $t_l(v_l)$ is a strictly increasing function of v_l and $\frac{-1}{\zeta_t}\ln q^{w,m}$ is a strictly increasing function of $q^{w,m}$, the above inequality implies that $v_l^\dagger = v_l^*$ and $q^{w,m\dagger} = q^{w,m*}$, or v_l^* and $q^{w,m*}$ are unique. Unique v_l^* further implies t_l^* is unique.

(c) If $\frac{\gamma^{AV}}{\gamma^{HV}} = \theta$, we reformulate the NE-VI as the following equivalent VI:

$$\sum_{w\in W}\sum_{l\in L}\left[t_l(v_l^*)\left(x_l^{w,h} - x_l^{w,h*}\right) + t_l(v_l^*)\theta\left(x_l^{w,a} - x_l^{w,a*}\right)\right]$$
$$+ \sum_{w\in W}\sum_{l\in L\setminus\hat{L}} t_l(v_l^*)\left(x_l^{w,\tilde{a}} - x_l^{w,\tilde{a}*}\right) + \sum_{w\in W}\sum_{l\in\hat{L}}\frac{\gamma^{AV}}{\gamma^{HV}} t_l(v_l^*)\left(x_l^{w,\tilde{a}} - x_l^{w,\tilde{a}*}\right)$$
$$- \sum_{w\in W}\sum_{m\in M}\frac{1}{\zeta_t}\left(\ln q^{w,m*} - \zeta_0^m - \frac{\zeta_p p^m}{\phi l^m}\right)(q^{w,m} - q^{w,m*}) \geq 0, \forall(\boldsymbol{x},\boldsymbol{q})$$
$$\in \Phi \text{ and } v_l \text{ and } t_l(v_l) \text{ are defined by constraints } (5-23)\text{-}(5-25)$$

The equivalence can be easily proved through comparing their KKT conditions.

Suppose that $(\boldsymbol{v}^*, \boldsymbol{x}^*, \boldsymbol{q}^*)$ and $(\boldsymbol{v}^\dagger, \boldsymbol{x}^\dagger, \boldsymbol{q}^\dagger)$ are two solutions of the above VI, then

$$\sum_{w\in W}\sum_{l\in L}\left[t_l(v_l^*)\left(x_l^{w,h\dagger} - x_l^{w,h*}\right) + t_l(v_l^*)\theta\left(x_l^{w,a\dagger} - x_l^{w,a*}\right)\right]$$
$$+ \sum_{w\in W}\sum_{l\in L\setminus\hat{L}} t_l(v_l^*)\left(x_l^{w,\tilde{a}\dagger} - x_l^{w,\tilde{a}*}\right)$$
$$+ \sum_{w\in W}\sum_{l\in\hat{L}}\frac{\gamma^{AV}}{\gamma^{HV}} t_l(v_l^*)\left(x_l^{w,\tilde{a}\dagger} - x_l^{w,\tilde{a}*}\right)$$
$$- \sum_{w\in W}\sum_{m\in M}\frac{1}{\zeta_t}\left(\ln q^{w,m*} - \zeta_0^m - \frac{\zeta_p p^m}{\phi l^m}\right)(q^{w,m\dagger} - q^{w,m*}) \geq 0$$
$$\sum_{w\in W}\sum_{l\in L}\left[t_l(v_l^\dagger)\left(x_l^{w,h*} - x_l^{w,h\dagger}\right) + t_l(v_l^\dagger)\theta\left(x_l^{w,a*} - x_l^{w,a\dagger}\right)\right]$$
$$+ \sum_{w\in W}\sum_{l\in L\setminus\hat{L}} t_l(v_l^\dagger)\left(x_l^{w,\tilde{a}*} - x_l^{w,\tilde{a}\dagger}\right)$$
$$+ \sum_{w\in W}\sum_{l\in\hat{L}}\frac{\gamma^{AV}}{\gamma^{HV}} t_l(v_l^\dagger)\left(x_l^{w,\tilde{a}*} - x_l^{w,\tilde{a}\dagger}\right)$$
$$- \sum_{w\in W}\sum_{m\in M}\frac{1}{\zeta_t}\left(\ln q^{w,m\dagger} - \zeta_0^m - \frac{\zeta_p p^m}{\phi l^m}\right)(q^{w,m*} - q^{w,m\dagger}) \geq 0$$

and consequently

$$\sum_{w\in W}\sum_{l\in L\setminus\hat{L}}\left(t_l(v_l^{\dagger})-t_l(v_l^{*})\right)\left(x_l^{w,h\dagger}+\theta x_l^{w,a\dagger}+x_l^{w,\tilde{a}\dagger}-x_l^{w,h*}-\theta x_l^{w,a*}-x_l^{w,\tilde{a}*}\right)$$
$$+\sum_{w\in W}\sum_{l\in\hat{L}}\left(t_l(v_l^{\dagger})-t_l(v_l^{*})\right)\left(x_l^{w,h\dagger}+\theta x_l^{w,a\dagger}+\frac{\gamma^{AV}}{\gamma^{HV}}x_l^{w,\tilde{a}\dagger}-x_l^{w,h*}\right.$$
$$\left.-\theta x_l^{w,a*}-\frac{\gamma^{AV}}{\gamma^{HV}}x_l^{w,\tilde{a}*}\right)$$
$$-\sum_{w\in W}\sum_{m\in M}\frac{1}{\zeta_t}(\ln q^{w,m\dagger}-\ln q^{w,m*})(q^{w,m\dagger}-q^{w,m*})\le 0$$

Based on the definition of v_l and the fact that $\frac{\gamma^{AV}}{\gamma^{HV}}=\theta$, the above equation is equivalent to

$$\sum_{l\in L}\left(t_l(v_l^{\dagger})-t_l(v_l^{*})\right)(v_l^{\dagger}-v_l^{*})-\sum_{w\in W}\sum_{m\in M}\frac{1}{\zeta_t}(\ln q^{w,m\dagger}-\ln q^{w,m*})(q^{w,m\dagger}-q^{w,m*})$$
$$\le 0$$

Because $t_l(v_l)$ is a strictly increasing function of v_l and $\frac{-1}{\zeta_t}\ln q^{w,m}$ is a strictly increasing function of $q^{w,m}$, the above inequality implies that $v_l^{\dagger}=v_l^{*}$ and $q^{w,m\dagger}=q^{w,m*}$, or v_l^{*} and $q^{w,m*}$ are unique. Unique v_l^{*} further implies t_l^{*} is unique. □

5.1.4 Solution algorithm

To solve the NE-VI, we apply the technique developed by Aghassi et al. (2006) using duality to reformulate the NE-VI as the following nonlinear optimization problem:

NE-NLP:

$$\min_{\boldsymbol{x},\boldsymbol{q},\boldsymbol{\rho},\boldsymbol{\pi}} \sum_{w\in W}\sum_{l\in L}\left(\gamma^{HV}t_l x_l^{w,h}+\gamma^{AV}t_l x_l^{w,a}\right)+\sum_{w\in W}\sum_{l\in L\setminus\hat{L}}\gamma^{HV}t_l x_l^{w,\tilde{a}}+\sum_{w\in W}\sum_{l\in\hat{L}}\gamma^{AV}t_l x_l^{w,\tilde{a}} - \sum_{w\in W}\sum_{m\in M}\frac{1}{\zeta_t}\left(ln\, q^{w,m}-\zeta_0^m-\frac{\zeta_p p^m}{\phi l^m}\right)q^{w,m}+\sum_{w\in W}q^w\pi^w$$

s.t.

$$\gamma^{HV}t_l+\rho_i^{w,h}-\rho_j^{w,h}\geq 0 \qquad \forall(i,j)=l\in L, w\in W$$

$$\gamma^{AV}t_l+\rho_i^{w,a}-\rho_j^{w,a}\geq 0 \qquad \forall(i,j)=l\in L, w\in W$$

$$\gamma^{HV}t_l+\rho_i^{w,\tilde{a}}-\rho_j^{w,\tilde{a}}\geq 0 \qquad \forall(i,j)=l\in L\setminus\hat{L}, w\in W$$

$$\gamma^{AV}t_l+\rho_i^{w,\tilde{a}}-\rho_j^{w,\tilde{a}}\geq 0 \qquad \forall(i,j)=l\in \hat{L}, w\in W$$

$$\frac{-1}{\zeta_t}\left(\ln q^{w,m}-\zeta_0^m-\frac{\zeta_p p^m}{\phi l^m}\right)+\pi^w-\boldsymbol{E}^w\boldsymbol{\rho}^{w,m}\geq 0 \qquad \forall w\in W, m\in M$$

$$(\boldsymbol{x},\boldsymbol{q})\in\Phi$$

where π^w is an auxiliary variable.

In solving the above optimization problem, if the optimal value of the objective function is zero, then one part of the optimal solution, $(\boldsymbol{x},\boldsymbol{q})$, would be the solution to the UE-VI problem. Detailed derivation of the NE-NLP can be found in Appendix B. Because the UE-NLP model is a regular nonlinear program, it can be solved using commercial nonlinear solvers such as CONOPT (Drud, 1994).

5.1.5 Numerical examples

Numerical examples in this section are based on the Nguyen-Dupuis network (Nguyen and Dupuis, 1984). As shown in Figure 5-1, the network consists of 13 nodes, 19 links (three of which are automated links), and four O-D pairs. Assume that, in the travel time function, $\alpha_l = 0.15$ and $\beta_l = 4$. Table 5-1 lists the link input parameters for links, including link free flow travel time and base link capacity with only HV flows. The total travel demand between each O-D pair is given by: $q^{1\text{-}2} = 800\ veh/h$, $q^{1\text{-}3} =$

$1600\ veh/h$, $q^{4\text{-}2} = 1200\ veh/h$, $q^{4\text{-}3} = 400\ veh/h$. The ratio between the average headway of autonomous driving vehicles and that of HVs is assumed to be $\theta = 0.4$ (Ghiasi et al., 2017). The value of time of drivers in human-driven mode is assumed to be $\gamma^{HV} = \$7.5/h$.[‡] For drivers in autonomous driving mode, the value of time is assumed to be half of γ^{HV}, i.e., $\gamma^{AV} = 0.5\gamma^{HV} = \$3.75/h$. The purchasing price of HVs is assumed to be $p^h = \$20{,}000$. The purchasing price of IIAVs is assumed to be $p^a = \$57{,}500$, based on the assumption of $37,500 added purchasing price for AV capabilities (Fagnant and Kockelman, 2015). The purchasing price of IEAVs is assumed to be $p^{\tilde{a}} = \$35{,}000$. Further assume all vehicle types have a service life of ten years, i.e., $l^m = 10, m = h, a, \tilde{a}$. The coefficients of purchasing price and travel cost in the vehicle choice model are set as $\zeta_p = \zeta_t = -3$ and assume $\zeta_0^m = 0, m = h, a, \tilde{a}$.[§] The annual number of trips made by each driver is set to be $\phi = 730$ (i.e., two trips per day). Note that the parameter values are for illustration purposes only.

Table 5-1: Link characteristics of the Nguyen-Dupuis network

Link	Free-flow travel time $\hat{t}_l$ (min)	Capacity c_l^{HV} (veh/h)	Link	Free-flow travel time $\hat{t}_l$ (min)	Capacity c_l^{HV} (veh/h)
1-5	7	1020	8-2	9	1500
1-12	9	1860	9-10	10	1980
4-5	9	900	9-13	9	420
4-9	12	420	10-11	6	1980
5-6	3	1260	11-2	7	1380
5-9	9	1380	11-3	8	1620

[‡] The value of time is assumed to be 50% of the hourly wage rate of road users (Concas and Kolpakov, 2009; Zhang et al., 2004). The hourly wage rate is set to be $15/h, which is computed based on the annual average income of $31,128 (Department of Numbers, 2018) and the working time of 52 weeks with 40 hours per week.

[§] In practice, parameters, ζ_0^m, ζ_p, and ζ_t can be calibrated based on empirical behavioral data. The values used here are for illustration purpose only.

6-7	5	1260	12-6	7	1980
6-10	13	1800	12-8	14	420
7-8	5	660	13-3	11	420
7-11	9	1200			

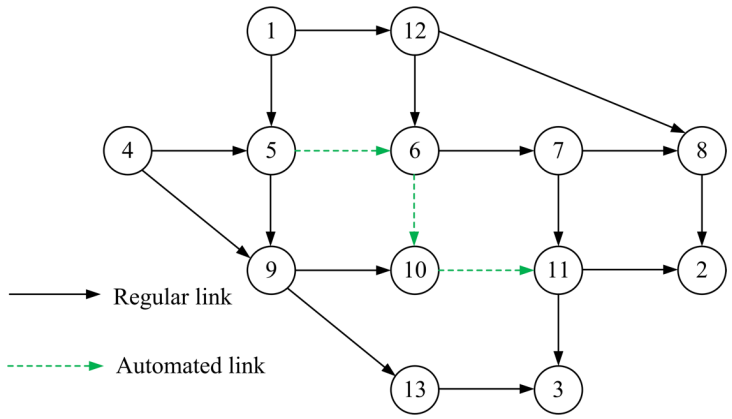

Figure 5-1. Nguyen-Dupuis network with automated links.

The network equilibrium solutions are shown in Table 5-2. From the last two columns in Table 5-2, we can observe that for each O-D pair, HVs have the highest equilibrium demand share, followed by IEAVs, and IIAVs have the smallest demand share of less than 0.1 percent. Although IIAVs have the lowest travel cost among the three vehicle classes, the purchasing price of IIAVs is so high that the utility associated with IIAVs is the lowest, and consequently the demand share of IIAVs is the lowest. Compared to IIAVs, IEAVs have higher travel cost but much lower price. Because the utility associated with IEAVs is higher than IIAVs, IEAVs have higher demand share than IIAVs.

To investigate the impact of purchasing price of IEAVs on the market share of different types of vehicles, six groups of IEAV prices are considered, with p^3 ranging from \$25,000 to \$50,000 with a step size of \$5,000. Table 5-3 lists the equilibrium

market shares under different prices of IEAVs. Note that the last three rows report the total market shares for the whole network. As expected, the total market share of IEAVs for the whole network increases with the decrease of IEAV price. However, the decrease of IEAV price does not necessarily lead to the market share increase for each O-D pair because the utility associated with each class of vehicles depends not only on the price but also on the travel cost. As shown in Table 5-3, for O-D pairs 1-2, 1-3, and 4-2, the market share of IEAVs increases with the decrease of IEAV price. For O-D pair 4-3, the market share of IEAVs increases as the price decreases from \$50,000 to \$35,000, then decreases as the price decreases from \$35,000 to \$30,000, and then increases again as the price decreases from \$30,000 to \$25,000.

Table 5-2: Equilibrium O-D travel cost and demand by class

O-D	Class	Capital cost per trip (\$)	Travel cost (\$)	Utility	Market share (%)	Demand (veh/h)
1-2	1	2.74	5.26	-23.99	83.63	669.02
	2	7.88	2.63	-31.52	0.05	0.36
	3	4.80	3.75	-25.63	16.33	130.62
1-3	1	2.74	5.51	-24.76	83.11	1329.76
	2	7.88	2.76	-31.90	0.07	1.06
	3	4.80	3.99	-26.36	16.83	269.20
4-2	1	2.74	5.30	-24.11	83.62	1003.49
	2	7.88	2.65	-31.58	0.05	0.58
	3	4.80	3.79	-25.74	16.33	195.94
4-3	1	2.74	5.46	-24.59	86.68	346.73
	2	7.88	2.73	-31.82	0.06	0.25
	3	4.80	4.03	-26.48	13.26	53.02

Table 5-3: Equilibrium market shares under different IEAV prices

O-D	Class	Market share (%)					
		$p^{\tilde{a}}$ =\$50,000	$p^{\tilde{a}}$ =\$45,000	$p^{\tilde{a}}$ =\$40,000	$p^{\tilde{a}}$ =\$35,000	$p^{\tilde{a}}$ =\$30,000	$p^{\tilde{a}}$ =\$25,000
1-2	1	99.90	99.57	97.081	83.63	70.52	58.25
	2	0.06	0.06	0.05	0.05	0.02	0.01

	3	0.05	0.38	2.86	16.33	29.46	41.74
1-3	1	99.87	99.54	97.06	83.11	61.36	36.43
	2	0.08	0.08	0.08	0.07	0.03	0.01
	3	0.05	0.38	2.86	16.83	38.61	63.56
4-2	1	99.89	99.56	97.07	83.62	70.52	52.24
	2	0.07	0.07	0.06	0.05	0.02	0.01
	3	0.05	0.38	2.86	16.33	29.46	47.75
4-3	1	99.86	99.53	97.05	86.68	89.53	83.84
	2	0.09	0.09	0.09	0.06	0.02	0.01
	3	0.05	0.38	2.86	13.26	10.45	16.15
Tot al	1	99.88	99.55	97.07	83.73	68.76	50.28
	2	0.07	0.07	0.07	0.06	0.03	0.01
	3	0.05	0.38	2.86	16.22	31.22	49.71

The value of time of road users will also affect the market share of different types of vehicles. We further considered six groups of road users' value of time in human-driven mode, with γ^{HV} ranging from \$5/h to \$17.5/h with a step size of \$2.5/h. Assume that road users' value of time in autonomous driving mode $\gamma^{AV} = 0.5\gamma^{HV}$. The market shares under different γ^{HV} are reported in Table 5-4 and shown in Figure 5-2. Note that the last three rows and Figure 5-2 show the market shares for the whole network. One can observe that the total market shares of both IIAVs and IEAVs increase as γ^{HV} increases from \$5.0/h to \$12.5/h, the total market share of IIAVs continues increasing as γ^{HV} increases from \$12.5/h to \$17.5/h but the total market share of IEAVs decreases as γ^{HV} increases from \$12.5/h to \$17.5/h. The total market share of HVs decreases with the increase of γ^{HV}. Intuitively, drivers will probably save more travel cost from autonomous driving mode with the increase of γ^{HV}. Therefore, the increase of γ^{HV} will probably augment the relative utilities associated with both IIAVs and IEAVs versus HVs (note that the utilities associated with all vehicle classes will probably decrease with the increase of γ^{HV}). Moreover, with the increase of γ^{HV} the relative utility associated with IIAVs will

probably increase faster than that for IEAVs because IIAVs are in autonomous driving mode on any links while IEAVs can only be driven autonomously on automated links.

The changes of market shares for O-D pairs 1-2, 1-3, and 4-2 have a similar trend as the changes of total market shares. For O-D pair 4-3, the market share of IIAVs increases with the increase of γ^{HV}, the market share of IEAVs increases as γ^{HV} increases from \$5.0/h to \$7.5/h and then decreases as γ^{HV} increases from \$7.5/h to \$17.5/h, the market share of HVs first decreases as γ^{HV} increases from \$5.0/h to \$7.5/h then increases as γ^{HV} increases from \$7.5/h to \$12.5/h and then decreases as γ^{HV} increases from \$12.5/h to \$17.5/h. As we can see, the impact of γ^{HV} on the market shares may be uneven among different O-D pairs.

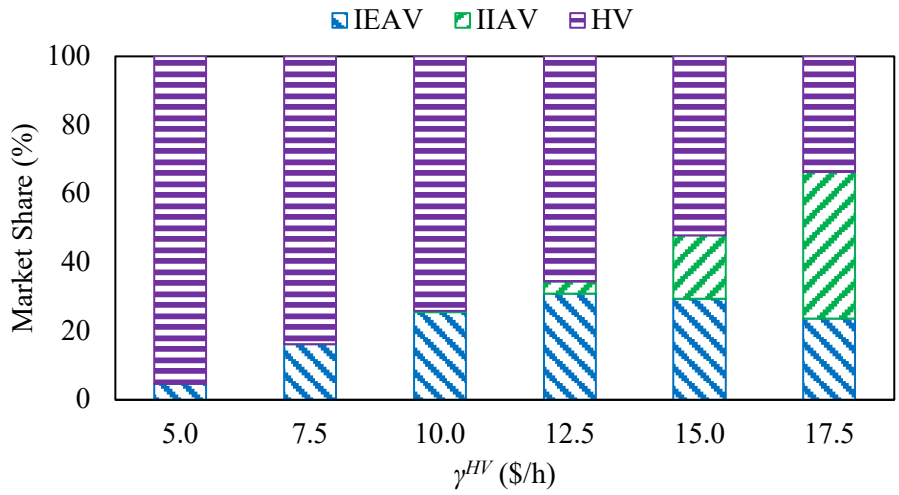

Figure 5-2. Equilibrium total market shares under different value of time

Table 5-4: Equilibrium market shares under different value of time.

O-D	Class	Market share (%)					
		γ^{HV} =\$5.0/h	γ^{HV} =\$7.5/h	γ^{HV} =\$10.0/h	γ^{HV} =\$12.5/h	γ^{HV} =\$15.0/h	γ^{HV} =\$17.5/h
1-2	1	95.41	83.63	75.65	68.64	58.85	40.83
	2	0.00	0.05	0.36	2.53	14.57	35.85

	3	4.59	16.33	23.99	28.83	26.58	23.32
1-3	1	95.41	83.11	68.00	54.97	37.01	19.71
	2	0.01	0.07	0.64	4.97	24.96	49.76
	3	4.59	16.83	31.36	40.06	38.03	30.53
4-2	1	95.41	83.62	75.63	68.47	57.32	36.55
	2	0.00	0.05	0.38	2.78	14.40	41.73
	3	4.59	16.33	23.99	28.76	28.28	21.72
4-3	1	95.41	86.68	90.27	92.23	84.02	66.25
	2	0.01	0.06	0.43	2.56	11.92	31.51
	3	4.59	13.26	9.30	5.21	4.06	2.24
Total	1	95.41	83.73	74.05	65.48	52.17	33.64
	2	0.00	0.06	0.49	3.58	18.41	42.75
	3	4.59	16.22	25.47	30.94	29.42	23.62

5.2 Deployment of automated roads

5.2.1 Model formulation

Given a limited budget, we now determine the deployment of automated roads with the aim of maximizing all road users' benefit. Denote y_l as a binary variable, representing whether to convert link $l \in L$ into an automated link. If yes, $y_l = 1$; otherwise, $y_l = 0$.

Because we assume the road users' vehicle type choice follow a logit model, the expected indirect utility received by a randomly sampled driver between O-D pair $w \in W$, in money terms, can be given as follows (Williams, 1977; Small and Rosen, 1981):

$$E(CS^w) = \frac{1}{-\zeta_p} \ln \sum_{m \in M} e^{\zeta_0^m + \frac{\zeta_p p^m}{\phi l^m} + \zeta_t \left(\rho_{d(w)}^{w,m} - \rho_{o(w)}^{w,m}\right)}$$

and the total user benefit can then be expressed as

$$\sum_{w \in W} \frac{1}{-\zeta_p} \ln \sum_{m \in M} e^{\zeta_0^m + \frac{\zeta_p p^m}{\phi l^m} + \zeta_t \left(\rho_{d(w)}^{w,m} - \rho_{o(w)}^{w,m}\right)} q^w$$

The optimal deployment problem (ODP) of automated roads can be formulated as follows:

ODP:

$$\max_{\boldsymbol{x},\boldsymbol{q},\boldsymbol{\rho},\boldsymbol{y}} \sum_{w\in W} \frac{1}{-\zeta_p} \ln \sum_{m\in M} e^{\zeta_0^m + \frac{\zeta_p p^m}{\phi l^m} + \zeta_t\left(\rho_{d(w)}^{w,m} - \rho_{o(w)}^{w,m}\right)} q^w$$

s.t. (5-8)-(5-14), (5-19)-(5-21)

$$t_l = \hat{t}_l\left[1 + \alpha_l\left(\frac{x_l^h + \theta x_l^a + (1 - y_l + \theta y_l)x_l^{\tilde{a}}}{c_l^{HV}}\right)^{\beta_l}\right] \qquad \forall l \in L \qquad (5\text{-}26)$$

$$\left(y_l\gamma^{AV}t_l + (1-y_l)\gamma^{HV}t_l + \rho_i^{w,\tilde{a}} - \rho_j^{w,\tilde{a}}\right)x_l^{w,\tilde{a}} = 0 \qquad \forall (i,j) = l \in L, w \in W \qquad (5\text{-}27)$$

$$y_l\gamma^{AV}t_l + (1-y_l)\gamma^{HV}t_l + \rho_i^{w,\tilde{a}} - \rho_j^{w,\tilde{a}} \geq 0 \qquad \forall (i,j) = l \in L, w \in W \qquad (5\text{-}28)$$

$$y_l \in \{0,1\} \qquad \forall l \in L \qquad (5\text{-}29)$$

$$\sum_{l\in L} y_l b_l \leq B \qquad (5\text{-}30)$$

where b_l is the cost for converting link l into an automated road, and B is the budget.

In the above, the objective function is to maximize the total user benefit. Constraints (5-8)-(5-14), (5-19)-(5-21), and (5-26)-(5-28) represent the optimality conditions of NE-VI as shown in Appendix A with the location variables of automated links. They describe road users' route and vehicle type choice behaviors. Constraint (5-29) specifies that y_a is a binary variable. Constraint (5-30) ensures that the total expense of deploying automated links are within the given budget.

5.2.2 Solution algorithm

As formulated, ODP is a mathematical program with complementarity constraints (MPCC), a class of problems difficult to solve. In this paper, we extend the active-set algorithm proposed by Zhang et al. (2009) to solve the ODP problem. Instead of solving

the MPCC directly, the active-set algorithm solves a restricted nonlinear program and a binary knapsack problem sequentially, and as proved by Zhang et al. (2009), the algorithm can converge to a strongly stationary solution to the original MPCC in a finite number of iterations. Note that the active-set algorithm has been adopted by many studies in the literature (see e.g., Chen et al., 2016; He et al., 2018; Song et al., 2015, 2017).

Given a feasible deployment plan of automated links, i.e., a certain solution of y_a, we can partition all binary variables y_a into two complementary sets $\Omega_0 = \{l: y_l = 0\}$ and $\Omega_1 = \{l: y_l = 1\}$, clearly $\Omega_0 \cup \Omega_1 = L$ and $\Omega_0 \cap \Omega_1 = \emptyset$. For a feasible deployment plan (Ω_0, Ω_1), a restricted problem of the ODP can be formulated as follows:

ODP-R:

$$\max_{\boldsymbol{x},\boldsymbol{q},\boldsymbol{\rho},\boldsymbol{y}} \sum_{w\in W} \frac{1}{-\zeta_p} \ln \sum_{m\in M} e^{\zeta_0^m + \frac{\zeta_p p^m}{\phi l^m} + \zeta_t\left(\rho_{d(w)}^{w,m} - \rho_{o(w)}^{w,m}\right)} q^w$$

s.t. (5-8)-(5-14), (5-19)-(5-21), (5-26)-(5-28)

$$y_l = 0 \qquad \forall l \in \Omega_0 \qquad (5\text{-}31)$$

$$y_l = 1 \qquad \forall l \in \Omega_1 \qquad (5\text{-}32)$$

The purpose of solving the above ODP-R is to obtain multipliers associated with constraints (5-31) and (5-32), which can be used to guide the updates of deployment plan (i.e., sets Ω_0, and Ω_1). Although ODP-R is still a MPCC, because it has given values for y_l, the solution of the ODP-R can be obtained by solving the NE-NLP problem with given deployment plan. The iterative solution procedure of the active-set algorithm is given as follows:

Step 0: Set $k = 1$ and solve NE-NLP with an initial feasible deployment plan (Ω_0^1, Ω_1^1).

Step 1: Solve ODP-R with the optimal solution of the NE-NLP. Denote the objective function value as S^k. Obtain the multipliers of constraints (5-31) and (5-32), denoted as μ_l^k and χ_l^k, respectively. Let Ψ denote a parameter and set $\Psi = +\infty$.

Step 2: Let $\bar{y}_l^*$ and e_l^* solve the following knapsack problem:

$$\max_{\boldsymbol{y},\boldsymbol{e}} \sum_{l\in\Omega_0^k} \mu_l^k e_l - \sum_{l\in\Omega_1^k} \chi_l^k e_l$$

s.t.

$$\bar{y}_l = e_l \qquad \forall l \in \Omega_0 \qquad (5\text{-}33)$$

$$\bar{y}_l = 1 - e_l \qquad \forall l \in \Omega_1 \qquad (5\text{-}34)$$

$$\sum_{l\in L} \bar{y}_l b_l \le B \qquad (5\text{-}35)$$

$$\sum_{l\in\Omega_0^k} \mu_l^k e_l - \sum_{l\in\Omega_1^k} \chi_l^k e_l \le \Psi \qquad (5\text{-}36)$$

$$e_l \in \{0,1\} \qquad \forall l \in \Omega_0^k \cup \Omega_1^k \qquad (5\text{-}37)$$

If the optimal objective function value is zero, stop and the current solution is the optimal. Otherwise, go to Step 3.

Step 3: Set:

i. $\Psi^* = \sum_{l\in\Omega_0^k} \mu_l^k e_l^* - \sum_{l\in\Omega_1^k} \chi_l^k e_l^*$

ii. $\bar{\Omega}_0 = \{l: \bar{y}_l^* = 0\}, \bar{\Omega}_1 = \{l: \bar{y}_l^* = 1\}$

Solve NE-NLP with the deployment plan $(\bar{\Omega}_0, \bar{\Omega}_1)$. If the total user benefit associated with the solution of NE-NLP is less than or equal to S^k, set $\Psi = \Psi^* - \varepsilon$, where ε is a sufficiently small positive value, and return to Step 2. Otherwise, set $\Omega_0^{k+1} = \bar{\Omega}_0$, $\Omega_1^{k+1} = \bar{\Omega}_1$, and $k = k + 1$, and go to Step 1.

At Step 2, the objective of the knapsack problem is to maximize the estimated improvement to the total user benefit by adjusting the current deployment plan. e_l is a "switch" variable, indicating whether to move the corresponding design variable to its complement set or not. If it is 1, shift the corresponding design variable to its complement set. If its value is 0, the corresponding design variable remains in the current set. Variable $\bar{y}_l$ represents a new deployment plan. Its feasibility is guaranteed by constraint (5-35). The left-hand side of constraint (5-37) is identical to the objective function of the knapsack problem and the constraint ensures that the objective function value is no greater than a predetermined parameter Ψ. Ψ is initially set to $+\infty$ to obtain the maximum positive objective function value Ψ^*, whose corresponding deployment plan may lead to the maximum improvement of total user benefit. However, because the Lagrangian multipliers μ_l^k and χ_l^k only provide estimates on how the objective function of the ODP changes, the new deployment plan $(\bar{\Omega}_0, \bar{\Omega}_1)$ may not lead to an actual improvement of total user benefit. Thus, Step 3 is to verify whether $(\bar{\Omega}_0, \bar{\Omega}_1)$ is a better plan or not. If $(\bar{\Omega}_0, \bar{\Omega}_1)$ doesn't yield a larger total user benefit, parameter Ψ is reduced slightly and the knapsack problem is solved again to generate another different deployment plan. Otherwise, the new deployment plan $(\bar{\Omega}_0, \bar{\Omega}_1)$ is adopted to update the current design.

5.2.3 Numerical Studies

In this section, two numerical examples are presented to demonstrate the proposed models and algorithms.

5.2.3.1 Nguyen-Dupuis network

We first solve the ODP model for the Nguyen-Dupuis network. Consider that the cost for converting a link into an automated road is 1 unit/mile. The length of a link is set to be equal to the link free flow travel time in minutes, i.e., $b_l = \hat{t}_{ij}$, which is based on the assumption that the free flow speed is 60 mile/h. The budget is set to be 40 units. Other input parameters are given in Section 5.1.5. The active set algorithm is implemented using GAMS (Rosenthal, 2012) on a 3.40 GHz Dell Computer with 16 GB of RAM. CPLEX 12.2 is used to solve the knapsack problem and CONOPT (Drud, 1994) is used to solve the NE-NLP and ODP-R problems.

The algorithm terminates at the third iteration (here the iteration means the outer loop of the active-set algorithm) and totally runs for 5.5 seconds. It provides a deployment plan that locate automated roads on links (1,5), (5,6), (6,7), (7.11), (11,2) and (11,3). Compared with the status quo condition (i.e., no automated roads), the optimal design improves the total user benefit from -32718.76 to -29175.86, an improvement of 10.8 percent. Table 5-5 illustrates the impacts of the deployed automated links on different O-D pairs and different vehicle classes. One can observe that, for all O-D pairs, the deployed automated links dramatically increase the market share of IEAVs. One can further observe that, for all four O-D pairs, the deployed automated links not only significantly reduce the equilibrium O-D travel cost of IEAVs, but also cut down the travel cost of HVs and IIAVs. The travel cost reduction for IEAVs is the direct benefit from deployed automated links because automated links enable IEAVs to drive autonomously and thus reduce their uses' travel costs. The travel cost reduction for HVs

and IIAVs demonstrates a potential indirect benefit of automated links. First, strategically deployed automated links promote the adoption of IEAVs by reducing the travel cost of IEAVs. Second, the road capacity of an automated link may be improved due to increased proportion of autonomous driving IEAVs. Last, the congestion level of the whole network may be reduced due to the capacity increase of automated links.

Table 5-5: Comparison between status quo and optimal design for the Nguyen-Dupuis network

O-D	Class	Status quo		Optimal design		Travel cost relative change (%)	Market share change (%)
		Travel cost ($)	Market share (%)	Travel cost ($)	Market share (%)		
1-2	1	5.28	99.74	4.37	54.83	-17.23	-44.91
	2	2.64	0.06	2.18	0.01	-17.42	-0.05
	3	5.28	0.21	2.38	45.16	-54.92	44.95
1-3	1	5.52	99.71	4.89	23.63	-11.41	-76.08
	2	2.76	0.08	2.45	0.01	-11.23	-0.07
	3	5.52	0.21	2.45	76.37	-55.62	76.16
4-2	1	5.38	99.73	5.00	75.51	-7.06	-24.22
	2	2.69	0.07	2.50	0.03	-7.06	-0.04
	3	5.38	0.21	3.32	24.47	-38.29	24.26
4-3	1	5.62	99.70	4.89	84.06	-12.99	-15.64
	2	2.81	0.09	2.45	0.03	-12.81	-0.06
	3	5.62	0.21	3.39	15.92	-39.68	15.71

5.2.3.2 Sioux Falls network

To further test the proposed model and algorithm, we implement them for the Sioux Falls network, which consists of 24 nodes, 76 links, as shown in Figure 5-3. In the travel time function, $\alpha_l = 0.15$ and $\beta_l = 4$. Table 5-6 lists the link input parameters. Note that the original link characteristics are revised slightly to better illustrate our model. To highlight the benefits of IEAVs and automated roads, we only considered 50 O-D pairs whose origins and destinations are far apart. The O-D demands can be found in

Table 5-7. In addition, we set $\theta = 0.4$, $\gamma^{HV} = \$7.5/h$, $\gamma^{AV} = 0.5\gamma^{HV} = \$3.75/h$, $p^h = \$20{,}000$, $p^a = \$57{,}500$, $p^{\tilde{a}} = \$35{,}000$, $l^m = 10$ for $m = h, a, \tilde{a}$, $\phi = 730$, $\zeta_p = \zeta_t = -3$ and $\zeta_0^m = 0$ for $m = h, a, \tilde{a}$. The cost for converting a link into an automated road is assumed to be 1 unit/mile. The length of a link is set to be equal to the link free flow travel time in minutes. The budget is set as 250 units. Note that the parameter values are for illustration purpose only.

Table 5-6: Link characteristics of the Sioux Falls network for deployment of automated roads

Link	Free-flow travel time (min)	Capacity (10^3veh/h)	Link	Free-flow travel time (min)	Capacity (10^3veh/h)	Link	Free-flow travel time (min)	Capacity (10^3veh/h)
1-2	18	25.90	10-11	15	10.00	17-19	6	4.82
1-3	12	23.40	10-15	18	13.51	18-7	6	23.40
2-1	18	25.90	10-16	12	4.85	18-16	9	19.68
2-6	15	4.96	10-17	24	4.99	18-20	12	23.40
3-1	12	23.40	11-4	18	4.91	19-15	9	14.56
3-4	12	17.11	11-10	15	10.00	19-17	6	4.82
3-12	12	23.40	11-12	18	4.91	19-20	12	5.00
4-3	12	17.11	11-14	12	4.88	20-18	12	23.40
4-5	6	17.78	12-3	12	23.40	20-19	12	5.00
4-11	18	4.91	12-11	18	4.91	20-21	18	5.06
5-4	6	17.78	12-13	9	25.90	20-22	15	5.08
5-6	12	4.95	13-12	9	25.90	21-20	18	5.06
5-9	15	10.00	13-24	12	5.09	21-22	6	5.23
6-2	15	4.96	14-11	12	4.88	21-24	9	4.89
6-5	12	4.95	14-15	15	5.13	22-15	9	9.60
6-8	6	4.90	14-23	12	4.92	22-20	15	5.08
7-8	9	7.84	15-10	18	13.51	22-21	6	5.23
7-18	6	23.40	15-14	15	5.13	22-23	12	5.00
8-6	6	4.90	15-19	9	14.56	23-14	12	4.92
8-7	9	7.84	15-22	9	9.60	23-22	12	5.00
8-9	30	5.05	16-8	15	5.05	23-24	6	5.08
8-16	15	5.05	16-10	12	4.85	24-13	12	5.09
9-5	15	10.00	16-17	6	5.23	24-21	9	4.89

9-8	30	5.05	16-18	9	19.68	24-23	6	5.08
9-10	9	13.92	17-10	24	4.99			
10-9	9	13.92	17-16	6	5.23			

Table 5-7: O-D demands of the Sioux Falls network for deployment of automated roads (veh/h)

O-D	Demand	O-D	Demand	O-D	Demand	O-D	Demand	O-D	Demand
1-13	9000	4-13	6000	7-13	4000	20-1	3000	23-1	7000
1-20	3000	4-20	3000	7-20	6000	20-2	8000	23-2	6000
1-21	3000	4-21	2000	7-21	6000	20-4	3000	23-4	2000
1-23	7000	4-23	2000	7-23	9000	20-5	5000	23-5	4000
1-24	5000	4-24	4000	7-24	7000	20-7	6000	23-7	9000
2-13	3000	5-13	2000	13-1	9000	21-1	3000	24-1	5000
2-20	8000	5-20	5000	13-2	3000	21-2	5000	24-2	4000
2-21	5000	5-21	9000	13-4	6000	21-4	2000	24-4	4000
2-23	6000	5-23	4000	13-5	2000	21-5	9000	24-5	6000
2-24	4000	5-24	6000	13-7	4000	21-7	6000	24-7	7000

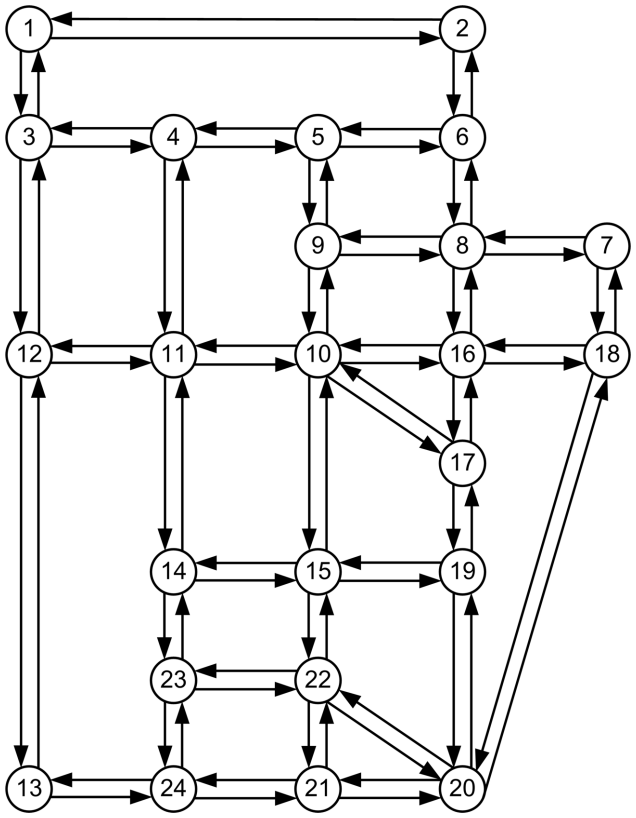

Figure 5-3. Sioux Falls network for the deployment of automated roads

The active-set algorithm terminates at the 4th iteration (here the iteration means the outer loop of the active-set algorithm) and totally runs for 58 min and 31.8 sec. It provides a deployment plan that locates automated roads on 22 links, as shown in Figure 5-4. The plan improves the total user benefit by 12.8 percent. The total market shares for the whole network in the status quo (i.e., no automated roads) and in the optimal deployment plan are compared in Table 5-8. One can observe that, in the status quo, 52.48% road users adopt IIAVs and only 0.10% road users adopt IEAVs, while in the optimal deployment plan only 13.14% road users still choose IIAVs and 58.79% road users choose IEAVs. Due to the deployment of automated roads, a large portion of HV users and majority of IIAV users in the status quo switch to IEAVs. The detailed market shares and travel costs comparison for each O-D pair can be found in Table 5-9 and Table 5-10.

Table 5-8: Total market shares and total user benefit in the status quo and in the optimal deployment plan

	Total market shares (%)			Total user benefit
	HVs	IIAVs	IEAVs	
The status quo	47.42	52.48	0.10	-3,140,229
Optimal deployment plan	28.07	13.14	58.79	-2,737,198

Table 5-9: Market shares in status quo and in optimal deployment plan

O-D	Market share (%)					
	The status quo			Optimal plan		
	HV	IIAV	IEAV	HV	IIAV	IEAV
1-13	99.68	0.11	0.21	24.34	0.01	75.66
1-20	1.10	98.90	0.00	0.72	10.24	89.04
1-21	2.15	97.85	0.01	0.00	0.03	99.97
1-23	3.72	96.28	0.01	1.33	4.26	94.42
1-24	15.81	84.16	0.03	0.00	0.01	99.99
2-13	96.71	3.09	0.20	24.28	0.23	75.49
2-20	24.58	75.37	0.05	62.53	29.73	7.74

2-21	0.08	99.93	0.00	0.61	22.03	77.36
2-23	0.13	99.87	0.00	0.58	58.07	41.35
2-24	0.64	99.36	0.00	0.00	0.30	99.70
4-13	99.71	0.08	0.21	78.05	0.02	21.93
4-20	58.73	41.15	0.12	26.36	5.17	68.47
4-21	17.40	82.56	0.04	0.10	0.04	99.86
4-23	54.41	45.48	0.11	93.40	5.64	0.96
4-24	19.73	80.23	0.04	5.26	1.96	92.78
5-13	99.53	0.26	0.21	78.01	0.07	21.92
5-20	81.70	18.13	0.17	27.47	1.18	71.35
5-21	39.93	59.99	0.08	0.10	0.01	99.89
5-23	27.46	72.48	0.06	30.42	5.74	63.84
5-24	7.23	92.76	0.02	0.03	0.03	99.94
7-13	66.80	33.06	0.14	67.08	28.79	4.13
7-20	99.79	0.00	0.21	88.98	0.00	11.02
7-21	87.83	11.99	0.19	6.12	0.01	93.87
7-23	80.53	19.31	0.17	60.79	1.47	37.73
7-24	46.12	53.78	0.10	0.17	0.01	99.83
13-1	99.68	0.11	0.21	25.96	0.01	74.03
13-2	96.71	3.09	0.20	25.91	0.21	73.88
13-4	99.71	0.08	0.21	27.40	0.01	72.59
13-5	99.53	0.26	0.21	27.39	0.03	72.58
13-7	66.80	33.06	0.14	49.35	11.75	38.90
20-1	1.10	98.90	0.00	1.71	83.24	15.05
20-2	24.58	75.37	0.05	36.39	58.65	4.96
20-4	58.73	41.15	0.12	57.65	34.51	7.85
20-5	81.70	18.13	0.17	75.33	14.42	10.26
20-7	99.79	0.00	0.21	88.02	0.00	11.98
21-1	2.15	97.85	0.01	0.02	2.27	97.70
21-2	0.08	99.93	0.00	0.35	88.24	11.41
21-4	17.40	82.56	0.04	35.69	41.01	23.30
21-5	39.93	59.99	0.08	72.96	26.81	0.24
21-7	87.83	11.99	0.19	4.52	0.01	95.48
23-1	3.72	96.28	0.01	1.09	13.97	84.94
23-2	0.13	99.87	0.00	0.22	82.89	16.90
23-4	54.41	45.48	0.11	84.23	14.50	1.27
23-5	27.46	72.48	0.06	55.54	43.62	0.84
23-7	80.53	19.31	0.17	64.91	0.46	34.64
24-1	15.81	84.16	0.03	0.00	0.03	99.97
24-2	0.64	99.36	0.00	0.00	1.57	98.43
24-4	19.73	80.23	0.04	1.00	2.23	96.78
24-5	7.23	92.76	0.02	4.05	18.35	77.60
24-7	46.12	53.78	0.10	0.38	0.01	99.61

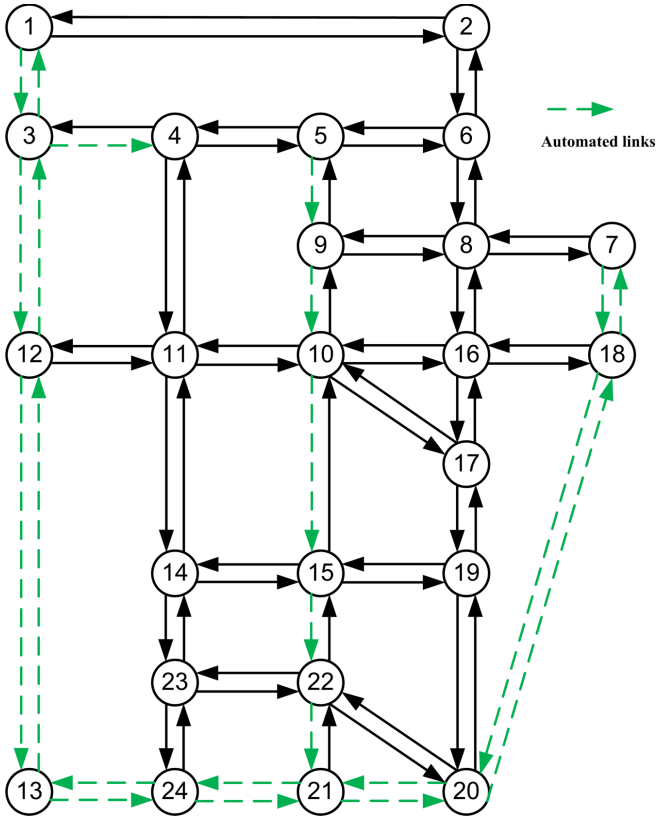

Figure 5-4. Deployment of automated links in Sioux Falls network

Table 5-10: Travel costs in status quo and in optimal deployment plan

O-D	Travel cost ($)					
	The status quo			Optimal plan		
	HV	IIAV	IEAV	HV	IIAV	IEAV
1-13	5.72	2.86	5.72	4.87	2.43	2.43
1-20	13.27	6.64	13.27	12.04	6.02	8.38
1-21	12.82	6.41	12.82	12.59	6.30	6.70
1-23	12.44	6.22	12.44	11.05	5.53	7.58
1-24	11.39	5.69	11.39	11.73	5.87	5.87
2-13	7.98	3.99	7.98	7.16	3.58	4.73
2-20	11.02	5.51	11.02	9.78	4.89	8.42
2-21	15.07	7.54	15.07	12.66	6.33	9.00
2-23	14.70	7.35	14.70	13.34	6.67	9.87
2-24	13.64	6.82	13.64	14.02	7.01	8.16
4-13	5.54	2.77	5.54	4.80	2.40	3.17
4-20	10.04	5.02	10.04	9.19	4.59	6.82
4-21	11.31	5.66	11.31	9.75	4.87	5.38
4-23	10.15	5.08	10.15	8.40	4.20	7.87

4-24	11.21	5.60	11.21	9.62	4.81	6.60
5-13	6.31	3.16	6.31	5.56	2.78	3.93
5-20	9.27	4.64	9.27	8.18	4.09	5.80
5-21	10.55	5.27	10.55	8.74	4.37	4.37
5-23	10.92	5.46	10.92	9.16	4.58	6.86
5-24	11.98	5.99	11.98	10.38	5.19	5.59
7-13	9.81	4.90	9.81	9.71	4.86	8.59
7-20	3.28	1.64	3.28	2.72	1.36	1.36
7-21	8.95	4.47	8.95	5.93	2.97	2.97
7-23	9.32	4.66	9.32	7.79	3.90	5.90
7-24	10.38	5.19	10.38	8.38	4.19	4.19
13-1	5.72	2.86	5.72	4.81	2.40	2.40
13-2	7.98	3.99	7.98	7.07	3.54	4.67
13-4	5.54	2.77	5.54	4.76	2.38	2.38
13-5	6.31	3.16	6.31	5.77	2.89	3.39
13-7	9.81	4.90	9.81	9.32	4.66	7.34
20-1	13.27	6.64	13.27	12.87	6.43	10.09
20-2	11.02	5.51	11.02	10.59	5.30	9.20
20-4	10.04	5.02	10.04	9.93	4.97	8.54
20-5	9.27	4.64	9.27	9.17	4.59	7.78
20-7	3.28	1.64	3.28	2.78	1.39	1.39
21-1	12.82	6.41	12.82	13.30	6.65	8.48
21-2	15.07	7.54	15.07	13.96	6.98	10.74
21-4	11.31	5.66	11.31	10.37	5.18	8.45
21-5	10.55	5.27	10.55	9.61	4.80	9.46
21-7	8.95	4.47	8.95	6.14	3.07	3.07
23-1	12.44	6.22	12.44	11.98	5.99	8.47
23-2	14.70	7.35	14.70	14.24	7.12	10.73
23-4	10.15	5.08	10.15	9.10	4.55	8.44
23-5	10.92	5.46	10.92	10.11	5.06	9.46
23-7	9.32	4.66	9.32	6.97	3.48	5.12
24-1	11.39	5.69	11.39	13.68	6.84	7.25
24-2	13.64	6.82	13.64	15.63	7.82	9.52
24-4	11.21	5.60	11.21	10.81	5.41	7.23
24-5	11.98	5.99	11.98	11.28	5.64	8.24
24-7	10.38	5.19	10.38	7.82	3.91	3.91

5.3 Model extensions

The proposed models in Section 5.2 and Section 5.3 can be extended in several directions. First, the network equilibrium model can be extended by considering IEAV

users' potential inconvenience costs and service charges associated with using autonomous driving service. Second, road users' vehicle choice behaviors can be modeled as a time-dependent evolution process, in which road users gradually adopt IIAVs and IEAVs. Third, the optimal deployment model can be modified by considering an objective of maximizing the net social benefit instead of only road users' benefit. Below we briefly discuss these extensions.

Some new notations are used in this section. For the convenience of readers, frequently used notations are listed below.

Sets	**Description**
T	Set of years, indexed by τ
N	Set of nodes, indexed by i, j
L	Set of links, indexed by $l = (i, j)$
$\hat{L}_\tau$	Set of automated links at year $\tau \in T$
W	Set of O-D pairs, indexed by w
M	Set of vehicles classes, indexed by $m = h, a, \tilde{a}$, where h represents HVs, a represents IIAVs, $\tilde{a}$ represents IEAVs
P^w	Set of paths between O-D pair w
$L(p)$	Set of links belonging to path p
$N(p)$	Set of nodes belonging to path p
$P^w(l)$	Set of paths between O-D pair w passing link l
B_τ^p	Set of automated sub-paths along path $p \in P^w$ at year $\tau \in T$, indexed by b
$\hat{L}(b)$	Set of automated links that belong to automated sub-path $b \in B_\tau^p$
$o(w)$	Origin node of O-D pair w
$d(w)$	Destination node of O-D pair w
n_b^+	The starting point of automated sub-path $b \in B_\tau^p$
n_b^-	The ending point of automated sub-path $b \in B_\tau^p$
Parameters	**Description**
q_τ^w	Total travel demand for O-D pair w by all classes at year τ
t_l^0	Free flow travel time of link l
$\bar{\eta}_l^{ha}, \bar{\eta}_l^{hh}, \bar{\eta}_l^{ah}, \bar{\eta}_l^{aa}$	Time headway parameters
$\bar{\eta}_{l,\tau}$	The average headway in mixed flow on link $l \in L$ at year $\tau \in T$
φ_l	Number of lanes on link $l \in L$
$\hat{c}_l^h$	The traffic capacity of link $l \in L$ when it is used by pure HVs

VOT^h	Value of time of drivers in human-driven mode
VOT^a	Value of time of drivers in autonomous driving mode
ε^{ah}	The inconvenience cost (in monetary unit) due to one transition from autonomous driving to manual driving
ε^{ha}	The inconvenience cost due to one transition from manual driving to autonomous driving.

Variables	**Description**
$q_\tau^{w,m}$	Travel demand between O-D pair w by class m at year τ
$f_{p,\tau}^m$	Traffic flow of class $m \in M$ on path $p \in P^w$ at year $\tau \in T$
$x_{l,\tau}^m$	Aggregate flow of class m on link l at year τ
$x_{l,\tau}^{\tilde{a}a}$	The aggregate flow of IEAV users using autonomous driving mode on an automated link $l \in \hat{L}_\tau$ at year $\tau \in T$
$t_{l,\tau}$	Travel time on link $l \in L$ at year $\tau \in T$
$r_{l,\tau}$	The percentage of flow of autonomous driving vehicles on link $l \in L$ at year $\tau \in T$
$c_{l,\tau}$	The capacity of link $l \in L$ at year $\tau \in T$
$\theta_{l,\tau}$	Service charge of autonomous driving per unit time on link $l \in \hat{L}_\tau$ at year $\tau \in T$
$y_{b,\tau}^p$	The proportion of IEAV users between O-D pair $w \in W$ who choose autonomous driving service at year $\tau \in T$
$y_{l,\tau}^p$	The proportion of IEAV users on path $p \in P^w$ between O-D pair $w \in W$ who choose autonomous driving service on automated link l at year $\tau \in T$
$HVE_{l,\tau}$	Human-driven vehicle equivalent for autonomous driving vehicles on link $l \in L$ at year $\tau \in T$
$v_{l,\tau}$	Aggregate link flow in HVE on link $l \in L$ at year $\tau \in T$
$\zeta_{b,\tau}^p$	Auxiliary variable representing the multiplier associated with constraint $y_{b,\tau}^p \leq 1$
$\lambda_{p,\tau}^m$	The travel cost of class $m \in M$ users between O-D pair $w \in W$ along path $p \in P^w$ at year $\tau \in T$
$\mu_\tau^{w,m}$	An auxiliary variable representing the equilibrium travel cost of class $m \in M$ users between O-D pair $w \in W$ at year $\tau \in T$

5.3.1 Network equilibrium model considering service charges and inconvenience costs

We consider a general transportation network over a prescribed planning horizon. The planning horizon is divided into $|T|$ years, where T represents the set of years within the planning horizon and is indexed by τ. Let $G(N, L)$ denote a directed road network,

where N is the set of nodes and L is the set of directed links. Links in the road network are designated by $l \in L$, or represented as node pairs (i, j), where $i, j \in N$. Let $\hat{L}_\tau$ represent the set of automated links in the network at year $\tau \in T$. Let W denote the set of origin-destination (O-D) pairs. Let $o(w)$ and $d(w)$ represent the origin node and destination node of O-D pair $w \in W$, respectively. Let $M = \{h, a, \tilde{a}\}$ denote the set of vehicle classes, where class h refers to HV, class a refers to IIAV, and class $\tilde{a}$ refers to IEAV. Let $q_\tau^{w,m}$ be the demand between O-D pair $w \in W$ by class $m \in M$ at year $\tau \in T$, and q_τ^w be the total demand between O-D pair $w \in W$ by all classes at year $\tau \in T$. Without loss of generality, we assume that the total travel demand between each O-D pair remains the same during the entire planning horizon. That is, $q_\tau^w = q_1^w, \forall \tau \in T$. Let P^w denote the set of paths between O-D pair $w \in W$. Let $f_{p,\tau}^m$ denote the traffic flow of class $m \in M$ on path $p \in P^w$ at year $\tau \in T$. Let $x_{l,\tau}^m$ denote the aggregate flow of class $m \in M$ on link $l \in L$ at year $\tau \in T$.

Let $t_{l,\tau}$ denote the travel time on link $l \in L$ at year $\tau \in T$. Assume $t_{l,\tau}$ is given by the well-known Bureau of Public Roads (BPR) travel time function with capacity being a function of the proportion of self-driving vehicles on link $l \in L$:

$$t_{l,\tau} = t_l^0 \left[1 + \alpha_l \left(\frac{x_{l,\tau}^h + x_{l,\tau}^a + x_{l,\tau}^{\tilde{a}}}{c_{l,\tau}(r_{l,\tau})} \right)^{\beta_l} \right] \tag{5-38}$$

where t_l^0 represents the free-flow travel time of link $l \in L$; $r_{l,\tau}$ denotes the percentage of flow of autonomous driving vehicles on link $l \in L$ at year $\tau \in T$; $c_{l,\tau}(r_{l,\tau})$ represents the capacity of link $l \in L$ at year $\tau \in T$; and α_l and β_l are two positive parameters.

As discussed in Section 3.1.2, $c_{l,\tau}(r_{l,\tau})$ is given by the following equation:

$$c_{l,\tau}(r_{l,\tau}) = \frac{\hat{c}_l^h}{\frac{\bar{\eta}_l^{ha} + \bar{\eta}_l^{ah}}{\bar{\eta}_l^{hh}} r_{l,\tau}(1 - r_{l,\tau}) + (1 - r_{l,\tau})^2 + \frac{\bar{\eta}_l^{aa}}{\bar{\eta}_l^{hh}}(r_{l,\tau})^2} \quad \forall l \in L, \tau \in T \tag{5-39}$$

In a traffic flow, an IEAV in human-driven mode is identical to a HV and an IEAV in autonomous driving mode is identical to an IIAV. The calculation of $r_{l,\tau}$ thus depends on IEAV users' driving mode choices, which will be discussed in the following section.

5.3.1.1 Driving mode choice of IEAV users on automated links

The travel cost for a HV or IIAV driver is defined as his/her travel time multiplied by his/her value of travel time (VOT). For an IEAV driver, in addition to travel time costs, he/she might also experience service charges of autonomous driving on automated roads and inconvenience costs due to transitions between autonomous driving and manual driving. The service charge on an automated road is determined by the provider of the automated road. The inconvenience cost might capture the delay of driving mode transitions (see e.g., Merat et al., 2014; Eriksson and Stanton, 2017) and drivers' anxiety of driving mode change. An IEAV driver might or might not choose to use autonomous driving service on an automated road depending on whether the autonomous driving service leads to lower total travel cost than manual driving.

Let VOT^h and VOT^a denote the value of time for travelers in manual driving mode and autonomous driving mode, respectively. We assume that the service charge of autonomous driving on a link is proportional to the travel time on the link. Let parameter

$\theta_{l,\tau}$ denote the service charge per unit time of autonomous driving on automated link $l \in \hat{L}_\tau$ at year $\tau \in T$. A reasonable $\theta_{l,\tau}$ must satisfy $\theta_{l,\tau} < VOT^h - VOT^a$ because otherwise IEAV users would never have any incentive to use the autonomous driving service on link $l \in \hat{L}_\tau$.

Compared with IIAVs, IEAVs can only be driven autonomously on automated links and must be manually driven on regular links. Therefore, IEAV users may experience inconvenience due to transitions between autonomous driving and manual driving. First, it might take time and effort to do the control transitions. Second, the control transitions might impact the efficiency of the autonomous driving service. Many studies have investigated the control transitions between autonomous driving and manual driving. Merat et al., (2014) conducted a driving simulator study and found that drivers may take around 15 seconds to regain control from a high level of automation and up to 40 seconds to completely stabilize the vehicle control. Using driving simulator experiments, Eriksson and Stanton (2017) found that it takes drivers between 2.8 and 23.8 seconds to switch from manual to automated control, and it takes drivers between 1.9 and 25.7 seconds to resume control from autonomous driving. In this study, we assume fixed and predetermined transition costs between autonomous driving and manual driving. Let parameter ε^{ah} represent the inconvenience cost (in monetary unit) due to one transition from autonomous driving to manual driving, and ε^{ha} represent the inconvenience cost due to one transition from manual driving to autonomous driving.

Let $N(p)$ denote the set of nodes along path $p \in P^w$. For a node $i \in N(p)\backslash\{o(w), d(w)\}$, $p \in P^w$, its incoming link and outgoing link along the path p potentially have four different combinations, as shown in Figure 5-5.

In scenario (a), the node i has an incoming automated link and an outgoing regular link. When traveling from node 1 to node 2, if an IEAV user utilize autonomous driving service on automated link $(1, i)$, he/she will experience an inconvenience cost ε^{ah} at node i. If an IEAV user chooses manual driving mode on automated link $(1, i)$, his/her inconvenience cost at node i will be zero.

In scenario (b), the node i has an incoming regular link and an outgoing automated link. When traveling from node 1 to node 2, if an IEAV user utilize autonomous driving service on automated link $(i, 2)$, he/she will experience an inconvenience cost ε^{ha} at node i. If an IEAV user chooses manual driving mode on automated link $(i, 2)$, his/her inconvenience cost at node i will be zero.

In scenario (c), both the incoming link and the outgoing link of the node i are automated links. When traveling from node 1 to node 2, if an IEAV user utilize autonomous driving service on automated link $(1, i)$, he/she will also utilize autonomous driving service on automated link $(i, 2)$ because he/she will have an additional travel cost savings of $\left(VOT^h - VOT^a - \theta_{i2,\tau}\right)t_{i2,\tau}$ without inducing additional inconvenience cost. Similarly, If an IEAV user utilize autonomous driving service on automated link $(i, 2)$, he/she will always utilize autonomous driving service on automated link $(1, i)$ because he/she will have an additional travel cost savings of $\left(VOT^h - VOT^a - \theta_{1i,\tau}\right)t_{1i,\tau}$ without inducing additional inconvenience cost. Therefore, IEAV users will always have identical

driving mode choices along two consecutive automated links. Note that we assume a reasonable service charge rate $\theta_{l,\tau}$ must satisfy $\theta_{l,\tau} < VOT^h - VOT^a$ as previously discussed.

In scenario (d), both the incoming link and the outgoing link of the node i are regular links. When traveling from node 1 to node 2, IEAV users can only use manual driving mode and will not have driving mode change at the node i.

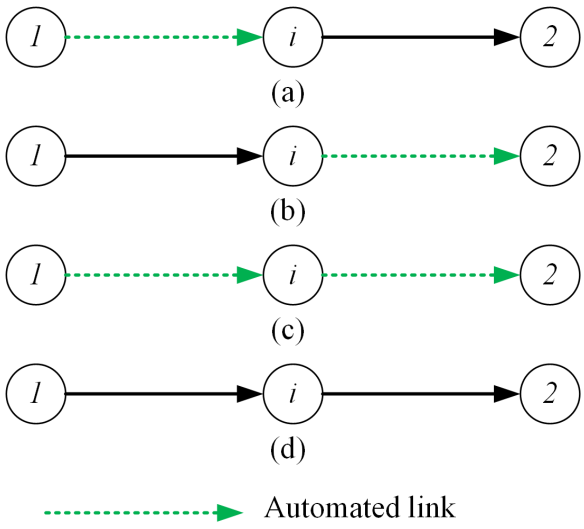

Figure 5-5. Different combinations of two consecutive links

We first use a toy network with four nodes and one O-D pair (1, 4), as shown in Figure 5-6, to illustrate IEAV users' driving mode choices. At a given year $\tau \in T$, we assume the travel demands are given by $q_\tau^{1-4,a} = 0, q_\tau^{1-4,h} = 0$, and $q_\tau^{1-4,\tilde{a}} = 2000$. Set $t_l^0 = 5, \alpha_l = 1, \beta_l = 1, \forall l \in \{(1,2),(2,3),(3,4)\}$. Set $\hat{c}_l^h = 2000, \bar{\eta}_l^{hh} = \bar{\eta}_l^{ah} = 1.8s, \bar{\eta}_l^{aa} = \bar{\eta}_l^{ha} = 0.9s$, then $c_{l,\tau}(r_{l,\tau}) = \frac{4000}{2-r_{l,\tau}}, \forall l \in \{(1,2),(2,3),(3,4)\}$. Assume $VOT^h = 10, VOT^a = 7$, and autonomous driving service charge rate $\theta_{23,\tau} = 1$. Let $y \in [0,1]$ denote the proportion of IEAV users who utilize autonomous driving service on the

automated link (2, 3), then $r_{23,\tau} = y$, $c_{23,\tau} = \frac{4000}{2-y}$, and $t_{23,\tau} = 5\left(2 - \frac{y}{2}\right)$. For regular links (1, 2) and (3, 4), $r_{12,\tau} = r_{34,\tau} = 0$, $c_{12,\tau} = c_{34,\tau} = 2000$, and $t_{12,\tau} = t_{34,\tau} = 10$.

Figure 5-6. A toy network with four nodes

The total travel cost for an IEAV user who chooses autonomous driving on link (2, 3) can be calculated as $VOT^h\left(t_{12,\tau} + t_{34,\tau}\right) + VOT^a t_{23,\tau} + \theta_{23,\tau} t_{23,\tau} + \varepsilon^{ah} + \varepsilon^{ha} = 280 - 20y + \varepsilon^{ah} + \varepsilon^{ha}$, which includes the travel time costs on the three links, autonomous driving service charge on link (2, 3), and two inconvenience costs due to transitions between autonomous driving and manual driving. The total travel cost for an IEAV user who chooses manual driving on link (2, 3) can be calculated as $VOT^h\left(t_{12,\tau} + t_{23,\tau} + t_{34,\tau}\right) = 300 - 25\,y$, which is simply the total travel time cost on the three links.

Below we show that the 2000 units of IEAV users might have different driving mode choices under different scenarios.

Scenario 1. If $\varepsilon^{ah} + \varepsilon^{ha} > 20$, we have $280 - 20y + \varepsilon^{ah} + \varepsilon^{ha} > 300 - 20y \geq 300 - 25\,y$ (because $y \in [0,1]$), i.e., using autonomous driving will have higher travel cost than using manual driving. Therefore, all IEAV users will choose manual driving mode on link (2, 3).

Scenario 2. If $\varepsilon^{ah} + \varepsilon^{ha} = 20$, we have $280 - 20y + \varepsilon^{ah} + \varepsilon^{ha} = 300 - 20y \geq 300 - 25\,y$ (because $y \in [0,1]$), and $300 - 20y = 300 - 25\,y$ only when $y = 0$. Therefore, all IEAV users will choose manual driving mode on link (2, 3).

Scenario 3. If $\varepsilon^{ah} + \varepsilon^{ha} < 15$, we have $280 - 20y + \varepsilon^{ah} + \varepsilon^{ha} < 295 - 20y \leq 300 - 25\,y$ (because $y \in [0,1]$), i.e., using autonomous driving will have smaller travel cost than using manual driving. Therefore, all IEAV users will choose autonomous driving mode on link (2, 3).

Scenario 4. If $\varepsilon^{ah} + \varepsilon^{ha} = 15$, we have $280 - 20y + \varepsilon^{ah} + \varepsilon^{ha} = 295 - 20y \leq 300 - 25\,y$ (because $y \in [0,1]$), and $295 - 20y = 300 - 25\,y$ only when $y = 1$. Therefore, all IEAV users will choose autonomous driving mode on link (2, 3).

Scenario 5. If $\varepsilon^{ah} + \varepsilon^{ha} \in (15,20)$, we will show that the 2000 units of IEAV users cannot have identical driving mode choice on link (2, 3). First, if $y = 0$, we have $280 - 20y + \varepsilon^{ah} + \varepsilon^{ha} = 280 + \varepsilon^{ah} + \varepsilon^{ha} < 300 = 300 - 25\,y$, which means using autonomous driving will have smaller travel cost than using manual driving, and this contradicts with $y = 0$. Second, if $y = 1$, we have $280 - 20y + \varepsilon^{ah} + \varepsilon^{ha} = 260 + \varepsilon^{ah} + \varepsilon^{ha} > 275 = 300 - 25\,y$, which means using autonomous driving will have higher travel cost than using manual driving, and this contradicts with $y = 1$. Therefore, y can neither be 0 nor 1. Furthermore, in the equilibrium state, all the 2000 units of IEAV users must have identical travel cost otherwise those have higher travel costs will switch

to the other driving mode. Therefore, we must have $280 - 20y + \varepsilon^{ah} + \varepsilon^{ha} = 300 - 25\,y$ or $y = \frac{1}{5}(20 - \varepsilon^{ah} - \varepsilon^{ha})$.

The above five scenarios show that the IEAV users between the same O-D pair might have identical or different driving modes along an automated road although they must always have identical travel cost in the equilibrium state. We further note that, for all the above five scenarios, we can collectively use $VOT^h\left(t_{12,\tau} + t_{34,\tau}\right) + VOT^h t_{23,\tau}(1-y) + \left(VOT^a + \theta_{23,\tau}\right)t_{23,\tau}y + (\varepsilon^{ah} + \varepsilon^{ha})y$ to calculate the equilibrium O-D travel cost for IEAV users. First, if $y = 0$, the equilibrium cost will be $VOT^h\left(t_{12,\tau} + t_{23,\tau} + t_{34,\tau}\right)$, which is the cost for the scenario using manual driving. Second, if $y = 1$, the equilibrium cost will be $VOT^h\left(t_{12,\tau} + t_{34,\tau}\right) + VOT^a t_{23,\tau} + \theta_{23,\tau}t_{23,\tau} + \varepsilon^{ah} + \varepsilon^{ha}$, which is the cost for the scenario using autonomous driving. Last, if $y \in (0,1)$, the scenario using manual driving and the scenario using autonomous driving must have identical cost, i.e., $VOT^h\left(t_{12,\tau} + t_{34,\tau}\right) + VOT^a t_{23,\tau} + \theta_{23,\tau}t_{23,\tau} + \varepsilon^{ah} + \varepsilon^{ha} = VOT^h\left(t_{12,\tau} + t_{23,\tau} + t_{34,\tau}\right)$, and consequently it is easy to verify that $VOT^h\left(t_{12,\tau} + t_{34,\tau}\right) + VOT^h t_{23,\tau}(1-y) + \left(VOT^a + \theta_{23,\tau}\right)t_{23,\tau}y + (\varepsilon^{ah} + \varepsilon^{ha})y = y\left(VOT^h\left(t_{12,\tau} + t_{34,\tau}\right) + VOT^a t_{23,\tau} + \theta_{23,\tau}t_{23,\tau} + \varepsilon^{ah} + \varepsilon^{ha}\right) + (1-y)VOT^h\left(t_{12,\tau} + t_{23,\tau} + t_{34,\tau}\right) = VOT^h\left(t_{12,\tau} + t_{34,\tau}\right) + VOT^a t_{23,\tau} + \theta_{23,\tau}t_{23,\tau} + \varepsilon^{ah} + \varepsilon^{ha} = VOT^h\left(t_{12,\tau} + t_{23,\tau} + t_{34,\tau}\right)$.

As aforementioned, an IEAV user will always have identical driving mode choice along two consecutive automated links. We thus collectively consider a set of

consecutive automated links along a path and define them as an automated sub-path as follows.

Definition 5-1. Along a path $p \in P^w$, an automated sub-path is a sub-path that starts from the origin node $o(w)$ or an ending point of a regular link along path $p \in P^w$, consists of a set of consecutive automated links, and ends at a starting point of a regular link along path $p \in P^w$ or the destination node $d(w)$.

As shown in Figure 5-7, the automated sub-path 1 starts from the origin node, includes one automated link (o, 1), and ends at the starting point of a regular link. The automated sub-path 2 starts from the ending point of a regular link, includes two automated links (2, 3) and (3, 4), and ends at the starting point of a regular link. The automated sub-path 3 starts from the ending point of a regular link, includes one automated link (5, d), and ends at the destination node.

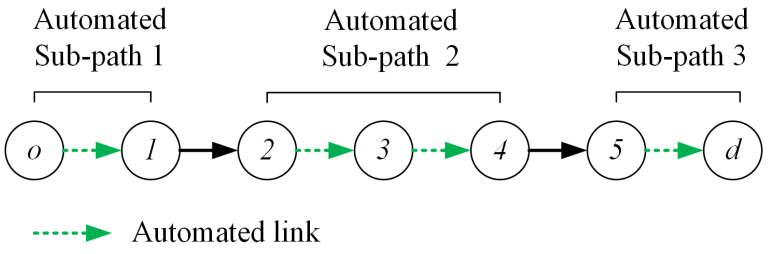

Figure 5-7. Illustration of automated road segments

Along a path $p \in P^w$, let B_τ^p denote the set of all automated sub-paths at year $\tau \in T$. Let $\hat{L}(b)$ denote the set of automated links that belong to automated sub-path $b \in B_\tau^p$. Further let n_b^+ and n_b^- respectively represent the starting point and ending point of

automated sub-path $b \in B_\tau^p$. We assign the potential inconvenience cost ε^{ha} and ε^{ah} associated with an automated sub-path $b \in B_\tau^p$ to nodes n_b^+ and n_b^-,respectively. For an IEAV user between O-D pair $w \in W$, we assume that there will be an inconvenience cost ε^{ha} at the origin node $o(w)$ if the IEAV user utilizes autonomous driving on an automated sub-path starting from node $o(w)$, and that there will be an inconvenience cost ε^{ah} at the destination node $d(w)$ if the IEAV user utilizes autonomous driving on an automated sub-path ending at node $d(w)$. For each automated sub-path $b \in B_\tau^p$, where $p \in P^w$, we define a variable $y_{b,\tau}^p \in [0,1]$ to represent the proportion of IEAV users between O-D pair $w \in W$ who choose autonomous driving service at year $\tau \in T$. Based on the above discussions, below we formally define the equilibrium state of IEAV users' driving mode choices along an automated sub-path.

Definition 5-2. At equilibrium, all IEAV users between O-D pair $w \in W$ on an automated sub-path $b \in B_\tau^p$ along path $p \in P^w$ have identical and minimum travel cost on the automated sub-path. If all those IEAV users choose identical driving mode on the automated sub-path, the travel cost for the chosen driving mode must be less than or equal to the unutilized driving mode. If both manual driving and autonomous driving are utilized, their associated travel costs must be identical.

Mathematically, we propose the following equilibrium conditions to describe IEAV users' driving mode choices along automated sub-paths:

$$y_{b,\tau}^p \leq 1 \qquad \forall b \in B_\tau^p, p \in P^w, w \in W, \tau \in T \quad (5\text{-}40)$$

$$\zeta_{b,\tau}^{p} \geq 0 \qquad \forall b \in B_{\tau}^{p}, p \in P^{w}, w \in W, \tau \in T \quad (5\text{-}41)$$

$$\zeta_{b,\tau}^{p}\left(1 - y_{b,\tau}^{p}\right) = 0 \qquad \forall b \in B_{\tau}^{p}, p \in P^{w}, w \in W, \tau \in T \quad (5\text{-}42)$$

$$y_{b,\tau}^{p} \geq 0 \qquad \forall b \in B_{\tau}^{p}, p \in P^{w}, w \in W, \tau \in T \quad (5\text{-}43)$$

$$\sum_{l \in \hat{L}(b)} \left(VOT^{a} + \theta_{l,\tau} - VOT^{h}\right) t_{l,\tau} + \sum_{n_b^+} \varepsilon^{ha} + \sum_{n_{\bar{b}}} \varepsilon^{ah} + \zeta_{b,\tau}^{p} \geq 0 \qquad \forall b \in B_{\tau}^{p}, p \in P^{w}, w \in W, \tau \in T \quad (5\text{-}44)$$

$$\left(\sum_{l \in \hat{L}(b)} \left(VOT^{a} + \theta_{l,\tau} - VOT^{h}\right) t_{l,\tau} + \sum_{n_b^+} \varepsilon^{ha} + \sum_{n_{\bar{b}}} \varepsilon^{ah} + \zeta_{b,\tau}^{p}\right) y_{b,\tau}^{p} = 0 \qquad \forall b \in B_{\tau}^{p}, p \in P^{w}, w \in W, \tau \in T \quad (5\text{-}45)$$

The following proposition reveals that under conditions (5-40)-(5-45), IEAV users between O-D pair $w \in W$ on an automated sub-path $b \in B_{\tau}^{p}$ along path $p \in P^{w}$ cannot reduce their individual travel costs by unilaterally changing driving mode, namely, the equilibrium state has been obtained.

Proposition 5-4. Constraints (5-40)-(5-45) are the sufficient and necessary equilibrium conditions for the driving mode choice behaviors of IEAV users between O-D pair $w \in W$ on an automated sub-path $b \in B_{\tau}^{p}$ along path $p \in P^{w}$.

Proof. If all the IEAV **users** between O-D pair $w \in W$ on an automated sub-path $b \in B_{\tau}^{p}$ along path $p \in P^{w}$ choose autonomous driving, i.e., $y_{b,\tau}^{p} = 1$, from constraint (5-45) we have

$$\sum_{l \in \hat{L}(b)} \left(VOT^{a} + \theta_{l,\tau} - VOT^{h}\right) t_{l,\tau} + \sum_{n_b^+} \varepsilon^{ha} + \sum_{n_{\bar{b}}} \varepsilon^{ah} + \zeta_{b,\tau}^{p} = 0.$$

With constraint (5-41), we further have

$$\sum_{l\in\hat{L}(b)}\left(VOT^{a}+\theta_{l,\tau}-VOT^{h}\right)t_{l,\tau}+\sum_{n_b^+}\varepsilon^{ha}+\sum_{n_b^-}\varepsilon^{ah}=-\zeta_{b,\tau}^{p}\leq 0,$$

and consequently

$$\sum_{l\in\hat{L}(b)}\left(VOT^{a}+\theta_{l,\tau}\right)t_{l,\tau}+\sum_{n_b^+}\varepsilon^{ha}+\sum_{n_b^-}\varepsilon^{ah}\leq\sum_{l\in\hat{L}(b)}VOT^{h}t_{l,\tau},$$

which means using autonomous driving on the automated sub-path b has equal or lower cost than using manual driving. Therefore, no IEAV users will switch to manual driving. If all the IEAV users between O-D pair $w\in W$ on an automated sub-path $b\in B_\tau^p$ along path $p\in P^w$ choose manual driving on the automated sub-path b, i.e., $y_{b,\tau}^{p}=0$, from constraint (5-42) we have $\zeta_{b,\tau}^{p}=0$. With constraint (5-44), we further have

$$\sum_{l\in\hat{L}(b)}\left(VOT^{a}+\theta_{l,\tau}-VOT^{h}\right)t_{l,\tau}+\sum_{n_b^+}\varepsilon^{ha}+\sum_{n_b^-}\varepsilon^{ah}\geq 0,$$

and consequently

$$\sum_{l\in\hat{L}(b)}\left(VOT^{a}+\theta_{l,\tau}\right)t_{l,\tau}+\sum_{n_b^+}\varepsilon^{ha}+\sum_{n_b^-}\varepsilon^{ah}\geq\sum_{l\in\hat{L}(b)}VOT^{h}t_{l,\tau},$$

which means using autonomous driving on the automated sub-path b has equal or higher cost than using manual driving. Therefore, no IEAV users will switch to autonomous driving. If $y_{b,\tau}^{p}\in(0,1)$ of the IEAV users between O-D pair $w\in W$ on an automated sub-path $b\in B_\tau^p$ along path $p\in P^w$ choose autonomous driving on the automated sub-path b while the rest $1-y_{b,\tau}^{p}$ choose manual driving, from constraints (5-42) and (5-45) we have $\zeta_{b,\tau}^{p}=0$ and

$$\sum_{l\in\hat{L}(b)}\left(VOT^{a}+\theta_{l,\tau}-VOT^{h}\right)t_{l,\tau}+\sum_{n_b^+}\varepsilon^{ha}+\sum_{n_b^-}\varepsilon^{ah}+\zeta_{b,\tau}^{p}=0,$$

and consequently

$$\sum_{l\in\hat{L}(b)}\left(VOT^{a}+\theta_{l,\tau}\right)t_{l,\tau}+\sum_{n_b^+}\varepsilon^{ha}+\sum_{n_b^-}\varepsilon^{ah}=\sum_{l\in\hat{L}(b)}VOT^{h}t_{l,\tau},$$

which means using autonomous driving and manual driving on the automated sub-path b have identical travel cost. Therefore, no IEAV users will switch their driving modes. The above analysis includes all the possible cases when IEAV users will not change their driving modes on an automated sub-path. Hence Constraints (5-40)-(5-45) are the sufficient and necessary equilibrium conditions for the driving mode choice behaviors of IEAV users between O-D pair $w\in W$ on an automated sub-path $b\in B_\tau^p$ along path $p\in P^w$. □

In the following proposition, we further establish IEAV users' travel cost functions on automated sub-paths.

Proposition 5-5. At equilibrium, the travel cost for an IEAV user between O-D pair $w\in W$ on an automated sub-path $b\in B_\tau^p$ along path $p\in P^w$ can always be calculated as $\left(\sum_{l\in\hat{L}(b)}\left(VOT^{a}+\theta_{l,\tau}\right)t_{l,\tau}+\sum_{n_b^+}\varepsilon^{ha}+\sum_{n_b^-}\varepsilon^{ah}\right)y_{b,\tau}^{p}+\sum_{l\in\hat{L}(b)}VOT^{h}t_{l,\tau}\left(1-y_{b,\tau}^{p}\right)$.

Proof. From the proof of Proposition 5-4, we can easily verify that: (1) if $y_{b,\tau}^{p}=1$, i.e., all the IEAV users between O-D pair $w\in W$ on an automated sub-path $b\in B_\tau^p$ along

path $p \in P^w$ choose autonomous driving on the automated sub-path b, $\left(\sum_{l\in\hat{L}(b)}\left(VOT^a + \theta_{l,\tau}\right)t_{l,\tau} + \sum_{n_b^+}\varepsilon^{ha} + \sum_{n_b^-}\varepsilon^{ah}\right)y_{b,\tau}^p$ calculates the travel cost of each of these IEAV users who use autonomous driving; (2) if $y_{b,\tau}^p = 0$, i.e., all the IEAV users choose manual driving on the automated sub-path b, $\sum_{l\in\hat{L}(b)} VOT^h t_{l,\tau}\left(1 - y_{b,\tau}^p\right)$ calculates the travel cost of each of these IEAV users who use manual driving; and (3) if $y_{b,\tau}^p \in (0,1)$, i.e., $y_{b,\tau}^p \in (0,1)$ of the IEAV users between O-D pair $w \in W$ on an automated sub-path $b \in B_\tau^p$ along path $p \in P^w$ choose autonomous driving on the automated sub-path b while the rest $1 - y_{b,\tau}^p$ choose manual driving, then $\left(\sum_{l\in\hat{L}(b)}\left(VOT^a + \theta_{l,\tau}\right)t_{l,\tau} + \sum_{n_b^+}\varepsilon^{ha} + \sum_{n_b^-}\varepsilon^{ah}\right) = \sum_{l\in\hat{L}(b)} VOT^h t_{l,\tau} = \left(\sum_{l\in\hat{L}(b)}\left(VOT^a + \theta_{l,\tau}\right)t_{l,\tau} + \sum_{n_b^+}\varepsilon^{ha} + \sum_{n_b^-}\varepsilon^{ah}\right)y_{b,\tau}^p + \sum_{l\in\hat{L}(b)} VOT^h t_{l,\tau}\left(1 - y_{b,\tau}^p\right)$ calculates the identical travel cost of IEAV users who use either autonomous driving or manual driving. □

5.3.1.2 Proportion of autonomous driving vehicles in mixed traffic and travel time function reformulation

On a regular link, IEAVs must be driven manually, thus only IIAVs are autonomous driving vehicles. The proportion of flow of autonomous driving vehicles on a regular link is given by

$$r_{l,\tau} = \frac{x_{l,\tau}^a}{x_{l,\tau}^h + x_{l,\tau}^a + x_{l,\tau}^{\tilde{a}}} \qquad \forall l \in L\backslash\hat{L}_\tau, \tau \in T \qquad (5\text{-}46)$$

On an automated link, both IIAVs and IEAVs using autonomous driving mode are autonomous driving vehicles. With a slightly abuse of notation, we use $x_{l,\tau}^{\tilde{a}a}$ to represent the aggregate flow of IEAV users using autonomous driving mode on an automated link $l \in \hat{L}_\tau$ at year $\tau \in T$. The proportion of flow of autonomous driving vehicles on an automated link is given by

$$r_{l,\tau} = \frac{x_{l,\tau}^{a} + x_{l,\tau}^{\tilde{a}a}}{x_{l,\tau}^{h} + x_{l,\tau}^{a} + x_{l,\tau}^{\tilde{a}}} \qquad \forall l \in \hat{L}_\tau, \tau \in T \qquad (5\text{-}47)$$

Let $L(p)$ denote the set of links along path $p \in P^w$. Let variable $y_{l,\tau}^{p}$, where $l \in L(p) \cap \hat{L}_\tau$, represent the proportion of IEAV users on path $p \in P^w$ between O-D pair $w \in W$ who choose autonomous driving service on automated link l at year $\tau \in T$. $y_{l,\tau}^{p}$ satisfies the following equation:

$$y_{l,\tau}^{p} = y_{b,\tau}^{p} \qquad \forall l \in \hat{L}(b), b \in B_\tau^p, p \in P^w, w \in W, \tau \in T \qquad (5\text{-}48)$$

Let $P^w(l)$ denote the set of paths between O-D pair $w \in W$ that pass link $l \in L$. Note that $p \in P^w(l)$ is equivalent to $l \in L(p)$. Variables $x_{l,\tau}^{\tilde{a}a}$ and $x_{l,\tau}^{m}$ can then be calculated as

$$x_{l,\tau}^{\tilde{a}a} = \sum_{w \in W} \sum_{p \in P^w(l)} y_{l,\tau}^{p} f_{p,\tau}^{\tilde{a}} \qquad \forall l \in \hat{L}_\tau, \tau \in T \qquad (5\text{-}49)$$

$$x_{l,\tau}^{m} = \sum_{w \in W} \sum_{p \in P^w(l)} f_{p,\tau}^{m} \qquad \forall l \in L, m \in M, \tau \in T \qquad (5\text{-}50)$$

In Section 3.1.3, we defined two new concepts: human-driven vehicle equivalent (HVE) and aggregate link flow in HVE. Similarly, if $HVE_{l,\tau}$ and $v_{l,\tau}$ denote the HVE and

aggregate link flow in HVE on link $l \in L$ at year $\tau \in T$, they are defined by the following equations

$$HVE_{l,\tau} = \frac{\bar{\eta}_l^{hh} + \bar{\eta}_l^{aa} - \bar{\eta}_l^{ha} - \bar{\eta}_l^{ah}}{\bar{\eta}_l^{hh}} r_{l,\tau} + \frac{\bar{\eta}_l^{ha} + \bar{\eta}_l^{ah} - \bar{\eta}_l^{hh}}{\bar{\eta}_l^{hh}} \quad \forall l \in L, \tau \in T \qquad (5\text{-}51)$$

$$v_{l,\tau} = x_{l,\tau}^h + x_{l,\tau}^{\tilde{a}} + HVE_{l,\tau} x_{l,\tau}^a \quad \forall l \in L \backslash \hat{L}_\tau, \tau \in T \qquad (5\text{-}52)$$

$$v_{l,\tau} = x_{l,\tau}^h + x_{l,\tau}^{\tilde{a}} - x_{l,\tau}^{\tilde{a}a} + HVE_{l,\tau}\left(x_{l,\tau}^a + x_{l,\tau}^{\tilde{a}a}\right) \quad \forall l \in \hat{L}_\tau, \tau \in T \qquad (5\text{-}53)$$

The travel time function can then be given by the following equation

$$t_{l,\tau} = t_l^0 \left[1 + \alpha_l \left(\frac{v_{l,\tau}}{\hat{c}_l^h}\right)^{\beta_l}\right] \quad \forall l \in L, \tau \in T \qquad (5\text{-}54)$$

Based on the above discussions, we can then formulate and analyze the user equilibrium problem in networks with automated roads and mixed flows of HVs, IIAVs and IEAVs.

5.3.1.3 Formulation of UE model

When travelling between origins and destinations, all road users are assumed to selfishly choose their routes to minimize their individual travel costs. In a network with automated links, the equilibrium flow distributions of HVs, IIAVs, and IEAVs can be described by the following nonlinear complementarity problem:

[UE-NCP]
Constraints (5-40)-(5-54), and

$$\sum_{p \in P^w} f_{p,\tau}^m = q_\tau^{w,m} \quad \forall w \in W, m \in M, \tau \in T \qquad (5\text{-}55)$$

$$\lambda_{p,\tau}^h = \sum_{l \in L(p)} VOT^h t_{l,\tau} \quad \forall p \in P^w, w \in W, \tau \in T \qquad (5\text{-}56)$$

$$\lambda_{p,\tau}^{a} = \sum_{l \in L(p)} VOT^{a} t_{l,\tau} \qquad \forall p \in P^{w}, w \in W, \tau \in T \qquad (5\text{-}57)$$

$$\lambda_{p,\tau}^{\tilde{a}} = \sum_{l \in L(p) \setminus \hat{L}_{\tau}} VOT^{h} t_{l,\tau} + \sum_{b \in B_{\tau}^{p}} \left(\left(\sum_{l \in \hat{L}(b)} \left(VOT^{a} + \theta_{l,\tau} \right) t_{l,\tau} + \sum_{n_b^{+}} \varepsilon^{ha} + \sum_{n_{\bar{b}}} \varepsilon^{ah} \right) y_{b,\tau}^{p} + \sum_{l \in \hat{L}(b)} VOT^{h} t_{l,\tau} \left(1 - y_{b,\tau}^{p} \right) \right) \qquad \forall p \in P^{w}, w \in W, \tau \in T \qquad (5\text{-}58)$$

$$f_{p,\tau}^{m} \geq 0 \qquad \forall p \in P^{w}, w \in W, m \in M, \tau \in T \qquad (5\text{-}59)$$

$$\lambda_{p,\tau}^{m} - \mu_{\tau}^{w,m} \geq 0 \qquad \forall p \in P^{w}, w \in W, m \in M, \tau \in T \qquad (5\text{-}60)$$

$$\left(\lambda_{p,\tau}^{m} - \mu_{\tau}^{w,m} \right) f_{p,\tau}^{m} = 0 \qquad \forall p \in P^{w}, w \in W, m \in M, \tau \in T \qquad (5\text{-}61)$$

where variable $\lambda_{p,\tau}^{m}$ represents the travel cost of class $m \in M$ users between O-D pair $w \in W$ along path $p \in P^{w}$ at year $\tau \in T$; variable $\mu_{\tau}^{w,m}$ is an auxiliary variable representing the equilibrium travel cost of class $m \in M$ users between O-D pair $w \in W$ at year $\tau \in T$. In equation (5-58), $\sum_{l \in L(p) \setminus \hat{L}_{\tau}} VOT^{h} t_{l,\tau}$ calculates the total travel time cost on all regular links along path p, and $\sum_{b \in B_{\tau}^{p}} \left(\left(\sum_{l \in \hat{L}(b)} \left(VOT^{a} + \theta_{l,\tau} \right) t_{l,\tau} + \sum_{n_b^{+}} \varepsilon^{ha} + \sum_{n_{\bar{b}}} \varepsilon^{ah} \right) y_{b,\tau}^{p} + \sum_{l \in \hat{L}(b)} VOT^{h} t_{l,\tau} \left(1 - y_{b,\tau}^{p} \right) \right)$ calculates the total cost on all automated sub-paths along path p (see Proposition 5-5).

In the above, constraints (5-40)-(5-45) are equilibrium conditions describing IEAV users' driving mode choices along automated sub-paths. Constraints (5-46)-(5-54) are definitional constraints. Constraint (5-55) is the flow conservation constraint. Constraints (5-56)-(5-58) define the travel cost for each user class. Constraint (5-59) describes the non-negativity of path flows. Constraints (5-59)-(5-61) ensures that, for the

same class between each O-D pair, the travel costs on all utilized paths are the same and equal to $\mu_\tau^{w,m}$, and less than or equal to those on unutilized paths. Note that the travel costs are all in monetary unit.

The proposed UE model has three distinct characteristics: First, the travel time functions have different structures for regular links and automated links (i.e., the difference between equations (5-52) and (5-53)); Second, the value of times for IEAV users may be different on regular links and automated links; Third, in addition to making route choices, IEAV users also need to choose their driving modes on automated links.

5.3.1.4 Solution algorithm

To solve the [UE-VI], we apply the technique developed by Aghassi et al. (2006) using duality to reformulate the [UE-VI] as the following nonlinear optimization problem:

[UE-NLP]

$$\min_{\boldsymbol{f},\boldsymbol{x},\boldsymbol{v},\boldsymbol{y},\tilde{\boldsymbol{\zeta}},\tilde{\boldsymbol{\mu}}} \sum_{w\in W}\sum_{p\in P^w}\sum_{m\in M}\lambda_{p,\tau}^{m} f_{p,\tau}^{m} + \sum_{w\in W}\sum_{p\in P^w}\sum_{b\in B_\tau^p}\left(\sum_{l\in\tilde{L}(b)}\left(VOT^a+\theta_{l,\tau}-VOT^h\right)t_{l,\tau}+\sum_{n_b^+}\varepsilon^{ha}+\sum_{n_b^-}\varepsilon^{ah}\right)y_{b,\tau}^{p}-\sum_{w\in W}\sum_{m\in M}q_\tau^{w,m}\tilde{\mu}_\tau^{w,m}+\sum_{w\in W}\sum_{p\in P^w}\sum_{b\in B_\tau^p}\tilde{\zeta}_{b,\tau}^{p}$$

s.t.

$$\tilde{\zeta}_{b,\tau}^{p}\geq 0 \qquad \forall b\in B_\tau^p, p\in P^w, w\in W, \tau\in T$$

$$-\tilde{\zeta}_{b,\tau}^{p} \le \sum_{l\in\hat{L}(b)} \left(VOT^{a} + \theta_{l,\tau} - VOT^{h}\right) t_{l,\tau} + \sum_{n_b^+} \varepsilon^{ha} + \sum_{n_b^-} \varepsilon^{ah} \qquad \forall b \in B_{\tau}^{p}, p \in P^{w}, w \in W, \tau \in T$$

$$\tilde{\mu}_{\tau}^{w,m} \le \lambda_{p,\tau}^{m} \qquad \forall p \in P^{w}, w \in W, m \in M, \tau \in T$$

$$(\boldsymbol{f}, \boldsymbol{x}, \boldsymbol{v}, \boldsymbol{y}) \in \Phi$$

where $\tilde{\zeta}_{b,\tau}^{p}$ and $\tilde{\mu}_{\tau}^{w,m}$ are auxiliary variables.

In solving the above optimization problem, if the optimal value of the objective function is zero, then one part of the optimal solution, $(\boldsymbol{f}^*, \boldsymbol{x}^*, \boldsymbol{v}^*, \boldsymbol{y}^*)$, would be the solution to the [UE-VI] problem. Because the [UE-NLP] model is a regular nonlinear programming, it can be solved using commercial nonlinear solvers such as CONOPT (Drud, 1994). However, the [UE-NLP] is path-flow-based and thus requires prior path enumeration. To solve the [UE-NLP] in large-scale networks, we propose an iterative solution procedure based on the column generation algorithm developed by Leventhal et al., (1973). We first construct a subset of P^w and solve a restricted version of the [UE-NLP] over the subset. Based on the obtained solution, a series of shortest-path sub-problems are solved to determine whether the solution of the restricted [UE-NLP] also solves the original formulation. If not, new paths generated from the sub-problems are added to the path subset and the iteration proceeds until termination.

Given the link travel time solution $\tilde{\boldsymbol{t}}$ obtained from solving the restricted [UE-NLP], the shortest-path problem for HVs and IIAVs (i.e., for $m \in \{h, a\}$) can be formulated as follows for each O-D pair $w \in W$:

[SP-HV&IIAV]

$$\min_{\boldsymbol{z}} \sum_{l \in L} \tilde{t}_{l,\tau}\, z_{l,\tau}^{w,m}$$

s.t.

$$\boldsymbol{\Delta} \boldsymbol{z}_{\tau}^{w,m} = \boldsymbol{E}^{w}$$

$$z_{l,\tau}^{w,m} \in \{0,1\} \qquad \forall l \in L$$

where $\boldsymbol{\Delta}$ is the node-link incidence matrix associated with the network; $\boldsymbol{z}_{\tau}^{w,m}$ is the vector of $\{\cdots, z_{l,\tau}^{w,m}, \cdots\}$; $z_{l,\tau}^{w,m}$ is a binary variable, which is equal to 1 if link $l \in L$ is utilized and 0 otherwise; $\boldsymbol{E}^{w}$ represents an "input-output" vector, which has exactly two non-zero components: one has the value 1 corresponding to the origin node $o(w)$ and the other has the value -1 corresponding to the destination node $d(w)$.

Problem [SP-HV&IIAV] belongs to the classical shortest path problem. The conventional shortest path algorithm such as the Dijkstra's algorithm (Dijkstra,1959), can be applied to solve the model [SP-HV&IIAV] efficiently.

For an IEAV user, his/her travel cost includes three parts: travel time costs on regular links, travel time costs and potential autonomous driving service charges on automated links, and potential inconvenience costs due to driving mode changes. To formulate the shortest path problem, we can also use the binary variable $z_{l,\tau}^{w,m}$ defined above to indicate whether a link $l \in L$ is utilized. For an automated link $l \in \hat{L}$, however, we also need to determine the driving mode of IEAVs on the link if it is utilized. A straightforward method to do so is to further define another binary variable, denoted as $\check{z}_{l,\tau}^{w,m}$, on top of $z_{l,\tau}^{w,m}$ to indicate the driving mode of IEAVs on an automated link $l \in \hat{L}$: $\check{z}_{l,\tau}^{w,m} = 1$ if autonomous driving is used, and $\check{z}_{l,\tau}^{w,m} = 0$ otherwise. With this method, however, the total travel cost on automated links will be given by $\sum_{l \in \hat{L}} \Big(\big(VOT^{a} +$

$\theta_{l,\tau}\big)\check{z}_{l,\tau}^{w,m} + VOT^h\big(1-\check{z}_{l,\tau}^{w,m}\big)\Big) z_{l,\tau}^{w,m}\tilde{t}_{l,\tau}$, which is nonlinear. Consequently, the shortest path problem will be a binary nonlinear programming, which is not easy to solve.

Instead of following the above approach, we developed a novel binary linear programming formulation for the shortest path problem for IEAVs (i.e., for $m = \tilde{a}$). For each O-D pair $w \in W$, the formulation is given as follows:

[SP-IEAV]

$$\min_{\boldsymbol{z},\boldsymbol{g},\boldsymbol{\psi}} \sum_{l\in L\setminus\hat{L}} VOT^h z_{l,\tau}^{w,m}\tilde{t}_{l,\tau} + \sum_{l\in\hat{L}}\Big(\big(VOT^a+\theta_{l,\tau}\big)g_{l,\tau}^{1,w} + VOT^h g_{l,\tau}^{2,w}\Big)\tilde{t}_{l,\tau} + \sum_{i\in N}\big(\psi_{i,\tau}^{1,w}\varepsilon^{ha} + \psi_{i,\tau}^{2,w}\varepsilon^{ah}\big)$$

s.t.

$$\boldsymbol{\Delta z}_{\tau}^{w,m} = \boldsymbol{E}^w \tag{5-62}$$

$$z_{l,\tau}^{w,m} \in \{0,1\} \quad \forall l \in L \tag{5-63}$$

$$g_{l,\tau}^{1,w} \in \{0,1\} \quad \forall l \in \hat{L} \tag{5-64}$$

$$g_{l,\tau}^{2,w} \in \{0,1\} \quad \forall l \in \hat{L} \tag{5-65}$$

$$\psi_{i,\tau}^{1,w} \in \{0,1\} \quad i \in N \tag{5-66}$$

$$\psi_{i,\tau}^{2,w} \in \{0,1\} \quad i \in N \tag{5-67}$$

$$z_{l,\tau}^{w,m} = g_{l,\tau}^{1,w} + g_{l,\tau}^{2,w} \quad \forall l \in \hat{L} \tag{5-68}$$

$$\psi_{i,\tau}^{1,w} \le 1 - \sum_{(j,i)=l\in\hat{L}} g_{l,\tau}^{1,w} \quad i \in N \tag{5-69}$$

$$\psi_{i,\tau}^{1,w} \le \sum_{(i,j)=l\in\hat{L}} g_{l,\tau}^{1,w} \quad i \in N \tag{5-70}$$

$$\psi_{i,\tau}^{1,w} \ge \sum_{(i,j)=l\in\hat{L}} g_{l,\tau}^{1,w} - \sum_{(j,i)=l\in\hat{L}} g_{l,\tau}^{1,w} \quad i \in N \tag{5-71}$$

$$\psi_{i,\tau}^{2,w} \le \sum_{(j,i)=l\in\hat{L}} g_{l,\tau}^{1,w} \quad i \in N \tag{5-72}$$

$$\psi_{i,\tau}^{2,w} \le 1 - \sum_{(i,j)=l\in\hat{L}} g_{l,\tau}^{1,w} \quad i \in N \tag{5-73}$$

$$\psi_{i,\tau}^{2,w} \geq \sum_{(j,i)=l\in\hat{L}} g_{l,\tau}^{1,w} - \sum_{(i,j)=l\in\hat{L}} g_{l,\tau}^{1,w} \qquad i \in N \qquad (5\text{-}74)$$

where $g_{l,\tau}^{1,w}$ is a binary variable, which is equal to 1 if automated link $l \in \hat{L}$ is utilized and autonomous driving is used on the link, and 0 otherwise; $g_{l,\tau}^{2,w}$ is a binary variable, which is equal to 1 if automated link $l \in \hat{L}$ is utilized and manual driving is used on the link, and 0 otherwise; $\psi_{i,\tau}^{1,w}$ is a binary variable, which is equal to 1 if node $i \in N$ is utilized and driving mode is changed from manual driving to autonomous driving at the node, and 0 otherwise; $\psi_{i,\tau}^{2,w}$ is a binary variable, which is equal to 1 if node $i \in N$ is utilized and driving mode is changed from autonomous driving to manual driving at the node, and 0 otherwise. Note that we assume IEAVs are in manual driving mode at the origin and destination nodes, which means that an IEAV user will experience an driving mode change from manual driving to autonomous driving at the origin node $o(w)$ (i.e., $\psi_{o(w),\tau}^{1,w} = 1$) if he/she utilizes autonomous driving on an automated link starting from node $o(w)$, and that an IEAV user will experience an driving mode change from autonomous driving to manual driving at the destination node $d(w)$ (i.e., $\psi_{d(w),\tau}^{2,w} = 1$) if he/she utilizes autonomous driving on an automated link ending at node $d(w)$.

In the above formulation, the objective function is to minimize the total travel cost for an IEAV user. The first term $\sum_{l\in L\setminus\hat{L}} VOT^h z_{l,\tau}^{w,m} \tilde{t}_{l,\tau}$ calculated the total travel cost on all utilized regular links. The second term $\sum_{l\in\hat{L}} \left(\left(VOT^a + \theta_{l,\tau}\right) g_{l,\tau}^{1,w} + VOT^h g_{l,\tau}^{2,w}\right) \tilde{t}_{l,\tau}$ calculates the total travel time cost and service charge on all utilized automated links. The last term $\sum_{i\in N}\left(\psi_{i,\tau}^{1,w}\varepsilon^{ha} + \psi_{i,\tau}^{2,w}\varepsilon^{ah}\right)$ calculates the total inconvenience cost. Constraint

(5-62) ensures flow balance. Constraints (5-63)-(5-67) ensure that variables $z_{l,\tau}^{w,m}$, $g_{l,\tau}^{1,w}$, $g_{l,\tau}^{2,w}$, $\psi_{i,\tau}^{1,w}$, and $\psi_{i,\tau}^{2,w}$ are binary variables. Constraint (5-68) specifies the relationship among $z_{l,\tau}^{w,m}$, $g_{l,\tau}^{1,w}$, and $g_{l,\tau}^{2,w}$: if $z_{l,\tau}^{w,m} = 1$, i.e., the automated link $l \in \hat{L}$ is utilized, we must have $g_{l,\tau}^{1,w} + g_{l,\tau}^{2,w} = 1$, i.e., one driving mode must be utilized; if $z_{l,\tau}^{w,m} = 0$, i.e., the automated link $l \in \hat{L}$ is not utilized, we must have $g_{l,\tau}^{1,w} + g_{l,\tau}^{2,w} = 0$, i.e., neither driving modes is utilized. Constraint (5-69) ensures that if a node $i \in N$ has an incoming automated link being utilized in autonomous driving mode (i.e., $\sum_{(j,i)=l\in\hat{L}} g_{l,\tau}^{1,w} = 1$), the node i cannot be a utilized node with a mode change from manual driving to autonomous driving (i.e., $\psi_{i,\tau}^{1,w}$ must be 0). Constraint (5-70) ensures that if a node $i \in N$ does not have any outgoing automated links being utilized in autonomous driving mode (i.e., $\sum_{(i,j)=l\in\hat{L}} g_{l,\tau}^{1,w} = 0$), the node i cannot be a utilized node with a mode change from manual driving to autonomous driving (i.e., $\psi_{i,\tau}^{1,w}$ must be 0). Constraint (5-71) ensures that if a node $i \in N$ has an outgoing automated link being utilized in autonomous driving mode (i.e., $\sum_{(i,j)=l\in\hat{L}} g_{l,\tau}^{1,w} = 1$) and does not have any incoming automated links being utilized in autonomous driving mode (i.e., $\sum_{(j,i)=l\in\hat{L}} g_{l,\tau}^{1,w} = 0$), the node i must be a utilized node with a mode change from manual driving to autonomous driving (i.e., $\psi_{i,\tau}^{1,w}$ must be 1). Constraint (5-72) ensures that if a node $i \in N$ does not have any incoming links being utilized in autonomous driving mode (i.e., $\sum_{(j,i)=l\in\hat{L}} g_{l,\tau}^{1,w} = 0$), the node i cannot be a utilized node with a mode change from autonomous driving to manual driving (i.e., $\psi_{i,\tau}^{2,w}$ must be 0). Constraint (5-73) ensures that if a node $i \in N$ has an

outgoing automated link being utilized in manual driving mode (i.e., $\sum_{(i,j)=l\in\hat{L}} g_{l,\tau}^{1,w} = 1$), the node i cannot be a utilized node with a mode change from autonomous driving to manual driving (i.e., $\psi_{i,\tau}^{2,w}$ must be 0). Constraint (5-74) ensures that if a node $i \in N$ has an incoming automated link being utilized in autonomous driving mode (i.e., $\sum_{(j,i)=l\in\hat{L}} g_{l,\tau}^{1,w} = 1$) and does not have any outgoing automated links being utilized in autonomous driving mode (i.e., $\sum_{(i,j)=l\in\hat{L}} g_{l,\tau}^{1,w} = 0$), the node i must be a utilized node with a mode change from autonomous driving to manual driving (i.e., $\psi_{i,\tau}^{2,w}$ must be 1).

As formulated, [SP-IEAV] is a binary linear programming that can be solved using commercial solvers such as CPLEX 12.9. However, since binary linear programming is NP-hard, it might be challenging to solve [SP-IEAV] for large-scale networks. We thus further develop a network expansion method to solve [SP-IEAV] efficiently. As shown in Figure 5-8, the original network i.e., $G(N, L)$ (see Figure 5-8 (a)), can be expanded into a new network, i.e., $G(\underline{N}, \underline{L})$ (see Figure 5-8 (b)), by the following steps:

(1) For each node $i \in N$ that has either incoming or outgoing automated links, we make a copy of the node, denoted as i'.

(2) For each automated link $(i, j) = l \in \hat{L}$, we can then make a copy of it as (i', j').

(3) For each node pair i' and i, we add two dummy links (i, i') and (i', i).

In the expanded network $G(\underline{N}, \underline{L})$, let $\underline{L}_0$ denote the set of all newly added duplicate automated links (i', j'), $\underline{L}_1$ denote the set of all dummy links (i, i'), $\underline{L}_2$ denote

the set of all dummy links (i', i), and $\underline{L} = L \cup \underline{L}_0 \cup \underline{L}_1 \cup \underline{L}_2$. Link travel cost in the expanded network, denoted as $s_{l,\tau}$, is defined as follows:

(1) The travel cost on link $l = (i, j) \in L$ is defined as $s_{ij,\tau} = VOT^h \tilde{t}_{ij,\tau}$.

(2) The travel cost on link $(i', j') \in \underline{L}_0$ is defined as $s_{i'j',\tau} = \left(VOT^a + \theta_{ij,\tau}\right)\tilde{t}_{ij,\tau}$, where (i', j') is the copy of $(i, j) \in \hat{L}$.

(3) The travel cost on link $(i, i') \in \underline{L}_1$ is defined as $s_{ii',\tau} = \varepsilon^{ha}$.

(4) The travel cost on link $(i', i) \in \underline{L}_2$ is defined as $s_{i'i,\tau} = \varepsilon^{ah}$.

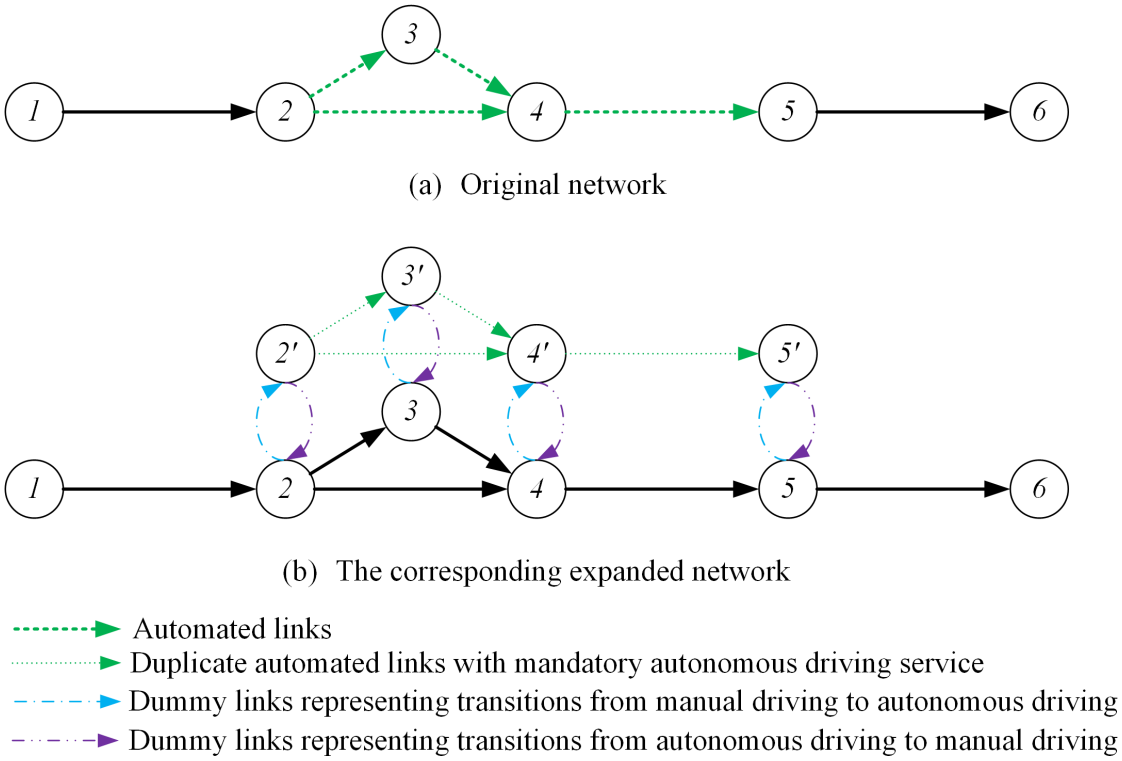

Figure 5-8. Illustration of the network expansion

With the above link travel cost definitions, we can decompose an IEAV user's joint path and driving mode choice behavior in the original network into a pure path

choice behavior in the expanded network. For example, if an IEAV user between O-D pair (1, 6) chooses route $1 \rightarrow 2 \rightarrow 3 \rightarrow 4 \rightarrow 5 \rightarrow 6$ and utilizes autonomous driving on links (2, 3), (3, 4), and (4, 5) in the original network (see Figure 5-8(a)), his/her behavior can be equivalently represented as using the path $1 \rightarrow 2 \rightarrow 2' \rightarrow 3' \rightarrow 4' \rightarrow 5' \rightarrow 5 \rightarrow 6$ in the expanded network. Within the expanded network $G(\underline{N}, \underline{L})$, the [SP-IEAV] can be reformulated into the following shortest path problem:

[SP-IEAV-2]

$$\min_{\boldsymbol{z}} \sum_{l \in L} s_{l,\tau} \, z_{l,\tau}^{w,m}$$

s.t.

$$\boldsymbol{\Delta} \boldsymbol{z}_{\tau}^{w,m} = \boldsymbol{E}^{w}$$

$$z_{l,\tau}^{w,m} \in \{0, 1\} \qquad \forall l \in \underline{L}$$

[SP-IEAV-2] is a classical shortest path problem and can be solved efficiently using the Dijkstra's algorithm (Dijkstra,1959).

SP-HV&IIAV and SP-IEAV-2 can be solved for each O-D pair after we solve a restricted [UE-NLP] problem. The optimal solution of SP-HV&IIAV, denoted by $\tilde{\boldsymbol{z}}_{\tau}^{w,m}$, can be used to construct the shortest path for HV and IIAV users ($m \in \{h, a\}$), denoted as $\tilde{p}_{\tau}^{w,m}$. The optimal solution of SP-IEAV-2, also denoted by $\tilde{\boldsymbol{z}}_{\tau}^{w,m}$, can be used to construct the shortest path for IEAV users ($m = \tilde{a}$), denoted as $\tilde{p}_{\tau}^{w,m}$. If for each class of users and every O-D pair, the calculated minimal travel cost from SP-HV&IIAV or SP-IEAV-2 is not smaller than the equilibrium travel cost from the restricted [UE-NLP], then the solution of the restricted [UE-NLP] also solves the original formulation. Otherwise, we add those new paths that have smaller travel costs than the corresponding equilibrium

travel costs to the path subset and proceed to the next iteration. The iterative solution procedure is outlined as follows:

Step 0: Set $\tilde{t}_{l,\tau} = t_l^0$. For each O-D pair $w \in W$, solve SP-HV&IIAV and SP-IEAV-2 and construct initial path subsets $\tilde{P}_\tau^{w,m} = \{\tilde{p}_\tau^{w,m}\}$ accordingly.

Step 1: Solve the [UE-NLP] over the path subset $\bigcup_{w\in W} \bigcup_{m\in M} \tilde{P}_\tau^{w,m}$ and obtain the link travel time $\tilde{t}_{l,\tau}$ and the equilibrium O-D travel cost $\tilde{\mu}_\tau^{w,m}$.

Step 2: For each O-D pair $w \in W$, solve SP-HV&IIAV and SP-IEAV-2 to obtain the optimal solution $\tilde{\boldsymbol{z}}_\tau^{w,m}$ and construct the shortest path $\tilde{p}_\tau^{w,m}$ for each user class $m \in M$. If for each O-D pair $w \in W$, $\sum_{l\in L} \tilde{t}_{l,\tau}\, \tilde{z}_{l,\tau}^{w,m} = \frac{\tilde{\mu}_\tau^{w,h}}{VOT^h} = \frac{\tilde{\mu}_\tau^{w,a}}{VOT^a}$ for user class $m \in \{h, a\}$ and $\sum_{l\in L} VOT^h \tilde{t}_{l,\tau}\, \tilde{z}_{l,\tau}^{w,m} + \sum_{l\in \underline{L}_0} \big(VOT^a + \theta_{l,\tau}\big)\tilde{t}_{l,\tau}\, \tilde{z}_{l,\tau}^{w,m} + \sum_{l\in \underline{L}_1} \varepsilon^{ha}\, \tilde{z}_{l,\tau}^{w,m} + \sum_{l\in \underline{L}_2} \varepsilon^{ah}\, \tilde{z}_{l,\tau}^{w,m} = \tilde{\mu}_\tau^{w,m}$ for user class $m = \tilde{a}$, then terminate and the current solution of the restricted [UE-NLP] is the UE solution. Otherwise, add all the shortest paths $\tilde{p}_\tau^{w,m}$ for user class $m \in \{h, a\}$ that satisfy $\sum_{l\in L} \tilde{t}_{l,\tau}\, \tilde{z}_{l,\tau}^{w,m} < \frac{\tilde{\mu}_\tau^{w,h}}{VOT^h} = \frac{\tilde{\mu}_\tau^{w,a}}{VOT^a}$, and the shortest path $\tilde{p}_\tau^{w,m}$ for user class $m = \tilde{a}$ that satisfy $\sum_{l\in L} VOT^h \tilde{t}_{l,\tau}\, \tilde{z}_{l,\tau}^{w,m} + \sum_{l\in \underline{L}_0} \big(VOT^a + \theta_{l,\tau}\big)\tilde{t}_{l,\tau}\, \tilde{z}_{l,\tau}^{w,m} + \sum_{l\in \underline{L}_1} \varepsilon^{ha}\, \tilde{z}_{l,\tau}^{w,m} + \sum_{l\in \underline{L}_2} \varepsilon^{ah}\, \tilde{z}_{l,\tau}^{w,m} < \tilde{\mu}_\tau^{w,m}$ to the corresponding path subset $\tilde{P}_\tau^{w,m}$ and return to Step 1.

Note that we add a user class dimension to the path subset so that each user class can have a separate path subset. By doing so, we might be able to reduce the problem size of the restricted [UE-NLP].

5.3.1.5 Numerical studies

This section provides a numerical example to assess the proposed model and algorithm for the UE problem. The algorithm was implemented using GAMs (Rosenthal, 2012) on a 3.40 GHz Dell Computer with 16 GB of RAM. CONOPT (Drud, 1994) was used to solve the UE-NLP.

We solved the UE problem in the Nguyen-Dupuis network (Nguyen and Dupuis, 1984) shown in Figure 5-1. This network consists of 13 nodes, 19 links, and four O-D pairs. We consider a certain year in the future and assume that three links (5,6), (6,10), and (10,11) are converted into automated links. The total travel demand between each O-D pair is given by: $q^{1\text{-}2} = 9600\ veh/h$, $q^{1\text{-}3} = 19200\ veh/h$, $q^{4\text{-}2} = 14400\ veh/h$, $q^{4\text{-}3} = 4800\ veh/h$. We assume that the adoption rates of IIAVs and IEAVs for each O-D pair are 10% and 40%, respectively. Table 5-11 lists a new set of link input parameters that are different from those in Table 5-1 in Section 5.1.5. We set $\alpha_l = 0.15$ and $\beta_l = 4$ in the travel time function. Other default model parameters include: (1) headways: $\bar{\eta}_l^{hh} = \bar{\eta}_l^{ah} = 1.8s, \bar{\eta}_l^{aa} = 0.6s, \bar{\eta}_l^{ha} = 0.9s$; (2) value of travel times: $VOT^h = \$7.5/h$, $VOT^a = 0.5VOT^h = \$3.75/h$; (3) inconvenience costs: $\varepsilon^{ah} = \$0.2$, $\varepsilon^{ha} = \$0.1$; (4) service charge of autonomous driving: $\theta_{l,\tau} = \$0.5/h, \forall l$. Note that the above values are chosen for illustrative purpose.

Table 5-11: A new set of link characteristics of the Nguyen-Dupuis network

Link	Free-flow travel time t_a^0 (min)	Capacity u_a (veh/h)	Link	Free-flow travel time t_a^0 (min)	Capacity u_a (veh/h)
1-5	7	6000	8-2	9	8000
1-12	9	8000	9-10	10	8000

4-5	9	6000	9-13	9	4000
4-9	12	4000	10-11	6	8000
5-6	3	6000	11-2	7	6000
5-9	9	6000	11-3	8	8000
6-7	5	6000	12-6	7	8000
6-10	13	8000	12-8	14	4000
7-8	5	4000	13-3	11	4000
7-11	9	6000			

Table 5-12 reports the equilibrium travel cost for each O-D pair and each vehicle class. One can observe from Table 5-12 that for each O-D pair, HVs have the highest equilibrium travel cost, followed by IEAVs, and IIAVs have the smallest equilibrium travel cost. This result is expected because: (1) HVs experience the high value of travel time VOT^h throughout the network because they can only be driven manually; (2) IIAVs experience the low value of travel time VOT^a throughout the network due to their autonomous driving capability; and (3) Although IEAVs experience the high value of travel time VOT^h in manual driving mode, they are able to reduce their value of travel time to VOT^a on automated links. Note that for the same O-D pair, IEAVs will always have lower or equal travel cost than HVs because IEAVs can always reduce themselves to HVs by not using autonomous driving service. One can also observe from the fifth column in Table 5-12 that for each O-D pair, the equilibrium travel cost for IIAVs is half of that for HVs. This result is expected because based on our travel cost definitions for IIAVs and HVs (i.e., Equations (23) and (24)), IIAVs and HVs will always have identical travel time at equilibrium and thus the ratio between the equilibrium travel cost for IIAVs and that for HVs will always be $\frac{VOT^a}{VOT^h}$.

Table 5-12: Equilibrium O-D travel cost by vehicle class

O-D	Equilibrium travel cost ($)			Cost reduction compared to HVs	
	HVs	IIAVs	IEAVs	IIAVs	IEAVs
1-2	6.866	3.433	5.581	50.0%	18.7%
1-3	7.448	3.724	6.163	50.0%	17.3%
4-2	6.574	3.287	5.290	50.0%	19.5%
4-3	7.156	3.578	5.872	50.0%	17.9%

As shown in the last column in Table 5-12, the equilibrium travel cost for IEAVs between each O-D pair is significantly reduced compared to that for HVs. Figure 5-9 shows the paths used by IEAVs between the four O-D pairs. We can see that for each O-D pair, all IEAVs share an identical path. All four paths for the four O-D pairs pass through the three automated links. We further checked the driving mode choices of IEAVs on automated links and found that all IEAVs choose autonomous driving mode.

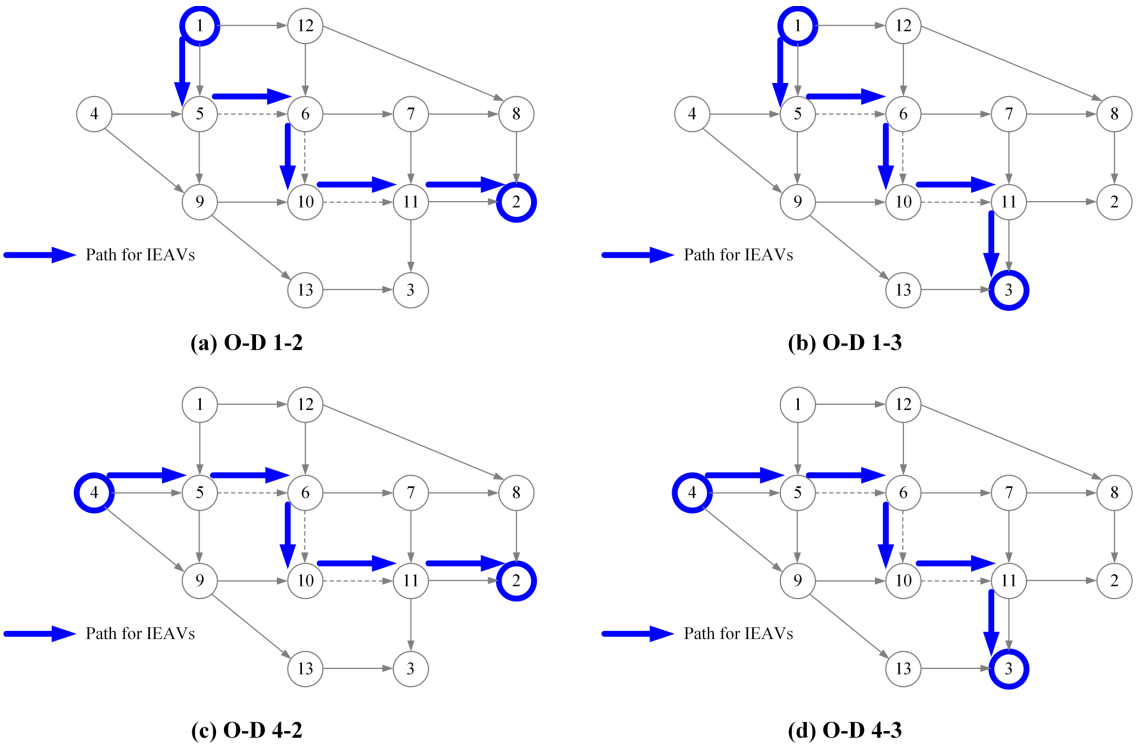

Figure 5-9. Illustration of the paths used by IEAVs

We further considered another scenario in which no automated links are deployed in the network and all other model parameters remain unchanged. We solved the UE model and compared the solutions with the scenario with automated links. Table 5-13 shows the equilibrium O-D travel costs comparison between the two scenarios. We can observe from Table 5-13 that, compared to the scenario without automated links, the scenario with automated links have smaller equilibrium O-D travel costs for all four O-D pairs and all three vehicle classes. The deployed automated links not only significantly reduce the travel costs for IEAVs but also slightly reduce the travel costs for HVs and IIAVs. Properly deployed automated links may benefit a transportation network in two ways: (1) automated links enable autonomous driving for IEAVs and thus reduce the value of travel time of IEAV users; and (2) automated links attract IEAVs to use them in autonomous driving mode and thus increase their traffic capacities.

Table 5-13: Equilibrium O-D travel cost comparison between the scenarios with and without automated links

O-D	O-D travel cost without automated links ($)			O-D travel cost with automated links ($)			Relative difference		
	HVs	IIAVs	IEAVs	HVs	IIAVs	IEAVs	HVs	IIAVs	IEAVs
1-2	7.333	3.666	7.333	6.866	3.433	5.581	-6.4%	-6.4%	-23.9%
1-3	7.974	3.987	7.974	7.448	3.724	6.163	-6.6%	-6.6%	-22.7%
4-2	7.164	3.582	7.164	6.574	3.287	5.290	-8.2%	-8.2%	-26.2%
4-3	7.805	3.903	7.805	7.156	3.578	5.872	-8.3%	-8.3%	-24.8%

To analyze the impacts of the inconvenience costs associated with using autonomous driving service, we further considered another two scenarios in which the inconvenience costs ε^{ah} and ε^{ha} are increased to 4.0 and 8.0 times of the current values,

respectively. For the scenario in which $\varepsilon^{ah} = \$0.8$ and $\varepsilon^{ha} = \$0.4$, all IEAVs between each O-D pair still use the path passing through the three automated links and choose autonomous driving mode on these automated links. For the scenario in which $\varepsilon^{ah} = \$1.6$ and $\varepsilon^{ha} = \$0.8$, no IEAVs use autonomous driving service on the automated links due to the excessive inconvenience costs.

Similar results can be observed when we try different service charges of autonomous driving on automated links. If the service charges are low, IEAVs will use autonomous driving service on automated links. When the service charges become too high, IEAVs will no longer use autonomous driving service on the automated links.

The above results are expected because as discussed in Section 5.3.1.1, an IEAV driver considers a total travel cost including travel time costs, inconvenience costs due to driving mode changes, and service charges of autonomous driving on automated links, and he/she might or might not choose to use autonomous driving service depending on whether it leads to lower total travel cost than manual driving.

5.3.2 Vehicle choice model

Road users' adoption of new vehicle technologies is a complicated process that are influenced by many factors such as vehicle characteristics, purchase prices, users' demographic and socioeconomic characteristics, and built-environment factors. To highlight the overall structure of the proposed modeling framework and reduce the computation burden of the deployment model of automated roads (proposed in Section 5), we adopt a simplified multinomial logit model to predict road users' adoption of IIAVs and IEAVs, although more complicated and accurate adoption models might be

used within our modeling framework based on data availability and computing capability. Logit models have been widely adopted in the literature to capture automotive consumers' choices of different types of conventional gasoline vehicles (e.g., Lave and Train, 1979; Boyd and Mellman, 1980), alternative-fuel vehicles (e.g., Ewing and Sarigöllü, 1998; Brownstone et al., 2000; Lin and Greene, 2010; Yip et al., 2018; Cen et al., 2018), and autonomous vehicles (e.g., Yap et al., 2015; Daziano et al., 2017; Bansal and Kockelman, 2017; Haboucha et al., 2017; Chen et al., 2019).

In our model, we made the following assumptions: (1) All vehicles have identical life time. (2) At the first year $\tau = 1$, all users are using HVs and the ages of these HVs follow a uniform distribution between 0 and the vehicle life time. (3) A user decides to buy a new vehicle if and only if his/her vehicle reaches the life time of the vehicle. Assumption (1) might me relaxed by considering increase of vehicle life time due to technology development. Assumption (2) might be relaxed by considering existing adoption of IIAVs and IEAVs and data-calibrated vehicle age distribution. Assumption (3) might be relaxed by adopting more realistic models to predict road users' decisions on whether to purchase vehicles. For instance, another layer of logit model might be calibrated with survey data to capture the influence of the demographic and built-environment factors on road users' vehicle purchase decisions (Bansal and Kockelman, 2017). Note, however, that doing so might significantly complicate the automated road deployment model (proposed in Section 5) and even make it intractable.

At each year $\tau \in T\backslash\{1\}$, road users who plan to purchase vehicles choose HVs, IIAVs, or IEAVs by following the logit model. The probability of road users between O-

D pair w choosing vehicle type $m \in M$ at year $\tau \in T$, denoted as $\sigma_\tau^{w,m}$, is specified by the following equation:

$$\sigma_\tau^{w,m} = \frac{\exp(u_\tau^{w,m})}{\sum_{m' \in M} \exp\left(u_\tau^{w,m'}\right)} \qquad \forall w \in W, m \in M \qquad (5\text{-}75)$$

where $u_\tau^{w,m}$ denotes the utility of road users between O-D pair w choosing vehicle type m at year $\tau \in T$. Note that the scale factor is normalized to 1 in the logit model. The utility $u_\tau^{w,m}$ is defined as follows:

$$u_\tau^{w,m} = \frac{\chi_e e_\tau^m}{\kappa\pi} + \chi_t \mu_{\tau-1}^{w,m} + \chi_0^m \qquad \forall w \in W, m \in M, \tau \in T\backslash\{1\} \qquad (5\text{-}76)$$

where e_τ^m is the purchasing price of vehicle type m at year τ; π is the life time of vehicles; κ is the annual average number of trips made by each driver, $\mu_{\tau-1}^{w,m}$ is the equilibrium travel cost of road users between O-D pair w choosing vehicle type m at year $\tau - 1$, χ_e and χ_t are respectively the coefficients for vehicle purchase cost and travel cost, and χ_0^m is a vehicle-specific constant that encapsulates all "hidden" attributes. Note that $\frac{e_\tau^m}{\kappa\pi}$ represents vehicle's capital cost per trip, and that we assume the equilibrium travel cost $\mu_{\tau-1}^{w,m}$ can represent the average travel cost for all the trips made by a road user. In addition, coefficients χ_e and χ_t should have a negative sign. Similar utility definition has been adopted by the studies of Nie et al. (2016) and Liu and Wang (2017) to model road users' choice of different type of electric vehicles. We note that users may also consider other vehicle or trip related costs when choosing vehicle types, such as government subsidy, auto insurance and parking cost. For simplicity and to highlight the

price and travel cost differences, this study assumes that all other vehicle or trip related costs are identical for the three types of vehicles. The utility model (5-76) can be readily extended to consider government subsidy, auto insurance and parking cost, via adding corresponding terms to the model. Finally, the travel demand of road users between O-D pair w using vehicle type m at year $\tau \in T$, i.e., $q_\tau^{w,m}$ is calculated as follows:

$$q_1^{w,h} = q_1^w \qquad \forall w \in W \tag{5-77}$$

$$q_1^{w,m} = 0 \qquad \forall w \in W, m \in \{a, \tilde{a}\} \tag{5-78}$$

$$q_\tau^{w,h} = q_{\tau-1}^{w,h} - \frac{1}{\pi} q_1^w + \frac{1}{\pi} q_1^w \sigma_\tau^{w,h} \qquad \forall w \in W, \tau \in T\backslash\{1\}, \tau \le \pi + 1 \tag{5-79}$$

$$q_\tau^{w,m} = q_{\tau-1}^{w,m} + \frac{1}{\pi} q_1^w \sigma_\tau^{w,m} \qquad \forall w \in W, m \in \{a, \tilde{a}\}, \tau \in T\backslash\{1\}, \tau \le \pi + 1 \tag{5-80}$$

$$q_\tau^{w,m} = q_{\tau-1}^{w,m} - \frac{1}{\pi} q_1^w \sigma_{\tau-\pi-1}^{w,m} + \frac{1}{\pi} q_1^w \sigma_\tau^{w,m} \qquad \forall w \in W, m \in M, \tau \in T\backslash\{1\}, \tau > \pi + 1 \tag{5-81}$$

In the above, constraints (5-77) and (5-78) specify the initial value of $q_\tau^{w,m}$ at the first year $\tau = 1$ according to our assumption (2). Constraints (5-79)-(5-81) specify the travel demand evolution for each O-D pair and each vehicle class. According to our assumptions (1)-(3), the travel demand devolution process can be described as follows: At the first year $\tau = 1$, all travel demands are HVs, i.e., $q_1^{w,h} = q_1^w, \forall w \in W$ and $q_1^{w,m} = 0, \forall w \in W, m \in \{a, \tilde{a}\}$. At each year from year $\tau = 2$ to year $\tau = \pi + 1$, $\frac{1}{\pi} q_1^w$ HV demands (the second term in constraint (5-79)) are replaced with new HV, IIAV, and IEAV demands due to vehicle aging. The share of each vehicle class $m \in M$ is calculated as $\frac{1}{\pi} q_1^w \sigma_\tau^{w,m}$ (the last term in constraints (5-79) and (5-80)), i.e., the allocation of the $\frac{1}{\pi} q_1^w$ new demands among the three vehicle classes follows the logit model. At each year

after year $\tau = \pi + 1$, each class $m \in M$ has $\frac{1}{\pi} q_1^w \sigma_{\tau-\pi-1}^{w,m}$ demands (the second term in constraint (5-81)) to be replaced with new vehicle demands due to vehicle aging. In total, those demands are $\sum_{m \in M} \frac{1}{\pi} q_1^w \sigma_{\tau-\pi-1}^{w,m} = \frac{1}{\pi} q_1^w$. Again, the allocation of the $\frac{1}{\pi} q_1^w$ new demands among the three vehicle classes follows the logit model as given by the last term in constraint (5-81).

For simplicity of representation, the vehicle choice model defined by constraints (5-77)-(5-81) is denoted as [VCM].

5.3.3 Time-dependent deployment model of automated roads

In this section, based on the UE model and the vehicle choice model, we will investigate how to optimally deploy automated roads in a general transportation network.

Denote $s_{l,\tau}$ as a binary variable, representing whether to convert link $l \in L$ into an automated link at year $\tau \in T$. If yes, $s_{l,\tau} = 1$; otherwise, $s_{l,\tau} = 0$. If a link is converted into an automated link, the charge rate for autonomous driving service, i.e., $\theta_{l,\tau}$, also needs to be determined. Due to the introduction of the variable $\boldsymbol{s} = \{\cdots, s_{l,\tau}, \cdots\}$ and the fact that $\boldsymbol{\theta} = \{\cdots, \theta_{l,\tau}, \cdots\}$ becomes a variable, other decision variables in the UE model [UE-NCP] and the vehicle choice model [VCM] now become functions of $\boldsymbol{s}$ and $\boldsymbol{\theta}$. Therefore, we denote the UE model and the vehicle choice model as [UE-NCP$(\boldsymbol{s}, \boldsymbol{\theta})$] and [VCM$(\boldsymbol{s}, \boldsymbol{\theta})$], respectively. The time-dependent optimal deployment problem (T-ODP) for automated roads can then be formulated as follows:

[T-ODP]

$$\min_{\boldsymbol{s},\boldsymbol{\theta}} \sum_{\tau\in T}\sum_{w\in W}\sum_{p\in P^w}\sum_{m\in M}\frac{\varrho\lambda_{p,\tau}^{m} f_{p,\tau}^{m}}{(1+\omega)^{\tau-1}} - \sum_{\tau\in T}\sum_{w\in W}\sum_{p\in P^w}\frac{\sum_{b\in B_\tau^p}\sum_{l\in\hat{L}(b)}\varrho\theta_{l,\tau}t_{l,\tau}\,y_{b,\tau}^{p} f_{p,\tau}^{\tilde{a}}}{(1+\omega)^{\tau-1}} + \sum_{\tau\in T\setminus\{1\}}\sum_{w\in W}\sum_{m\in M}\frac{1}{\pi}q_1^w\sigma_\tau^{w,m}\varsigma_\tau^m + \sum_{\tau\in T}s_{l,\tau}\varpi_{l,\tau}$$

s.t.

[UE-NCP($\boldsymbol{s},\boldsymbol{\theta}$)]

[VCM($\boldsymbol{s},\boldsymbol{\theta}$)]

$$\sum_{\tau\in T} s_{l,\tau} \le 1 \qquad \forall l\in L \qquad (5\text{-}82)$$

$$\theta_{l,\tau} \ge 0 \qquad \forall l\in L \qquad (5\text{-}83)$$

$$\theta_{l,\tau} < VOT^h - VOT^a \qquad \forall l\in L \qquad (5\text{-}84)$$

where ω is the discount rate per year, ϱ is a factor converting cost from an hourly basis to a yearly basis, ς_τ^m is the total amortized cost within the planning horizon for purchasing a class $m \in M$ vehicle at year $\tau \in T$, $\varpi_{l,\tau}$ is the total amortized cost within the planning horizon for constructing, maintaining and operating an automated road on link $l \in L$ deployed at year $\tau \in T$.

In the above, the objective function is to minimize the social cost. The first term calculates the total travel cost of all road users. The second term calculates the total service charges paid by IEAV users on automated roads, which are considered as a transfer from users to the government/operator and do not represent either a social gain or social cost. The third term calculates the total amortized cost of newly purchased vehicles within the planning horizon. The last term calculates the total amortized cost of automated roads within the planning horizon. Constraint [UE-NCP($\boldsymbol{s},\boldsymbol{\theta}$)] describes road users' route choice behaviors. Constraint [VCM($\boldsymbol{s},\boldsymbol{\theta}$)] describes road users' vehicle choice behaviors. Constraint (5-82) ensures that a link can be converted into an automated link at most once during the planning horizon. Constraints (5-83) and (5-84)

specify the lower and upper bounds for the service charges of autonomous driving on automated links.

Due to the complexity of [UE-NCP($\boldsymbol{s}, \boldsymbol{\theta}$)], the active-set algorithm cannot be used to solve [T-ODP]. Alternatively, a genetic-algorithm-based approach (see e.g., Yin, 2000) can be designed to solve the above deployment model.

5.4 Summary

In this chapter, we developed a modeling framework for the planning and evaluation of an infrastructure-enabled autonomous driving system. The system suggests realizing autonomous driving by the combination of smart infrastructure, which is equipped with roadside sensing, computing and communicating devices, and low-cost IEAVs, which only carry minimum necessary on-board devices. An IEAV can be much cheaper and more affordable than an IIAV. Such a system has drawn increasing attention from researchers. We envision that there will be three major types of vehicles in the market: HVs, IIAVs and IEAVs, and that the government will deploy automated roads to serve IEAVs. A network equilibrium model was first formulated to describe road users' vehicle type and route choice behaviors in a transportation network with automated roads. Two special characteristics of IEAVs are considered in the model. First, IEAVs are driven by human drivers on regular roads while they are driven autonomously on automated roads. Second, IEAV users will experience different VOTT on regular and automated roads. Road users are assumed to minimize their individual trip costs when choosing routes. Their vehicle type choices are modeled using a multinomial logit model. Based on the network equilibrium model, an optimal deployment model was further

developed to help the government strategically convert regular roads into automated roads so that road users' total benefits are maximized. The model was formulated as a MPCC, and an active-set algorithm was applied to solve it. The Nguyen-Dupuis network and the Sioux Falls network were used for the numerical demonstration of the proposed models. The results show that automated roads can significantly improve the market share of IEAVs, reduce road users' travel costs, and improve road users' consumer surpluses. The infrastructure-enabled autonomous driving system is of great potential in promoting the adoption of autonomous driving technology. Several extensions of the proposed models are also discussed. A more general UE model is formulated. A time-dependent deployment model for automated roads is proposed.

Appendix A: Proof of the equivalence between NE-VI and the network equilibrium conditions

To prove the optimal solution of the NE-VI problem satisfies network equilibrium conditions, derive the KKT conditions of the MMUE-VI formulation as follows:

$$\left(\gamma^{HV} t_l + \tilde{\rho}_i^{w,h} - \tilde{\rho}_j^{w,h}\right) x_l^{w,h} = 0 \qquad \forall (i,j) = l \in L, w \in W \qquad \text{(A.1)}$$

$$\gamma^{HV} t_l + \tilde{\rho}_i^{w,h} - \tilde{\rho}_j^{w,h} \geq 0 \qquad \forall (i,j) = l \in L, w \in W \qquad \text{(A.2)}$$

$$\left(\gamma^{AV} t_l + \tilde{\rho}_i^{w,a} - \tilde{\rho}_j^{w,a}\right) x_l^{w,a} = 0 \qquad \forall (i,j) = l \in L, w \in W \qquad \text{(A.3)}$$

$$\gamma^{AV} t_l + \tilde{\rho}_i^{w,a} - \tilde{\rho}_j^{w,a} \geq 0 \qquad \forall (i,j) = l \in L, w \in W \qquad \text{(A.4)}$$

$$\left(\gamma^{HV} t_l + \tilde{\rho}_i^{w,\tilde{a}} - \tilde{\rho}_j^{w,\tilde{a}}\right) x_l^{w,\tilde{a}} = 0 \qquad \forall (i,j) = l \in L \backslash \hat{L}, w \in W \qquad \text{(A.5)}$$

$$\gamma^{HV} t_l + \tilde{\rho}_i^{w,\tilde{a}} - \tilde{\rho}_j^{w,\tilde{a}} \geq 0 \qquad \forall (i,j) = l \in L \backslash \hat{L}, w \in W \qquad \text{(A.6)}$$

$$\left(\gamma^{AV} t_l + \tilde{\rho}_i^{w,\tilde{a}} - \tilde{\rho}_j^{w,\tilde{a}}\right) x_l^{w,\tilde{a}} = 0 \qquad \forall (i,j) = l \in \hat{L}, w \in W \qquad \text{(A.7)}$$

$$\gamma^{AV} t_l + \tilde{\rho}_i^{w,\tilde{a}} - \tilde{\rho}_j^{w,\tilde{a}} \geq 0 \qquad \forall (i,j) = l \in \hat{L}, w \in W \qquad \text{(A.8)}$$

$$\frac{-1}{\zeta_t}\left(\ln q^{w,m} - \zeta_0^m - \frac{\zeta_p p^m}{\phi l^m}\right) + \tilde{\pi}^w - \boldsymbol{E}^w \tilde{\boldsymbol{\rho}}^{w,m} = 0 \qquad \forall w \in W, m \in M \qquad \text{(A.9)}$$

$$(\boldsymbol{x}, \boldsymbol{q}) \in \Phi$$

where vector $\tilde{\boldsymbol{\rho}}^{w,m}$ is the multiplier associated with constraint (5-8) and $\tilde{\pi}^{w}$ is the multiplier associated with constraint (5-22).

From equation (A.9), we have

$$q^{w,m} = e^{\zeta_t\left(\tilde{\rho}_{d(w)}^{w,m} - \tilde{\rho}_{o(w)}^{w,m} + \tilde{\pi}^{w}\right) + \zeta_0^m + \frac{\zeta_p p^m}{\phi l^m}} \qquad \forall w \in W, m \in M \qquad \text{(A.10)}$$

From equation (A.10) and constraint (5-22) we have

$$q^{w} = \sum_{m \in M} q^{w,m} = \sum_{m \in M} e^{\zeta_t\left(\tilde{\rho}_{d(w)}^{w,m} - \tilde{\rho}_{o(w)}^{w,m} + \tilde{\pi}^{w}\right) + \zeta_0^m + \frac{\zeta_p p^m}{\phi l^m}} \quad \forall w \in W, m \in M \qquad \text{(A.11)}$$

$$\frac{q^{w,m}}{q^{w}} = \frac{e^{\zeta_0^m + \frac{\zeta_p p^m}{\phi l^m} + \zeta_t\left(\tilde{\rho}_{d(w)}^{w,m} - \tilde{\rho}_{o(w)}^{w,m}\right)}}{\sum_{m' \in M} e^{\zeta_0^{m'} + \frac{\zeta_p p^{m'}}{\phi l^{m'}} + \zeta_t\left(\tilde{\rho}_{d(w)}^{w,m'} - \tilde{\rho}_{o(w)}^{w,m'}\right)}} \qquad \forall w \in W, m \in M \qquad \text{(A.12)}$$

Comparing the optimality conditions of NE-VI with the network equilibrium conditions (5-6)-(5-21) eliminating $\lambda^{w,m}$ and $u^{w,m}$, we can find that they are exactly the same except that $\tilde{\rho}_i^{w,m} = \rho_i^{w,m}$. Therefore, NE-VI is equivalent to the network equilibrium conditions. □

Appendix B: Derivation of the NE-NLP Model

The NE-VI is given as follows:

$$\sum_{w \in W} \sum_{l \in L} \left[\gamma^{HV} t_l^*\left(x_l^{w,h} - x_l^{w,h*}\right) + \gamma^{AV} t_l^*\left(x_l^{w,a} - x_l^{w,a*}\right)\right] + \sum_{w \in W} \sum_{l \in L \setminus \hat{L}} \gamma^{HV} t_l^*\left(x_l^{w,\tilde{a}} - x_l^{w,\tilde{a}*}\right) + \sum_{w \in W} \sum_{l \in \hat{L}} \gamma^{AV} t_l^*\left(x_l^{w,\tilde{a}} - x_l^{w,\tilde{a}*}\right) - \sum_{w \in W} \sum_{m \in M} \frac{1}{\zeta_t}\left(\ln q^{w,m*} - \zeta_0^m - \frac{\zeta_p p^m}{\phi l^m}\right)\left(q^{w,m} - q^{w,m*}\right) \geq 0, \forall (\boldsymbol{v}, \boldsymbol{x}) \in \Phi$$

By the definition of VI problem, $(\boldsymbol{x}^*, \boldsymbol{q}^*)$ solves the above VI if and only if the following relationship holds:

$$\sum_{w\in W}\sum_{l\in L}\left(\gamma^{HV}t_l^* x_l^{w,h*} + \gamma^{AV}t_l^* x_l^{w,a*}\right) + \sum_{w\in W}\sum_{l\in L\setminus\hat{L}}\gamma^{HV}t_l^* x_l^{w,\tilde{a}*} + \sum_{w\in W}\sum_{l\in\hat{L}}\gamma^{AV}t_l^* x_l^{w,\tilde{a}*} - \sum_{w\in W}\sum_{m\in M}\frac{1}{\zeta_t}\left(\ln q^{w,m*} - \zeta_0^m - \frac{\zeta_p p^m}{\phi l^m}\right)q^{w,m*}$$
$$= \min_{\boldsymbol{x},\boldsymbol{q}} \sum_{w\in W}\sum_{l\in L}\left(\gamma^{HV}t_l^* x_l^{w,h} + \gamma^{AV}t_l^* x_l^{w,a}\right) + \sum_{w\in W}\sum_{l\in L\setminus\hat{L}}\gamma^{HV}t_l^* x_l^{w,\tilde{a}} + \sum_{w\in W}\sum_{l\in\hat{L}}\gamma^{AV}t_l^* x_l^{w,\tilde{a}} - \sum_{w\in W}\sum_{m\in M}\frac{1}{\zeta_t}\left(\ln q^{w,m*} - \zeta_0^m - \frac{\zeta_p p^m}{\phi l^m}\right)q^{w,m}$$

s.t. $(\boldsymbol{x}, \boldsymbol{q}) \in \Phi$.

The above relationship implies that $(\boldsymbol{x}^*, \boldsymbol{q}^*)$ must optimize the above linear programing (LP) problem, where $(\boldsymbol{x}, \boldsymbol{q})$ is the vector of decision variables. The dual problem of the above LP problem is as follows:

$$\max_{\tilde{\boldsymbol{\rho}},\tilde{\boldsymbol{\pi}}} \sum_{w\in W} -q^w\tilde{\pi}^w$$

s.t.

$$\gamma^{HV}t_l^* + \tilde{\rho}_i^{w,h} - \tilde{\rho}_j^{w,h} \geq 0 \qquad \forall (i,j) = l \in L, w \in W$$
$$\gamma^{AV}t_l^* + \tilde{\rho}_i^{w,a} - \tilde{\rho}_j^{w,a} \geq 0 \qquad \forall (i,j) = l \in L, w \in W$$
$$\gamma^{HV}t_l^* + \tilde{\rho}_i^{w,\tilde{a}} - \tilde{\rho}_j^{w,\tilde{a}} \geq 0 \qquad \forall (i,j) = l \in L\setminus\hat{L}, w \in W$$
$$\gamma^{AV}t_l^* + \tilde{\rho}_i^{w,\tilde{a}} - \tilde{\rho}_j^{w,\tilde{a}} \geq 0 \qquad \forall (i,j) = l \in \hat{L}, w \in W$$
$$\frac{-1}{\zeta_t}\left(\ln q^{w,m*} - \zeta_0^m - \frac{\zeta_p p^m}{\phi l^m}\right) + \tilde{\pi}^w - \boldsymbol{E}^w\tilde{\boldsymbol{\rho}}^{w,m} \geq 0 \qquad \forall w \in W, m \in M$$

where vector $\tilde{\boldsymbol{\rho}}^{w,m}$ is the multiplier associated with constraint (5-8) and $\tilde{\pi}^w$ is the multiplier associated with constraint (5-22). Consequently, by LP strong duality theorem, if $(\boldsymbol{x}^*, \boldsymbol{q}^*)$ is the optimal solution of the primal problem, the dual problem also has an

optimal solution and there is no duality gap. By corollary 1 of Aghassi et al. (2006), $(\boldsymbol{x}^*, \boldsymbol{q}^*)$ solves the VI problem if and only if the following mathematical program has an optimal value of zero and $(\boldsymbol{x}^*, \boldsymbol{q}^*, \tilde{\boldsymbol{\rho}}^*, \tilde{\boldsymbol{\pi}}^*)$ is the optimal solution to the following optimization problem:

$$\min_{\boldsymbol{x},\boldsymbol{q},\tilde{\boldsymbol{\rho}},\tilde{\boldsymbol{\pi}}} \sum_{w\in W}\sum_{l\in L}\left(\gamma^{HV} t_l x_l^{w,h} + \gamma^{AV} t_l x_l^{w,a}\right) + \sum_{w\in W}\sum_{l\in L\setminus\hat{L}} \gamma^{HV} t_l x_l^{w,\tilde{a}} + \sum_{w\in W}\sum_{l\in \hat{L}} \gamma^{AV} t_l x_l^{w,\tilde{a}} - \sum_{w\in W}\sum_{m\in M} \frac{1}{\zeta_t}\left(\ln q^{w,m} - \zeta_0^m - \frac{\zeta_p p^m}{\phi l^m}\right) q^{w,m} + \sum_{w\in W} q^w \tilde{\pi}^w$$

s.t.

$$\gamma^{HV} t_l + \tilde{\rho}_i^{w,h} - \tilde{\rho}_j^{w,h} \geq 0 \qquad \forall (i,j) = l \in L, w \in W$$

$$\gamma^{AV} t_l + \tilde{\rho}_i^{w,a} - \tilde{\rho}_j^{w,a} \geq 0 \qquad \forall (i,j) = l \in L, w \in W$$

$$\gamma^{HV} t_l + \tilde{\rho}_i^{w,\tilde{a}} - \tilde{\rho}_j^{w,\tilde{a}} \geq 0 \qquad \forall (i,j) = l \in L\setminus\hat{L}, w \in W$$

$$\gamma^{AV} t_l + \tilde{\rho}_i^{w,\tilde{a}} - \tilde{\rho}_j^{w,\tilde{a}} \geq 0 \qquad \forall (i,j) = l \in \hat{L}, w \in W$$

$$\frac{-1}{\zeta_t}\left(\ln q^{w,m} - \zeta_0^m - \frac{\zeta_p p^m}{\phi l^m}\right) + \tilde{\pi}^w - \boldsymbol{E}^w \tilde{\boldsymbol{\rho}}^{w,m} \geq 0 \qquad \forall w \in W, m \in M$$

$$(\boldsymbol{x}, \boldsymbol{q}) \in \Phi$$

Let $\rho_i^{w,m} = \tilde{\rho}_i^{w,m}$ and $\pi_l = \tilde{\pi}_l$, we have the NE-NLP model.

CHAPTER 6

CONCLUSIONS AND FUTURE WORKS

6.1 Summary of major findings

This dissertation focuses on the modeling and optimization of network infrastructure modification and enhancement planning for AVs. The summary and findings of each chapter are discussed as follow:

Chapter 2 provided the related literature on network equilibrium and congestion pricing studies involving AVs, lane management studies for AVs, and infrastructure-enabled autonomous driving studies. Based on the discussions of the properties and limitations of existing studies, the contributions of this dissertation are highlighted.

Chapter 3 investigated the UE and congestion pricing problems in networks with mixed AV and HV flows. One key finding is that the UE problems might have unique or non-unique flow patterns depending on the realizations of future AV technologies and HV drivers' headway choices. In addition, numerical examples revealed that the adoption of AVs doesn't necessary reduce network congestion. Under certain scenarios, AVs may worsen the system performance and increase the network delay. The system optimum in both time units and monetary units as well as the corresponding pricing for user equilibrium are further investigated. It was found that, under general scenarios, it may be difficult to identify and realize system optimal flow distributions with the marginal-cost pricing scheme because the tolled UE might also have non-unique solutions for link travel times and equilibrium O-D travel times. For the second-best pricing problem, a robust optimization model, which is a min-max program, is proposed and solved by a

genetic-algorithm-based solution procedure. The model aims at optimizing the system performance under the worst-case flow distributions. Numerical studies demonstrate the importance of considering the non-uniqueness property of the tolled UE problem and the effectiveness of the robust congestion pricing model. The robust toll design can significantly reduce the worst-case total system travel time as well as the gap between the best-case and worst-case total system travel time, which implies more stable system performance.

Chapter 4 proposed a new form of managed lanes for AVs, designated as autonomous vehicle/toll (AVT) lanes and then investigated the optimal deployment of dedicated AV lanes and AVT lanes in general transportation networks with mixed AV and HV flows. Different from dedicated AV lanes that can only be used by AVs, AVT lanes grant free access to AVs while allowing HVs to use by paying tolls. The first key finding of this chapter is that dedicated AV lanes may be underutilized when AV flows are low. Based on the relationship between road capacity and the proportion of AV flows, we then identified the potential of AVT lanes in selling redundant road capacity to HVs when AV flows are low. The UE problem in a transportation network with mixed traffic of AVs and HVs and dedicated AV lanes and AVT lanes is formulated. It was found that the UE problem might have non-unique flow patterns under general cases. The deployment model of AV and AVT lanes was thus formulated as a robust min-max problem, which optimizes the system performance under the worst-case flow distributions. A genetic-algorithm-based approach was proposed to solve the model. Numerical studies based on the Nguyen-Dupuis network and the Sioux Falls network

demonstrated the effectiveness of the proposed deployment model and showed that AV and AVT lanes can significantly improve the system performance.

Chapter 5 explored an infrastructure-enabled autonomous driving system. The system combines vehicles and infrastructure in the realization of autonomous driving. Equipped with roadside sensing, computing, and communicating devices, a regular road can be upgraded into an "automated road" enabling or providing autonomous driving service to vehicles. Those vehicles only need to carry minimum required on-board devices to enable their autonomous driving on an automated road. The costs of vehicles can thus be significantly reduced. Moreover, the liability associated with autonomous driving can now be shared by vehicle makers, infrastructure providers, and/or some third-party players. This chapter developed a modeling framework for the evaluation and planning of the infrastructure-enabled autonomous driving system. A new network equilibrium model is developed to describe road users' route and vehicle choice behaviors and the resulting equilibrium traffic flow distributions in a road network with automated roads and mixed traffic of HVs, IIAVs, and IEAVs. The model considers the impact of mixed traffic on road capacity, the impact of autonomous driving on drivers' value of travel time, and the unique features of IEAVs that they are driven manually on regular roads and can switch to autonomous driving on automated roads. A deployment model for automated roads is then formulated and solved by an active-set algorithm. Numerical results show that the infrastructure-enabled autonomous driving system is promising in promoting the adoption and benefit realization of autonomous driving

technology, and that the proposed modeling framework provides a valuable tool for decision makers in evaluating and planning such a system.

6.2 Future research

In this dissertation, we assume that AVs will have smaller following headways than HVs and consequently link capacity is an increasing function of the proportion of AV flow on the link. However, as mentioned by Ghiasi et al. (2017), AV technologies are yet to be fully developed and thus may have quite some uncertainties. If future AV technologies are conservative and AVs have larger critical headways than HVs, link capacity may be a decreasing function of the proportion of AV flow on the link (Seo and Asakura, 2017). Under such conservative scenario of future AV technologies, AVs should be the one to be tolled in mixed traffic. Future research could analyze the impact of this conservative scenario and propose corresponding strategies for toll designing and infrastructure planning.

In the numerical studies involving travelers VOT, we assume that the VOT of AV users is significantly reduced compared to that of HV users (by 50%). However, some researchers have pointed out that the impact of AVs on drivers' VOT might be more modest than anticipated (see e.g., Singleton, 2019; de Almeida Correia et al., 2019). Sensitivity analysis could be conducted to further investigate the impact of AV users' VOT savings on toll designing and infrastructure planning.

The proposed models in Chapter 4 can be extended in several directions. First, the network equilibrium model can be extended by considering the mode choice of travelers between AVs and HVs. Second, the robust deployment model can be extended by

considering the risk-neutral and risk-acceptant preferences of planners. Third, a further study is planned to consider the equality of different user groups when employing the proposed model. In addition, the development of even more efficient algorithms for solving the proposed models will be undertaken.

Following the works done in Chapter 5, our future research will be undertaken in the following directions. First, numerical studies and sensitivity analysis will be conducted to demonstrate the use of the proposed time-dependent deployment model for automated roads. Second, other types of financing scheme for deploying automated roads, such as build-operate-transfer, will be investigated. Third, the combination of automated roads with other types of infrastructure, such as dedicated autonomous vehicle lanes (Chen et al., 2016) and zones (Chen et al., 2017b), will be considered.

REFERENCES

Aghassi, M., Bertsimas, D., & Perakis, G. (2006). Solving asymmetric variational inequalities via convex optimization. *Operations Research Letters*, *34*(5), 481-490.

Arbex, R. O., & da Cunha, C. B. (2015). Efficient transit network design and frequencies setting multi-objective optimization by alternating objective genetic algorithm. *Transportation Research Part B: Methodological*, *81*, 355-376.

Bansal, P., & Kockelman, K. M. (2017). Forecasting Americans' long-term adoption of connected and autonomous vehicle technologies. *Transportation Research Part A: Policy and Practice*, *95*, 49-63.

Braess, D., Nagurney, A., & Wakolbinger, T. (2005). On a paradox of traffic planning. *Transportation science*, *39*(4), 446-450.

Bose, A., & Ioannou, P. (2003). Mixed manual/semi-automated traffic: a macroscopic analysis. *Transportation Research Part C: Emerging Technologies*, *11*(6), 439-462.

Bagloee, S. A., Tavana, M., Asadi, M., & Oliver, T. (2016). Autonomous vehicles: challenges, opportunities, and future implications for transportation policies. *Journal of modern transportation*, *24*(4), 284-303.

Basar, G., & Cetin, M. (2017). Auction-based tolling systems in a connected and automated vehicles environment: Public opinion and implications for toll revenue and capacity utilization. *Transportation Research Part C: Emerging Technologies*, *81*, 268-285.

Bierstedt, J., Gooze, A., Gray, C., Peterman, J., Raykin, L., & Walters, J. (2014). Effects of next-generation vehicles on travel demand and highway capacity. *FP Think Working Group*, 10-11.

Boyd, J. H., & Mellman, R. E. (1980). The effect of fuel economy standards on the US automotive market: an hedonic demand analysis. *Transportation Research Part A: General*, *14*(5-6), 367-378.

Brownstone, D., Bunch, D. S., & Train, K. (2000). Joint mixed logit models of stated and revealed preferences for alternative-fuel vehicles. *Transportation Research Part B: Methodological, 34(5),* 315-338.

Cen, X., Lo, H. K., Li, L., & Lee, E. (2018). Modeling electric vehicles adoption for urban commute trips. *Transportation Research Part B: Methodological*, *117*, 431-454.

Congress, N. (1994). The Automated Highway System: an idea whose time has come. *Public Roads*, *58*(1).

Ceylan, H., & Bell, M. G. (2004). Traffic signal timing optimisation based on genetic algorithm approach, including drivers' routing. *Transportation Research Part B: Methodological*, *38*(4), 329-342.

Chen, A., Kim, J., Lee, S., & Kim, Y. (2010). Stochastic multi-objective models for network design problem. *Expert Systems with Applications*, *37*(2), 1608-1619.

Chen, D., Ahn, S., Chitturi, M., & Noyce, D. A. (2017a). Towards vehicle automation: Roadway capacity formulation for traffic mixed with regular and automated vehicles. *Transportation research part B: methodological*, *100*, 196-221.

Chen, Z., He, F., Zhang, L., & Yin, Y. (2016). Optimal deployment of autonomous vehicle lanes with endogenous market penetration. *Transportation Research Part C: Emerging Technologies*, *72*, 143-156.

Chen, Z., He, F., Yin, Y., & Du, Y. (2017b). Optimal design of autonomous vehicle zones in transportation networks. *Transportation Research Part B: Methodological*, *99*, 44-61.

Chen, S., Wang, H., & Meng, Q. (2019). Designing autonomous vehicle incentive program with uncertain vehicle purchase price. *Transportation Research Part C: Emerging Technologies*, *103*, 226-245.

Concas, S., & Kolpakov, A. (2009). *Synthesis of research on value of time and value of reliability* (No. BD 549-37).

Department of Numbers (2018). US Household Income. https://www.deptofnumbers.com/income/us/ (accessed November 20, 2018)

Dijkstra, E. W. (1959). A note on two problems in connexion with graphs. *Numerische mathematik*, *1*(1), 269-271.

Drud, A. S. (1994). CONOPT—a large-scale GRG code. *ORSA Journal on computing*, *6*(2), 207-216.

de Andrade, G. R., Chen, Z., Elefteriadou, L., & Yin, Y. (2017). Multiclass Traffic Assignment Problem with Flow-Dependent Passenger Car Equivalent Value of Trucks. *Transportation Research Record: Journal of the Transportation Research Board*, (2667), 131-141.

de Almeida Correia, G. H., Looff, E., van Cranenburgh, S., Snelder, M., & van Arem, B. (2019). On the impact of vehicle automation on the value of travel time while performing work and leisure activities in a car: Theoretical insights and results from a stated preference survey. *Transportation Research Part A: Policy and Practice*, *119*, 359-382.

Di, X., Liu, H. X., & Ban, X. J. (2016). Second best toll pricing within the framework of bounded rationality. *Transportation Research Part B: Methodological*, *83*, 74-90.

Drezner, Z., & Salhi, S. (2002). Using hybrid metaheuristics for the one-way and two-way network design problem. *Naval Research Logistics (NRL)*, *49*(5), 449-463.

Dahlgren, J. (2002). High-occupancy/toll lanes: where should they be implemented?. *Transportation Research Part A: Policy and Practice*, *36*(3), 239-255.

Daziano, R. A., Sarrias, M., & Leard, B. (2017). Are consumers willing to pay to let cars drive for them? Analyzing response to autonomous vehicles. *Transportation Research Part C: Emerging Technologies*, *78*, 150-164.

Eriksson, A., & Stanton, N. A. (2017). Takeover time in highly automated vehicles: noncritical transitions to and from manual control. *Human factors*, *59*(4), 689-705.

Ewing, G. O., & Sarigöllü, E. (1998). Car fuel-type choice under travel demand management and economic incentives. *Transportation Research Part D: Transport and Environment*, *3*(6), 429-444.

Fielding, G. J., & Klein, D. B. (1993). High occupancy/toll lanes: Phasing in conjestion pricing a lane at a time. *Reason Foundation, Policy Study*, (170).

Fagnant, D. J., & Kockelman, K. (2015). Preparing a nation for autonomous vehicles: opportunities, barriers and policy recommendations. *Transportation Research Part A: Policy and Practice*, *77*, 167-181.

Fan, W., & Machemehl, R. B. (2006). Optimal transit route network design problem with variable transit demand: genetic algorithm approach. *Journal of transportation engineering*, *132*(1), 40-51.

Ghiasi, A., Hussain, O., Qian, Z. S., & Li, X. (2017). A mixed traffic capacity analysis and lane management model for connected automated vehicles: A Markov chain method. *Transportation Research Part B: Methodological*, *106*, 266-292.

Gopalswamy, S., & Rathinam, S. (2018, June). Infrastructure enabled autonomy: A distributed intelligence architecture for autonomous vehicles. In *2018 IEEE Intelligent Vehicles Symposium (IV)* (pp. 986-992). IEEE.

Goldberg, D. E. (1989). Genetic Algorithms in Search. Optimization and Machine Learning. Addism1—Wesley. *Reading, MA*.

Guo, X., & Yang, H. (2010). Pareto-improving congestion pricing and revenue refunding with multiple user classes. *Transportation Research Part B: Methodological*, *44*(8-9), 972-982.

Haboucha, C. J., Ishaq, R., & Shiftan, Y. (2017). User preferences regarding autonomous vehicles. *Transportation Research Part C: Emerging Technologies*, *78*, 37-49.

Hall, M. A. (1978). Properties of the equilibrium state in transportation networks. *Transportation Science*, *12*(3), 208-216.

He, Y., Song, Z., & Zhang, L. (2018). Time-dependent transportation network design considering construction impact. *Journal of Advanced Transportation*, *2018*.

Horst, T., Mudge, R., Ellis, R., & Rubin, K. (2016). 40 Proposed U.S. Transportation and Water Infrastructure Projects of Major Economic Significance*. AECOM. Tech. rep.*

Honda (2019). Automated drive. https://global.honda/innovation/automated-drive/detail.html (Accessed January 30, 2019)

Harker, P. T., & Pang, J. S. (1990). Finite-dimensional variational inequality and nonlinear complementarity problems: a survey of theory, algorithms and applications. *Mathematical programming*, *48*(1-3), 161-220.

Hoogendoorn, S. (2010). *Traffic flow theory and simulation, vk4821* (Vol. 152). TU Delft, Delft.

Hartman, P., & Stampacchia, G. (1966). On some non-linear elliptic differential-functional equations. *Acta mathematica*, *115*, 271-310.

Jun, M., & Markel, A. J. (2017). *Infrastructure-Based Sensors Augmenting Efficient Autonomous Vehicle Operations* (No. NREL/CP-5400-62390). National Renewable Energy Lab.(NREL), Golden, CO (United States).

Jiang, N. (2017). Optimal signal design for mixed equilibrium networks with autonomous and regular vehicles. *Journal of Advanced Transportation*, *2017*.

Lamotte, R., De Palma, A., & Geroliminis, N. (2017). On the use of reservation-based autonomous vehicles for demand management. *Transportation Research Part B: Methodological*, *99*, 205-227.

Levin, M. W., & Boyles, S. D. (2015). Effects of autonomous vehicle ownership on trip, mode, and route choice. *Transportation Research Record*, *2493*(1), 29-38.

Levin, M. W., & Boyles, S. D. (2016a). A cell transmission model for dynamic lane reversal with autonomous vehicles. *Transportation Research Part C: Emerging Technologies*, *68*, 126-143.

Levin, M. W., & Boyles, S. D. (2016b). A multiclass cell transmission model for shared human and autonomous vehicle roads. *Transportation Research Part C: Emerging Technologies*, *62*, 103-116.

Leventhal, T., Nemhauser, G., & Trotter Jr, L. (1973). A column generation algorithm for optimal traffic assignment. *Transportation Science*, *7*(2), 168-176.

Le Vine, S., Zolfaghari, A., & Polak, J. (2015). Autonomous cars: The tension between occupant experience and intersection capacity. *Transportation Research Part C: Emerging Technologies*, *52*, 1-14.

Litman, T. (2017). *Autonomous vehicle implementation predictions* (p. 28). Victoria, Canada: Victoria Transport Policy Institute.

Lu, G., Nie, Y. M., Liu, X., & Li, D. (2019). Trajectory-based traffic management inside an autonomous vehicle zone. *Transportation Research Part B: Methodological*, *120*, 76-98.

Liu, H., & Wang, D. Z. (2017). Locating multiple types of charging facilities for battery electric vehicles. *Transportation Research Part B: Methodological*, *103*, 30-55.

Lawphongpanich, S., & Yin, Y. (2010). Solving the Pareto-improving toll problem via manifold suboptimization. *Transportation Research Part C: Emerging Technologies*, *18*(2), 234-246.

Lazar, D. A., Coogan, S., & Pedarsani, R. (2017, December). Capacity modeling and routing for traffic networks with mixed autonomy. In *2017 IEEE 56th Annual Conference on Decision and Control (CDC)* (pp. 5678-5683). IEEE.

Liu, Z., & Song, Z. (2018a). Network user equilibrium of battery electric vehicles considering flow-dependent electricity consumption. *Transportation Research Part C: Emerging Technologies*, *95*, 516-544.

Liu, Z., & Song, Z. (2018b). Dynamic charging infrastructure deployment for plug-in hybrid electric trucks. *Transportation Research Part C: Emerging Technologies*, *95*, 748-772.

Liu, Z., & Song, Z. (2019). Strategic planning of dedicated autonomous vehicle lanes and autonomous vehicle/toll lanes in transportation networks. *Transportation Research Part C: Emerging Technologies*, *106*, 381-403.

Lou, Y., Yin, Y., & Lawphongpanich, S. (2010). Robust congestion pricing under boundedly rational user equilibrium. *Transportation Research Part B: Methodological*, *44*(1), 15-28.

Liu, Y., Guo, X., & Yang, H. (2009). Pareto-improving and revenue-neutral congestion pricing schemes in two-mode traffic networks. *NETNOMICS: Economic Research and Electronic Networking*, *10*(1), 123-140.

Lave, C. A., & Train, K. (1979). A disaggregate model of auto-type choice. *Transportation research part A: general*, *13*(1), 1-9.

Lin, Z., & Greene, D. L. (2010). A plug-in hybrid consumer choice model with detailed market segmentation. *Transportation research board*, 10-1698.

Merat, N., Jamson, A. H., Lai, F. C., Daly, M., & Carsten, O. M. (2014). Transition to manual: Driver behaviour when resuming control from a highly automated vehicle. *Transportation research part F: traffic psychology and behaviour*, *27*, 274-282.

Mehr, N., & Horowitz, R. (2019). How Will the Presence of Autonomous Vehicles Affect the Equilibrium State of Traffic Networks?. *IEEE Transactions on Control of Network Systems*.

Marchant, G. E., & Lindor, R. A. (2012). The coming collision between autonomous vehicles and the liability system. *Santa Clara L. Rev.*, *52*, 1321.

Meyer, J., Becker, H., Bösch, P. M., & Axhausen, K. W. (2017). Autonomous vehicles: The next jump in accessibilities?. *Research in transportation economics*, *62*, 80-91.

National Academies of Sciences, Engineering, and Medicine (NASEM). (2018). Dedicating Lanes for Priority or Exclusive Use by Connected and Automated Vehicles. *Washington, DC: The National Academies Press.* https://doi.org/10.17226/25366.

Nissan (2017). NISSAN'S SELF-DRIVING CAR. https://www.nissanusa.com/experience-nissan/news-and-events/self-driving-autonomous-car.html (Accessed January 30, 2019)

nuTonomy (2018). nuTonomy and Lyft Launch Boston Self-Driving Pilot. https://www.nutonomy.com/company-news/nutonomy-and-lyft-launch-boston-self-driving-pilot/ (accessed January 20, 2019)

Nayak, A., Chour, K., Marr, T., Ravipati, D., Dey, S., Gautam, A., ... & Rathinam, S. (2018). A Distributed Hybrid Hardware-In-the-Loop Simulation framework for Infrastructure Enabled Autonomy. *arXiv preprint arXiv:1802.01787*.

Nguyen, S., & Dupuis, C. (1984). An efficient method for computing traffic equilibria in networks with asymmetric transportation costs. *Transportation Science*, *18*(2), 185-202.

Nie, Y. M., Ghamami, M., Zockaie, A., & Xiao, F. (2016). Optimization of incentive polices for plug-in electric vehicles. *Transportation Research Part B: Methodological*, *84*, 103-123.

Noruzoliaee, M., Zou, B., & Liu, Y. (2018). Roads in transition: Integrated modeling of a manufacturer-traveler-infrastructure system in a mixed autonomous/human driving environment. *Transportation Research Part C: Emerging Technologies*, *90*, 307-333.

Ntousakis, I. A., Nikolos, I. K., & Papageorgiou, M. (2015). On microscopic modelling of adaptive cruise control systems. *Transportation Research Procedia*, *6*, 111-127.

Park, B., Messer, C., & Urbanik, T. (1999). Traffic signal optimization program for oversaturated conditions: genetic algorithm approach. *Transportation Research Record: Journal of the Transportation Research Board*, (1683), 133-142.

Polak, E., & Royset, J. O. (2005). On the use of augmented Lagrangians in the solution of generalized semi-infinite min-max problems. *Computational Optimization and Applications*, *31*(2), 173-192.

Pan, T., Lam, W. H., Sumalee, A., & Zhong, R. (2019). Multiclass multilane model for freeway traffic mixed with connected automated vehicles and regular human-piloted vehicles. *Transportmetrica A: Transport Science*, 1-29.

Ran, B., Cheng, Y., Leight, S., Parker, S. (2019a). Development of an Integrated Transportation System of Connected Automated Vehicles and Highways. *ITE Journal*, *89*(11).

Ran, B., Cheng, Y., Li, S., Ding, F., Jin, J., Chen, X., & Zhang, Z. (2019b). *U.S. Patent No. 10,380,886*. Washington, DC: U.S. Patent and Trademark Office.

Rebsamen, B., Bandyopadhyay, T., Wongpiromsarn, T., Kim, S., Chong, Z. J., Qin, B., ... & Rus, D. (2012, November). Utilizing the infrastructure to assist autonomous vehicles in a mobility on demand context. In *TENCON 2012 IEEE Region 10 Conference* (pp. 1-5). IEEE.

Rosenthal, E. (2012). GAMS, A User's Guide Tutorial by Richard E. *Rosenthal, GAMS Development Corporation, Washington, DC, USA*.

Seo, T., & Asakura, Y. (2017). Endogenous market penetration dynamics of automated and connected vehicles: Transport-oriented model and its paradox. *Transportation Research Procedia*, *27*, 238-245.

Sharon, G., Levin, M. W., Hanna, J. P., Rambha, T., Boyles, S. D., & Stone, P. (2017). Network-wide adaptive tolling for connected and automated vehicles. *Transportation Research Part C: Emerging Technologies*, *84*, 142-157.

Shladover, S. E. (2012). Highway capacity increases from automated driving. *California PATH Program*.

Simoni, M. D., Kockelman, K. M., Gurumurthy, K. M., & Bischoff, J. (2019). Congestion pricing in a world of self-driving vehicles: An analysis of different strategies in alternative future scenarios. *Transportation Research Part C: Emerging Technologies*, *98*, 167-185.

Singleton, P. A. (2019). Discussing the "positive utilities" of autonomous vehicles: will travellers really use their time productively?. *Transport reviews*, *39*(1), 50-65.

Sheffi Y. (1985) Urban Transportation Networks: Equilibrium Analysis with Mathemafical Programming Methods. Prentice-Hall, New Jersey.

Shepherd, S., & Sumalee, A. (2004). A genetic algorithm based approach to optimal toll level and location problems. *Networks and Spatial Economics*, *4*(2), 161-179.

Shladover, S. E., Su, D., & Lu, X. Y. (2012). Impacts of cooperative adaptive cruise control on freeway traffic flow. *Transportation Research Record*, *2324*(1), 63-70.

Small, K. A., & Rosen, H. S. (1981). Applied welfare economics with discrete choice models. *Econometrica (pre-1986)*, *49*(1), 105.

Song, Z., Yin, Y., & Lawphongpanich, S. (2009). Nonnegative Pareto-improving tolls with multiclass network equilibria. *Transportation Research Record*, *2091*(1), 70-78.

Song, Z., Yin, Y., Lawphongpanich, S., & Yang, H. (2014). A Pareto-improving hybrid policy for transportation networks. *Journal of Advanced Transportation*, *48*(3), 272-286.

Song, Z., Yin, Y., & Lawphongpanich, S. (2015). Optimal deployment of managed lanes in general networks. *International Journal of Sustainable Transportation*, *9*(6), 431-441.

Song, Z., He, Y., & Zhang, L. (2017). Integrated planning of park-and-ride facilities and transit service. *Transportation Research Part C: Emerging Technologies*, *74*, 182-195.

Sanchez, F., Blanco, R., & Diez, J. L. (2016). Better together: cooperative technologies will be vital to the development of highly autonomous vehicles operating in complex urban environments. *Vision Zero International*.

Talebpour, A., Mahmassani, H. S., & Elfar, A. (2017). Investigating the effects of reserved lanes for autonomous vehicles on congestion and travel time reliability. *Transportation Research Record*, *2622*(1), 1-12.

Tientrakool, P., Ho, Y. C., & Maxemchuk, N. F. (2011, September). Highway capacity benefits from using vehicle-to-vehicle communication and sensors for collision

avoidance. In *2011 IEEE Vehicular Technology Conference (VTC Fall)* (pp. 1-5). IEEE.

Tscharaktschiew, S., & Evangelinos, C. (2019). Pigouvian road congestion pricing under autonomous driving mode choice. *Transportation Research Part C: Emerging Technologies*, *101*, 79-95.

Talebian, A., & Mishra, S. (2018). Predicting the adoption of connected autonomous vehicles: A new approach based on the theory of diffusion of innovations. *Transportation Research Part C: Emerging Technologies*, *95*, 363-380.

TOYOTA (2019). Message From Toyota Chief Safety Technology Officer Kiyotaka Ise. http://automatedtoyota.com/ (Accessed January 30, 2019)

Transportation Research Board (TRB), (2016). Highway Capacity Manual, Sixth Edition: A Guide for Multimodal Mobility Analysis. *Washington, DC*.

van den Berg, V. A., & Verhoef, E. T. (2016). Autonomous cars and dynamic bottleneck congestion: The effects on capacity, value of time and preference heterogeneity. *Transportation Research Part B: Methodological*, *94*, 43-60.

van Wee, B., Annema, J. A., & Banister, D. (Eds.). (2013). *The transport system and transport policy: an introduction*. Edward Elgar Publishing. (pp. 125-159)

Wang, B. (2018). Uber' self-driving system was still 400 times worse Waymo in 2018 on key distance intervention metric. https://www.nextbigfuture.com/2018/03/uber-self-driving-system-was-still-400-times-worse-waymo-in-2018-on-key-distance-intervention-metric.html (accessed September 20, 2018)

Waymo (2018a). Riding with Waymo One today. https://medium.com/waymo/riding-with-waymo-one-today-9ac8164c5c0e (Accessed January 30, 2019)

Waymo (2018b). On the Road. https://waymo.com/ontheroad/ (accessed September 20, 2018)

Waymo (2019). The world's first premium electric self-driving vehicle. https://waymo.com/whats-next/ (Accessed January 30, 2019)

Williams, H. C. (1977). On the formation of travel demand models and economic evaluation measures of user benefit. *Environment and planning A*, *9*(3), 285-344.

Xiong, Y., & Schneider, J. B. (1992). Transportation network design using a cumulative genetic algorithm and neural network. *Transportation Research Record*, (1364).

Yang, H., & Huang, H. J. (2004). The multi-class, multi-criteria traffic network equilibrium and systems optimum problem. *Transportation Research Part B: Methodological*, *38*(1), 1-15.

Yang, H., & Huang, H. J. (2005). *Mathematical and economic theory of road pricing*. Elsevier, Kidlington, Oxford, UK.

Yang, X., Chen, A., Ning, B., & Tang, T. (2016). A stochastic model for the integrated optimization on metro timeFigure and speed profile with uncertain train mass. *Transportation Research Part B: Methodological*, *91*, 424-445.

Yin, Y. (2000). Genetic-algorithms-based approach for bilevel programming models. *Journal of transportation engineering*, *126*(2), 115-120.

Yin, Y., & Yang, H. (2004). Optimal tolls with a multiclass, bicriterion traffic network equilibrium. *Transportation Research Record*, *1882*(1), 45-52.

Yip, A. H., Michalek, J. J., & Whitefoot, K. S. (2018). On the implications of using composite vehicles in choice model prediction. *Transportation Research Part B: Methodological*, *116*, 163-188.

Yap, M. D., Correia, G., & van Arem, B. (2015). Valuation of travel attributes for using automated vehicles as egress transport of multimodal train trips. *Transportation Research Procedia*, *10*, 462-471.

Ye, Y., & Wang, H. (2018). Optimal Design of Transportation Networks with Automated Vehicle Links and Congestion Pricing. *Journal of Advanced Transportation*, *2018*.

Ye, L., & Yamamoto, T. (2018). Impact of dedicated lanes for connected and autonomous vehicle on traffic flow throughput. *Physica A: Statistical Mechanics and its Applications*, *512*, 588-597.

Zhang, K., & Nie, Y. M. (2018). Mitigating the impact of selfish routing: An optimal-ratio control scheme (ORCS) inspired by autonomous driving. *Transportation Research Part C: Emerging Technologies*, *87*, 75-90.

Zhang, X., & Yang, H. (2004). The optimal cordon-based network congestion pricing problem. *Transportation Research Part B: Methodological*, *38*(6), 517-537.

Zhang, A., Boardman, A. E., Gillen, D., & Waters II, W. G. (2004). Towards estimating the social and environmental costs of transportation in Canada. *Report for Transport Canada*, *7*.

Zhang, L., Lawphongpanich, S., & Yin, Y. (2009). An active-set algorithm for discrete network design problems. In *Transportation and Traffic Theory 2009: Golden Jubilee* (pp. 283-300). Springer, Boston, MA.

CURRICULUM VITAE

ZHAOCAI LIU

Utah State University
435-764-1080 | email: zhaocai.liu@aggiemail.usu.edu

EDUCATION

Utah State University, Utah, USA — Aug. 2015 −Dec. 2019
Ph.D. candidate in Transportation Engineering

Southeast University, Nanjing, China — Aug. 2012 −Jun. 2015
M.S. in Transportation Engineering

Southeast University, Nanjing, China. — Aug. 2008 −Jul. 2012
B.S. in Road Bridge and River-Crossing Engineering

RESEARCH INTEREST

Transportation network modeling, operations research, sustainable transportation systems, electric vehicles, electric bus systems, dynamic wireless charging, autonomous vehicles

HONORS AND AWARDS

1. USUSA Graduate Enhancement Award, Utah State University 2019
2. Ellis L. Mathes Scholarship, ITE Intermountain Section 2019
3. Outstanding Engineering PhD Scholar of the Year, College of Engineering, Utah State University 2019
4. First Place in Technical Writing Competition, College of Engineering, Utah State University 2019
5. RGS Graduate Student Travel Award, Utah State University 2019
6. Best Student Paper Award, ITE Utah Chapter 2018
7. RGS Graduate Student Travel Award, Utah State University 2018
8. RGS Graduate Student Travel Award, Utah State University 2017
9. Scholarship Sponsored by China Road &Bridge Corporation 2011
10. Grant Sponsored by China Merchants Bank 2010
11. Second prize in mathematics competition in Southeast University 2009
12. Scholarship Sponsored by Huijiao Ji 2009
13. National Encouragement Scholarship 2009

14. Scholarship Sponsored by Yingda technology Co., Ltd. 2009

PUBLICATIONS

1. Liu, Z., Song, Z. Strategic planning of dedicated autonomous vehicles lanes and autonomous vehicle/toll lanes in transportation networks. *Transportation Research Part C: Emerging Technologies, 106, 381-403.*
2. Liu, Z., Song, Z., He, Y., 2019. Economic analysis of on-route fast charging for battery electric buses: A case study in Utah. *Transportation Research Record.* https://doi.org/10.1177/0361198119839971
3. He, Y., Song, Z., Liu, Z., Sze, N. N., 2019. Factors Influencing Electric Bike Share Ridership: Analysis of Park City, Utah. *Transportation Research Record,* 0361198119838981.
4. He, Y., Song, Z., Liu, Z., 2019. Fast-charging station deployment for battery electric bus systems considering electricity demand charges. *Sustainable Cities and Society,* 101530. https://doi.org/10.1016/j.scs.2019.101530
5. Liu, Z., Song, Z., 2018. Dynamic charging infrastructure deployment for plug-in hybrid electric trucks. *Transportation Research Part C: Emerging Technologies, 95,* 748-772.
6. Liu, Z., Song, Z., 2018. Network user equilibrium of battery electric vehicles considering flow-dependent electricity consumption. *Transportation Research Part C: Emerging Technologies, 95,* 516-544.
7. Liu, Z., Song, Z., He, Y., 2018. Planning of Fast-Charging Stations for a Battery Electric Bus System under Energy Consumption Uncertainty. *Transportation Research Record*, 0361198118772953.
8. Liu, Z., Song, Z., 2017. Robust planning of dynamic wireless charging infrastructure for battery electric buses. *Transportation Research Part C: Emerging Technologies, 83,* 77-103.
9. Liu, Z., Song, Z., He, Y., 2017. Optimal Deployment of Dynamic Wireless Charging Facilities for an Electric Bus System. *Transportation Research Record: Journal of the Transportation Research Board*, (2647), 100-108.
10. He, Y., Song, Z., Liu, Z., 2017. Updating highway asset inventory using airborne LiDAR. *Measurement, 104,* 132-141.

In Preparation

11. Liu, Z., Song, Z. User equilibrium and congestion pricing problems for the mixed autonomous vehicles and human-driven vehicles. To be submitted to *Transportation Research Record*

12. Liu, Z., Zhibin Chen, Song, Z., He Y. Strategic planning of automated roads for infrastructure-enabled autonomous vehicles. To be submitted to *Transportation Research Part B*
13. Liu, Z., He, Y., Song, Z. Optimal charging schedule and management for a fast-charging battery electric bus system. To be submitted to *Transportation Research Part E*
14. He, Y., Liu, Z., Song, Z. Integrated strategic and operational planning for a fast-charging battery electric bus system. To be submitted to *Transportation Research Record*
15. He, Y., Liu, Z., Song, Z. Network design, charging station deployment, and battery sizing for a battery electric bus system. To be submitted to *Transportation Research Part E*

CONFERENCE PRESENTATIONS

1. Transportation Research Board (TRB) 98th Annual Meeting (2019)
   Podium presentation: Liu, Z., Song, Z., He, Y. Economic analysis of on-route fast charging for battery electric buses: A case study in Utah.
2. Transportation Research Board (TRB) 98th Annual Meeting (2019)
   Podium presentation: He, Y., Song, Z., Liu, Z. Factors Influencing Electric Bike Share Ridership: Analysis of Park City, Utah
3. Transportation Research Board (TRB) 98th Annual Meeting (2019)
   Poster: He, Y., Song, Z., Liu, Z. Recharging scheduling for a fast-charging battery electric bus system considering electricity demand charges.
4. 2018 INFORMS Annual Meeting
   Podium presentation: Liu, Z., Song, Z., 2018. Dynamic charging infrastructure deployment for plug-in hybrid electric trucks.
5. Transportation Research Board (TRB) 97th Annual Meeting (2018)
   Podium presentation: Liu, Z., Song, Z., He, Y. Planning of Fast-Charging Stations for a Battery Electric Bus System under Energy Consumption Uncertainty.
6. Transportation Research Board (TRB) 97th Annual Meeting (2018)
   Oral presentation: He, Y., Song, Z., Liu, Z. Fast-Charging Station Deployment for Electric Bus Systems Considering Electricity Demand Charges.
7. 5th Annual Conference on Electric Roads & Vehicles (2018)
   Poster: Liu, Z., Song, Z. Dynamic charging infrastructure deployment for plug-in hybrid electric trucks.
8. 2017 INFORMS Annual Meeting

Podium presentation: Liu, Z., Song, Z., He, Y. Robust planning of dynamic wireless charging infrastructure for battery electric buses.

9. 2017 Sustainable Electrified Transportation Center (SELECT) Annual Meeting
   Poster: Liu, Z., Song, Z. Dynamic charging infrastructure deployment for plug-in hybrid electric trucks.
10. 2017 Sustainable Electrified Transportation Center (SELECT) Annual Meeting
    Poster: He, Y., Song, Z., Liu, Z. Fast-Charging Station Deployment for Electric Bus Systems Considering Electricity Demand Charges.
11. 4th Annual Summer Conference on Livable Communities (ACLC) (2017).
    Podium presentation: Liu, Z., Song, Z., A Chen, S Ryu. Exploring bicycle route choice behavior with space syntax analysis.
12. 4th Annual Summer Conference on Livable Communities (ACLC) (2017).
    Poster: Liu, Z., Song, Z., He, Y. Robust planning of dynamic wireless charging infrastructure for battery electric buses.
13. Transportation Research Board (TRB) 96th Annual Meeting (2017)
    Poster: Liu, Z., Song, Z., He, Y. Optimal Deployment of Dynamic Wireless Charging Facilities for an Electric Bus System.
14. Transportation Research Board (TRB) 96th Annual Meeting (2017)
    Poster: He, Y., Song, Z., Liu, Z. Highway Asset Inventory Data Collection Using Airborne LiDAR.
15. 2016 Sustainable Electrified Transportation Center (SELECT) Annual Meeting
    Poster: Liu, Z., Song, Z., He, Y. Optimal Deployment of Dynamic Wireless Charging Facilities for an Electric Bus System.

RESEARCH EXPERIENCE

Utah State University, Utah, USA. Aug. 2015 −Dec. 2019
Graduate Research Assistant, Advisor: Ziqi Song, PhD
Dissertation Topic: Strategic Infrastructure Planning for Autonomous Vehicles

- Developed a bi-level optimization model to determine the deployment of automated roads for infrastructure-enabled autonomous vehicles.
- Proposed a robust optimization model to determine the deployment of dedicated autonomous vehicle lanes and autonomous vehicle/toll lanes in a network.

- Investigated network equilibrium and congestion patterns for a transportation network with mixed autonomous vehicles and human-driven vehicles.
- Proposed an optimal recharging scheduling model for a battery electric bus system.
- Developed an excel-based tool to help transit agencies design and analyze a battery electric bus corridor.
- Conducted economic analysis of on-route fast charging for battery electric buses.
- Proposed a robust optimization model to determine the deployment of charging lanes for plug-in hybrid electric trucks in a transportation network.
- Proposed a robust optimization model to solve the problem of deploying fast-charging stations for a battery electric bus system.
- Formulated the traffic assignment problem of battery electric vehicles with flow-dependent energy consumption.
- Proposed a robust optimization model to determine the deployment of dynamic wireless charging facilities for an electric bus system.
- Developed an ArcGIS-based approach to process aerial LiDAR data for highway feature inventory.

TEACHING EXPERIENCE

Utah State University, Utah, USA. Aug. 2016 −Dec. 2019
Teaching Assistant

- CEE 3210: Introduction to Transportation Engineering, Spring 2017, Spring 2018
- CEE 6220: Traffic Engineering, Fall 2016, Fall 2017, Fall 2018
- CEE 6250: Transportation Safety, Spring 2018, Spring 2019
- CEE 6290: Transportation Network Analysis, Spring 2018, Spring 2019

Southeast University, Nanjing, China Aug. 2012 −Jun. 2015

Private Tutor

- High School Physics
- High School Math
- High School Chemistry

RESEARCH REPORTS

1. Song, Z., Liu, Z., He, Y., 2018. Optimal Deployment of Wireless Charging Facilities for an Electric Bus System, MPC-18-359. North Dakota State University - Upper Great Plains Transportation Institute, Fargo: Mountain-Plains Consortium, 2018.
2. Liu, Z., Song, Z., Chen, A., Ryu, S., 2016. Exploring bicycle route choice behavior with space syntax analysis (No. TRCLC 15-13). Western Michigan University. Transportation Research Center for Livable Communities.
3. He, Y., Song, Z., Liu, Z., Lindsey, R., 2016. Implementation of aerial LiDAR technology to update highway feature inventory (No. Report No. UT-17.06). Utah. Dept. of Transportation. Research Division.

SKILLS

Programming Languages: GAMS, MATLAB, C++

Software/Tools: ArcGIS, Cube, AutoCAD

Hobbies: singing, badminton, table tennis, hiking, movies